

THE
STEREOCHEMISTRY
OF
ALKANES
AND
NON-CONJUGATED ALKENES

A Thesis presented for
the degree of Doctor of Philosophy
in the
Faculty of Science
of the
University of Glasgow
by
Moira Jane M^cCaffer

September 1977

ProQuest Number: 13804129

All rights reserved

INFORMATION TO ALL USERS

The quality of this reproduction is dependent upon the quality of the copy submitted.

In the unlikely event that the author did not send a complete manuscript and there are missing pages, these will be noted. Also, if material had to be removed, a note will indicate the deletion.



ProQuest 13804129

Published by ProQuest LLC (2018). Copyright of the Dissertation is held by the Author.

All rights reserved.

This work is protected against unauthorized copying under Title 17, United States Code
Microform Edition © ProQuest LLC.

ProQuest LLC.
789 East Eisenhower Parkway
P.O. Box 1346
Ann Arbor, MI 48106 – 1346

ACKNOWLEDGEMENTS

I wish to acknowledge my indebtedness to Dr.D.N.J.White and Professor G.A.Sim for their interest and direction throughout this period of research. I am also grateful to other members of the X - ray analysis group of the University of Glasgow, particularly Dr.C.J.Gilmore,Dr.P.Mallinson and Mr.A.A.Freer for helpful discussions and advice.

Thanks are due to the staff of the chemistry and computing departments and to the photographer, Mr.R.Munro, who assisted me in my research.

Financial support from the Science Research Council is gratefully acknowledged.

Finally, I am very grateful to my husband without whose help and encouragement I could not have completed this project.

Glasgow, 1977

M.J.M^CCaffer

CONTENTS

	Page
<u>Summary</u>	1
<u>Chapter one</u> - Molecular mechanics: An introduction	5
1.1 Introduction	6
1.2 Potential functions and force fields	10
1.3 Determination of heats of formation	20
1.4 Parametrization of force fields	24
1.5 Energy minimisation	27
1.6 References	37
 <u>Chapter two</u> - The development of a molecular force field for calculations on alkanes and non-conjugated alkenes	 39
2.1 Introduction	40
2.2 The force field	41
2.3 Results and discussion for compounds included in the parametrization	55
2.4 Some applications of the White-Bovill force field	71
2.5 References	81
 <u>Chapter three</u> - Application of the White-Bovill force field to the conformational analysis of cyclic hydrocarbons, C ₆ -C ₁₂	 86
3.1 Introduction	87
3.2 The effect of introducing a double bond into cycloalkanes, C ₆ -C ₁₀	90
3.3 The effect of introducing a second double bond into cycloalkenes, C ₈ -C ₁₀	92

Contents (contd.)

	Page
3.4 Conformations of the individual cyclenes	101
3.5 References	148
 <u>Chapter four</u> - Molecular mechanics calculations on the stability of bridgehead olefins in bicyclo(m.n.1)alk-1-ene systems	152
4.1 Introduction	153
4.2 Review	154
4.3 Molecular mechanics calculations and results	159
4.4 Discussion	169
4.5 References	183
 <u>Chapter five</u> - Prediction of the stereoselectivity of hindered substrates	185
5.1 Introduction	186
5.2 Prediction of the stereoselectivity in the hydroboration of hindered cyclohexenes using molecular mechanics calculations and steric congestion calculations	191
5.3 Discussion	199
5.4 References	203
 <u>Chapter six</u> - The correlation of Raman optical activity in methyl torsion modes with molecular mechanics calculations of chiral hind- ering potentials	204
6.1 Introduction	205
6.2 Molecular mechanics calculations	213

Contents (contd.)

	Page
6.3 Discussion	225
6.4 References	229
 <u>Chapter seven</u> - Some aspects of crystallography	230
7.1 Historical	231
7.2 Corrections to the measured intensities	232
7.3 Structure factors	235
7.4 Structure factors and the electron density distribution	238
7.5 Direct methods of phase determination	239
7.6 Fourier synthesis	246
7.7 Least squares refinement	247
 <u>Chapter eight</u> - X-ray analysis of 1,8-dimethyl-2- naphthyl acetate	252
8.1 Introduction	253
8.2 Experimental	256
8.3 Results	260
8.4 Discussion of results	291
8.5 References	301
 <u>Chapter nine</u> - The crystal structure of bicyclo(4.4.1)- undecane-1,6-diol	302
9.1 Introduction	303
9.2 Experimental	307
9.3 Results	310
9.4 Discussion of results	346
9.5 References	357

SUMMARY

Molecular force fields, which were developed before 1973 to deal with calculations on alkanes and/or non-conjugated alkenes, were each known to have certain defects in that they could not adequately reproduce all the experimental data. The parametrization of a new and improved force field for calculations on alkanes and non-conjugated alkenes was therefore undertaken. The force field, which was subsequently developed (referred to as the White-Bovill force field or WBFF, for short), incorporated into its parametrization large amounts of recently published experimental data concerning the thermodynamic and structural properties of a carefully selected group of 75 compounds and was found to be more general and reliable than the previously developed force fields. The final form of the WBFF consisted of 22 parameters for aliphatic functions and 18 parameters for double bonds and its surroundings. The mean deviation between the calculated and experimental enthalpies of 60 compounds was 0.55 kcal./mole and the corresponding figures for geometric properties were 0.009 Å, 0.6° and 0.9° in bond lengths, bond angles and torsion angles.

Molecular mechanics(MM) calculations, utilising the WBFF, were then undertaken on a series of cyclenes which had one double bond in the ring, ranging from C₆ - C₁₀ and with two double bonds in the ring, ranging from C₈ - C₁₀, so that detailed knowledge of the relationship between conformational structure and energy would be obtained. The WBFF produced extremely reliable results for geometries, heats of formation and heats of hydrogenation of a number of medium ring compounds so that it was possible to place a certain degree of confidence in the results from this investigation of the plethora of conformations and transannular

interactions exhibited by medium rings. In addition, the minimum energy conformation (MEC) of cis,cis,cis-1,5,9-cyclododecatriene was assigned on the basis of MM calculations and an NMR analysis.

A series of MM calculations was performed on a carefully selected group of sixteen bicyclic bridgehead olefins with the aim of assessing the limits of the application of the rules, proposed by Bredt, Fawcett and Wiseman, regarding the stability of bridgehead olefins and providing guidelines or rules for situations not covered by the previous rules. The experimental data, which were mostly of a qualitative nature, were satisfactorily reproduced by the WBFF and it was found that, within a given skeleton, systems with a double bond placed in the second largest bridge will be less strained than those with a double bond located in the largest bridge, which in turn are less strained than those with a double bond situated in the smallest bridge.

The recent publication of results of a series of hydroboration/oxidation experiments on hindered 1,3,5-tri- and tetra-substituted alkylcyclohexenes provided reference data for testing the application of summed atom centred congestion ratios (based on the Wipke and Gund congestion algorithm) in the prediction of the outcome of stereoselective additions to hindered double bonds since hydroboration is known to be sensitive to the balance of steric hindrance to the two faces of the double bond. The agreement between the predicted and experimentally observed stereoselectivity was favourable (within 15% of each other) when steric control dominates the reaction.

It has been suggested that Raman optical activity in methyl torsion modes of vibration in chiral molecules can be correlated with the chiral part of the electronic potential barrier hindering the rotation of the methyl group. In a

perturbed harmonic oscillator approximation, the chiral part is proportional to the displacement of the equilibrium position of the methyl group from the symmetric position. MM calculations of this displacement in (+)-3-methylcyclohexanone, (+)-3-methylcyclopentanone, (-)-limonene, (+)-carvone and (-)-menthol was found to correlate in sign, and approximately in magnitude, with the observed Raman optical activity in bands assigned to methyl torsion modes.

A structure analysis of 1,8-dimethyl-2-naphthyl acetate was carried out as part of a series of investigations, by Dr. J. Carnduff, into the autoxidation of 2-naphthols. On the basis of the rates of autoxidation reactions, the 1,8-dimethyl derivative was expected to be more strained than the 1-isopropyl derivative, which, in turn, should be more strained than the 1-methyl derivative. This hypothesis was supported by the corresponding structure analyses and, from a comparison of structural data for eight C1 and/or C8 substituted naphthalenes, the only consistent indicators of steric crowding are the C1-C9-C8 valence angle and C1....C8 nonbonded distance.

An X-ray crystal structure analysis of bicyclo(4.4.1)-undecane-1,6-diol was undertaken to determine the MEC of the bicyclo(4.4.1)undecane system and the conformation of the 10-membered ring and to obtain structural details of the MEC of cycloheptane. The X-ray results reveal that the bicyclo(4.4.1)-undecane ring system consists of two cycloheptane rings, both in the C_2 -symmetric twist-chair conformation, fused back-to-back in a 1,3-manner. MM calculations on a number of plausible conformations of the bicyclo(4.4.1)undecane system confirm the X-ray results. The conformation of the 10-membered ring in the bicyclo(4.4.1)undecane-1,6-diol was of interest on account of the

fact that it belongs to a class which had not yet been considered in MM calculations or diffraction studies of the low-energy conformations of cyclodecane.

CHAPTER ONE

Molecular mechanics: An introduction

1.1 Introduction

Through chemistry, in conjunction with all the other sciences and technologies, civilization has made tremendous headway during the last century. In chemistry, the success of John Dalton's atomic theory and the concept of isomerism, proposed by Berzelius led to radical changes of method. Chemistry ceased to be the science of 'material principles' and was transformed into the science of 'molecular structure'. Before Dalton, there had been no way of labelling the constitutions of chemical substances, except by reference to their large-scale observable properties. But now a new phase began: by paying close attention to their molecular weights and reactions, one could establish the underlying molecular structures of chemical substances directly. The development of the concept of valency was decisive, for it led to rules governing the writing of structural formulae.

Another conceptual scheme of great significance for ideas of structure of matter was the idea of Le Bel and van't Hoff (1874) of the three-dimensional arrangement of atoms. This idea did not realise its full impetus until 1950 when D.H.R. Barton published his pioneering paper¹ on conformational analysis, relating chemical reactivity of steroids and polycyclic terpenoids to conformation. Since then, the organic chemist has been concerned with the physical and chemical properties and reactivity of organic molecules in greater depth and therefore he will

utilise experimental and theoretical methods, which supply detailed information of the geometry and thermodynamic properties of molecules, and which are simple, reliable and economical.

When structural features of the molecule (bond angles, bond lengths, torsional angles, nonbonded distances) depart from their optimal values, the molecule is said to be strained. Often, functional units are the standards of choice and, for example, non-linear carbon - carbon triple bonds, twisted olefinic linkages, and nonplanar benzene rings are features indicating molecular strain. While strain is qualitatively an intuitive and simple subject, a good deal of complexity enters when quantitative results are desired e.g. in the study of chemical reactivity or when comparison between formally unrelated molecules is attempted, and, as a result, data concerning molecular strain is relatively scarce.

Existing experimental techniques for determining molecular structure and energy e.g. spectroscopy (NMR, IR, ORD/CD), diffraction (X-rays, electrons, neutrons), calorimetry and electrochemistry all have their limitations and drawbacks. All are time-consuming at best and, with the exception of diffraction, give rise to incomplete descriptions of geometry and/or energy, while the diffraction methods give no information regarding energies.

For many years, chemists have attempted to overcome

experimental difficulties by calculating the geometry and energy of a given molecule using different approaches. One approach involves the calculation of molecular properties e.g. energy, geometry, electron density, by quantum mechanics. Although ab-initio quantum mechanical calculations are theoretically sound, they are impractical for molecules of about more than twenty atoms as they use vast amounts of computer time - the time requirement goes up as n^4 where n is the number of orbitals. Alternatively, semi-empirical (simplified) quantum mechanical treatments (EHT, CNDO, MINDO) could be used but the results obtained are rather restricted because of the uncertainties introduced by the various approximations.

Molecular mechanics calculations (or empirical force-field calculations), on the other hand, are less time-consuming than the quantum mechanical calculations - the computer time requirement goes up by N^2 where N is the number of atoms and are relatively easy to perform. In addition, the results obtained by this method, under suitable conditions, can be highly reliable and their accuracy is comparable to that obtained by many of the experimental techniques. Unfortunately, the success of this technique depends on the existence of a large body of good experimental data for the initial parametrisation of an assumed force-field, which subsequently provides information on further compounds, some of which may be new or unobserved, by a process of extrapolation.

In the past few years, molecular mechanics calculations have been used to investigate features of the BORN-OPPENHEIMER surface of a wide class of organic molecules and have thus helped considerably in the understanding of various aspects of organic chemistry including molecular conformations, molecular thermodynamic properties, reaction mechanisms, kinetics, vibrational spectra and the interpretation of dynamic NMR spectra. At present reliable calculations can only be made for a limited range of compounds comprising alkanes, alkenes, aldehydes, ketones, esters and peptides with up to 40 to 50 atoms per molecule.

There are many reviews on molecular mechanics
calculations which are relevant to the present discussion. 2 - 8

1.2 Potential Functions and Force Fields

Although there are often considerable differences in the detailed techniques, all methods express the molecular strain energy as a sum of contributions from interactions such as bond-stretching, valence angle deformations and nonbonded contacts.

In valence force-field methods, the molecular geometry is usually specified by a set of ordinary crystal or orthogonal co-ordinates. It is assumed that there is a natural (or strain-free) bond length between two atoms bonded together and a natural bond angle between a given set of atoms. Deviations cause energy changes defined by interaction potentials. Similarly torsion and van der Waal's potentials can be related to standard values. A computer program now moves atoms by a specified increment (usually $0.00001 \overset{\circ}{\text{A}}$), derives the total resultant energy and continues until it finds a minimum of energy. Using interaction potentials, derived in part experimentally, one can calculate the energies of organic molecules as a function of various geometric parameters.

The total molecular potential energy (or the steric energy), V_s , of a molecule is given by the sum of six components, which are assumed to be independent of one another in the simplest treatments and which are model dependent:-

$$V_s = V_l + V_e + V_\omega + V_\chi + V_q + V_r \quad (1)$$

where V_l , V_e , V_ω , V_χ , V_q and V_r are the components of

energy which results from bond length deformation, bond angle deformation (Baeyer strain), torsional strain (Pitzer strain), out-of-plane deformations at trigonal atoms, coulombic interactions and nonbonded interactions respectively.

In the above treatment, cross terms which account for coupling between the components e.g. stretch-stretch term, stretch-bend term and bend-bend terms are neglected as they usually are very small.

(a) Bond Length Deformations

Intuitively, a chemical bond may be envisioned as a spring and thus there is a "natural" bond length. The potential energy stored in a molecule due to bond length deformation may be computed using Hooke's Law.

$$V_1 = \sum_1 \frac{1}{2} k_1 (l - l_0)^2 \quad (2)$$

where l_0 is the unstrained length, l is the observed length and k_1 is the force constant depending on the stiffness of the bond.

This term will be significant if there are, in the molecule, one or more bonds which are forced by their environment to have unnatural bond lengths. Deformation of bond lengths is an energetically costly process e.g. to stretch or compress a single bond by only 0.03 \AA costs 0.3 kcal./mole .

(b) Bond Angle Deformation

The use of Hooke's law to describe bond angle deformations is only a good approximation for small angular

displacements because of the anharmonic nature of molecules. In order to quantify large deformations (ca.25°), it is necessary to introduce additional terms into the harmonic expression. This is usually in the form of a cubic term and the following type of expression is best suited to our model.⁹

$$V_e = \sum_e \frac{1}{2} k_e (\Delta e^2 - k_e^1 \Delta e^3), \quad (3)$$

where $\Delta e = e - e_0$, e being observed bond angle, e_0 is the equilibrium bond angle, k_e is the force constant depending on the stiffness of the valency angles and k_e^1 is the cubic force constant.

Bond angle deformation is an energetically cheap process e.g. to deform a C-C-C bond angle by 1° from its preferred lowest energy value costs only about 0.01 kcal/mole and thus bond angle variation is common.

(c) Torsional strain

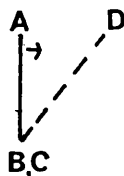
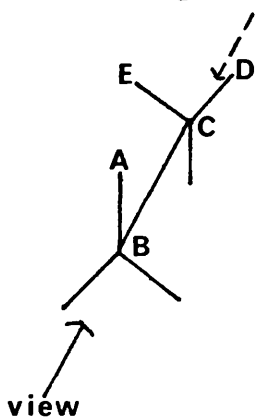
A concept, long labelled as Pitzer strain, arises from 1, 2 interactions between groups attached to contiguous carbon atoms. Variations of torsion angles from their most energetically favourable position is taken into account in the following manner -

$$V_\omega = \sum_\omega \frac{1}{2} k_\omega (1 + S \cos n\omega), \quad (4)$$

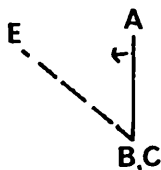
where k_ω is the barrier to free rotation, S assumes the value of -1 for C=C-C-C and C-C-C-H rotations i.e. where the minimum is an eclipsed conformation, and the value of +1 for all rotations around single bonds, n is the periodicity i.e. the no. of times the same conformation occurs in one revolution, and ω is the observed dihedral angle.

This expression assumes that the barrier height is insensitive to the changes in the nature of the substituent and that each eclipsing interaction makes an equal contribution to the barrier. The energy barriers have been found, experimentally, to be dependent, to some extent, on the number of substituents but reasonably insensitive to their nature.

The torsion angles are signed quantities corresponding to the Prelog-Ingold convention which is adopted by conformational analysts (as opposed to spectroscopists):



A must be rotated clockwise to eclipse D and the torsion angle is positive.



A must be rotated anti-clockwise to eclipse E and the torsion angle is negative.

Theory, to account for the origin or physical phenomena from which the rotational barrier arises, is far from mute and is filled with apparent conceptual conflicts. 10

The quantum mechanical results are consistent with the view that the barrier arises from interactions among atoms not formally bound to one another and it is therefore

necessary to consider repulsion energy between substituents, electronic kinetic energy, electron-electron repulsion and nuclear-electronic attraction. Whatever the explanation, the omission of this term from the model, introduces grave errors.

(d) Out - of - Plane Deformation

When four groups (or atoms) attached to an olefinic linkage or two groups (or atoms) attached to a carbonyl group deviate significantly from coplanarity with the trigonal centres, the π -bond is weakened due to poor overlap. Out - of - plane bending potentials, in addition to pure torsional potentials, must be added to ensure proper geometry and energy representation of ethylenic compounds and ketones. The potential energy stored in the molecule as a result of this deformation is accounted for in the following manner.

$$V_X = \sum_X \frac{1}{2} k_X (180 - X)^2 \quad (5)$$

where k_X is the out-of-plane bending force constant and X is the improper torsion angle at trigonal atoms.

(e) Coulombic Interaction Energy

Coulombic (or electrostatic) interactions influence steric repulsions in molecules which possess a dipole e.g. ketones, amides, and consequently must be taken into account in any quantitative treatment of molecular conformation and energy. According to classical electrostatic theory, the electrostatic interaction energy V_q is given by:-

$$V_q = q_i q_j / D r_{ij} , \quad (6)$$

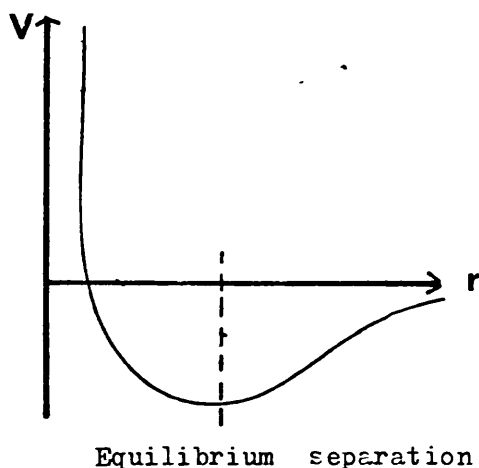
where D is the effective dielectric constant for interactions between charged atoms, q_i, q_j is the charge on

atoms i and j and r_{ij} is the distance between atoms i and j .

(f) Nonbonded Interaction Energies

Non-bonded interactions are the most troublesome components of the steric energy and are the attractive and repulsive forces that exist between two atoms or groups of atoms sufficiently close in space (either intra- or intermolecular) but not directly bonded to one another. These forces are qualitatively apparent from the existence of liquids and solids on one hand and from their relative incompressibility on the other.

For an isolated pair of spherically symmetric atoms (or molecules), the potential energy is a function of the separation of the atomic (or molecular) centres and has the approximate form, illustrated below.



For non-spherical atoms (or molecules), the potential energy depends also on the orientation of the atoms (or molecules)^{11, 12} and would therefore require an additional parameter in the potential function, but this problem has not as yet been solved.

The forces between atoms (or molecules) may be obtained from the gradient of the potential energy curve and for small separations (less than $3A^0$), the forces are repulsive and for larger separations (greater than $4A^0$), they are attractive.

In principle, the potential curve (also referred to as van der Waals potential) for any particular pair of atoms can be calculated from a consideration of the deviation of the corresponding gas from ideal behaviour. However, in practice, the potential curves have proved difficult to measure experimentally and accurate van der Waals potentials are available only for rare gases¹³ and a few special cases e.g. N_2 and CH_4 . This is unfortunate since they are responsible for a large proportion of the strain-causing deformations in molecules and consequently, strongly influence molecular geometry, vibrational frequencies and enthalpy.

The functional form V_r which describes intramolecular nonbonded interactions is usually taken over from known or assumed interatomic or intermolecular interaction potentials.¹⁴ Although there is no clear physical basis for this extrapolation, this method has proved to be satisfactory and reasonably successful even although it neglects the nature of the material between the atoms. The two most widely used types of intermolecular inter-

action potentials which have been used to describe intramolecular nonbonded interactions are the two - parameter Lennard-Jones potential (7) and three-parameter Buckingham potential (8).

$$V(r) = A/R^N - B/R^6, \text{ with } N = 12 \text{ or } 9 \quad (7)$$

$$V(r) = A \exp (-BR) - C/R^6 \quad (8)$$

In both (7) and (8), the first term describes the repulsive short range forces which occur when the distance between the central atoms is less than the sum of the van der Waals radii and which result from a balance between nuclear repulsions, electronic kinetic energies, electronic repulsions and nuclear- electronic attractions. The second term in (7) and (8) is easier to estimate and accounts for the London dispersion forces.

The precise form of the potential which was used in the development of the White-Bovill alkane/alkene force-field⁹, was derived by Williams¹⁵ by a least-squares procedure to represent intermolecular interactions in crystalline hydrocarbons e.g. heats of sublimation, lattice constants and structural details and has the following form,

$$V_r = \sum_r \epsilon (- 2/\alpha^6 + \exp (12(1-\alpha))) \quad (9)$$

where the expressions is summed over all pairs of nonbonded atoms separated by three or more bonds (different conventions are adopted by other workers in the field). Bond stretching potentials take account of the van der Waals interaction between atoms that are bonded to each

other, while bond angle bending potentials allow for nonbonded interactions between atoms bound to a common atom.

This expression (9) assumes that the total van der Waals interaction energy is equal to the sum of the energies of each pair of (spherical) atoms ("pairwise additive formulation"). It has been shown that this method gives some incorrect representations, particularly if interacting systems are not localised, but, at present, there is no satisfactory alternative and it is hoped that some of these approximations may be averaged out or absorbed in the parametrization of the force-field, particularly if care is taken in the evaluation of adjustable parameters (α and ϵ) in (9), for example, by including experimental data with small separations since potential functions are least reliable in this area.

In (9) α is a function of the distance co-ordinate alone and is equal to $\frac{r}{r_1^* + r_2^*}$ where r is van der Waals distance between atoms 1 and 2, and r_1^* and r_2^* are the van der Waals radii of atoms 1 and 2. ϵ is a function of the energy co-ordinate and is a parameter which varies with the size of the atom, since it is clearly more difficult to push two large atoms, like iodine, together to some small value of α than it is to push two small atoms to the same value of α . In some force fields, the value of ϵ for a pair of dissimilar atoms is taken to be the geometric mean of the values for identical pairs of the different atoms

interacting, while in others, ϵ is an independent parameter. However, in view of the aforementioned approximations, it would appear more sensible to have as many independent non-bonded parameters as possible and use the geometric mean as the starting value of ϵ in parametrisations in such cases.

Some terms which will appear in future discussions concerning nonbonded potential functions and parameters are defined as follows.

- a "hard" atom is one for which the plot of the force versus distance shows a steep slope.
- a "soft" atoms is one for which the plot of force versus distance shows a gentle slope.
- a "bigger" atoms is one where the equilibrium separation is slid further to the right.
- a "smaller" atom is one where the equilibrium separation is slid further to the left.

The reference geometries, force constants and the expressions for the potential energy components of the steric energy are referred to collectively as the force field. The major types of force field used in vibrational analysis and molecular mechanics are the valence force field (VFF), which is described above, and the Urey-Bradley force field (UBFF). The UBFF contains contributions due to bond stretching, bond rotation and angle bending, includes all nonbonded interactions, even those between atoms separated by two bonds i.e. 1, 3 interactions and omits cross terms.

The VFF is more general and can always be modified in such a way as to achieve a better fit between observed and calculated quantities, however, there are computer programming complexities associated with the introduction of cross terms and the time-consuming effort to assess them. The UBFF is, however, less complicated than the VFF.

There is another type of force field, the central force field, which assumes that molecules are held together by forces acting along lines between each pair of atoms, but this type of force field is rarely used.

1.3 Determination of Heats of Formation

The energy minimisation program used in force field calculations, minimises the energy with respect to the cartesian co-ordinates and supplies the detailed geometry, the steric energy components and the total steric energy, V_s , of different conformational minima of a molecule. The steric energy, V_s , corresponds to an isolated molecule in a "hypothetical motionless state at 0°K" ¹⁶. In order to compare the calculated steric energy, V_s , (of a molecule) with an experimental quantity, usually the heat of formation, ΔH_f° (which is defined as the heat absorbed or released upon formation of the compound from the standard states of the elements composing it.) it is necessary to take account of the enthalpies of vibration, rotation and translation and the vibrational zero point energy. These can be induced by making empirical corrections

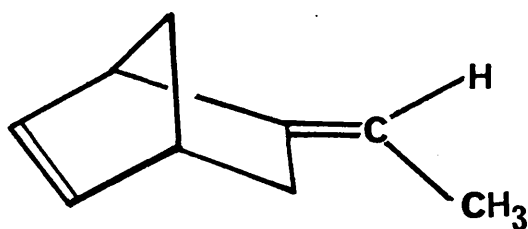
(group or bond contributions) or via statistical mechanics.

The first approach e.g. group increment scheme, assumes that, within limits, molecular structural groups have the same contribution to the heat of formation regardless of the nature of the total molecular structure. This is not an unreasonable assumption (see Table 1) if it is remembered that experimental heats of formation are themselves uncertain to a few tenths of a kcal./mole. The enthalpy of formation of a molecule

Table 1

Compound	ΔH_f° (gas, 25°C) kcal./mole.	Increment, kcal./mole.
C_2H_6	-20.24	-4.59
C_3H_8	-24.83	-5.53
C_4H_{10}	-30.36	-4.74
C_5H_{12}	-35.10	-4.82
C_6H_{14}	-39.92	-4.93
C_7H_{16}	-44.85	-5.01
C_8H_{18}	-49.86	-4.80
C_9H_{20}	-54.66	-4.96
$C_{10}H_{22}$	-59.62	

is calculated by adding the steric energy, V_s , to the sum of appropriate group enthalpy increments, which can be obtained from the steric energies and experimental enthalpies by a linear least-squares procedure ¹⁷, e.g. for 5-ethylidene norbornene -



$$\Delta H_f^\circ(\text{gas}, 25^\circ\text{C}) = E_s + 3I(=\text{CH}) + 1I(=\text{C}) + 1I(-\text{CH}_3) + 2I(-\text{CH}_2) + 2I(-\text{CH}) \quad (10)$$

Bond increment schemes are adopted in a similar fashion. These group and bond enthalpy increment schemes are more convenient than the statistical mechanics scheme and they also take into account errors which exist in the parametrization.

In the alternative statistical mechanics approach, it is necessary to add to the calculated steric energy, the rotational and translational enthalpies ($= 3RT$), the vibrational enthalpy and zero point energy in order to obtain the calculated heat of formation. The $3N - 6$ vibrational frequencies, ν_i , necessary for the evaluation of the latter two components, can be obtained by diagonalising the matrix, $M^{-\frac{1}{2}} B M^{-\frac{1}{2}}$, where B is the matrix of the potential energy second derivatives and M is the diagonal matrix of the atomic masses. The vibrational zero point energy, E_{VIB}^0 , is given by $E_{\text{VIB}}^0 = \frac{1}{2} h \sum_{i=1}^{3N-6} \nu_i$, where h is Planck's constant, while at Temperature T , the vibrational enthalpy, H_{VIB} , is calculated as

$$H_{\text{VIB}} = kT \sum_{i=1}^{3N-6} \ln(1 - \exp(-h \nu_i / kT)),$$

where k is Boltzman's constant and h is Planck's constant.

If the enthalpies of vibration are evaluated for the different conformational minima of one molecule, it is found that the values seldom differ by about more than 1 k cal/mole, which implies that differences in steric energies can be equated with conformational energies.

It is important that care should be taken when equating differences in steric energy, differences in enthalpy and differences in free energy. Energy is more intuitively convenient while enthalpy is more experimentally and thermodynamically convenient and they are interrelated by $P\Delta V$ terms,

$$\Delta H = \Delta E + P\Delta V , \quad (11)$$

usually the errors involved in these terms are small under the conditions of interest: 25°C (298K) and 1 atm. pressure.

Free energy (ΔG) is the thermodynamic variable which determines relative stability:

$$\Delta G = \Delta H - T\Delta S = -RT \ln K$$

where ΔH is the enthalpy change, ΔS is the entropy and K is the equilibrium constant. From this equation, it is evident that the free energy is composed of an enthalpy (or energy) term as well as an entropy term (ΔS).

Whereas ΔH is essentially temperature independent, increasing the temperature increases the entropy term. In most cases, near ambient temperatures, the enthalpy term dominates. As such, it is usually safe to assume

tacitly that information about ΔH is conceptually equivalent to that about ΔG . In any case, it is ΔH differences that define strain energy and ΔG differences that define relative thermodynamic stability.

From a knowledge of the free energy difference between two conformers at a particular temperature, it is possible to deduce the extent to which the conformers are present e.g. ΔG° for the change gauche to anti butane is -0.39 k cal/mole, which corresponds to an equilibrium constant K value of 1.9. Thus at 300°K, butane is approximately 65% anti and 35% gauche.

1.4 Parametrization of Force Fields

As previously mentioned, the force constants, reference geometrics and the potential functions are referred to collectively as a force field, which therefore 'describes the restoring forces which occur in a molecule when the geometry of minimal potential energy is disturbed'⁷. It is therefore necessary to derive optimum values for the force field parameters in such a manner that the resultant force field will correctly predict the geometric and/or spectroscopic and/or thermodynamic properties of a large variety of multiform molecules, within the limits of experimental error.

In order to achieve this success, it is essential to have available a large body of experimental data which is both diverse and, equally important, accurate and also to use the minimum number of necessary adjustable parameters e.g. to omit negligible cross-terms, otherwise serious problems resulting from overparametrization will

arise.

Initial estimates for force constants and potential functions for bond stretching, angle bending and out-of-plane bending are usually borrowed from vibrational analysis while bond lengths and angles are chosen from electron diffraction, microwave or X-ray results. In bond angle deformation, it has been proved^{18, 19} that to reproduce accurately experimental energies as well as geometries that it is vitally important to use different strain-free angles for different substitution of the central carbon in the force field. The starting force constant and potential function for torsional interactions are taken from microwave analysis of rotational barrier data.

An accurate description of van der Waals curves for nonbonded interactions is most essential, but they are now known only in the crudest way and consequently the nonbonded energies are the most difficult to parametrize for. Since the Lennard-Jones and Buckingham type potentials are known to be least reliable at small interatomic separation, it is vital to include as much experimental data which exhibit this feature as possible.

In practice, it is possible to obtain numerous sets of optimised parameters each of which will give essentially the same results, but extreme care must be taken with the balance between the functions and with the interpretation of the results.

Most workers adopt one of two methods to derive

optimum values for force field parameters - (a) trial-and-error method or (b) least-squares procedure.

In method (a), the force field parameters are altered in a trial-and-error manner in an attempt to find optimum values. This method consumes large amounts of human and computer resources as it is difficult to predict accurately the effect of a parameter change on the overall geometry and energy of all molecules involved in the parametrization.

Method (b) was implemented by Lifson and Warshel in 1968²⁰ and involves an elaborate linear least-squares procedure to find the best possible values for the force field parameters from structural, thermodynamic and vibrational data by minimising the squares of the differences between experimental and calculated properties with respect to force field parameters and produce a CONSISTENT FORCE FIELD. The squared term is usually weighted by an amount which is inversely proportional to the square of the standard deviation of the corresponding experimental observation. This method has the advantage of giving information concerning the omission of parameters (i.e. ones which do not differ significantly from zero) and the dependence or independence within groups of parameters but, because of the need to evaluate the second derivatives of potential energy in the calculation of vibrational frequencies, this method requires the availability of large amounts of computer time. The agreement with experimental data is reliable - Ermer and Lifson²¹ developed an alkene consistent force field where the average absolute differences between observed and calculated bond lengths, bond

angles and torsion angles used in the optimisation are 0.003 \AA , 0.5° and 1.0° respectively over a total of 44 structural quantities, between observed and calculated heats of hydrogenation 0.92 kcal/mole over 10 thermochemical quantities and between observed and calculated frequencies 15.4 cm^{-1} over 259 vibrational frequencies. It is noteworthy that method (a) produces equally good results.

An alternative method, which may be regarded as a hybrid of methods (a) and (b), may be used and it is a consequence of the fact that it is more difficult to reproduce properties associated with the energy of molecules than those associated with the geometry i.e. energy parameters are more force field dependent than geometric parameters. To overcome this problem efficiently the force constants in the force field i.e. k_1 , k_θ , k_ω and ϵ may be included in a linear least-squares optimisation along with the group enthalpy increments.

1.5 Energy Minimisation

Generally the co-ordinates of a molecule, which are initially used in a molecular mechanics study are only approximate as, for example, they have been derived from molecular models. In order to obtain information regarding the equilibrium properties of a molecule, it is necessary to adopt an energy minimisation scheme which will minimise the steric energy of the molecule, V_s , with respect to the co-ordinates by systematically adjusting the positions of the atoms and which will also produce

results which are both consistent and reliable. At present, there is no single scheme which is generally accepted as all the minimisation methods which are used, have known shortcomings²². However, the success or failure of one scheme depends largely on the position on the potential energy hypersurface that the model molecule lies.

The input co-ordinates are usually cartesian since they are simpler to use and easier to programme than internal co-ordinates which are, however, indispensable for molecules composed of more than 60 atoms.

The most widely used energy minimisation schemes will be discussed in the following sections, although the overall minimisation method, which is adopted, is often a combination of two different schemes.

At a potential energy minimum, the net force acting on any one atom is zero i.e. a necessary condition for an energy minimum is that the partial derivatives of the energy with respect to each co-ordinate equal zero,

$$\text{i.e. } \frac{\partial V_s(x)}{\partial x_i} = 0, \quad i = 1, 2, \dots, 3N$$

where N is the number of atoms in the molecule and x is a co-ordinate vector.

The potential energy of the trial model can be expanded in a Taylor series (truncated after the linear term) about an energy minimum:

$$V_s(x + \delta x)_{x=x_s} = V_s(x)_{x=x_s} + \sum_{i=1}^{3N} \left(\frac{\partial V_s(x)}{\partial x_i} \right)_{x=x_s} \Delta x_i \quad (12)$$

where x_s is a given starting point not far from the minimum.

In order to satisfy the condition for an energy minimum, the derivatives of the energy with respect to each of the $3N$ co-ordinates are taken:

$$\sum_{j=1}^{3N} \left(\frac{\partial V_s(x + \delta x)}{\partial x_j} \right)_{x=x_s} = \sum_{j=1}^{3N} \left(\frac{\partial V_s(x)}{\partial x_j} \right)_{x=x_s} +$$

$$\sum_{j=1}^{3N} \sum_{i=1}^{3N} \left(\frac{\partial^2 V_s(x)}{\partial x_j \partial x_i} \right)_{x=x_s} \Delta x_i = 0 \quad (13)$$

Equation (13) is equivalent, in matrix notation to:

$$\nabla V_s(x_s + \delta x) = \nabla V_s(x_s) + F_s \delta x = 0 \quad (14)$$

where ∇V_s is the gradient of V , and F is the matrix of the second derivatives of V . From (14), it can be deduced that

$$\delta x = -F_s^{-1} \cdot \nabla V_s(x_s) \quad (15),$$

where F^{-1} is the inverse of F .

(a) Scheme 1: Steepest Descent

This was the first general scheme to be introduced into molecular mechanics calculations, by Wiberg²³, in 1965 and it involves changing, in turn, each co-ordinate of the molecule by a small increment, calculating the

corresponding energy change and then restoring the co-ordinate to its initial value. After this procedure has been applied to each co-ordinate in the molecule, the co-ordinates are then each moved by an amount proportional to its partial derivative of energy with respect to the co-ordinate, in a direction which lowers the energy. This procedure is repeated until the difference in energy from one cycle to the next is less than a stipulated value.

To obtain a mathematical description of the steepest descent method, it is necessary to substitute a diagonal matrix D with $D_{ii} = 1/L$, where L is a scaling constant, for F in equation (15), which gives:

$$\delta x_i = -L \left(\frac{\partial V_s(x)}{\partial x_i} \right)_{x=x_s} \quad (16)$$

Bixon and Lifson²⁴ determine the constant L from a given value for the root-mean-square change of the Cartesian co-ordinates (σ_0)

$$L = \sigma_0 \left(\frac{1}{3N} \sum_{i=1}^{3N} \left(\frac{\partial V}{\partial x_i} \right)^2 \right)^{-\frac{1}{2}} \quad (17)$$

The value of σ_0 must be properly chosen during the various stages of the minimisation process, otherwise the convergence is unnecessarily slow.

Allinger and other workers have found that this minimisation method avoids the difficulty of getting stuck in a saddle point on the hypersurface and that it is most efficient (i.e. rapid minimisation) when the energy and geometry of the molecule are far removed from its minimum but becomes less efficient as the

minimum is approached. Another disadvantage, apart from the scaling problems, is that this method finds both global and local minima as well as maxima. The final absolute partial derivative attained by this method is about $0.1 \text{ k cal mole}^{-1} \text{ \AA}^{-1}$.

(b) Scheme 2: Pattern Search

This method²⁵, which was first applied to molecular mechanics calculations by Schleyer, is similar to the steepest descent method. It differs from steepest descent in that the perturbed co-ordinate is not returned to its starting point, if it is a favourable energy change, so that the pattern search method does not require the evaluation of derivatives and is scale invariant. The minimisation is accomplished by a combination of exploratory moves and pattern moves to generate a sequence of improving approximations. Exploratory moves examine the local behaviour of the function and seek to locate the direction of any sloping valleys present; pattern moves utilize the information yielded by the explorations by progressing along any such valleys. This method has the advantage that the rate of descent down valleys is more rapid than in the steepest descent method.

Schleyer's modified pattern-search method², has given lower energy and more reasonable distribution of strain than the steepest descent method, but like the steepest descent method, finds local minima and convergence near minimum is relatively slow. The difficulty

of the occurrence of local minima can be partially eliminated by employing a variety of starting geometries, when flexible molecules are being considered, which will hopefully converge to the same geometry and energy. Convergence is assumed and the search terminated when the exploration steps have been reduced below some specified limit (e.g. 10^{-40} Å).

The pattern search method is clearly a simple strategy which is easily programmed, requires very little computer storage and hence faster than the steepest descent method and like the steepest descent method, is relatively tolerant of the approximate trial structure.

(c) Scheme 3: Newton - Raphson method

This procedure was first used independently by Jacob, Thompson and Bartell¹⁹, Boyd²⁶ and Lifson and Warshel²⁰ and was found to be versatile and to produce results which were reproducible and reliable.

In equation (15), F is the matrix of second derivatives of V i.e.

$$F = \frac{\partial^2 V_s}{\partial x_j \partial x_i}$$

If F is set equal to $\frac{\partial^2 V_s}{\partial x_j \partial x_i} : i, j \leq 3$ for each atom i.e. F is then equal to the block diagonal matrix^{27,28}, this overcomes the scaling problems encountered in the steepest descent method. This block diagonal approximation method is, however, less tolerant of the approximate trial structure than the steepest descent and

pattern search methods, but it is more effective for bringing a crude, trial conformation into the vicinity of the minimum. After 50 - 100 iterations, the first derivatives of potential energy with respect to the cartesian co-ordinates are reduced to about 0.1 kcal. mole⁻¹ Å⁻¹, but thereafter convergence is slow. More recently it has been found⁸ that the block diagonal method is, in fact, less tolerant of the trial structure than the pure diagonal approximation i.e. where $F = \frac{\partial^2 V}{\partial x_i^2}$ for each atom, although the convergence properties are roughly the same. It would therefore seem to be more advantageous to use the pure diagonal approach which would use less computer time.

Regardless of whether the pure or block diagonal approach is adopted in the initial stages of minimisation, it becomes necessary in later stages to use a method which has better convergence properties. Such a method is the full-matrix Newton-Raphson i.e. where $F = \frac{\partial^2 V}{\partial x_j \partial x_i}$;
 $i, j = 1, 3N$ (18)

The matrix F is singular with six eigenvalues zero because rotations and translations have not been excluded, and so the set of equations(15) cannot be solved directly.

Two methods are available for inverting F. The first "generalised inverse" method²⁹ requires the diagonalisation of F:-

$$F^+ = E \text{ diag } (1/\lambda) E^*$$

where F^+ is the generalised inverse of F , λ and E are eigenvalues and eigenvectors of F respectively. The second approach, sometimes call the "reduced F - matrix technique" or Rao's method^{4,30}, involves keeping six co-ordinates constant by removing the corresponding rows and columns from the matrix and solving the remaining set of equations by standard methods.

However, although this second method is significantly faster than the first, it does not produce the unique generalised inverse F^+ - instead it yields a non unique F^{r2} generalised reciprocal, where F^{r2} is a matrix which is a two condition generalised reciprocal matrix, satisfying conditions (1) and (2), discussed below^{31,32}. For any matrix P , square or rectangular, there exists a unique matrix Q satisfying the conditions:-

$$PQP = P \quad (1)$$

$$QPQ = Q \quad (2)$$

$$(PQ)^* = PQ \quad (3)$$

$$(QP)^* = QP \quad (4)$$

Furthermore, the unique generalised inverse matrix of P is a matrix $Q = P^+$, which satisfies the conditions (1) - (4). This shortcoming of the second method is manifested by the observation that the convergence of the process depends on the orientation of the molecule in the frame, although, in the case of molecular mechanics, the difference in

results for one orientation and another is usually not significant.

This quadratically convergent Newton-Raphson process has to be iterative (series of successive approximations) because of the linear relationship between the first derivatives of V_s and the cartesian co-ordinates, implied by (15) and because of the truncation of the Taylor series. The full-matrix minimisation method has good convergence properties as it converges, after about 3 cycles, with the first derivatives being lowered to 10^{-10} kcal mole $^{-1}$ Å $^{-1}$. The geometry, mostly torsion angles, will usually be changed significantly, and this method thus gives a better representation of the true molecular geometry and its inherent symmetry than any of the methods previously discussed, an account of the fact that the full-matrix method takes into consideration the interaction of each atom with all the other atoms in the molecule. The energy, on the other hand, is not usually significantly altered on going to the full-matrix from the block-diagonal method. Since the full-matrix method requires a good initial estimate of the trial structure, it is only used in the second stages of minimisation - steepest descent, pattern search, block diagonal or pure diagonal methods may be used in the first stages. One major disadvantage is the necessity of solving a set of linear equations at each iteration, which requires vast amounts of computer resources, but this is not a very serious problem, due to the availability of

very fast computers with large core stores.

The matrix elements F_{ij} , calculated for the equilibrium structure, correspond to the mass independent generalised force constants of the system. The force constants corresponding to the normal vibrations of the molecule are the eigenvalues of the matrix with elements $(G_{ij}F_{ij})$ where G is the matrix of reduced masses and so normal modes of vibration and thermodynamic variables can be easily derived. Second derivative schemes give access to both minimisation and maximisation and provides a means of distinguishing between the two possibilities.

(d) Numerical versus analytical derivatives⁸.

Analyticals are faster in computer execution time but numericals are easier to program and more versatile. This latter feature can be vitally important e.g. when a force-field is in the process of being parametrized. During the parametrization, it is usually necessary to change the form of one or more of the potential forms in the force-field. In a scheme utilising numerical derivatives, it is necessary to change only a few lines in the program, whereas, when analytical derivatives are used the new expressions for these must be derived and incorporated into the program which must be amended substantially to accommodate the changes. For production work, there is preference for analytical derivatives⁹, since they use less computer time.

1.6 References

1. D.H.R. Barton, Experientia 6, 316 (1950).
2. J.D. Williams, P.J. Stang and P. von R. Schleyer, Annu. Rev. Phys. Chem., 19, 531 (1968).
3. E.M. Engler, J.D. Andose and P. von R. Schleyer, J. Amer. Chem. Soc., 95, 8005 (1973).
4. C. Altona and D.H. Faber, Topics in Current Chemistry, 45, 1 (1974).
5. J.D. Dunitz and H.B. Burgi in, International Review of Science, Physical Chemistry Series Two., Butterworths, London, Vol. II, Ch. 4 (1976).
6. N.L. Allinger, Advances in Physical Organic Chemistry, 13, 1 (1976).
7. O. Ermer, Structure and Bonding, 27, 161 (1976).
8. D.N.J. White, Computers in Chemistry, (1977), in press.
9. D.N.J. White and M.J. Bovill, J. Chem. Soc. Perkin II, in press.
10. J.P. Lowe, Science, 179, 527 (1973), presents a comparison of the explanations for ethane.
11. H. Margenau, Phys. Rev., 63, 385 (1943); 64, 131 (1943); 66, 303 (1944).
12. L. Pauling, The Nature of the Chemical Bond, Cornell University Press, 1940.
13. I. Amdur and E.A. Mason, J. Chem. Phys., 22, 670 (1954).
14. For a review see G.C. Maitland and E.B. Smith, Chem. Soc. Rev., 2, 181 (1973).
15. a) D.E. Williams, J. Chem. Phys., 45, 3770 (1966).
b) D.E. Williams, ibid., 47, 4680 (1967).

16. S. Chang, D. McNally, S. Shary-Tehrany, M.J. Hickey
and R.H. Boyd, J. Amer. Chem. Soc., 92, 3109 (1970).
17. H.L. Lipson and W. Cochran, The Crystalline State,
Ed. W.L. Bragg, Vol. III, 340 (1966).
18. N.L. Allinger, J.A. Hirsch, M.A. Miller, I. Tyminski,
and F.A. van Catledge, J. Amer. Chem. Soc., 90,
1199 (1968).
19. E.J. Jacob, H.B. Thompson, L.S. Bartell, J. Chem. Phys.,
47, 3736 (1967).
20. S. Lifson and A. Warshel, J. Chem. Phys., 49, 5116 (1968).
21. O. Ermer and S. Lifson, J. Amer. Chem. Soc., 95,
4121 (1973).
22. W. Murray (ed.) in Numerical Methods for Unconstrained
Optimization, London, Academic Press (1972).
23. K.B. Wiberg, J. Amer. Chem. Soc., 87, 1070 (1965).
24. I. Suzuki, Bull. Chem. Soc. Japan, 35, 540 (1962);
35, 1279 (1962).
25. R. Hooke and T.A. Jeeves, J. Assoc. Computing
Machinery, 8, 212 (1961).
26. R.H. Boyd, J. Chem. Phys. 49, 2574 (1968).
27. D.N.J. White and G.A. Sim, Tetrahedron, 29, 3933 (1973).
28. N.L. Allinger and G.A. Lane, J. Amer. Chem. Soc.,
96, 2937 (1974).
29. A. Warshel and S. Lifson, J. Chem. Phys., 53, 582 (1970).
30. C.R. Rao, Sankhyā, 15, 253 (1955).
31. D.N.J. White, Acta Cryst, (A), in preparation.
32. A.L. Mackay, Acta Cryst., A33, 212 (1977).

CHAPTER TWO

The development of a molecular force field
for calculations on
alkanes and non-conjugated alkenes

2.1 Introduction

By 1973, there were several force-fields ^{1,2,3,4} in existence which were developed to deal with calculations on alkanes and/or non-conjugated alkenes. Unfortunately, each one of these force fields was known to have certain defects in that they could not adequately reproduce all the available experimental data e.g. heats of formation of polycyclic hydrocarbons⁵. Such shortcomings are usually a result of a biased selection of molecules included in the parametrization of the force field, unnecessary overparametrization, lack of experimental data and incorrect derivation of the balance between non-bonded interaction potentials and other contributions to the steric energy.

Since an alkane/alkene force-field can form the basis for other force fields describing all other functional types of molecules e.g. carbonyl compounds, halogens, it is important that the basic alkane/alkene force field is a reliable one, otherwise vast amounts of human and computer resources are wasted.

Since 1973, a number of papers, supplying potentially useful experimental data, have appeared in the literature. This data include heats of formation of polycyclic hydrocarbons^{6, 7}, heats of hydrogenation of medium ring dienes and trienes⁸ and structural data e.g. neutron diffraction study of a cyclodecane derivative⁹ and X-ray and electron diffraction studies of medium ring dienes.

The time was therefore considered to be right for the parametrization of a new and improved force field which would be more general and reliable than the previously developed

force fields.

2.2. The Force Field

The force field which was subsequently developed (referred to as the White-Evill force field or WBFF, for short), incorporated into its parametrization large amounts of experimental data concerning the thermodynamic and structural properties of a carefully selected group of about 75 compounds, which range from the simplest alkene, ethylene through other straight and branched chain compounds, cyclic compounds from $C_5 - C_{12}$, bicyclic, polycyclic and highly strained hydrocarbons¹⁰.

In order to keep the force field as simple as possible, a truncated (i.e. no cross-terms used) valence force field model, identical in form to that used in Schleyer's alkane force field (SFF) was adopted. The H.....H potentials in SFF were found too 'hard' and were therefore revised. As described in Chapter 1, the steric energy, V_s , for alkanes/alkene is composed of 5 components:-

$$V_s = \sum_1 \frac{1}{2} k_1 (1 - l_0)^2 + \sum_{\theta} \frac{1}{2} k_{\theta} (\Delta \theta^2 - k^1_{\theta} \Delta \theta^3) +$$

$$\sum_{\omega} \frac{1}{2} k_{\omega} (1 + s \cos n \omega) + \sum_r \epsilon (-2/\alpha^6 + \exp$$

$$(12(1-\alpha))) + \sum_X \frac{1}{2} k_X (180 - X)^2$$

where $\alpha = r / (r_1^* + r_2^*)$.

The trial force constants were carefully adjusted in a trial and error manner until the fit between all the calculated and observed properties was satisfactory - heats of formation, heats of hydrogenation, conformational energies, barrier heights between conformations and

geometries of molecules.

The final form of the force field consisted of 22 parameters for aliphatic functions and 18 parameters for double bonds and its surroundings and is given in Table 1. A Group enthalpy increment scheme was adopted to obtain heats of formation and hydrogenation with the increments being determined from the steric energies and experimental heats of formation by a linear least-squares process. The values of the increments and their e.s.d's (estimated standard deviations) are reported in Table 2.

In total, 60 experimental enthalphy values were used in the parametrization and the final mean deviation between the calculated and experimental enthalpies was 0.55 kcal/mole which compares favourably with the 0.61 kcal/mole over 39 compounds, 0.72 kcal/mole over 39 compounds and 0.92 over 10 compounds obtained by Schleyer¹, Allinger² and Ermer and Lifson³ respectively. The corresponding figures for geometric properties are 0.009 Å, 0.6° and 0.9° in bond lengths, bond angles and torsion angles respectively over a set of 93 observations. The enthalphy and geometric data on the individual molecules are listed in Tables 3 and 4 respectively. It can thus be seen that these results are within the acceptable limits of experimental error and are more reliable than the aforementioned force fields and hence a certain amount of confidence can be placed in the results for compounds, not included in the parametrization but whose structural features are represented in it.

The energy minimisation scheme was a tandem quasi-Newton (Block Diagonal followed by Full Matrix) minimis-

Atom Key

1 = H, 2 = C_{sp2}, 3 = C_{sp3}

Force constants are in k.cal.mol⁻¹Å⁻² or in k.cal.mol⁻¹deg⁻², Energies are in k.cal.mol⁻¹

Bond Stretching

Type 1	Type 2	$\frac{1}{2}k_b$	λ_o
1	2	346.0	1.089
1	3	331.2	1.100
2	2	670.0	1.335
2	3	319.5	1.501
3	3	316.8	1.520

Van der Waals

Type 1	Type 2	r_1^*	r_2^*	ϵ
1	1	3.10	0.0	0.0160
1	2	3.53	0.0	0.0330
1	3	3.35	0.0	0.0299
2	2	4.00	0.0	0.0760
2	3	3.60	0.0	0.0800
3	3	3.85	0.0	0.1200

Table 1: Force Field Parameters

Angle Bending

Type 1	Type 2	Type 3	$\frac{1}{2}k_{\theta}$	k'_{θ}	$*\theta^1_{\text{O}}$	θ^2_{O}	θ^3_{O}	θ^4_{O}
1	2	1	0.0055	0.0096	118.6			
1	2	2	0.0060	0.0	121.7	120.4		
1	2	3	0.0060	0.0		117.5		
2	2	3	0.0120	0.0096		122.3	121.0	
3	2	3	0.0233	0.0096			116.4	
1	3	1	0.0072	0.0096	108.2	109.1		
1	3	2	0.0088	0.0096	110.5	110.0	110.2	
1	3	3	0.0088	0.0096	109.0	109.2	109.2	
2	3	2	0.0090	0.0096		111.0	110.1	109.5
2	3	3	0.0090	0.0096		110.4	110.1	109.5
3	3	3	0.0120	0.0096		110.4	110.1	109.5

* Superscript indicates the degree of substitution at the central atom

Torsion

Type 1	Type 2	Type 3	Type 4	k_w	s	n
1	2	2	1	6.2500	-1.0	2.0
1	2	2	3	6.2500	-1.0	2.0
3	2	2	3	6.2500	-1.0	2.0
1	2	3	1	0.1367	1.0	3.0
1	2	3	2	0.1367	1.0	3.0
1	2	3	3	0.1367	1.0	3.0
2	2	3	1	0.0629	-1.0	3.0
2	2	3	2	0.0629	-1.0	3.0
2	2	3	3	0.0629	-1.0	3.0
3	2	3	1	0.0629	1.0	3.0
3	2	3	2	0.0629	1.0	3.0
3	2	3	3	0.0629	1.0	3.0
1	3	3	1	0.1100	1.0	3.0
1	3	3	2	0.1100	1.0	3.0
1	3	3	3	0.1100	1.0	3.0
2	3	3	2	0.0200	1.0	3.0
2	3	3	3	0.0629	1.0	3.0
3	3	3	3	0.0629	1.0	3.0

Out of Plane Bending

Type 1	Type 2	Type 3	Type 4	k_x
3	2	2	1	0.0020

Table 1 (contd)

TABLE 2. GROUP ENTHALPY INCREMENTS

≡C/2	6.28	E.5.6.
≡C/1	8.36	1.19
≡C	8.70	1.07
-C/3	9.26	1.32
-C/2	-1.20	1.11
-C/1	-5.20	1.94
-C	-2.38	1.36
	-1.12	1.23

UNITS KCAL./MOL.

TABLE 3(a). CALCULATED AND EXPERIMENTAL HEATS OF FORMATION, ΔH_f° (GAS, 25°C) AND CALCULATED STERIC ENERGIES, E_s (KCAL./MOL.)

COMPOUND	E_s	ΔH_f° (GAS) CALC	ΔH_f° (GAS) OBS	ΔC_{p-0}	REF.
ETHYLENE	0.11	12.67	12.47	0.20	50,20
PROPENE	0.44	4.91	4.88	0.03	50,20
1-BUTENE	0.80	-0.01	-0.11	0.10	50,20
CIS-2-BUTENE	1.99	-1.62	-1.77	0.15	50,20
TRANS-2-BUTENE	0.68	-2.93	-2.83	-0.10	50,20
ISOBUTENE	0.85	-3.61	-4.15	0.54	50,20
2-METHYL-1-BUTENE	1.48	-8.26	-8.55±0.18	0.29	50
3-METHYL-1-BUTENE	1.98	-6.19	-6.61±0.18	0.42	50
2-METHYL-2-BUTENE	2.53	-10.01	-10.15	0.14	50,20
2,3-DIMETHYL-1-BUTENE	2.47	-14.72	-15.19±0.50	0.47	50
2,3-DIMETHYL-2-BUTENE	4.91	-16.56	-16.42±0.25	-0.14	50
3,3-DIMETHYL-1-BUTENE	2.68	-14.50	-14.51±0.25	0.01	50
1-PENTENE	1.02	-5.08	-5.33±0.31	0.25	50
CIS-2-PENTENE	2.23	-6.67	-6.86	0.19	50,20
TRANS-2-PENTENE	0.98	-7.92	-7.76	-0.16	50,20
2-METHYL-2-PENTENE	2.66	-15.17	-15.13	-0.04	50,20
2-METHYL-TRANS-2-PENTENE	3.02	-14.81	-15.09±0.32	0.28	50
3-METHYL-CIS-2-PENTENE	2.67	-15.16	-14.89±0.36	-0.27	50
4-METHYL-TRANS-2-PENTENE	2.11	-14.15	-14.70±0.35	0.55	50
4-METHYL-CIS-2-PENTENE	2.60	-13.66	-13.74±0.29	0.08	50
4,4-DIMETHYL-1-PENTENE	2.16	-20.31	-19.32	-0.99	50,20
2,4,4-TRIMETHYL-1-PENTENE	3.43	-27.97	-26.37±0.30	-1.60	50
1,4-PENTADIENE	0.96	25.15	25.25±0.25	-0.10	50
TRANS-2-HEXENE	1.18	-13.01	-12.88±0.39	-0.13	50
CIS-2-HEXENE	2.40	-11.79	-12.51±0.33	0.72	50
1,5-HEXADIENE	1.29	20.19	20.05	0.14	50,20
METHYLCYCLOPENTANE	8.13	-25.66	-25.50	-0.16	50

TABLE 3(a). CALCULATED AND EXPERIMENTAL HEATS OF FORMATION, ΔH_f^0 (GAS, 25°C) AND CALCULATED STERIC ENERGIES, E_s (KCAL./MOL.) (CONT'D)

COMPOUND	E_s	ΔH_f^0 (GAS) CALC	ΔH_f^0 (GAS) OBS	$\Delta C-o$	REF.
CYCLOPENTENE	7.70	8.75	8.22	0.53	50,20,51
1-METHYLCYCLOPENTENE	7.76	-0.12	-0.6 \pm 0.5	0.48	50
3-METHYLCYCLOPENTENE	7.01	1.51	2.00 \pm 0.5	-0.49	50
CYCLOHEXANE	5.45	-20.27	-29.50 \pm 0.15	1.23	50
METHYLCYCLOHEXANE	5.47	-35.61	-36.98 \pm 0.25	1.37	50
CYCLOHEXENE	2.78	-1.45	-1.18	-0.27	50,20
1-METHYLCYCLOHEXENE	2.84	-10.32	-10.34 \pm 0.20	0.02	50
1,4-CYCLOHEXADIENE	3.17	26.43	26.3	0.13	51
CYCLOHEPTANE	8.33	-28.69	-28.22 \pm 0.18	-0.47	50
CYCLOHEPTENE	5.98	-3.54	-2.07	-1.47	50,20,51
CIS-CYCLOOCTENE	7.88	-6.93	-6.47	-0.46	50,20,51
TRANS-CYCLOOCTENE	18.60	3.79	4.1a	-0.31	51
NORBORNANE	19.47	-11.72	-12.42 \pm 0.70	0.70	52
NORBORNADIENE	31.32	55.11	54.80 \pm 0.55b	0.31	53
5-ETHYLDIENENORBORNENE	25.22	34.79	34.82 \pm 0.43	-0.03	54
ADAMANTANE	11.63	-29.61	-30.65 \pm 0.98	1.04	52
1-METHYLADAMANTANE	11.34	-38.90	-40.57 \pm 0.34	1.67	6
2-METHYLADAMANTANE	12.91	-35.69	-35.66 \pm 0.62	-0.03	6
1,3,5,7-TETRAETHYLADAMANTANE	13.23	-67.05	-67.15 \pm 0.80	0.10	6
PROTODADAMANTANE	21.79	-19.45	-20.54 \pm 0.60	1.09	6
DIAMANTANE	17.69	-33.06	-32.60 \pm 0.58	-0.46	6
4-METHYLDIAMANTANE	17.33	-42.43	-43.53 \pm 0.30	1.10	6
3-METHYLDIAMANTANE	18.76	-39.31	-37.60 \pm 0.58	-1.71	6
1-METHYLDIAMANTANE	19.30	-40.46	-39.85 \pm 0.85	-0.61	6
PERHYDROTRICQUINACENE	17.77	-23.46	-24.47 \pm 0.86	1.01	35
BICYCLO(3.3.1)NONANE	11.08	-30.69	-30.46 \pm 0.55	-0.23	7
BICYCLO(3.3.2)DECANE	18.97	-28.08	-25.3 \pm 1.7	-2.78	7

TABLE 3(b). CALCULATED AND OBSERVED HEATS OF HYDROGENATION, $-\Delta H$, AND CALCULATED STERIC ENERGY DIFFERENCES (KCAL./MOL.)

COMPOUND	E_s	$-\Delta H$ CALC.	$-\Delta H$ OBS	$\Delta c-o$	REF.
CIS, CIS-1,5-CYCLOOCTADIENE \rightarrow	2.22	29.71	30.70 \pm 0.07	-0.99	8
CIS-CYCLOOCTENE					
CIS, CIS, CIS-1,4,7-CYCLONONA-	-2.76	52.22	53.26 \pm 0.06	-1.04	8
TRIENE \rightarrow CIS-CYCLONONENE					
CIS, CIS-1,6-CYCLODECADIENE \rightarrow	-4.31	23.18	23.06 ^c	0.12	8
CIS-CYCLODECENE					
TRANS, TRANS-1,6-CYCLODECA-	-4.55	22.94	23.62 ^c	-0.68	8
DIENE \rightarrow TRANS-CYCLODECENE					
TRANS, TRANS-1,6-CYCLODECA-	-7.28	47.70	47.63 ^c	0.07	8
DIENE \rightarrow CYCLODECANE					
CIS, CIS-1,6-CYCLODECA-	-9.46	45.52	43.73 ^c	1.79	8
DIENE \rightarrow CYCLODECANE					

STANDARD DEVIATION
OVER 60 COMPOUNDS

0.79

- a THE EXPERIMENTAL ΔH_f° INCLUDES 1KCAL./MOL. ADDED TO CORRECT FOR WORK DONE IN SOLUTION.
- b MEAN OF 3 EXPERIMENTAL HEAT OF FORMATION VALUES.
- c SAMPLE SUFFICIENT FOR ONE DETERMINATION ONLY OF THE DIENE
- $\Delta c-o = \Delta H_f^\circ(\text{GAS})_{\text{CALC.}} - \Delta H_f^\circ(\text{GAS})_{\text{OBS.}}$ IN THE HEAT OF FORMATION CASES.
- $\Delta c-o = -\Delta H_{\text{CALC.}} - (-\Delta H)_{\text{OBS.}}$ IN THE HEAT OF HYDROGENATION CASES.
- STANDARD DEVIATION FOR THE EXPERIMENTAL HEATS OF FORMATION ARE REPORTED WHEN THE INFORMATION IS AVAILABLE.

Table 4: Experimental and Calculated Structural Parameters

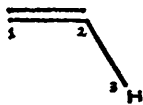
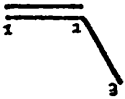
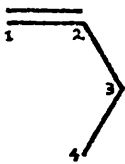
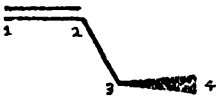
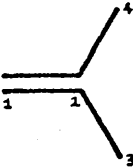
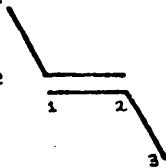
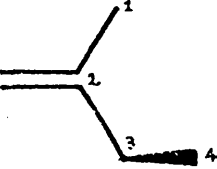
Compound	Structure		Expt	Calc.	Calc.- Expt	Ref.
Ethylene		ℓ_{12}	1.335	1.336	0.001	55
		ℓ_{23}	1.090	1.089	-0.001	
		θ_{123}	121.7	121.3	-0.4	
Propene		ℓ_{12}	1.336	1.337	0.001	56
		ℓ_{23}	1.501	1.505	0.004	
		θ_{123}	124.3	123.6	-0.7	
<u>cis</u> -1- Butene		θ_{123}	126.7	125.5	-1.2	18
		θ_{234}	114.8	115.4	0.6	
<u>skew</u> -1-Butene		θ_{123}	125.4	123.6	-1.7	18
		θ_{234}	112.1	111.5	-0.6	
Isobutene		θ_{423}	115.3	116.2	0.9	57
<u>trans</u> -2-Butene		ℓ_{23}	1.508	1.506	-0.002	22
		ℓ_{12}	1.347	1.338	-0.009	
		θ_{123}	123.8	123.6	-0.2	
2-Methyl- <u>skew</u> -1-Butene		ϕ_{1234}	72.7 ±5.0	71.5	-1.2	58

Table 4 (contd)

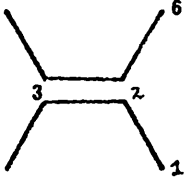
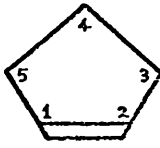
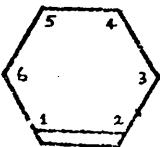
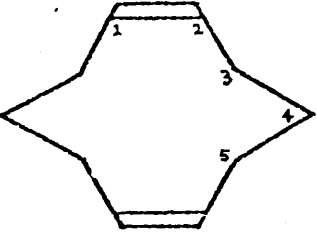
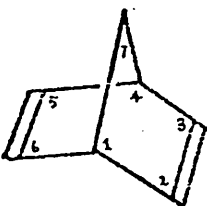
Compound	Structure		Expt	Calc.	Calc. - Expt	Ref.
2,3-Dimethyl- 2-Butene		ℓ_{12}	1.511	1.511	0.000	59
		ℓ_{23}	1.353	1.346	-0.007	
		θ_{12}	113.2	114.4	1.2	
Cyclopentene		ϕ_{1534}	156.7	160.9	4.2	60
Cyclohexene		ϕ_{1234}	-15.2	-15.3	-0.1	61
		ϕ_{2345}	44.9	45.4	0.5	
		ϕ_{3456}	-60.2	-62.2	-2.0	
<u>cis,cis</u> -1,6- Cyclodecadiene		ℓ_{12}	1.326	1.340	0.014	62
		ℓ_{23}	1.506	1.510	0.004	
		θ_{123}	128.2	127.0	-1.2	
		θ_{345}	114.1	113.6	-0.5	
		ϕ_{1234}	-114.7	-115.5	-0.8	
		ϕ_{2345}	58.2	59.5	1.3	
Norbornadiene		ℓ_{12}	1.535	1.510	-0.025	63, 4
		ℓ_{23}	1.343	1.337	-0.006	
		θ_{174}	94.1	94.3	0.2	
		$\langle \ell_{17} \rangle$	1.544	1.526	-0.018	
		ϕ_{2145}	115.6	116.3	0.7	

Table 4 (contd)

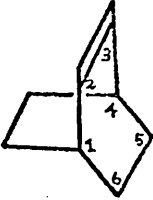
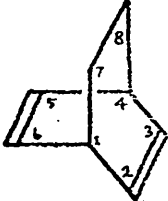
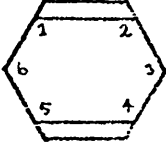
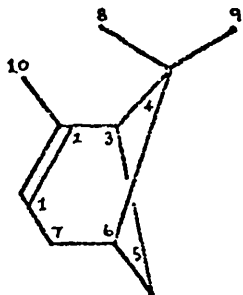

Compound	Structure		Expt	Calc.	Calc.- Expt	Ref
Bicyclo[2.2.2] Octene		ϕ_{6143}	121.2	120.4	-0.8	64
		ϕ_{1234}	0.0	0.0	0.0	
Bicyclo[2.2.2] Octadiene		ϕ_{2145}	123.4	123.4	0.0	64
		ϕ_{1784}	0.0	0.0	0.0	
1,4-Cyclohexadiene		χ_{12}	1.334	1.338	0.004	65
		χ_{16}	1.496	1.509	0.013	
		θ_{234}	113.3	113.2	-0.1	
		θ_{345}	123.5	123.4	0.1	
		ϕ_{1234}	0.0	0.0	0.0	
2-Pinene		χ_{12}	1.34	1.34	0.00	66
		θ_{176}	112 ± 3	108	-4	
		θ_{123}	118 ± 3	118	0	
		θ_{217}	118 ± 3	119	1	
		$\theta_{1,2,10}$	126	125	-1	
		ϕ_{4365}	146 ± 8	142	-4	
Cyclohexane		χ_{cc}	1.528	1.530	0.002	67, 68
		θ_{ccc}	111.3	111.3	0.0	
		ϕ_{cccc}	55.2	55.2	0.0	

Table 4 (contd)

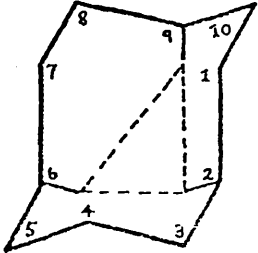
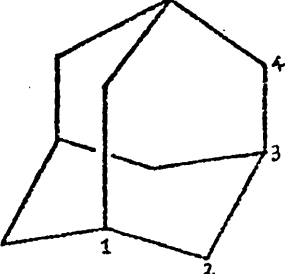
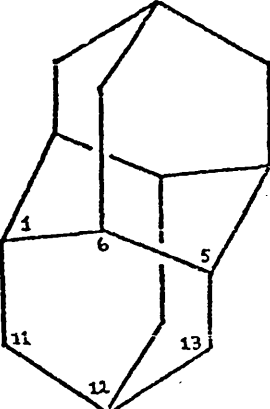
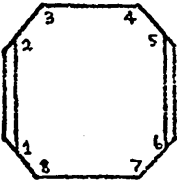
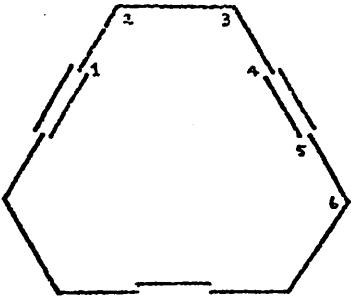
Compound	Structure		Expt	Calc.	Calc.- Expt	Ref.
Cyclodecane (C_{2h} average)		θ_{345}	118.0	117.9	-0.1	9, 31
		θ_{456}	118.1	117.6	-0.5	
		θ_{567}	114.7	114.9	0.2	
		$\phi_{10,1,2,3}$	-152	-152	0	
		ϕ_{1234}	55	55	0	
		ϕ_{2345}	66	68	2	
		$r(H6 \cdots H9)$	2.08	2.07	-0.01	
		$r(H2 \cdots H6)$	1.94	1.94	0.00	
Adamantane		θ_{123}	110.0	110.0	0.0	69
		θ_{234}	109.2	109.2	0.0	
		$\langle l_{CC} \rangle$	1.534	1.536	0.002	
Diamantane		$\langle l_{CC} \rangle$	1.535	1.537	0.002	70
		$\langle \theta_{CCC} \rangle$	109.5	109.4	-0.1	
		$\theta_{11,12,13}$	108.8	109.2	0.4	
		$\theta_{5,13,12}$	110.2	110.0	-0.2	
		$\theta_{6,5,13}$	110.2	109.9	-0.3	
		θ_{561}	108.7	109.0	0.3	

Table 4 (contd)

Compound	Structure		Expt	Calc.	Calc.- Expt	Ref
cis,cis-1,5-Cyclooctadiene		ℓ_{12}	1.341	1.340	-0.001	28, 71
		ℓ_{23}	1.502	1.512	0.010	
		ℓ_{34}	1.554	1.530	-0.024	
		θ_{123}	127.8	127.8	0.0	
		θ_{234}	116.8	115.8	-1.0	
		$r(C1 \cdots C5)$	3.30	3.39	0.09	
		$r(C1 \cdots C6)$	3.05	3.08	0.03	
		$r(C2 \cdots C6)$	3.32	3.31	-0.01	
		$r(C3 \cdots C7)$	3.82	3.81	-0.01	
		$r(C4 \cdots C7)$	3.19	3.19	0.00	
		$r(C4 \cdots C8)$	3.13	3.05	-0.08	
trans,trans,trans-1,5,9-Cyclododecatriene (D_3 average)		ℓ_{23}	1.54	1.53	-0.01	72
		ℓ_{34}	1.49	1.51	0.02	
		ℓ_{45}	1.32	1.34	0.02	
		θ_{234}	111.1	112.1	1.0	
		θ_{345}	124.1	123.5	-0.6	
		ϕ_{1234}	63.4	61.6	-1.8	
		ϕ_{2345}	-116.5	-115.0	1.5	
		ϕ_{3456}	178.0	177.9	-0.1	

ation which utilized numerical first and second derivatives. All compounds were minimised until $\partial V_s / \partial x$ was 10^{-8} kcal/mole \AA^{-1} .

2.3 Results and Discussion for compounds included in the Parametrization

(a) The Effect of non bonded H...H potentials on calculated molecular conformations and steric energies

Many different force field models have emerged since 1970^{1,2,3}. In general, they have reproduced geometric and thermodynamic properties of alkanes and alkenes in many instances and the results of different force fields are in fair agreement. These force fields, depending on the manner of the parametrization and the specific reason for the parametrization, contain a diverse balance of non-bonded potential functions superimposed on truncated valence force fields. Some workers^{1,11} have taken this to mean that differences between nonbonded potentials can be offset, in part at least, by suitable modification of the valence force field, whilst maintaining approximately spectroscopic values for the valence force constants.

During the parametrization of WBFF¹⁰, one interesting point that emerged was that the range of values that an acceptable choice of parameters for H...H function (and hence C...C, as the two are highly correlated) can assume is somewhat narrower and limited than previously believed and that, in fact, the first derivative of the H....H potential with respect to the internuclear separation should

not exceed $8 \text{ kcal mole}^{-1} \text{ \AA}^{-1}$ and the energy per H...H interaction at 2.0 \AA should not exceed $1.5 \text{ kcal mole}^{-1}$ ¹². Table 5 shows the values of the above functions calculated by eight force fields. Investigations ¹² have revealed that it is vital to employ an acceptable balance of forces between the different functions in the force field, otherwise the consequences can be serious - incorrect prediction of geometry, heats of formation, conformational energies (and hence minimum energy conformations) and incorrect interpretation of trends in molecular properties. These points will be illustrated in the following sections.

As an example of such defects, it is known that 1,1' - biadamantane has 6 short H...H contacts over the central bond and it has been found experimentally that the central bond ($\text{C1} - \text{C1}'$) is 1.578 \AA which is considerably longer than a $\text{Csp}^3 - \text{Csp}^3$ bond in an 'unstrained' molecule e.g. 1.533 \AA in propane. This stretching can be interpreted as a means of relieving the strain due to H...H contacts and hence a function of the hardness of the H...H potential used ¹¹. The harder the H...H potential used in a force field, the more the central bond length is overestimated. Allinger ¹⁷ and Schleyer ¹ calculate this bond length to be 1.617 \AA and 1.583 \AA respectively, the corresponding derivatives are 21.5 and $9.5 \text{ kcal mole}^{-1} \text{ \AA}^{-1}$, suggesting that the error increases rapidly with the value of the first derivative and that the H...H nonbonded potential in these two force fields are too 'hard'.

Table 5

The energy (kcal mol^{-1}) per H...H interaction at 2.0\AA , and its first derivative with respect to H...H distance ($\text{kcal mol}^{-1}\text{\AA}^{-1}$), for the potential function from a selection of current force fields.

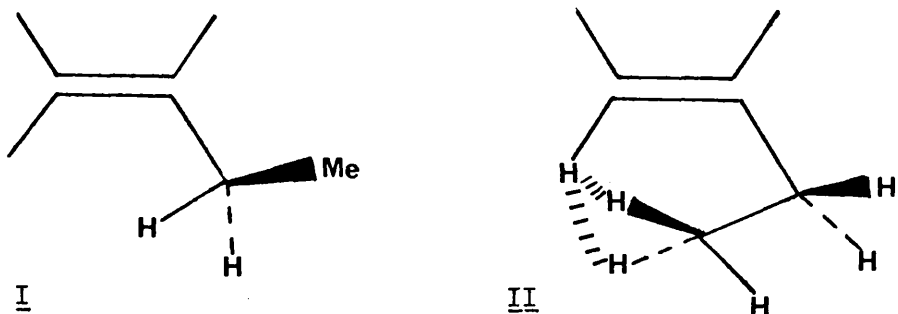
Force Field	V	dV/dr^a
Allinger and Sprague (2)	4.43	-21.49
Schleyer and co-workers (1)	2.26	-9.48
Ermer and Lifson (3)	1.32	-6.60
Bartell and co-workers (13)	1.12	-5.38
Montgomery and co-workers (14)	1.08	-5.10
Boyd and co-workers (15)	1.06	-4.31
Hendrickson (16)	0.95	-3.88
White and Bovill (10)	0.69	-3.05

^a

A direct measure of the "hardness" of the function.

(b) 1 - Butene

Two minimum energy conformations of 1-butene are the gauche form (I) and the eclipsed form (II).



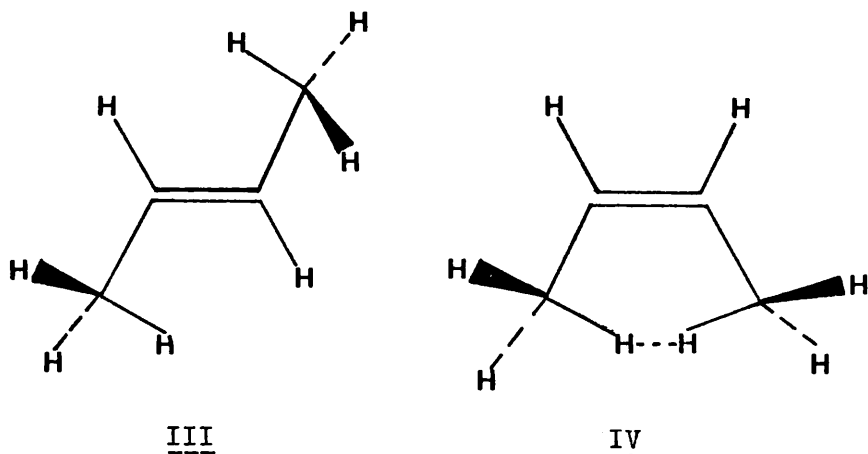
Experimental evidence implies that the two forms are of approximately the same energy^{18, 19}.

Force field calculations using Allinger's alkene force field (AFF)² and an extended version of Schleyer's alkane force field to deal with alkenes (SFF/E) overestimate the steric energy of the eclipsed form by over 1 kcal/mole. This is a direct consequence of using "hard" H...H potentials (see Table 5), which therefore exaggerate the two repulsive H...H interactions in the eclipsed form. The WBFF, on the other hand, calculates the gauche form (I) to be more stable than the eclipsed form (II) by only 0.6 kcal/mole, which is equivalent to a 70%:30% mixture.

(c) 2 - Butene

The most stable conformation of propene has a methyl hydrogen eclipsing the double bond, and two such eclipsing interactions are present in trans-2-butene (III), which is essentially strainfree with respect to steric interference between the hydrogen atoms. However in cis-2-butene (IV) maintenance of two such eclipsing interactions would place nonbonded hydrogens only 1.80 Å apart in an ideal geometry.

Thus potentially destabilising interaction is, in large measure, relieved by opening of the $C=C-C_{sp^3}$ and $H-C_{sp^3}-C_{sp^2}$ angles. The strain in cis-2-butene relative to trans is found experimentally to be only 1.24 kcal/mole²⁰. According to the microwave spectrum²¹, cis-2-butene possesses C_{2v} -symmetry with eclipsed methyl groups.



Overestimation of $H...H$ interactions, in this case, has three consequences; the cis/trans energy difference is calculated to be too high, the $C=C-C$ valency angles too large in the cis isomer and possibly an incorrect prediction of the symmetry of the cis isomer. The enthalpy difference may be corrected by the inclusion of a small one-fold component in the term which describes the torsion around the double bond², but the geometry can only be improved by revision of the $H...H$ potential. Force field calculations on cis- and trans-2-butene have been performed using AFF, SFF/E and WBFF and the results are tabulated in Table 6, which endorses the opinion that the $H...H$ potentials in AFF and SFF/E are 'hard' compared to the 'softer' potentials in WBFF, which gives a better representation of 2-butene. Furthermore, AFF calculated a molecular C_2 -symmetry with methyl groups twisted out of the eclipsed

Table 6

Calculated enthalpies of isomerisation for 2-butene and
C=C-C_{sp}³ valency angles for cis-2-butene.

	$\Delta \Delta H_{c/t}$	$\theta \text{ c=c-c}$
Experiment	1.20 ²⁰	125.4 ²² , 126.7 ²¹
^a AFF(2)	1.84	127.9
^a SFF/E	1.86	128.2
WBFF(10)	1.30	127.1

^aThe constribution due to the one-fold barrier around
C=C has been discounted for purposes of comparison.

Units of enthalpy difference is kcal/mole.

position by 8.6° , whereas WBFF predict the correct molecular symmetry (C_{2v}). The incorrect prediction of molecular symmetry by AFF, may be due, in part, to the incomplete convergence of the minimisation²³. The geometry calculated by WBFF is shown in Figure 1.

(d) cis, cis - Cyclo octa - 1,5 - diene (1,5 - COD)

Conformational interconversions of 1,5 - COD were first studied experimentally by Anet using the dynamic NMR method²⁴ and then theoretically by Anet²⁵, Allinger²⁶ and Ermer²⁷ using molecular mechanics calculations. This topic will be discussed in Chapter 3.

The minimum energy conformation of 1,5 -COD has been shown by spectroscopic²⁴ and diffraction^{28,29} studies and by molecular mechanics calculations^{10,25,26,27,30} to be unequivocally a C_2 symmetric twist boat, but the calculated degree of twist (i.e. the $Csp^2-Csp^3-Csp^3-Csp^2$ torsion angle) varies from 27° to 55° depending on which force field is used. This is not altogether surprising as the value of the degree of twist depends largely on the hydrogens on C4 and C8 as can be seen from Fig. 2. As the degree of twist is increased from 0° (corresponds to a C_{2v} boat conformation) upwards, the two hydrogen move closer together until a limiting value is reached where the decrease in torsional strain is offset by the increase in steric compression. The "harder" the H...H potential employed, the sooner this limiting value will be reached.

Figure 1: The calculated structure of cis-2-butene (C_{2v} symmetry).

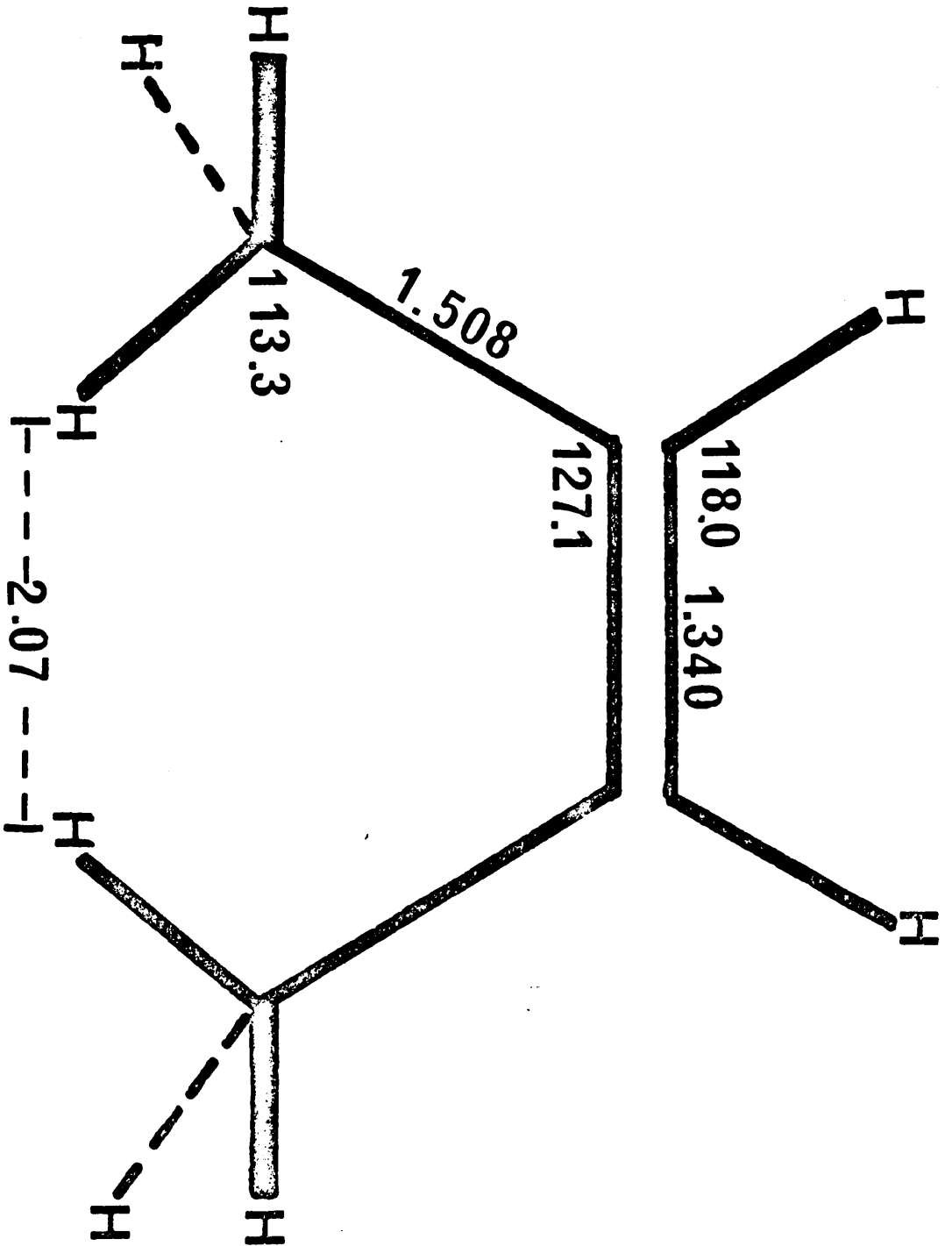


Figure 2: The calculated twist-boat conformation of
cis,cis-cycloocta-1,5-diene (C_2 symmetry).

AFF, SFF/E and WBFF calculate the degree of twist to be 38° , 50° and 52° respectively. X-ray crystal structure analysis²⁹ of a dibromo derivative and an electron diffraction study²⁸ of 1,5 - COD give experimental values of 65° and 45° respectively. Thus again confirmation is obtained that the H...H potentials employed by Allinger are much too 'hard'. The degree of twist and geometry calculated by the WBFF is in excellent agreement with the geometry obtained from the electron diffraction results (see Figure 2 and Table 4).

(e) Cyclodecane

Cyclodecane and many of its derivatives have been studied extensively by X-ray³¹ and neutron diffraction analysis⁹ and by IR/Raman spectroscopy³². All these studies point to the fact that the preferred conformation in the solid, liquid and gaseous states, is the boat-chair-boat (BCB) conformation. This is confirmed by molecular mechanics calculations in most cases - the WBFF calculates the BCB conformation to be the minimum energy conformation, which is 0.5 kcal/mole more stable than the next lowest conformation, the TCCC (T stands for "twisted"). However, only AFF and SFF calculate the TCCC to be the preferred minimum energy conformation by 1.7 and 0.6 kcal mole⁻¹ respectively over the BCB, which would contradict both the vast body of experimental data and other molecular mechanics calculations.

The neutron-diffraction study⁹ indicated that the preferred conformation, the ECB, possesses six short transannular H...H distances ($< 2.0\text{\AA}$) (see Table 4), which will therefore be a major contributor to the strain energy. The TCCC does have some transannular interactions but the H...H distances are longer and energy due to them less repulsive. This implies that if 'hard' H...H potentials, i.e. potentials which overestimate the repulsive term, are used, the contribution by the six short H...H interactions to the steric energy of the ECB is overestimated and as a consequence, the TCCC is predicted to be more stable than ECB. Since the latter six force fields in Table 5 correctly predict the ECB as the minimum energy conformation of cyclodecane, the validity of the limiting values for H...H potential functions, discussed in (a), is endorsed.

A recent electron diffraction study, by Montgomery¹⁴, revealed that gaseous cyclodecane at 130°C consists of a mixture of 49% ECB, 35% TBC, 8% TBCC and 8% BCC. Force fields calculations with WBFF, were performed on six conformations - the four conformation mentioned above, the TCCC and a low energy conformation, TCTC³⁴, which had not appeared to have been studied previously - Hendrickson¹⁶ and Ermer³³ only consider conformations in which the symmetry elements pass through atoms, the TCTC has, however, a two-fold axis which passes through the centre of the ring. The steric energy, relative to the ECB, and torsion angles calculated by the WBFF, for the six

FIGURE 3. TORSION ANGLES (DEG) AND STERIC ENERGIES RELATIVE TO THE BCB CONFORMATION (KCAL./MOLE) FOR SOME LOW-ENERGY CONFORMATIONS OF CYCLODECANE

TORSION ANGLES	BCB	TCCC	TBC	TBCC	BCC	TCTC
1,2,3,4	-55	-145	79	-65	-61	-55
2,3,4,5	-68	86	-70	-58	-73	96
3,4,5,6	68	-70	-70	131	61	-111
4,5,6,7	55	86	79	-68	52	150
5,6,7,8	-152	-145	60	-65	-142	-55
6,7,8,9	55	145	-138	151	133	-55
7,8,9,10	68	-86	53	-98	-87	96
8,9,10,1	-68	70	53	57	65	-111
9,10,1,2	-55	-86	-138	-98	-92	150
10,1,2,3	152	145	60	151	155	-55
Vs	0,00	0,48	0,52	0,61	0,66	2,41
SYMMETRY	C _{2h}	C _{2h}	C ₂	C ₂	-	C ₂

conformations are given in Figure 3. All six conformations were found to correspond to true minima in contrast to Ermer's finding that some were only partial minima³³. The calculations confirm that the BCB is the conformation of lowest energy out of the six and show that there is a correlation between the relative steric energy and the percentage of the four conformations, found in the electron diffraction study. In addition, the geometry calculated by the WBFF for the BCB closely mirrors that found in the accurate neutron diffraction study of trans-1,6-cyclodecanediol⁹(see Table 4).

(f) Polycyclic Alkanes

Experimental work on polycyclic alkanes^{6,35} has revealed certain deficiencies in some current parametrizations which in part has been attributed to "an undue emphasis on the repulsive nature of H...H interactions". Professor P. von R. Schleyer⁵ has reported a list of polycyclic hydrocarbons whose heats of formation are poorly reproduced by the AFF and SFF (see Table 7) The WBFF was subsequently applied to the same group of compounds and the mean deviation between the calculated and experimental heats of formation is 0.98 kcal/mole, which represents a considerable improvement over the corresponding values of 2.23 and 3.12 kcal/mole obtained by the SFF and AFF. However, the calculated heat of formation for manxane, by the WBFF, differs from the reported experimental value by about 6 kcal/mole, more than twice any of the other deviations, which, together with the fact that SFF's is in "error" by 4 kcal/mole, would perhaps cast some doubt on the accuracy of the

TABLE 2. HEATS OF FORMATION OF POLYCYCLIC ALKANES

MOLECULE	ΔH_f° (GAS) OBS.	Δ (SFF)	Δ (AFF)	Δ (WBFF)	REF.
ADAMANTANE	-31.76 \pm 0.32	-0.74	-2.06	1.04	6
	-30.65 \pm 0.57 ^b				
	-32.96 ^c				
1-MEADAMANTANE	-40.57 \pm 0.34	-1.25	-2.32	1.67	6
2-MEADAMANTANE	-35.66 \pm 0.62	-2.28	-3.38	-0.03	6
1,3,5,7-TETRAHEADAMANTANE	-67.15 \pm 0.80	-3.11	-3.06	0.10	6
PROTODAMANTANE	-20.54 \pm 0.60	-0.59	-2.09	1.09	6
DIAMANTANE	-32.60 \pm 0.58	-4.77	-5.53	-0.46	6
4-MEDIAMANTANE	-43.53 \pm 0.30	-3.29	-3.68	1.10	6
3-MEDIAMANTANE	-37.60 \pm 0.58	-5.31	-5.75	-1.71	6
1-MEDIAMANTANE	-39.85 \pm 0.85	-3.71	-4.58	-0.61	6
PERHYDROTRIQUINACENE	-24.47 \pm 0.86	0.73	4.73	1.01	35
BICYCLO(3.3.1)NONANE	-30.46 \pm 0.55	0.09	-0.18	-0.23	7
BICYCLO(3.3.2)DECANE	-25.3 \pm 1.7	-0.87	0.1	-2.78	7
MEAN DEVIATION		2.23	3.12	0.98	

$\Delta = \Delta H_f^\circ$ (GAS), CALC. - ΔH_f° (GAS) OBS.

a. REF. 52

b. REF. 73

c. REF. 74

AFF ALLINGER'S FORCE FIELD

SFF SCHLEYER'S FORCE FIELD

WBFF WHITE-BOVILL'S FORCE FIELD

ENERGIES ARE IN KCAL/MOL

experimental heat of formation.

Schleyer has also reported that AFF and SFF force fields predict 2, 4 and 2,8 - ethano-noradamantane to be isoenergetic, whereas in fact the former is the stablomer by about 1.5 kcal/mole³⁶. Our calculations (WBFF) correctly indicate the 2, 4 - isomer as the minimum energy isomer but the enthalpy difference is underestimated at 0.5 kcal/mole.

2.4 Some applications of the WBFF

Applications of the WBFF to medium ring and other cyclic compounds will be discussed in Chapter 3.

(a) n-Butane

n - Butane has three conformers, two of which are mirror images of each other and are known as the "gauche" or "skew" conformations and one, more stable by about 0.6 kcal/mole than either gauche conformational isomer, which is known as the "trans" or "anti" conformation.

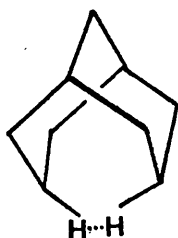
Recently, there has been some controversy over the explanation for the gauche destabilization. The conventional interpretation³⁷ is that the gauche instability can be largely attributed to 1...6 hydrogen repulsions between gauche methyl or methylene groups with a small contribution from the 1...4 hydrogen interactions about the central bond. Allinger's "gauche-hydrogen hypothesis"³⁸, on the

other hand, assigns 60% of the calculated enthalpy difference between gauche- and anti- butane to the 1...4 gauche-hydrogen interaction and claims that this interpretation is independent of the exact parametrization of the force field.

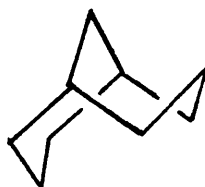
This hypothesis has been discounted on both points by various workers^{12,39,40} as alternative force field calculations with "softer" H...H potentials than AFF estimate the 1...4 H interaction contribution to be relatively minor at 24%³⁹ and 19%¹⁰. This hypothesis would therefore seem to depend strongly on the choice of nonbonded potentials, particularly the H...H potential and the balance of forces in the different force fields, so that although the overall results of different force fields agree fairly well, the individual components of the steric energy to differ significantly, as seen above. The interpretation of molecular properties, on the basis of the partitioning of the calculated steric energy, requires extreme caution, particularly when the force field is known to have faults and if organic chemists are to have faith in molecular mechanics calculations.

(b) Bicyclo (3.3.1) nonane

A recent gas phase electron diffraction study⁴¹ of bicyclo (3.3.1) nonane found that a twin-chair conformation (V) gives the best agreement with the intensity and radial distribution curves. The six-membered rings show a drastic



V



VI

flattening which is probably due to the C(3) - C(7) methylene nonbonded interactions since twinned ideal cyclohexane rings with tetrahedral valency angles would have a H...H separation of 0.75Å. X-ray studies of derivatives of bicyclo (3.3.1) nonane reveal that the ring system can adopt both a twin-chair (V) and a chair-boat (VI) conformation and that the twin-chair conformations show a similar flattening with the H...H separation at C(3), C(7) methylene groups being estimated at between 1.7Å - 2.0Å for the various studies. A twin-chair conformation is usually adopted when there are no endo substituents on positions 3 and 7⁴², whereas a chair-boat conformation, in which the H3...H7 interaction is absent but the familiar "bowsprit-flagpole interaction" and eclipsed hydrogen interaction of the cyclohexane boat are present, is usually adopted where there are bulky substituents at either or both these positions⁴³. From an inspection of the torsion angles in derivatives which have sp³-hybridised atoms at positions 2, 3, 4 and

6,7,8 it can be deduced that the flattening in the twin-chair conformations is effected by displacements of atoms 3 and 7 essentially parallel to the plane through 3,7,9 so that there is no skewing of the rings, which is observed when sp^2 -hybridised atoms are present at any of these positions. Equilibration experiments indicate that the twin-chair conformation is more stable than the chair boat by about 3 kcal mole⁻¹ ⁴⁴. This is supported by low temperature dynamic ¹³C NMR studies which furnish a limit for the free energy difference between the two conformations as being ≥ 1.40 kcal/mole⁴⁵.

The bicyclo (3.3.1) nonane systems has been investigated using molecular mechanics calculations by AFF¹⁷, SFF¹, and WBFF¹⁰, and from the foregoing discussion, it is obvious that the choice of the H...H potential used in each force field will strongly influence the reliability of the calculated geometry and steric energy of the two conformations. AFF, which employs 'hard' H...H potentials, calculate the H3...H7 separation to be 2.15Å and the enthalpy difference between the twin-chair and chair-boat conformations to be 1.24 kcal/mole, whereas the WBFF which uses "softer" H...H potentials, calculates the separation to be 1.97Å and the enthalpy difference to be 2.89 kcal/mole which are in much better agreement with the experimental values (estimated to be 1.7Å-2.0Å and 3 kcal/mole). AFF's value of 2.15Å is much too long as the corresponding distance in 9-thia bicyclo (3.3.1)-nonane-2,6-dione (a compound in which the rings in the twin-chair conformation

are skewed) is 2.07\AA ⁴⁶.

The calculated ring torsion angles for the twin-chair conformation are compared with those from an X-ray crystal structure analysis of bis-9-borabicyclo(3.3.1) - nonane⁴⁷ in Figure 4 and the calculated ring torsion angles for the boat-chair conformation are compared with those from an X-ray crystal structure analysis of 3-bromo-9-benzoyl-9-azabicyclo (3.3.1) nonane-2-one⁴³ in Figure 5.

(c) Sterically crowded double bonds

When four groups attached to an olefinic linkage deviate significantly from coplanarity with the trigonal centres, the Π -bond is weakened due to poor overlap. Such distortions may be induced by constraining the double bond in certain cyclic, bicyclic or polycyclic systems or in the presence of crowded bulky substituents. This weakening in the Π -bond can be detected by the low olefinic vibrational frequency and long ultraviolet absorption wavelength.

This seemed a good area to test the applicability of the WBFF, as it produced reliable results for 1-butene and 2-butene, where the double bonds are sterically crowded. Repulsive nonbonded interactions which result from steric crowding across a double bond may, in principle, be relieved by bond stretching, valence angle deformation and the twist of the central bond.

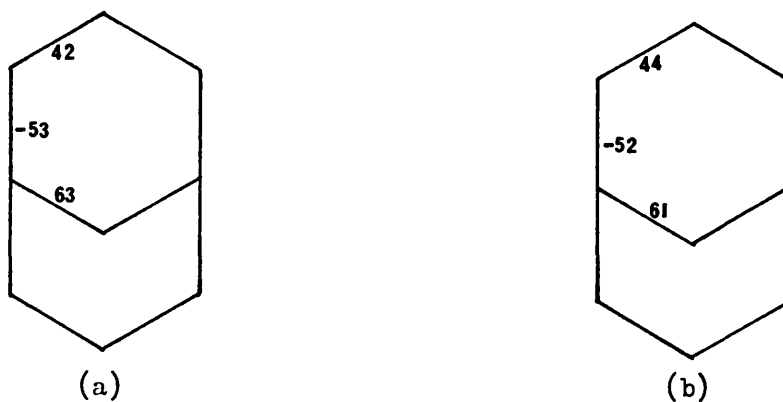


Figure 4: The calculated ring torsion angles (a) of the twin-chair conformation of bicyclo(3.3.1)nonane compared with the C_{2V} averaged experimental values of bis-9-borabicyclo(3.3.1)nonane (b).

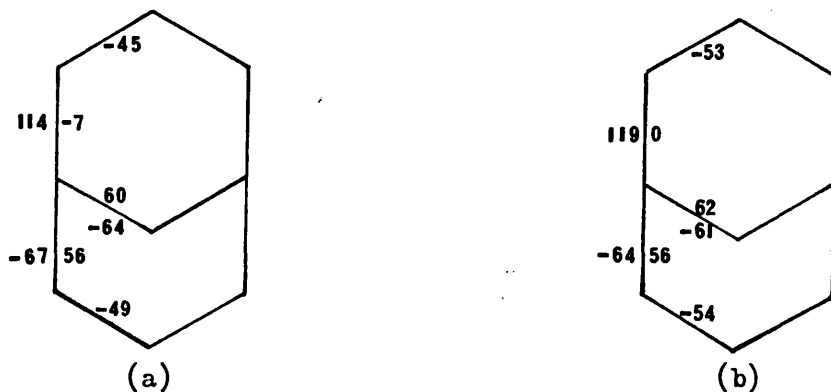
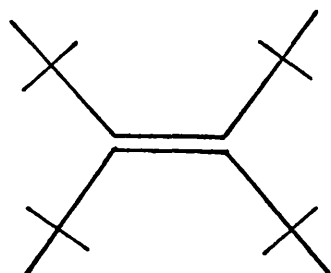


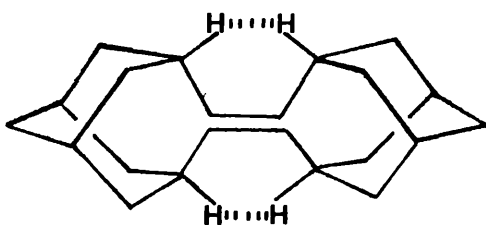
Figure 5: The calculated ring torsion angles(a) of the boat-chair conformation of bicyclo(3.3.1)nonane compared with the C_s averaged experimental values of 3-bromo-9-benzoyl-9-azabicyclo(3.3.1)nonane-2-one (b).



VII

Tetra-tert-butylethylene (VII) has not yet been reported but it may be expected that steric repulsion might be alleviated by a totally unrealistic stretch of the double bond or by substantial torsion. Calculations³ suggest a 75° twist which would thus give this compound substantial diradical character.

One compound which has been studied by spectroscopy⁴⁸ is biadamantylidene (VIII). This compound exhibits a planar double bond in spite of the presence of significantly repulsive nonbonded hydrogen interactions. Molecular mechanics calculations, with WBFF, were in excellent



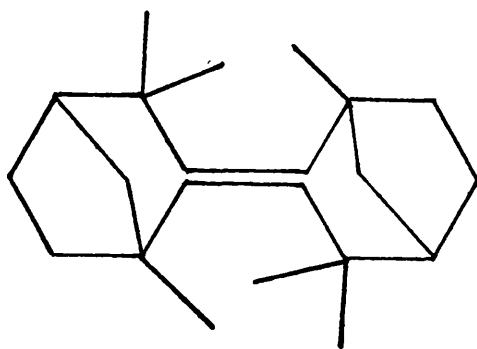
VIII

agreement with this observation - the calculated olefinic torsional angle was 0° - and the hydrogens were found to eclipse the double bond. The calculated steric energy, V_s , was only 24.00 kcal/mole, which indicates that the compound has about the same strain as 5-ethylidenenorbornene and which is about twice the steric energy of adamantane (11.34 kcal/mole). The central bond lengthening

is not very strong - 1.349\AA as compared to 1.335\AA in ethylene - and the $\text{Csp}^2 - \text{Csp}^3$ is 1.523\AA compared 1.501\AA in propene. The $\text{C} = \text{C} - \text{Csp}^2$ valency angle is only 123.6° and, as a result, the $\text{H} \dots \text{H}$ distance is only 1.87\AA . The rigid adamantane rings, in VIII, are not substantially different from an isolated adamantane molecule. These results indicate that the steric crowding in biadamantylidene is relieved mostly by bond stretching alone.

Opening of the $\text{C} = \text{C} - \text{Csp}^3$ valency angle to about 127° , as in cis-2-butene, would severely distort the preferred geometry of the adamantane rings and twisting about the double bond would minimise the $\text{H} \dots \text{H}$ interactions across the rings but would aggravate other repulsive nonbonded interactions and result in a weakening of the Π -bond.

An X-ray study of syn-bis-2,2¹-fenchylid-ene-E (IX) has been reported by Simonetta⁴⁹. There is considerable



IX

steric hindrance in this molecule as a result of the nonbonded interactions which arise from the presence of the six methyl groups about the double bond. Molecular mechanics calculations have been used to investigate this

molecule in an attempt to understand how the steric hindrance effects the molecular geometry and energy.

The steric energy, V_s , of this molecule is calculated to be 63.75 kcal/mole which indicates that the molecule is highly strained much of which is due to Baeyer strain.

Calculations indicate that the steric hindrance causes a slight deformation in the central bond length (1.360\AA) and a slightly larger deformation in the $\text{Csp}^2\text{-Csp}^3$ bond (1.534\AA). The valency angles are also adjusted to minimise the nonbonded interactions between the methyl groups. The C=C-Csp^3 valency angles are opened to 126.0° and 126.8° with the $\text{Csp}^2\text{-Csp}^3\text{-Csp}^3$ angle differing significantly from their equilibrium (109.5°) value - those involving the carbon with a single methyl group are observed to be 123.4° while the other four angles associated with the carbons which each bear two methyl groups have the average value of 115.8° . The olefinic torsional angle is observed to be 11.8° in the crystal. This is similar to the value of 15.3° calculated by the WBFF, but is significantly different from the value of 24° calculated by AFF. This supports the view that the AFF uses $\text{H}\dots\text{H}$ potentials which are unacceptably 'hard'. These deformations result in the shortest 1-6 contacts between the methyl groups being 3.10\AA and the longer ones being 3.44\AA .

It is interesting to note that Allinger has recently upgraded his 1972 force field^{2,75}. This was accomplished by the inclusion of one-fold and two-fold barriers in the torsional potentials with the result that the new H...H potential was made softer and smaller. As expected, the reliability of the force field is greatly improved. The standard deviation between the calculated and experimental heats of formation of 42 hydrocarbons is 0.42 kcal/mole. The new force field, in contrast to the old one, correctly predicts the BCB as the minimum energy conformation of cyclodecane. In addition, he also retracts his "gauche-hydrogen hypothesis"³⁸, but at the same time, does not accept the conventional explanations³⁷.

2.5 References

1. E.M. Engler, J.D. Andose and P. von R. Schleyer, J. Amer. Chem. Soc., 95, 8005 (1973)
2. N.L. Allinger, and J.T. Sprague, J. Amer. Chem. Soc., 94, 5734 (1972).
3. O. Ermer and S. Lifson, J. Amer. Chem. Soc., 95, 4121 (1973).
4. G. Buemi, F. Zuccarello and G. Favini, J. Mol. Struct., 21, 41 (1974).
5. P. von R. Schleyer, Private Communication.
6. T. Clark, T. McO. Knox, H. Mackle, M.A. McKervery and J.J. Rooney, J. Amer. Chem. Soc., 97, 3835 (1975)
7. W. Parker, W.V. Steele and I. Watt, submitted to J. Chem. Soc., Faraday
8. R.B. Turner, B.J. Mallon, M. Tichy, W. von E. Doering, W.R. Roth and G. Schroder, J. Amer. Chem. Soc., 95, 8605 (1973).
9. O. Ermer, J.D. Dunitz and I. Bernal, Acta Cryst., B29, 2278 (1973).
10. D.N.J. White and M.J. Bovill, J. Chem. Soc. Perkin Trans. 2, (in print).
11. C. Altona and D.H. Faber, Top. Curr. Chem., 45, 1 (1974).
12. D.N.J. White and M.J. Bovill, J. Mol. Struct., 33, 272 (1976)
13. E.J. Jacob, H.B. Thompson and L.S. Bartell, J. Chem. Phys., 47, 3736 (1967)
14. R.L. Hilderbrandt, J.D. Wieser and L.K. Montgomery, J. Amer. Chem. Soc., 95, 8598 (1973).

15. S. Chang, D. McNally, S. Shary-Tehrany, M.J. Hickey and R.H. Boyd, J. Amer. Chem. Soc., 92, 3109 (1970)
16. J.B. Hendrickson, J. Amer. Chem. Soc., 89, 7036, 7043, 7047 (1967).
17. N.L. Allinger, M.T. Tribble, M.A. Miller and D.H. Wertz, J. Amer. Chem. Soc., 93, 1637 (1971).
18. S. Kondo, E. Hirota and Y. Morino, J. Mol. Spectrosc., 28, 471 (1968).
19. A.A. Bothner - By, C. Naar-Colin and H. Gunther, J. Amer. Chem. Soc., 84, 2748 (1962).
20. D.R. Stull, E.F. Westrum Jr., and G.C. Sinke, "The Chemical Thermodynamics of Organic Compounds", Wiley, New York, N.Y., 1969.
21. S. Kondo, E. Hirota and Y. Morino, J. Mol. Spectrosc., 34, 231 (1970).
22. A. Almenmgen, L.M. Anfinsen and A. Haaland, Acta Chem. Scand., 24, 43 (1970)
23. D.N.J. White and O. Ermer, Chem. Phys. Lett., 31, 111 (1975).
24. F.A.L. Anet and L. Kozerski, J. Amer. Chem. Soc., 95, 3407 (1973).
25. F.A.L. Anet and R. Anet in Dynamic Nuclear Magnetic Resonance Spectroscopy, F.A. Cotton and L.M. Jackson, Ed., Academic Press, New York, p. 571 (1975).
26. N.L. Allinger and J.T. Sprague, Tetrahedron, 31, 21 (1975).
27. O. Ermer, J. Amer. Chem. Soc., 98, 3964 (1976).
28. L. Hedberg and K. Hedberg, Abs. Papers, Nat. Meeting Amer. Cryst. Ass., 1964, Bozeman, Montana.

29. R.K. MacKenzie, D.D. MacNicol, H.H. Mills, R.A. Raphael, F.B. Wilson and J.A. Zabkiewicz, J. Chem Soc., Perkin II, 1632 (1972).
30. G. Favini, F. Zuccarello and G. Buemi, J. Mol. Struct., 3, 385 (1969).
31. For a review see J.D. Dunitz, in J.D. Dunitz and J.A. Ibers (Eds.), Perspective in Structural Chemistry, No. 2, Wiley, New York, 1968, p.7.
32. R. Billeter and H.H. Gunthard, Helv. Chim. Acta., 41, 338 and 686 (1958).
33. O. Ermer, Structure and Bonding, 27, 1 (1976).
34. D.N.J. White and M.J. Bovill, Acta Cryst., B (in print).
35. T. Clark, T. McO. Knox, H. Mackie and M.A. McKervey, Chem. Comm., 666 (1975).
36. S.A. Godleski and P. von R. Schleyer, Chem. Comm., 38 (1976).
37. E.L. Eliel, N.L. Allinger, S.J. Angyal and G.A. Morrison, Conformational Analysis, Wiley-Interscience, New York, N.Y., 1965, p.13.
38. D.H. Wertz and N.L. Allinger, Tetrahedron, 30, 1579, (1974).
39. R.H. Boyd, J. Amer. Chem. Soc., 97, 5353 (1975)
(note ref. 19)
40. S. Fitzwater and S. Bartell, J. Amer. Chem. Soc., 98, 5107 (1976).
41. E.L. Osma, V.S. Mastryukov, L.V. Vilkov and N.A. Belikova, J. Chem. Soc., Chem Comm., 13 (1976)

42. W.A.C. Brown, G. Eglinton, J. Martin, W. Parker and G.A. Sim, Proc. Chem. Soc., 57 (1964)
43. P.D. Cradwick and G.A. Sim, J. Chem. Soc.(B), 2213(1971).
44. E.N. Marvell and R.S. Knutson, J. Org. Chem., 35, 388 (1970).
45. H.J. Schneider, Org. Mag. Res., 8, 363 (1976)
46. M.J. Bovill, P.J. Cox, H.P. Flitman, M.H.P. Guy, A.D.U. Hardy, G.A. Sim, D.N.J. White, Acta Cryst(B), in preparation.
47. D.J. Brauer and C. Kruger, Acta Cryst. B29, 1684(1973).
48. J.H. Wieringa, J. Strating, H. Wynberg and W. Adam, Tetrahedron, 28, 169 (1972).
49. M. Simonetta, private communication.
50. J.D. Cox and G. Pilcher, "Thermochemistry of Organic and Organometallic Compounds", Academic Press, New York, N.Y., (1970)
51. S.W. Benson, F.R. Cruickshank, D.M. Golden, G.R. Haugen, H.E. O'Neal, A.S. Rodgers, R. Shaw and R. Walsh, Chem. Rev., 69, 279 (1969).
52. R.H. Boyd, S.N. Sanwai, S. Shary-Tehrany and D. McNally, J. Phys. Chem., 75, 1264 (1971).
53. R. Walsh and J.M. Wells, J. Chem. Therm., 7, 149(1975).
54. M.P. Kozina, L.P. Timofeeva, the late S.M. Skuratov, N.A. Belikova, E.M. Milvitskaya and A.F. Plate, J. Chem. Therm., 3, 563 (1971).
55. K. Kuchitsu, J. Chem. Phys., 44, 906 (1966).
56. D.R. Lide and D. Christensen, J. Chem. Phys., 35, 1374 (1961).

57. L.H. Scharpen and V.W. Laurie, J. Chem. Phys., 39,
1732 (1963).
58. T. Shimanouchi, Y. Abe and K. Kuchitsu, J. Mol. Struct.,
2, 82 (1968).
59. I. Tokue, T. Fukuyama and K. Kuchitsu, J. Mol. Struct.,
23, 33 (1974).
60. J. Laane and R.C. Lord, J. Chem. Phys., 47, 4941 (1967)
61. J.F. Chiang and S.H. Bauer, J. Amer. Chem. Soc., 91,
1898 (1969).
62. A. Almenningen, G.G. Jacobsen and H.M. Seip, Acta
Chem. Scand., 23, 1495, (1969)
63. A. Yokozeki and K. Kochitsu, Bull. Chem. Soc., Japan,
44, 2356 (1971).
64. A. Yokozeki and K. Kochitsu, Bull. Chem. Soc., Japan,
44, 1783 (1971).
65. G. Dallinga and L.H. Toneman, J. Mol. Struct., 1,
117 (1967).
66. B.A. Arbuzov and V.A. Naumov, Doklady Akad Nauk S.S.S.R.,
158, 376 (1964).
67. H.J. Geise, H.R. Buys and F.C. Mijlhoff, J. Mol. Struct.,
9, 447 (1971).
68. M. Davis and O. Hassel, Acta Chem. Scand., 17, 1181 (1970)

CHAPTER THREE

Application of the White-Bovill force field (WBFF)

to the conformational analysis of

cyclic hydrocarbons, C₆-C₁₂

3.1. Introduction

Conformational analysis could profitably utilize more detailed knowledge of the relationship between conformational structure and energy. Molecular mechanics (MM) calculations supply this information and, in addition, predict properties of unobservable conformation, e.g. transition states.

It is usual to classify carbocyclic rings as follows:

small	3,4
"normal"	5,6,7
medium	8,9,10,11
large	11

The strain energies and geometries of cyclenes, with one double bond in the ring, ranging from C_6 - C_{10} and with two double bonds in the ring, ranging from C_8 - C_{10} have been calculated using the White-Bovill Force Field (WBFF), which was described in Chapter 2. In the parametrization of the WBFF*, use was made of what experimental data was available for medium ring compounds, which most of the study will be concerned with and which had been largely neglected in the parametrization of other force fields. It was therefore possible to place a certain degree of confidence in our results from the investigation of the plethora of conformations and transannular interactions exhibited by medium rings.

*The WBFF produced extremely reliable results for geometries, heats of formation and heats of hydrogenation of a number of medium ring compounds.

Combustion measurements allow an estimate to be made of the total strain in cycloalkanes relative to acyclic alkanes which are assumed to be strain-free.¹ All rings, except cyclohexane, have higher heats of combustion per methylene group, and the estimated total strain per mole is given below.

RING SIZE (n)	5	6	7	8	9	10	11	12	13	14
ESTIMATED TOTAL STRAIN (k cal. 1 mole)	7	0	6	10	13	12	12	4	5	0

The medium rings thus possess a special conformational situation in that they have more strain than the "normal" and large rings. On the basis of information from spectroscopic and X-ray diffraction and from inspection of molecular model, we can anticipate 3 types of strain in medium rings.

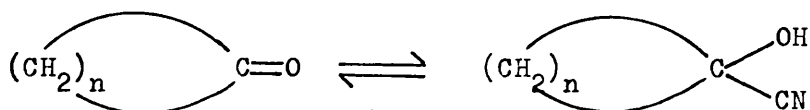
1. Transannular Strain, which is due to crowding of atoms, usually hydrogens, across the ring. In cyclodecane, the major contribution to the strain energy of the BCB conformation arises from six very short H H contacts which lie on the repulsive portion of the Van der Waals curve.
2. Pitzer Strain, is due to the existence of eclipsed conformations, e.g. in cyclodecane, there are 2 anti- and 8 gauche - butane interactions.
3. Baeyer or Angle Strain, e.g. in cyclodecane, the $C_{sp^3} - C_{sp^3} - C_{sp^3}$ angles are increased to a mean value of 117° to minimise Pitzer and transannular strain since valence angle deformation is energetically "cheap".

We also might anticipate that the conversion of sp^3 to sp^2 hybridization at one or more carbon atom is favoured

in some of these systems because the sp^2 configuration has a smaller number of C-H bonds than the sp^3 configuration and thus leads to a reduction in strain, due in part to the proximity of substituents on opposite sides of the rings and to bond oppositions. However, changes of bond hybridization may produce concomitant changes in angle strain and/or transannular strain. These changes may be either favourable or unfavourable.

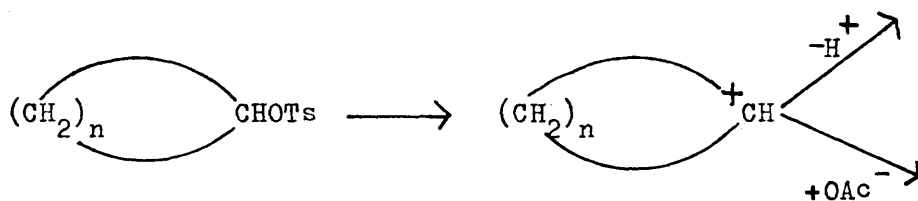
This supposition is supported by a number of reactions which show the effects of I-strain, which is defined as the "change in internal strain which results from change in coordination number of a ring atom involved in chemical reaction".²

1. Reactions of Cycloalkanones with Hydrogen Cyanide to give Cyanohydrins³



Ring Size	5	6	7	8	9	10	11	12	13	14
K	3.33	70	0.54	0.081	0.041	small	0.063	0.226	0.269	1.17

2. Acetolysis of Cycloalkyl Tosylates⁴



Ring Size	5	6	7	8	9	10	11	12	13	14
Relative k at 70°	10.5	0.75	19.0	144	129	286	30.8	2.44	2.63	0.99

In reaction 1, the dissociation of the cyanohydrin results in an increase of the already strained sp^3 -hybridized bond angles (distributed over the whole ring), but much more important, there is a reduction of transannular strain, so that, in the case of medium rings, the equilibrium lies to the left. In reaction 2, there is a relief of transannular strain in the transition state (sp^2 hybridised). The activation energy is lowest, hence the rate is higher, when the ground state compression is greatest, as it is in the medium rings. The increase in angular strain on going from sp^3 to sp^2 again is less important. Generally, in the region of medium rings, reactions which involve an increase in I-strain ($sp^2 \longrightarrow sp^3$) are slow and reactions which involve a decrease in I-strain ($sp^3 \longrightarrow sp^2$) are fast.

3.2. The Effect of introducing a double bond into Cycloalkanes, C₇-C₁₀

Columns (1) and (2) in Table 1 mirror the same trend

TABLE 1: CALCULATED STERIC ENERGIES OF MINIMUM ENERGY CONFORMATIONS OF MEDIUM RING COMPOUNDS.

RING SIZE	(1)	(2)	(3)	(4)	(5)	(6)
7	8.33	5.98	-	-	-	-
8	13.61*	7.88	18.68	10.85(1,5)	35.86(1,5)	24.67(1,5)
9	14.66*	10.47	15.08	7.26(1,5)	19.63(1,5)	12.82(1,5)
10	14.10	8.96	11.37	10.12(1,5)	10.81(1,5)	9.12(1,5)
				4.65(1,6)	6.82(1,6)	7.77(1,6)

COLUMN (1) STERIC ENERGY OF CYCLOALKANES
 COLUMN (2) STERIC ENERGY OF CIS-CYCLOALKENES
 COLUMN (3) STERIC ENERGY OF TRANS-CYCLOALKENES
 COLUMN (4) STERIC ENERGY OF CIS,CIS-CYCLOALKADIENES
 COLUMN (5) STERIC ENERGY OF TRANS,TRANS-CYCLOALKADIENES
 COLUMN (6) STERIC ENERGY OF CIS,TRANS-CYCLOALKADIENES

* STERIC ENERGY ESTIMATED FROM HEAT OF HYDROGENATION AND HEAT OF FORMATION OF CIS-ALKENE.

ENERGIES IN KCAL/MOLE

in strain as that derived from the heat of combustion measurements and confirm that the introduction of a cis double bond into the ring results in a reduction in strain, as predicted above. Column 3, however, does not show this trend. Molecular mechanics calculations indicate that the introduction of a trans rather than a cis double bond leads to unfavourable changes in torsional strain, and to a smaller but significant change, in angle strain and trans-annular strain. These strain components are largest in C_8 compound and decrease as ring size increases since the strain associated with the introduction of a trans double bond can be distributed more efficiently in the larger rings. Furthermore, the poor Π overlap, which arises as a result of the twisting of the double bonds in trans-cycloalkenes, the strained σ bonds and nonbonded repulsions make some of these compounds highly reactive and difficult to isolate e.g. trans-cycloheptene.

Heats of hydrogenation for cycloalkenes (cis and trans) agree favourably with the observed values and enables some confidence to be placed in the above observations (see Table 2).

3.3. The Effect of introducing a second double bond into Cycloalkenes, C_8-C_{10}

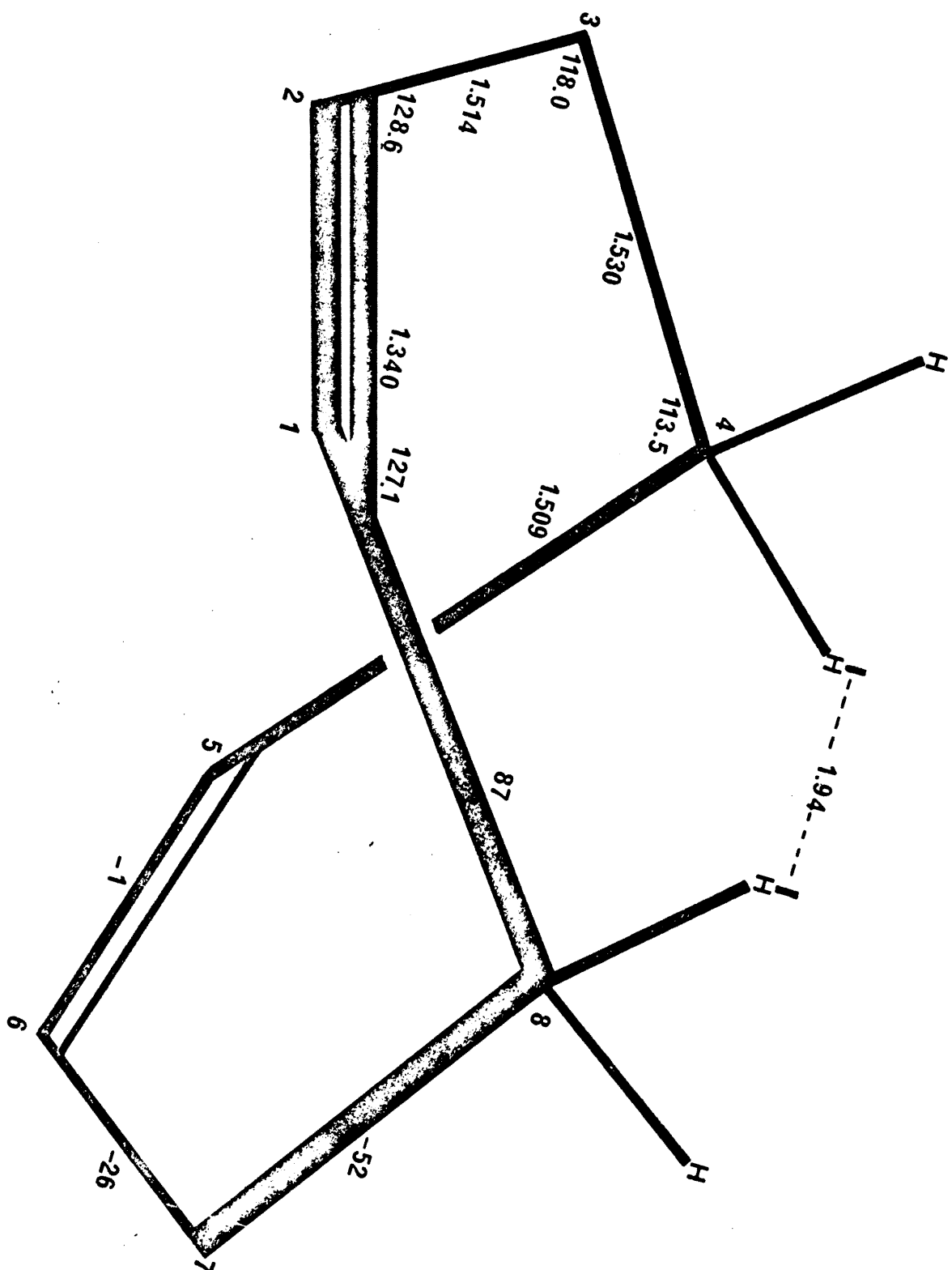
The introduction of a second cis double bond into cis-cyclooctene at carbon 5 results in an increase in strain of 2.17 kcal./mole. The minimum energy conformation of cis, cis-1,5-cyclooctadiene has been shown by spectroscopic and diffraction studies to be a twist-boat (Figure 1, see

TABLE 2: HEATS OF HYDROGENATION⁴ AND RELATIVE STABILITY OF CIS AND TRANS CYCLOOLEFINS⁵

RING SIZE	HEAT OF HYDROGENATION ΔH^0		$\Delta \Delta H^0$, KCAL./MOLE		Δ (CALC. - OBS.)
	CIS	TRANS	OBSERVED	CALCULATED *	
8	-22.98	-32.24	-9.26	-10.72	-1.46
9	-23.62	-26.49	-2.87	-4.61	-1.74
10	-20.67	-24.01	-3.34	-2.41	0.92

* IN ACETIC ACID
* CALCULATED BY THE MBFF

Figure 1: The calculated twist-boat conformation of
cis,cis-cycloocta-1,5-diene (C_2 symmetry).



also Chapter 2.3(d)). In Figure 1, The C1 ... C6 and C4 ... C7 nonbonded distances are found experimentally⁶ to be 3.05 Å and 3.19 Å respectively. The corresponding values, calculated by the WBFF are 3.08 Å and 3.19 Å respectively, which are in good agreement with the experimental values. The H4 ... H8 distance is calculated to be 1.94 Å. All these nonbonded interactions lie on the repulsive portion of the Van der Waals curves and thus give rise to transannular strain. The more important factor here is that the C = C - C_{sp}³ bond angles are increased to a mean value of 127.8° and the C_{sp}² - C_{sp}³ - C_{sp}³ angles to a mean value of 115.8° in order to accommodate the second cis double bond into the eight membered ring. This Baeyer strain and transannular strain are manifested in the strain energy components.

The introduction of a trans double bond into cis-cyclooctene, which yields 1,5-cis,trans-cyclooctadiene leads to an increase of 16.79 kcal./mole in the overall steric energy. Similarly, when a trans double bond is introduced into trans-cyclooctene to give 1,5-trans,trans-cyclooctadiene, the steric energy increases by 17.26 kcal./mole. As in the case of the introduction of the first trans double bond into an eight-membered cyclic compound, the introduction of the trans double bonds in the latter two cases results in large and unfavourable changes in torsional strain and transannular strain as well as smaller increases in Baeyer strain.

The steric energy of the minimum energy conformation of cis, cis-1,5-cyclononadiene, the chair (Figure 2) is 3.21 kcal./mole less than that of cis-cyclononene. This decrease is

Figure 2: The minimum energy conformation of cis,cis-1,5-cyclononadiene.

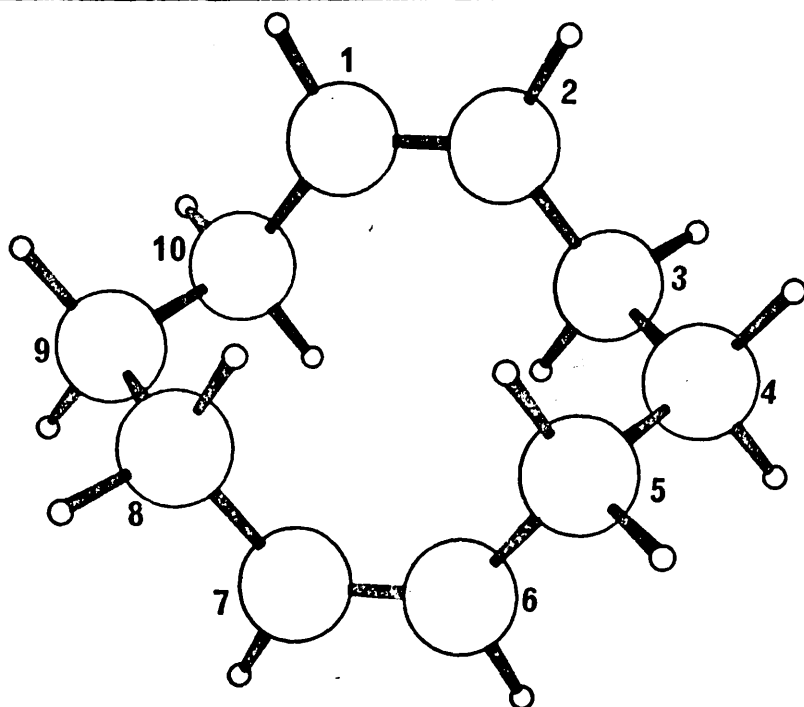
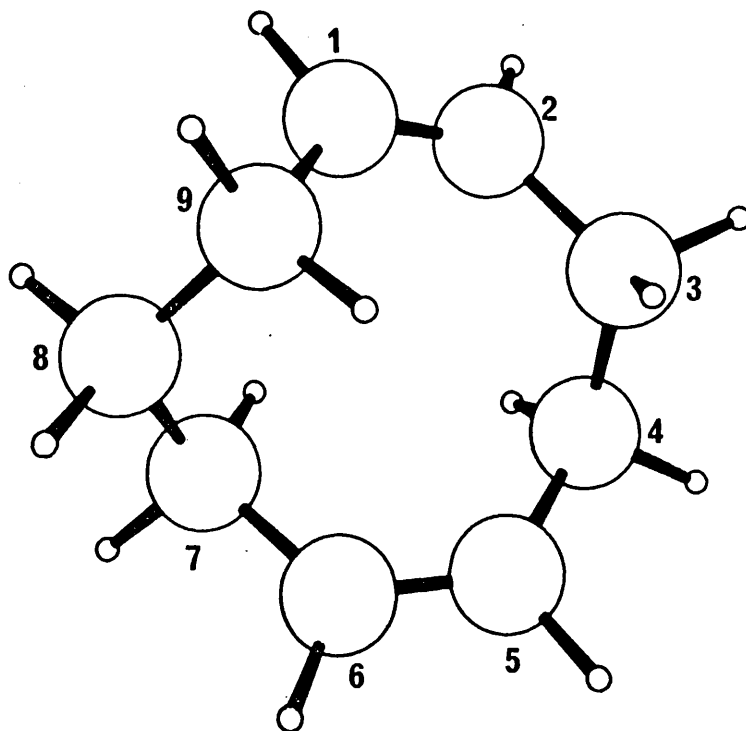


Figure 3: The minimum energy conformation of cis,cis-1,6-cyclodecadiene.

due to the fact that there is a decrease in the crowding of atoms across the ring because there are fewer hydrogens in the diene and also because the minimum energy conformation of the diene is a chair, in which C1 ... C6 nonbonded distance is $3.34 \overset{\text{O}}{\text{\AA}}$ and which is relatively strain-free.

Similarly, the steric energy of cis,cis-1,6-cyclodecadiene is 4.31 kcal./mole lower than cis-cyclodecene. The minimum energy conformation is again a chair (Figure 3), which is relatively strain-free and C2...C6 nonbonded is $3.65 \overset{\text{O}}{\text{\AA}}$. This decrease is mainly due to a decrease in transannular strain because there are fewer C-H bonds and to a decrease in angle strain because the internal ring angles do not have to increase as much to minimise the transannular strain.

The minimum energy conformation of cis, trans-1,6-cyclodecadiene (Figure 4) is only 1.9 kcal./mole lower than cis-cyclodecene. In Figure 4, the C1 ... C7 nonbonded distance is $2.99 \overset{\text{O}}{\text{\AA}}$ (the associated non bonded energy is 0.7 kcal./mole in WBFF), so that the transannular strain will not be reduced. The major reduction in energy is due to a reduction in Baeyer strain (which is a result of the decrease in the number of C-H bonds). However, it is interesting to note that the torsional energy is higher (by 0.34 kcal/mole) in the cis, trans-diene than in the cis ene which indicates that the introduction of the trans double bond into cis-cyclodecene still produces unfavourable changes in Pitzer strain.

The minimum energy conformation of trans,trans-1,6-

Figure 4: The minimum energy conformation of cis,trans-1,6-cyclodecadiene.

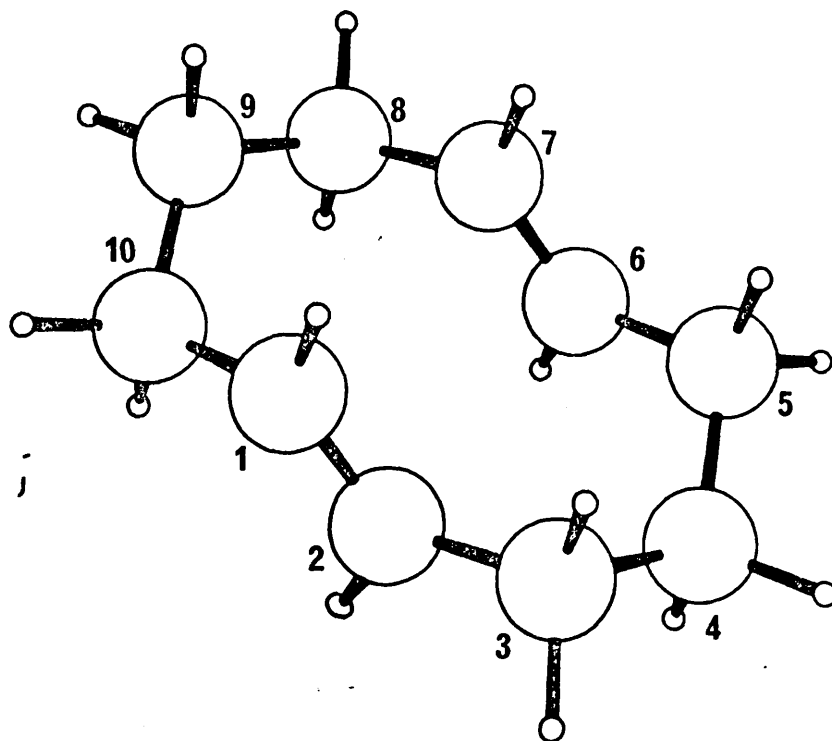
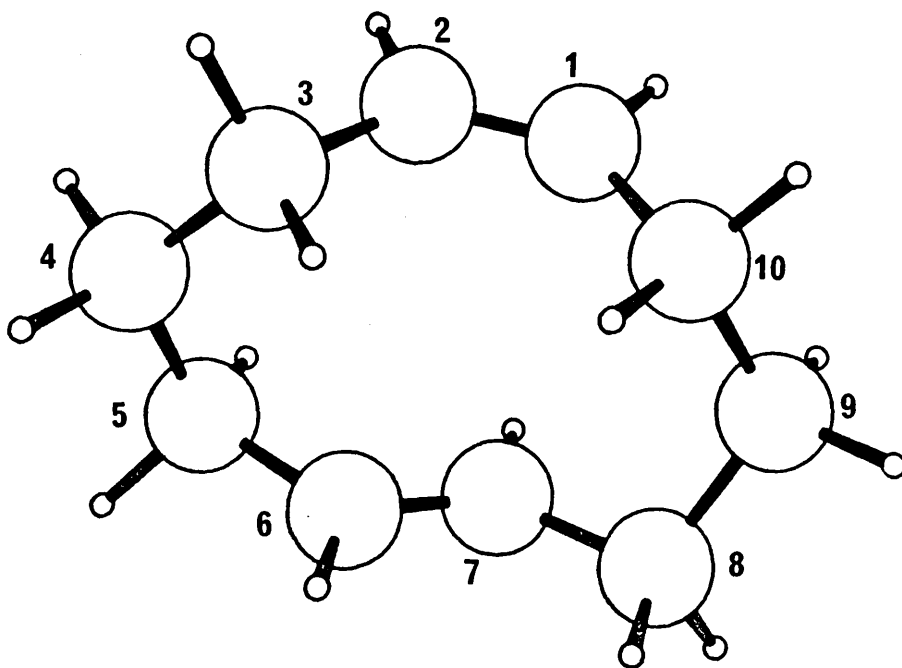


Figure 5: The minimum energy conformation of trans,trans-1,6-cyclodecadiene.

cyclodecadiene has been shown to be the "chair-chair" conformation (Figure 5). This conformation is computed to be 4.55 kcal./mole lower than that of trans-cyclodecene. The change in hybridisation in this case, produces a reduction in torsional strain and angle strain. It also produces a reduction in the transannular interactions involving the hydrogens, but, since the C1 ... C7 and C2 ... C6 nonbonded distances are both only 2.84 Å, the van der Waals profiles of the two double bonds are forced to interpenetrate and result in a strain energy component of 2.58 kcal./mole. Thus the transannular strain is 0.2 kcal./mole higher in the diene.

On the basis of the results in Table 1, the following points may be deduced:

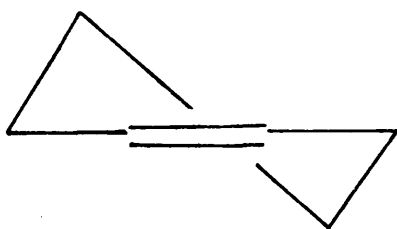
- (a) The least strained C₈ compound is cis-cyclooctene and the most strained is trans, trans-1,5-cyclooctadiene.
- (b) the least strained C₉ compound is cis, cis-1,5-cyclononadiene and the most strained is trans, trans-1,5-cyclononadiene.
- (c) the least strained C₁₀ compound is cis, cis-1,6-cyclodecadiene and the most strained is cyclodecane.
- (d) for C₈-C₁₀, cis-cycloalkenes are less strained than the corresponding trans-cycloalkenes.
- (e) for C₈ and C₉ rings, the cis, cis-cycloalkadienes are less strained than the corresponding cis, trans-isomers which, in turn, are less strained than the trans, trans-isomers.
- (f) the strain, associated with the introduction of a trans double bond, is significantly less in the ten-membered rings

than in the eight-or-nine membered ring, with the result that no generalization can be made regarding the stability of the various types of dienes that occur in ten-(and eleven-) membered rings. The controlling factor here is the particular minimum energy conformation that each type of diene adopts.

3.4. Conformations of the individual Cyclenes

(a) Cyclohexene

The half-chair conformation (I) with C_2 symmetry is the most stable conformation.⁷ The dihedral



$$V_s = 2.78 \text{ kcal. / mole}$$

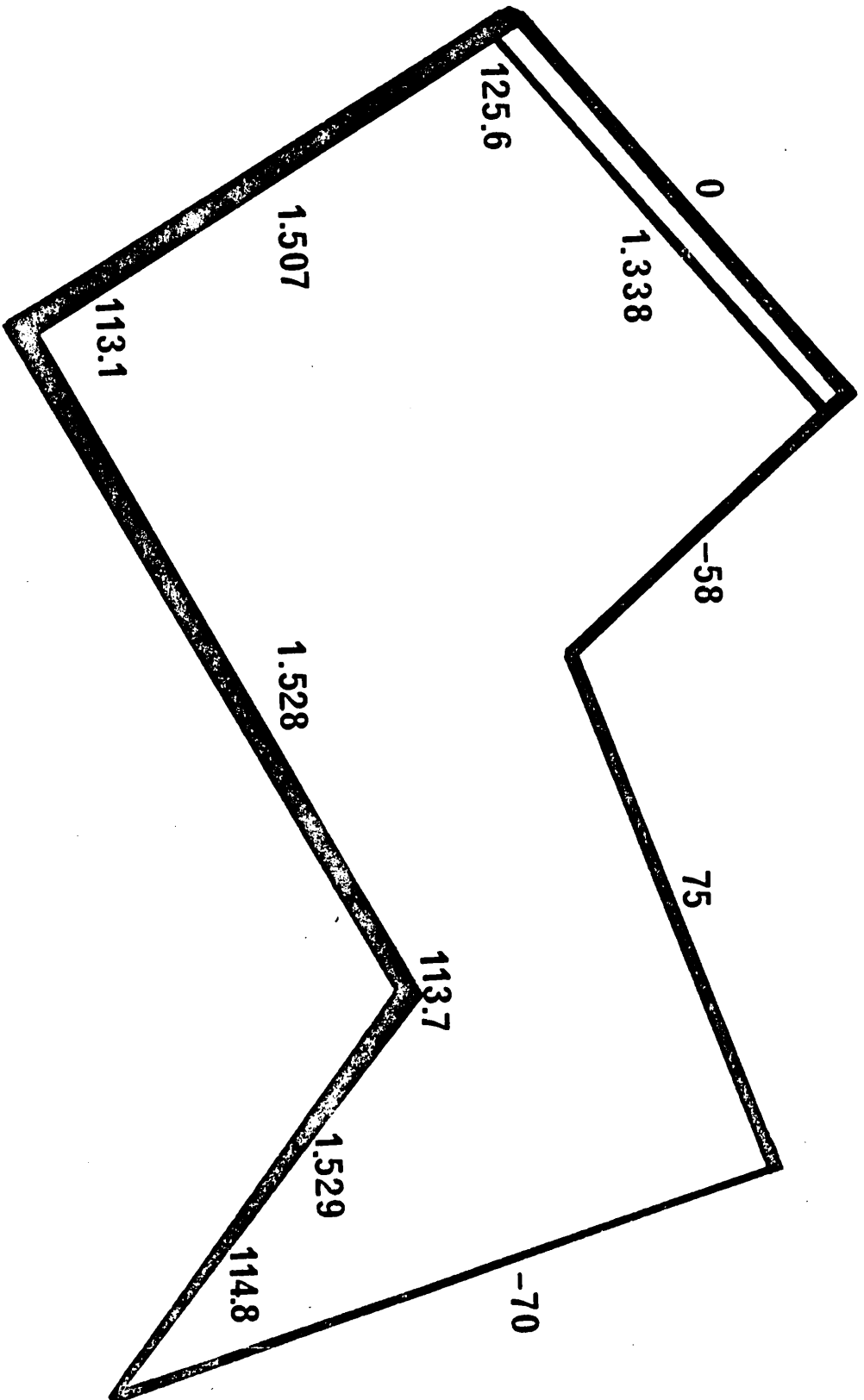
	<u>I</u> <u>Observed (7)</u>	<u>Calculated by WBFF</u>
ω_{1234}	-15.2	-15.3
ω_{2345}	44.9	45.4
ω_{3456}	-60.2	-62.3

angles, calculated by a modified Karplus equation, from NMR coupling constants $J_{23's}$ (43° and 77°) are in good agreement with the theoretically obtained (by WBFF) values of 44° and 74° .


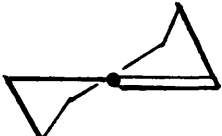


(b) cis-Cycloheptene

The problem is simpler than for cycloheptane, because the introduction of the double bond into the ring system affords a rigidity which prohibits the pseudorotation. WBFF, AFF^9 and CFF^{10} all calculate the C_s chair as the

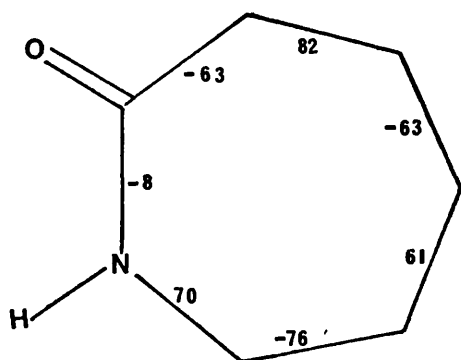
Figure 6: The calculated minimum energy conformation of
cycloheptene (C_s symmetry).



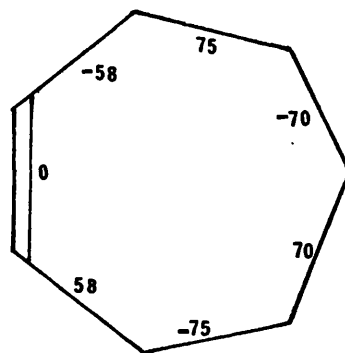
most stable form of cycloheptene, being 1.5 kcal./mole, (WBFF) and about 0.5 kcal./mole (AFF and CFF) lower in energy than the C_2 twist conformation.

<u>CHAIR(C_s)</u>	<u>TWIST-CHAIR(C_2)</u>	<u>TWIST-BOAT</u>	<u>BOAT(C_s)</u>
V_s 5.98 (kcal./mole)	7.51	8.37	9.64
			

The geometry calculated for the C_s chair is shown in Figure 6. Dihedral angles, calculated from NMR coupling constants J_{23} 's (11° and 109°) agree with the values calculated by the WBFF for the C_s chair (3° and 114°) conformation. The observed heat of hydrogenation of cycloheptene is 25.85 kcal./mole¹¹ and this agrees with the calculated value of 25.15 kcal./mole. Since derivatives of cycloalkenes are often low melting and difficult to crystallise, force field calculations provide a useful, and sometimes only, method for investigating conformations of cyclic compounds. However, the X-ray crystal structure analysis of ϵ -caprolactam has been performed¹² and was found to have a nearly symmetric chair conformation with torsion angles similar to those calculated by the WBFF for the C_s symmetric chair cycloheptene conformation, as shown over.



II. (a) ϵ -CAPROLACTAM-TORSION
ANGLES OBTAINED FROM
CRYSTAL STRUCTURE ANALYSIS.



(b) CHAIR CYCLOHEPTENE-
TORSION ANGLES
CALCULATED BY WBFF.

The discrepancy between the observed and calculated values of the torsion angles is, in part, due to the fact that the amide group has a far lower rotation barrier than the double bond and also has a much lower resistance to out-of-plane bending at the N-H group.

In contrast to the CFF¹⁰ the WBFF calculates the C_s boat to be an extremely shallow minimum closely flanked by a pair of maxima about 0.04 kcal./mole above the minimum (i.e. a saddle point) (see Figure 7).

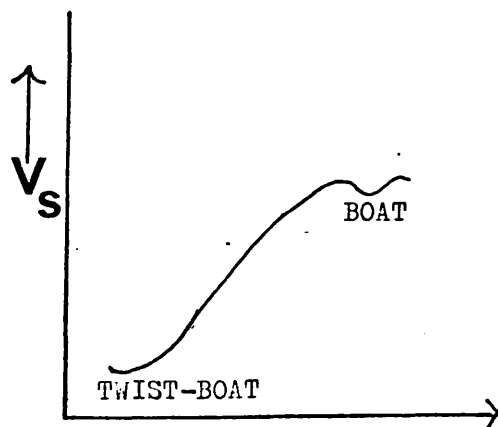
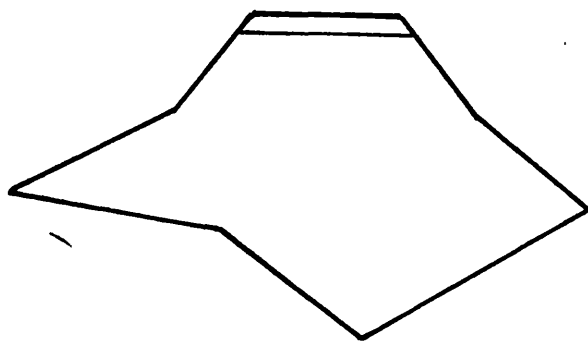


Figure 7

trans-cycloheptene has been generated and trapped, but not yet observed spectrophotometrically.¹⁴

(c) Cyclooctene

The cis and trans isomers of cyclooctene are both known and are of conformational interest. There is good experimental evidence as to the type of conformation of cis-cyclooctene¹⁴ though its detailed structure has not yet been determined (III).

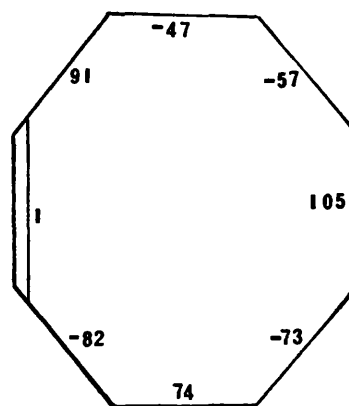
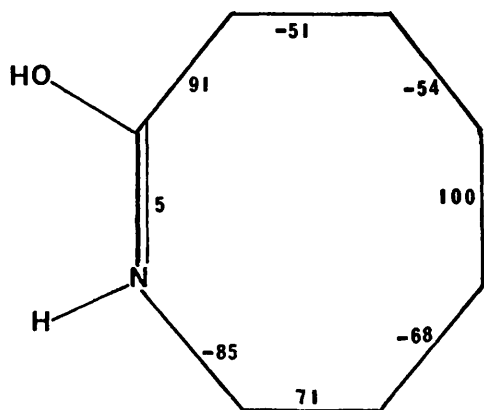


$$V_s = 7.88 \text{ kcal. / mole}$$

(III)

The torsional angles around the bonds of the ring confirm that the four atoms of this cis-double bond are essentially planar. The remaining atoms of the ring then arrange themselves to minimise transannular steric interactions and eclipsing of the substituents about each bond of the ring. The dihedral angles for cis-cyclooctene from NMR coupling constants $J_{23,s}$ (15° and 135°) agree with the values obtained by MM calculations using WBFF (23° and 140°). Good agreement is also obtained between the observed torsion

angles (from X-ray) for enantholactam hydrochloride¹⁵ and the calculated torsion angles for cis-cyclooctene, (IV).



(IV) (a) Torsion angles from X-ray study of Enantholactam Hydrochloride

(b) Torsion angles calculated for cis-cyclooctene by WBFF

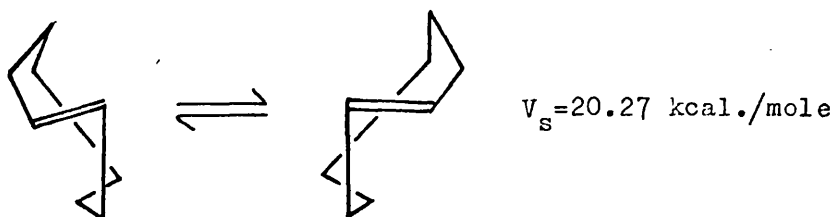
The smallest stable trans-cycloalkene to be isolated is trans-cyclooctene, which unlike the cis isomer, has an exceptionally high heat of hydrogenation, Model considerations show that the double bond and two attached methylenes in the trans isomer forms a trans-butene system and with only four remaining carbons to bridge the ends of the butene system, high distortion of the molecule is required. It has been shown that the molecule possesses a dipole moment which is extraordinarily large. for an olefin (0.82D compared with 0.15D for trans-cyclodecene) and this large moment has been interpreted in terms of a unique hybridisation at the olefinic carbons which puts considerable s character into the π -bond. The tight belt of saturated carbons joining the ends of the olefin leads to molecular asymmetry which cannot be destroyed by rotation of the belt

around the olefin and trans-cyclooctene has been optically resolved. The high barrier to racemization results from steric destabilization of the transition state caused by hydrogens forced into the interior of the ring en route to a 180° rotation around the double bond. Increased ring size allows more facile passage of the vinylic hydrogens through the centre of a ring, thus, at room temperature, trans cyclononene racemizes as it is formed.

In recent years, there has been some controversy as to whether the cross (V) (also called the crown) or chair (VI) conformation is the minimum energy conformation, both on the experimental and theoretical fronts.



V



VI

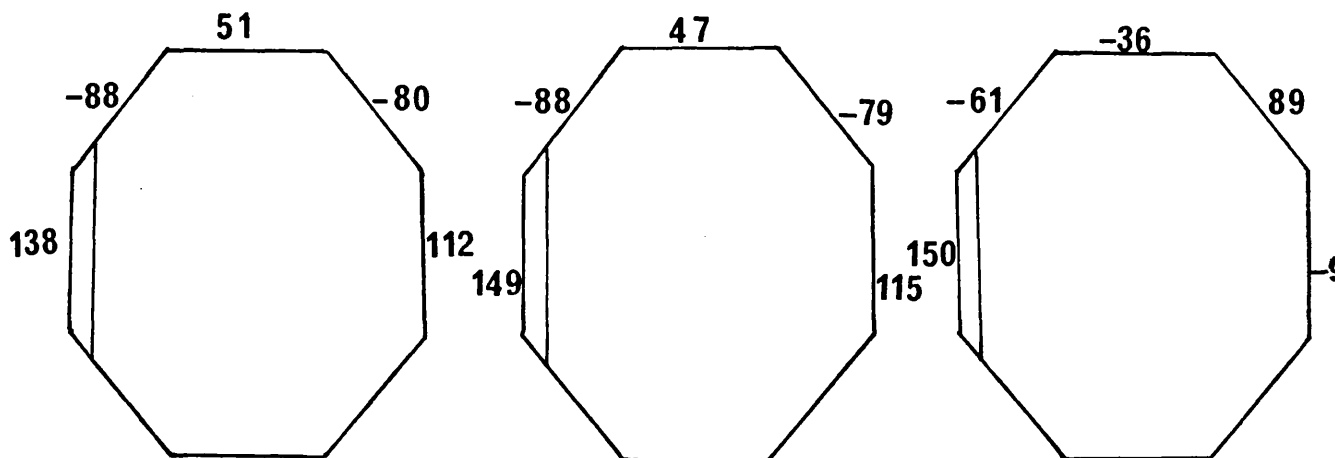
On the experimental side, the results of X-ray studies¹⁶ of adducts of trans-cyclooctene with complexing agents, such as silver nitrate, are to be treated with caution as the presence of heavy metal atoms introduce undesired perturbations of the double bond system and/or severely limit

the attainable accuracy of the studies. While the X-ray studies indicate that the cross conformation is the minimum energy conformer, gas phase electron diffraction studies by Gavin and Wang¹⁷ indicate a distorted chair (VI). However, recent X-ray results on trans -2-cyclooctenyl 3¹,5¹-dinitrobenzoate¹⁸ as well as more recent electron diffraction data on the parent compound by Traetteberg¹⁹ favour the cross conformation (V).

MM calculations with WBFF, AFF and CFF all calculate the cross conformation to be lower in energy by 1.67, 2.43 and 3.14 kcal. / mole respectively.

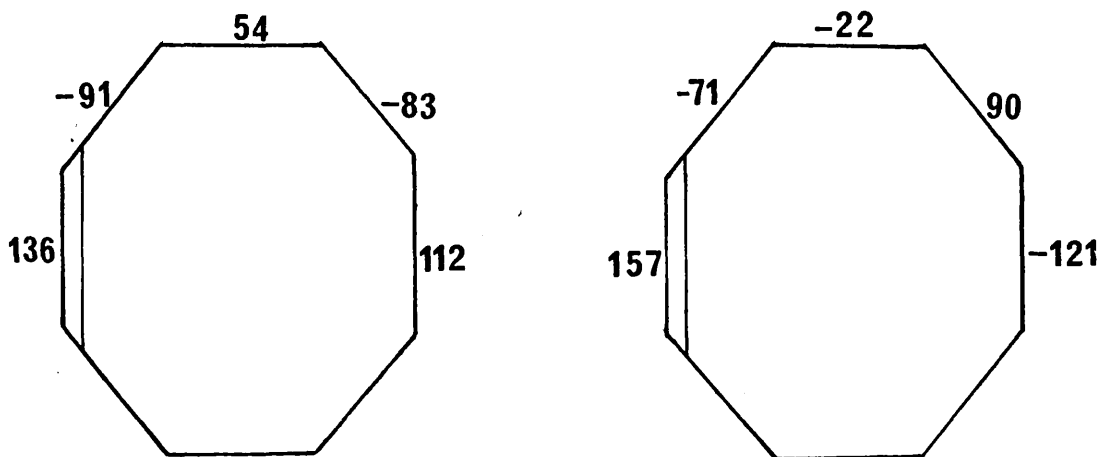
It would now seem that the cross conformation is, without doubt, the minimum energy conformer and that the trans-cyclooctene sample studied by Gavin and Wang had been prepared under non-equilibrium conditions and had consisted primarily of the chair conformation, which is prevented from rapidly converting to the cross conformation by a high interconversion barrier.

The torsion angles, obtained from an X-ray crystal structure analysis²⁰ of a non-complexed iodine containing derivative of trans-cyclooctene (VII(a)) is compared with the torsion angles of the cross (VII(b)) and chair conformations (VII(c)), calculated with WBFF. VII(d) and (e) show torsion angles obtained from the electron diffraction studies.



VII. (a) trans-Cyclooctene as observed in Iodine derivative (C_2 averaged) (b) trans-Cyclooctene Cross-Calculated Torsion Angles (C_2) (c) trans-Cyclooctene Chair-Calculated torsion angle (C_2)

Thus, the cross conformation is in good agreement with the crystal structure analysis.

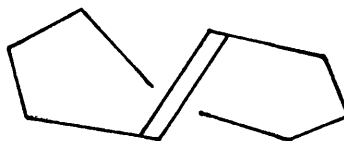
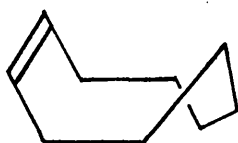


VII. (d) Torsion angles from Traetteberg electron diffraction (C_2)¹⁹

(e) Torsion angle from Gavin and Wang electron diffraction (C_s)¹⁷

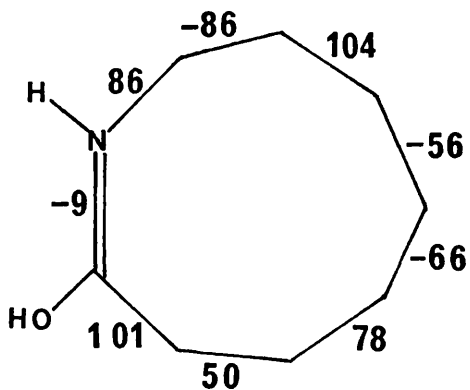
(d) Cyclononenes

No detailed conformational properties of cyclononenes are known. The *cis* isomer is calculated to be lower in energy than the *trans*, in agreement with the observed heat of hydrogenation values. Conformational models for *cis* and *trans* isomers were derived from two recent crystal structure analyses of caprylolactam and its hydrochloride.¹⁵ The *cis* isomer is asymmetric while the *trans* isomer has C_2 symmetry (VIII(a) and (b) respectively).

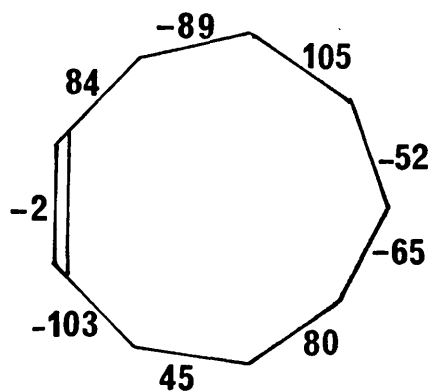


VIII(a) $V_s = 10.47$ kcal./mole (b) $V_s = 15.08$ kcal./mole

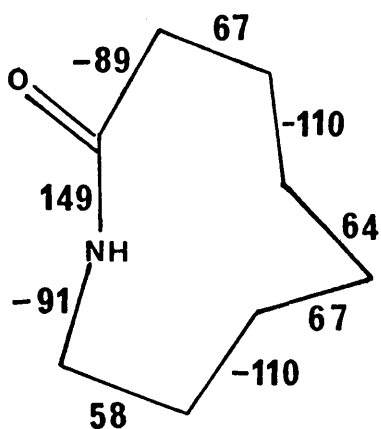
The calculated torsion angles for *cis* and *trans* cyclononene are compared with the experimental ones for caprylolactam and its hydrochloride in (IX(a) - (d)).



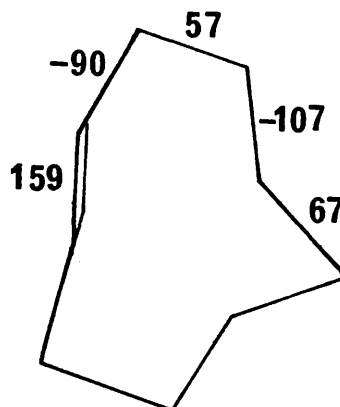
IX(a) Observed torsion angles
of caprylolactam
hydrochloride



(b) Calculated torsion
angles of cis-cyclononene.



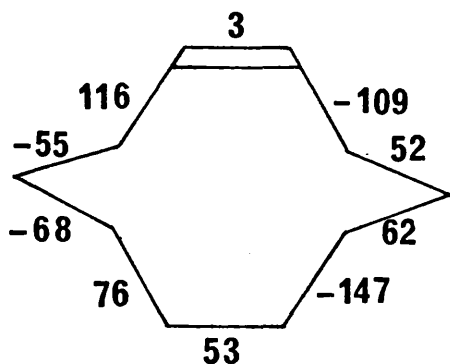
(c) Observed torsion
angles of caprylolactam



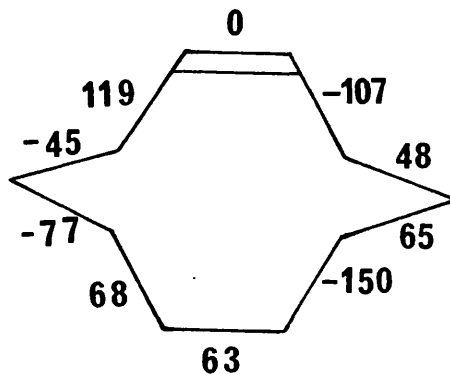
(d) Calculated torsion
angles of trans-
cyclononene

(e) Cyclodecene

The cis isomer is calculated to be lower in energy than the trans isomer. Conformation models for cis and trans isomers were derived from X-ray crystal structure analyses of silver nitrate adducts²¹ and the calculated torsion angles for cis and trans cyclodecene compare favourably with the X-ray results X(a) - (e).

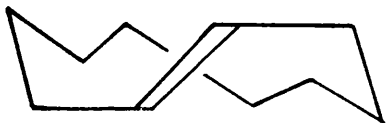


X(a) Observed torsion angles of AgNO_3 complex of cis-cyclodecene

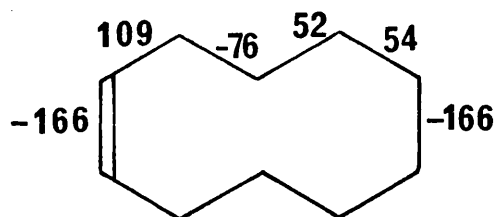
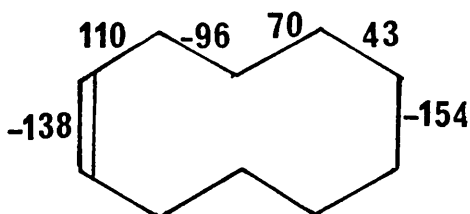


$$V_s = 8.96 \text{ kcal./mole}$$

(b) Calculated torsion angles for cis-cyclodecene



(c) The conformation of trans isomer (C_2 symmetry) - Twist



$$V_s = 11.37 \text{ kcal./mole}$$

(d) Observed torsion angles
in AgNO_3 adduct of trans-
cyclodecene

(e) Calculated torsion
angles in trans-cyclodecene

The reason for the large discrepancies in (d) and (e) may, in part, be due to perturbations of the double bond system by the silver atom and the limited accuracy of the experimental results.

(f) Cycloocta-1,5-diene (1,5-COD)

The minimum energy conformation of cis,cis-cycloocta-1,5-diene, the C_2 symmetric twist-boat conformation was discussed fully in Chapter 2. The various twist-boat interconversion pathways will be discussed in this section.

The dynamics of cis,cis-1,5-COD system was first studied experimentally using low-temperature NMR methods.²² These measurements show two distinct NMR processes, where the two barriers are calculated to be 4.4 and 4.9 kcal./mole. MM calculations^{23,24,25,26} have been used in an attempt to assign these barrier heights unambiguously to the appropriate

conformational interconversion. Anet²³ and Ermer²⁵ calculate that the route through the D_2 skew conformation is the lowest energy process followed by those through the C_{2v} boat and C_{2h} chair with approximately equal barrier heights. Allinger²⁴ on the other hand, calculates that the route through the C_{2v} boat is the minimum energy pathway followed by that through the chair and finally the route through the skew as the maximum energy interconversion route.

Because of the marked difference between these results, we decided to investigate this system rather closely. It seemed unlikely that such a dichotomy arose from differences between the various force fields, because of the usually similar results obtained for other calculations. Instead the differences in the methods in generating the transition states were thought to hold the key to the problem.

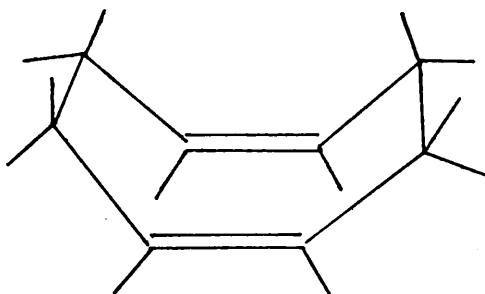
In the first instance, we used the method of Wiberg and Boyd²⁷ in order to map the energy changes from the twist boat to the boat and skew conformations and generated the transition state between twist boat and chair conformations with a molecule building program. In all three cases, we used a larger number of constraints on the system than was actually necessary. For example, in mapping from the twist boat to the skew all nine torsion angles around each of the $C_{sp^3} - C_{sp^3}$ bonds were driven instead of only $C_{sp^2} - C_{sp^3} - C_{sp^3} - C_{sp^2}$ torsion angles. In this case, we obtained the same order of preference for the various interconversion pathways as Allinger and similar values for the barrier heights.

In the next series of calculations, we used the Wiberg-Boyd algorithm, but with the minimum number of constraints, and obtained the same order of preference as Anet and Ermer. It therefore seemed as though Allinger had imposed too many constraints. In order to check this conclusion we repeated these calculations using AFF whereupon the route through the skew emerged as the minimum energy pathway.*

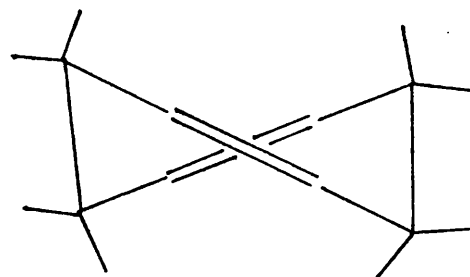
Finally, we repeated the calculations yet again using the Newton-Raphson maximisation procedure to define the three transition states. The results were very similar to those obtained using the Wiberg-Boyd algorithm with minimal constraints except that the energies of the transition states were some 0.02 kcal./mole lower, probably as a consequence of complete molecular relaxation (i.e. no artificial constraints). This lends additional support to the conclusion that a second-derivative minimisation/maximisation procedure, such as the Newton-Raphson, is the only safe optimisation algorithm for MM calculation.²⁸

The symmetry and the steric energy calculated by the WBFF for each of the five conformations considered in this study are shown in Figure 8 while the calculated (WBFF) barrier heights are compared with Ermer's and Anet's

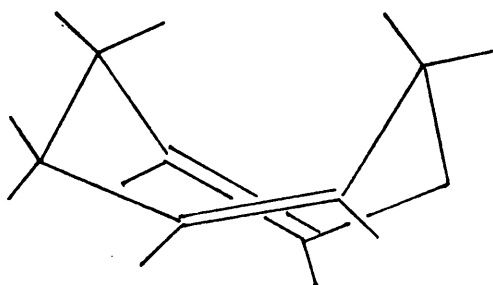
* Allinger's calculations were performed with AFF-73²⁴ whilst we used AFF-72⁹. Although full details of AFF-73 are not available it appears to be a slightly improved version of AFF-72. These do not affect the arguments above.



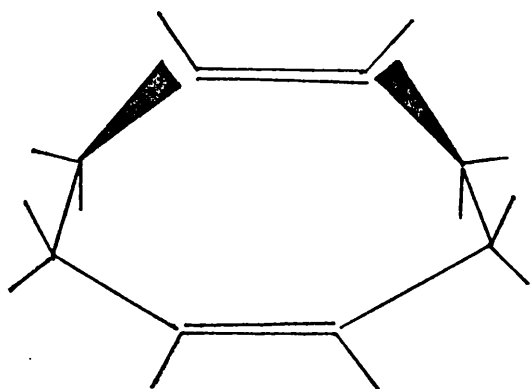
Boat \underline{C}_{2v}
 $V_s = 14.60 \text{ kcal./mole}$



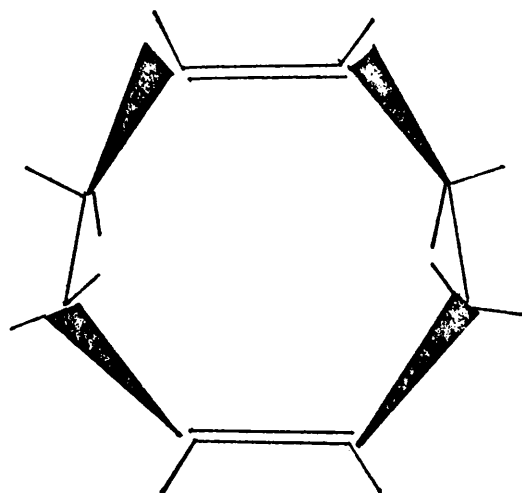
Skew \underline{D}_2
 $V_s = 12.32 \text{ kcal./mole}$



Twist-boat \underline{C}_2
 $V_s = 10.05 \text{ kcal./mole}$



Transition state \underline{C}_s
 $V_s = 14.69 \text{ kcal./mole}$

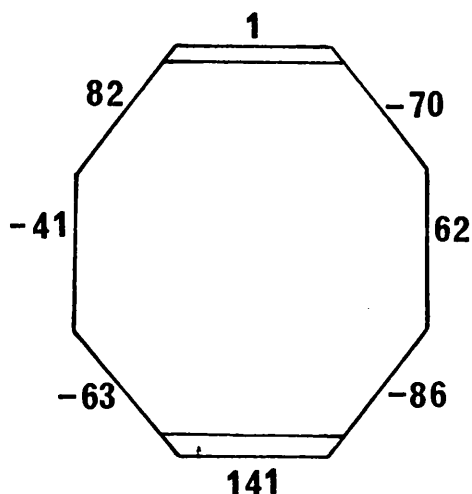


Chair \underline{C}_{2h}
 $V_s = 10.82 \text{ kcal./mole}$

Figure 8: Major conformations of cis,cis-cycloocta-1,5-diene.

in Table 3 along with the experimental values.

cis, trans-1,5-COD^{29,30} and trans,trans-1,5-COD³¹ have been isolated but no experimental data regarding conformational information is available. cis,trans-1,5-COD is optically active³² which implies that it is a highly strained and rigid molecule. From an inspection of molecular models, the minimum energy conformation is very similar to that of cis-cyclooctene (III). The torsion angles and steric energy calculated by the WBFF are shown below (XI)



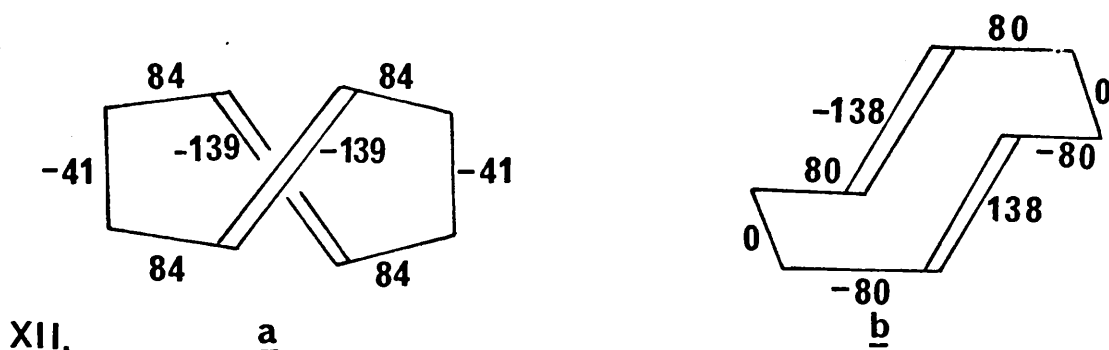
$$V_s = \frac{XI}{24.67} \text{ kcal/mole}$$

The NMR data on trans,trans-1,5-COD do not allow assignment of structure XII(a) or XII(b) to it.³¹ MM calculations using the WBFF, have been applied to this problem and it is found that the (a) is more stable than (b) by 5.14 kcal./mole, since (b) possesses unfavourable eclipsed torsion angles around the two C_{sp}³-C_{sp}³ bonds while in (a), the corresponding torsion angles are staggered.

TABLE 3: CALCULATED AND EXPERIMENTAL BARRIER HEIGHTS (KCAL/MOLE)
FOR THE VARIOUS CIS,CIS-CYCLOOCTA-1,5-DIENE CONFORMATIONAL
INTERCONVERSIONS.

	ANET ²³	ERMER ²⁵	WHITE AND BOVILL	EXPERIMENT ²²
ΔV(CHAIR)	7.2	5.9*	4.6	4.9*
ΔV(BOAT)	6.6	5.7*	4.5	4.9*
ΔV(SKEW)	4.2	4.2*	2.3	4.4*

* VALUES ARE ΔG



$$V_s = 35.86 \text{ kcal./mole}$$

$$V_s = 41.00 \text{ kcal./mole}$$

(g) Cyclonona-1,5-dienes (1,5-CND)

The structure of two cis,cis, two cis,trans and three trans,trans conformer of 1,5-CND have been calculated and the results are shown in Figure 9. The minimum energy conformation is the cis,cis-isomer of Figure 9(a), and equilibration³³ together with NMR experiments³⁴ are in complete agreement with this conclusion as to the favoured isomer but give no indication as to its conformation. However, Favini³⁵ also calculates the cis,cis-isomer of Figure 9(a) to be the global minimum and his calculated geometry is very similar to ours. It may also be pertinent that this conformation bears a strong resemblance to the known global minimum energy of cyclodeca-1,6-diene (Figure 15(a)). There is very little experimental structural data available for the 1,5-CND's but a recent X-ray crystal structure analysis of byssochlamic acid³⁶ has shown that the cis,cis-1,5-CND ring has a conformation very similar to that of Figure 9(b) and the two conformations are compared in Figure 10.

Figure 9: Cyclonona-1,5-diene conformations; peripheral values are torsion angles and the inner value is the steric energy in kcal./mole above the minimum. Symmetry is C_1 except as noted (a) C_2 , (c) C_s , (e) C_s .

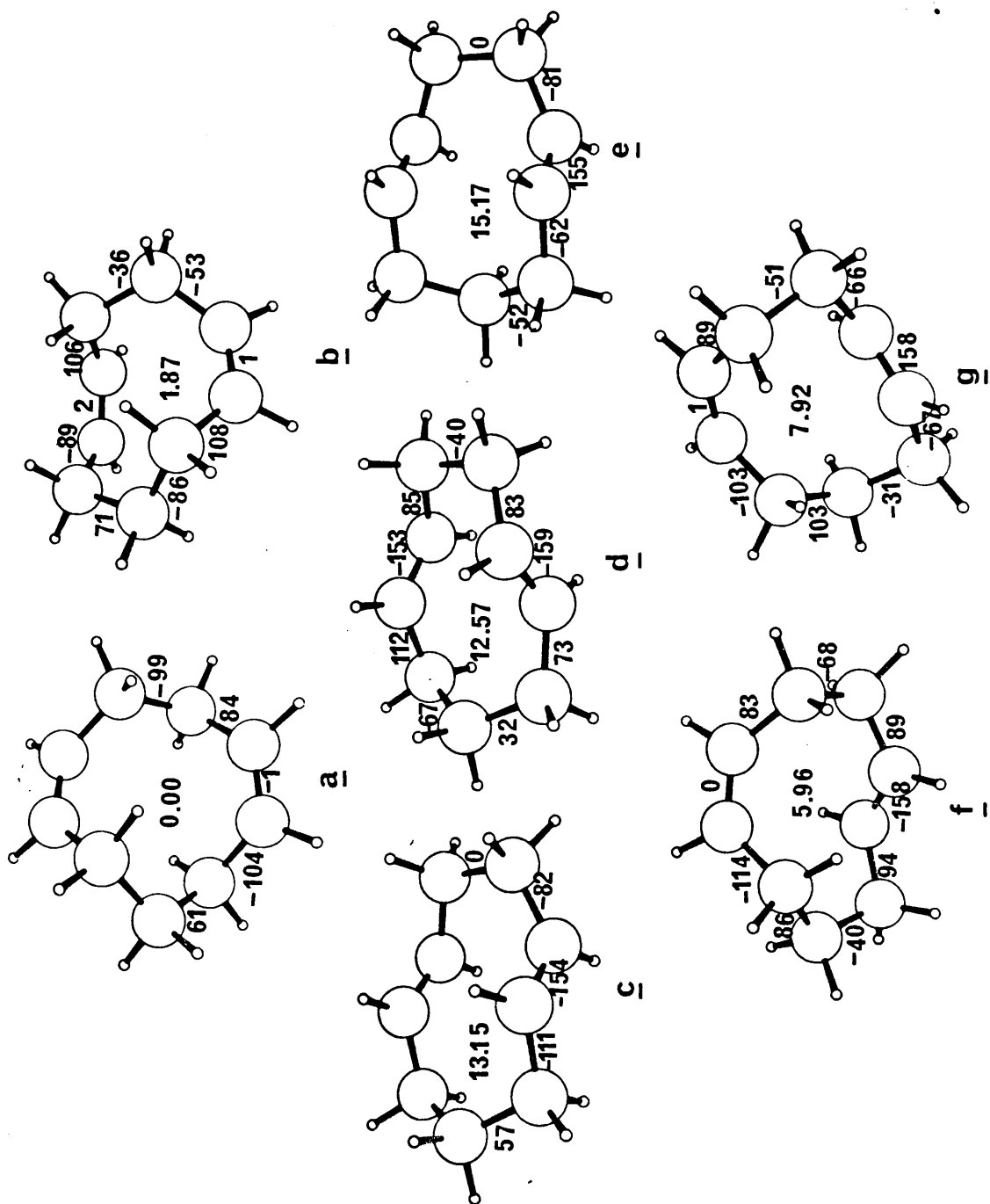
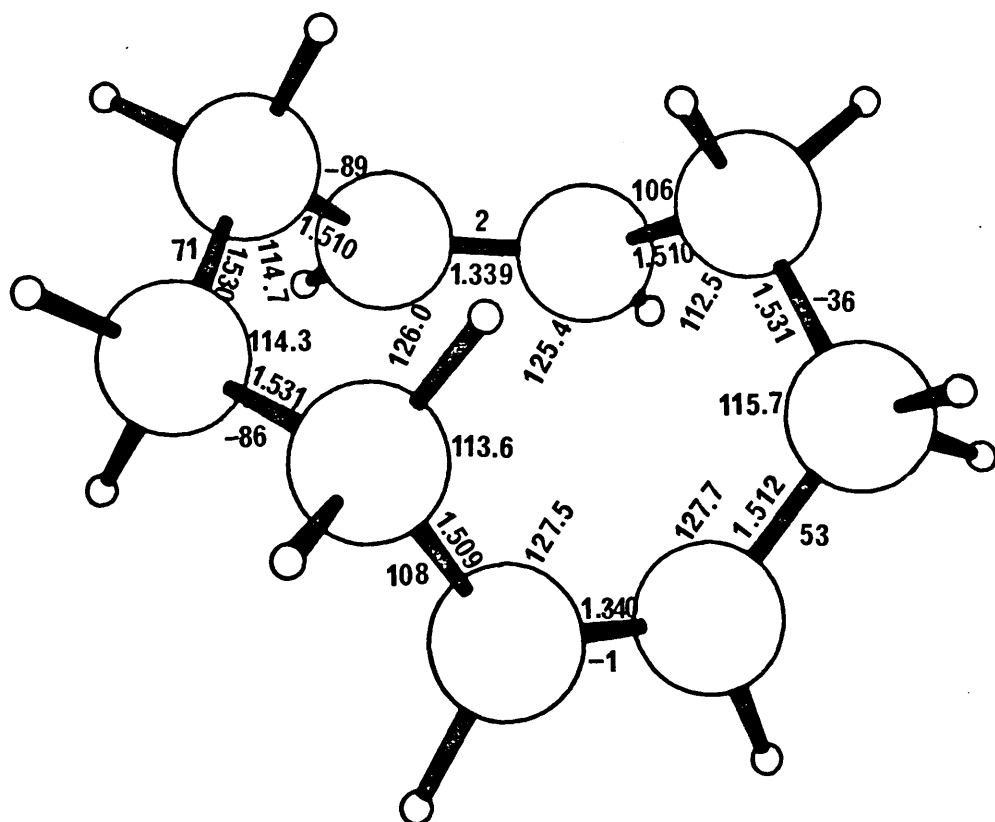
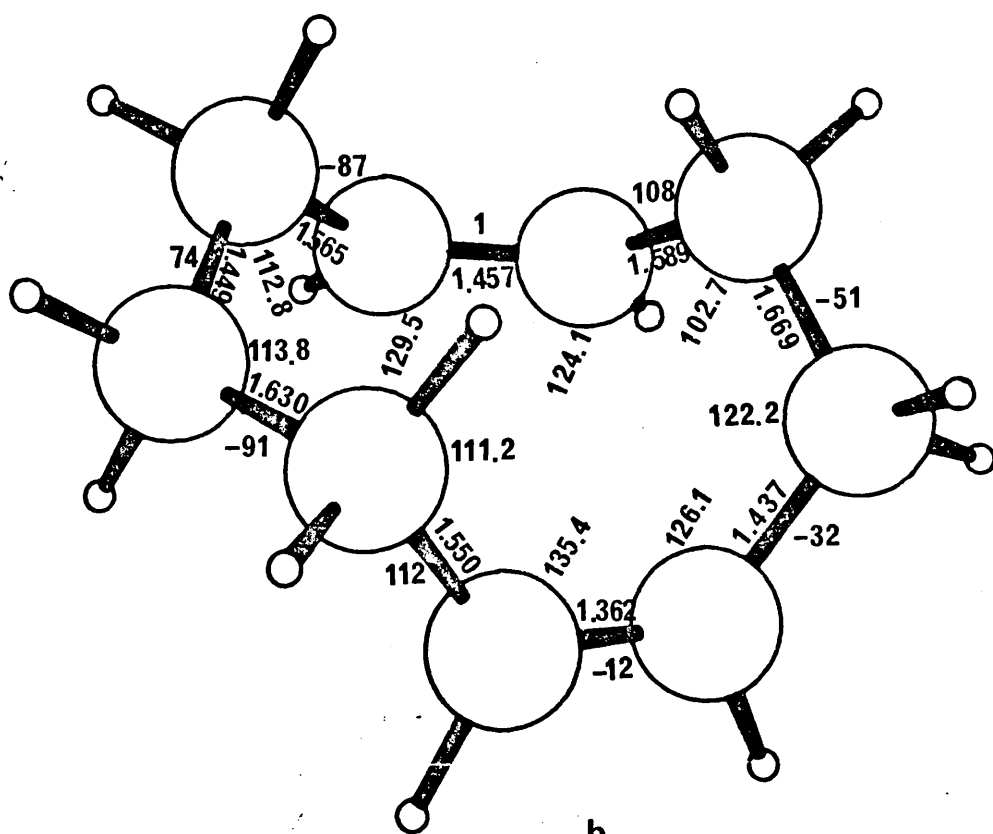


Figure 10: The calculated (a) and observed (b) structures of the cis,cis-cyclonona-1,5-diene ring as found in byssochlamic acid. Bond lengths and angles inner and torsion angles peripheral values.



a



b

The minimum energy cis,cis conformation is calculated to be 5.6 kcal./mole more stable than the lowest energy cis,trans conformation compared with a value of 4.3 kcal./mole derived from recent measurements of heats of hydrogenation. Some calculated and observed heats of hydrogenation are shown in Table 3 in Chapter 2.

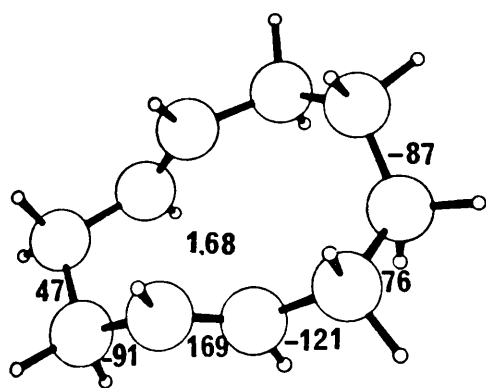
(h) Cyclodecadienes

The conformations of cyclodeca-1,5- and -1,6-dienes have not been previously studied in any great detail although the results of qualitative molecular mechanics calculations have been published,³⁷ and cis,cis-cyclodeca-1,6-dienes have been studied by Allinger³⁸ and Ermer.¹⁰

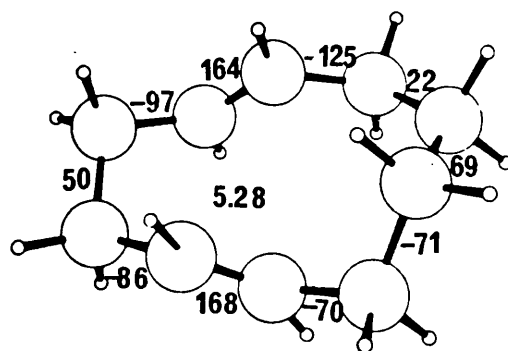
(i) Cyclodeca-1,5-diene (1,5-CDD)

The interest in this system stems from the fact that the 1,5-CDD ring is fairly widespread amongst naturally occurring germacranolides,³⁹ with one cis,trans and two trans,trans conformations observed via X-ray crystal structure analyses. The geometry and relative enthalpies of one cis,trans-, two cis,cis- and five trans,trans-conformers of 1,5-CDD have been calculated using the WBFF. The results are shown in Figure 11. The minimum energy conformation is the cis,trans-isomer shown in Figure 11(h) and its geometry is compared with that obtained from an X-ray crystal structure analysis of eupafornin⁴⁰ in Figure 12. There appears to be no experimental evidence regarding the minimum energy conformation of 1,5-CDD but the agreement of the calculated geometrical parameters for the cis,trans-isomer

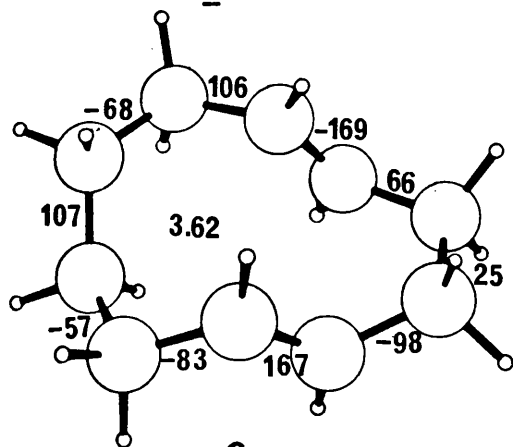
Figure 11: Cyclodeca-1,5-diene conformations; symmetries are
(a) C_2 , (e) C_2 .



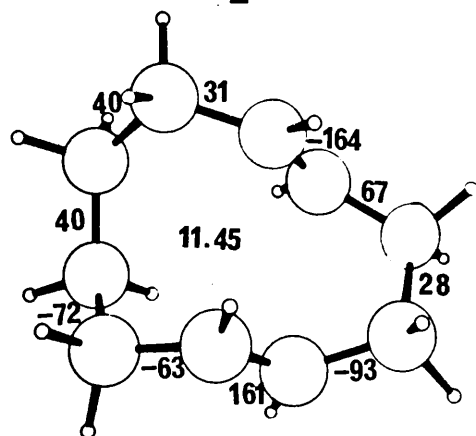
a



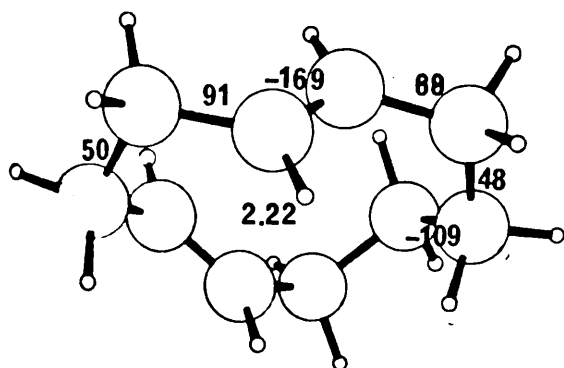
b



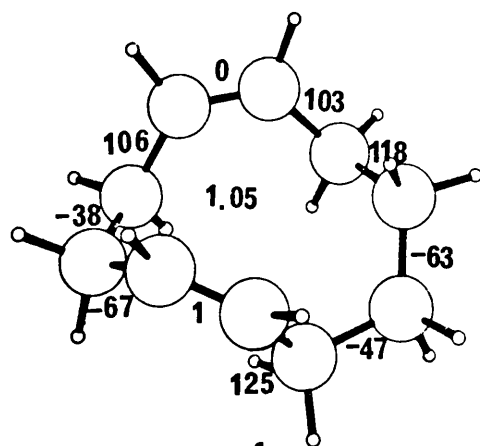
c



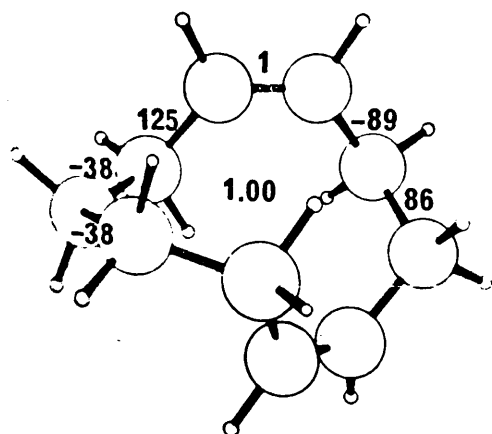
d



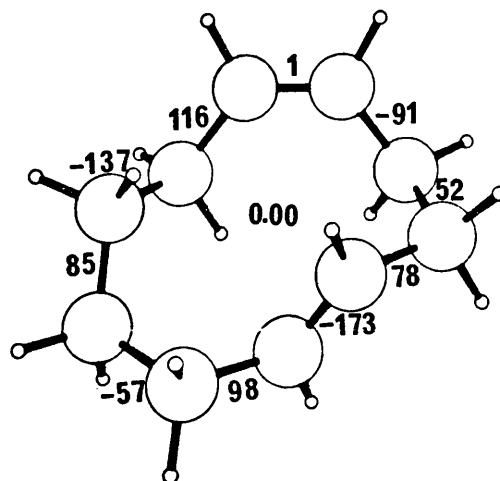
e



f

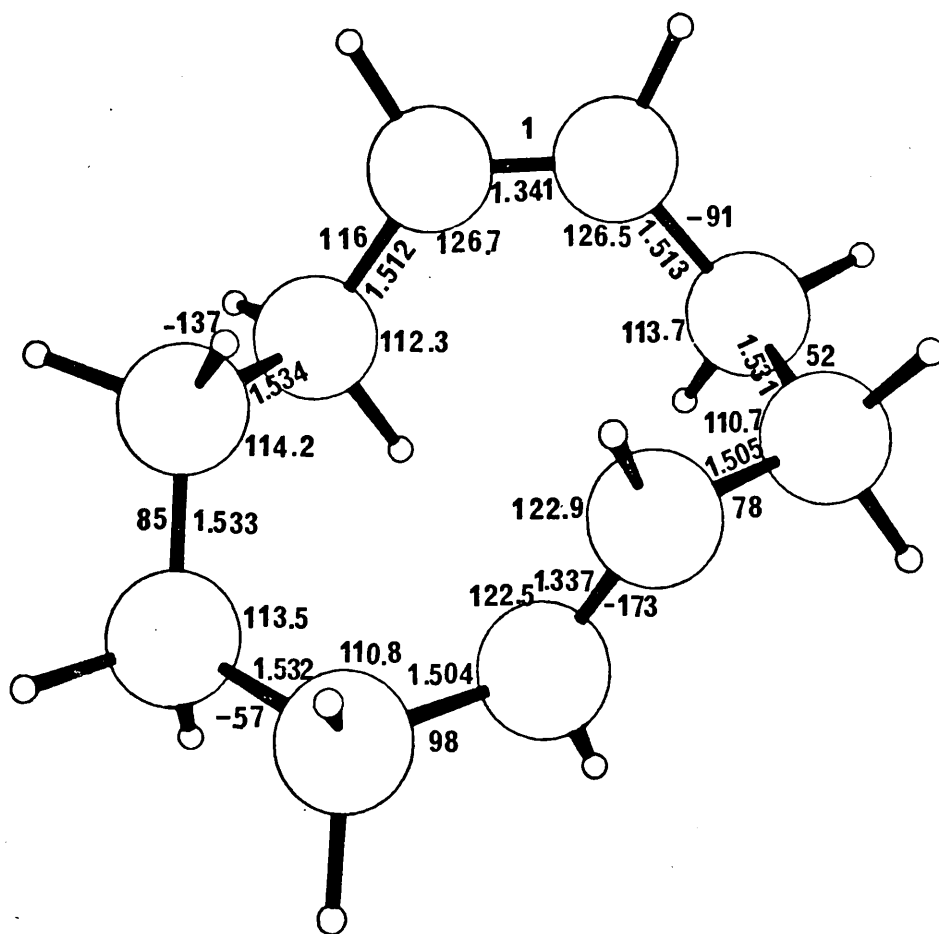


g

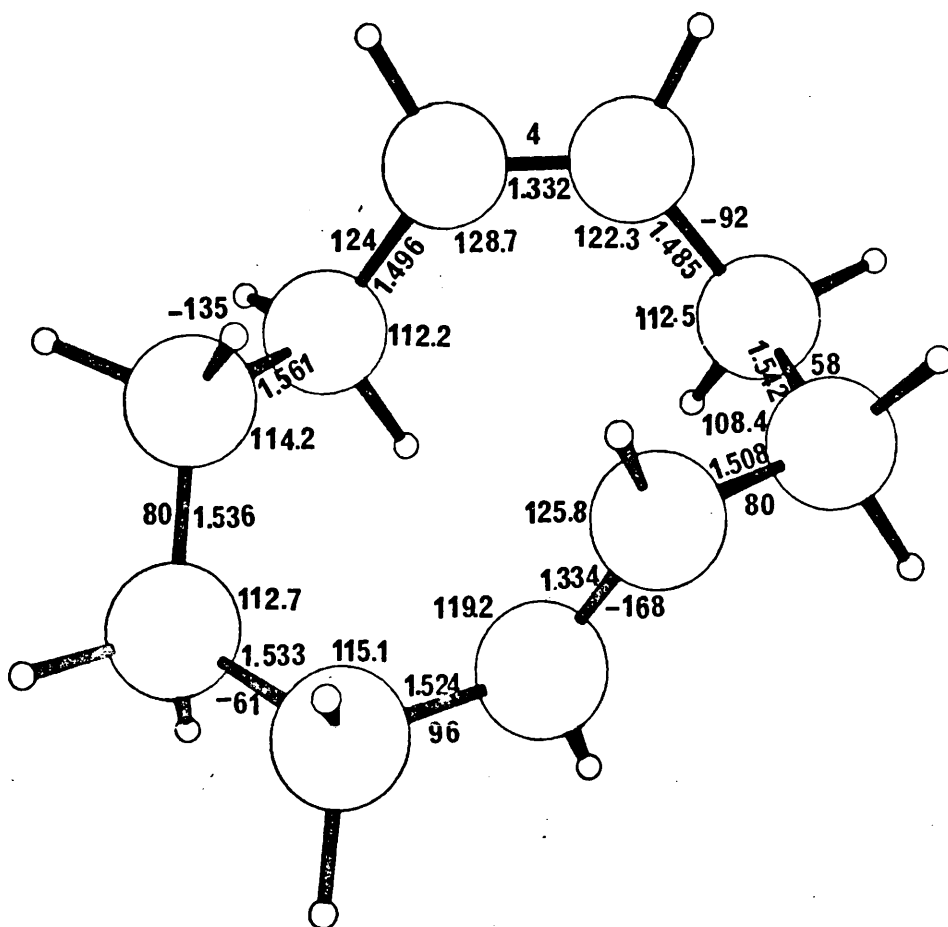


h

Figure 12: The calculated minimum energy conformation of cyclodeca-1,5-diene (a) compared with the geometry of the 10-ring of eupafornonin (b).



a



b

with the X-ray results is excellent, despite fairly heavy substitution of the 1,5-CDD ring in the latter instance. There are three other conformations within 2 kcal. /mole of the calculated global minimum; the two approximately isonergetic cis,cis isomers and the trans,trans-isomer shown in Figure 11(a). A conformation very similar to that of the lowest energy trans,trans-isomer has been observed in a series of germacranolides of which costunolide⁴¹ is a good representative. The conformer in Figure 11(a) has C_2 symmetry whilst the macrocycle in costunolide has only approximate C_2 symmetry because of its various substituents. Nevertheless, there is good agreement between the calculated geometry and the C_2 -averaged result from the X-ray crystal structure analysis,⁴¹ which are shown in Figure 13. There are also some experimental data regarding the conformation of Figure 11(e) and the calculated ring torsion angles are compared with those from an X-ray crystal structure analysis of Shiromodiol⁴² in Figure 14. A detailed comparison cannot be made because one of the double bonds is replaced by a trans-fused epoxide in the natural product; but the two conformations are qualitatively similar.

(ii) Cyclodeca-1,6-diene (1,6-CDD)

The 1,6-CDD system is better defined experimentally than the 1,5-isomer and a number of useful structural and thermodynamic measurements are available. Nine conformations of 1,6-CDD were studied by a development version of the WBFF and the results were published.⁴³ The geometries and relative enthalpies of eleven conformations of 1,6-CDD

Figure 13: The geometry of the calculated (a) minimum energy conformation of trans,trans-cyclodeca-1,5-diene compared with the C_2 averaged geometry of the macrocycle in costunolide (b).

- 132 -

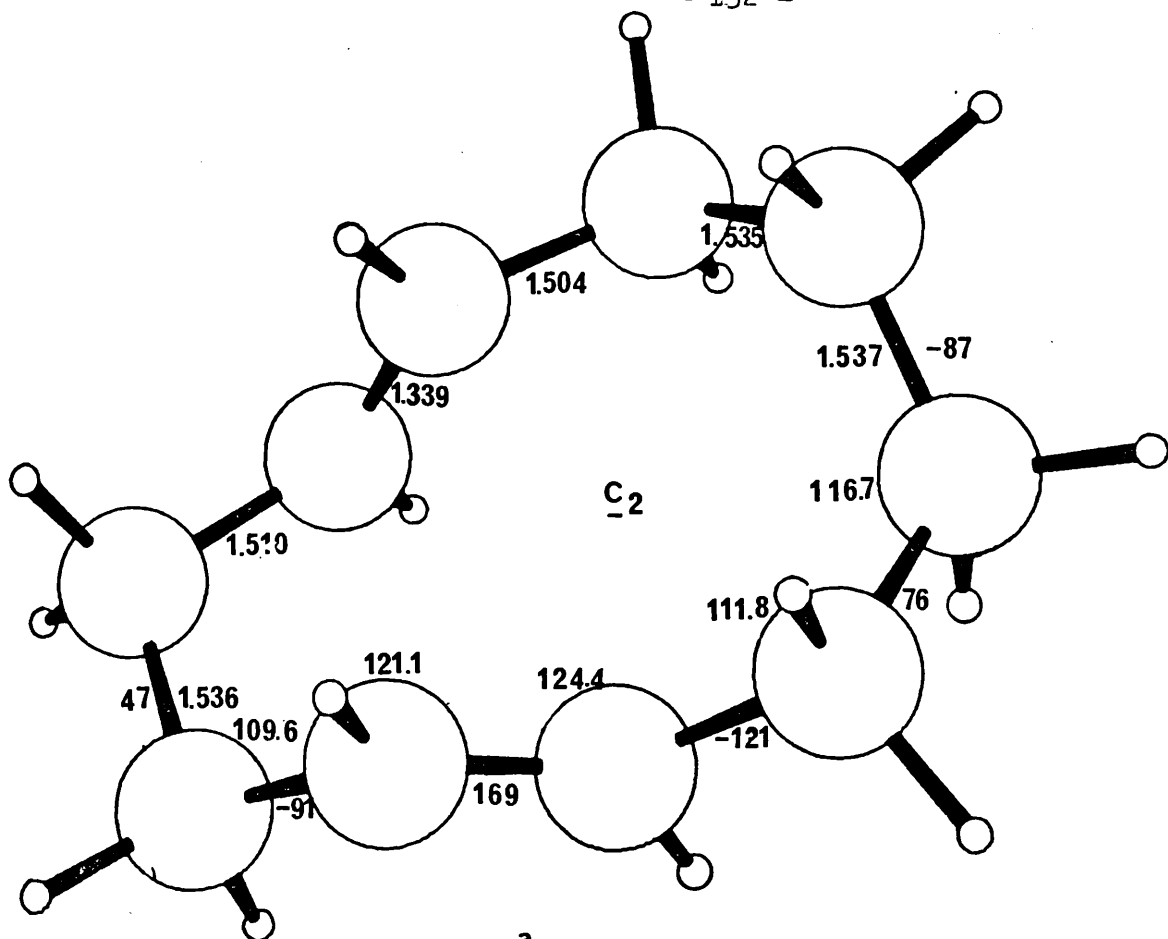
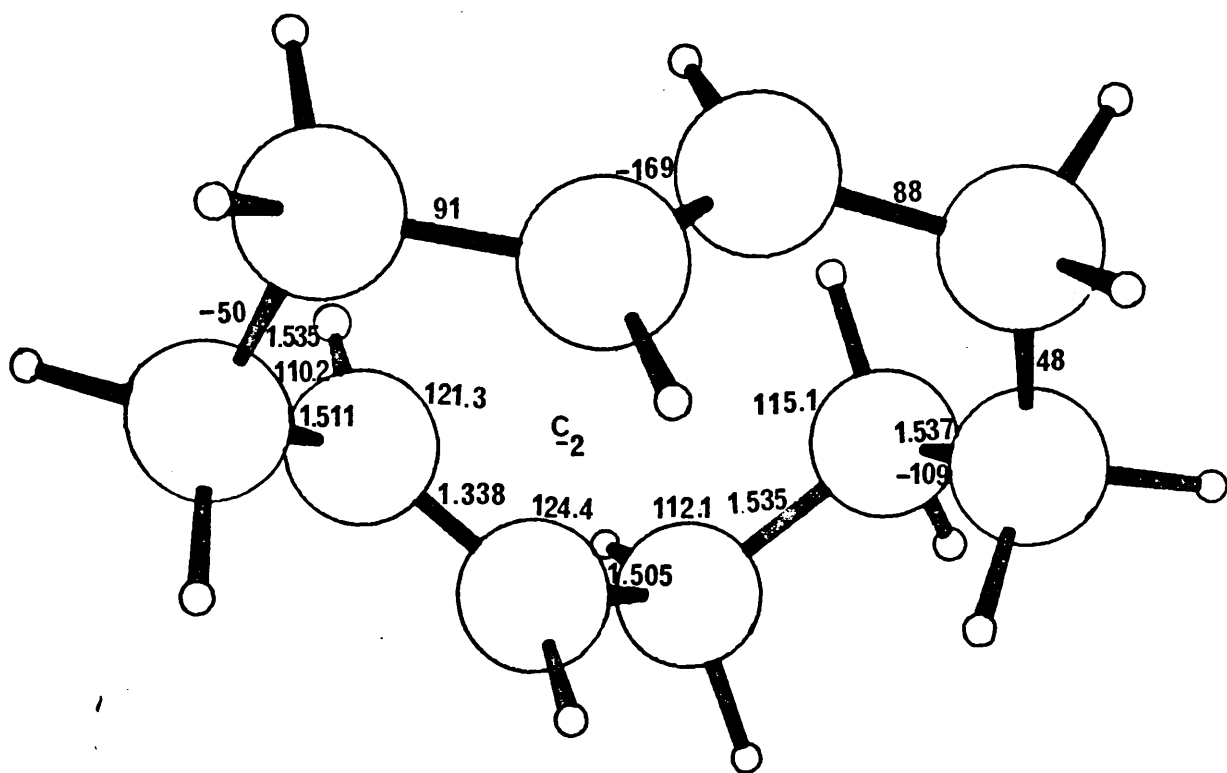
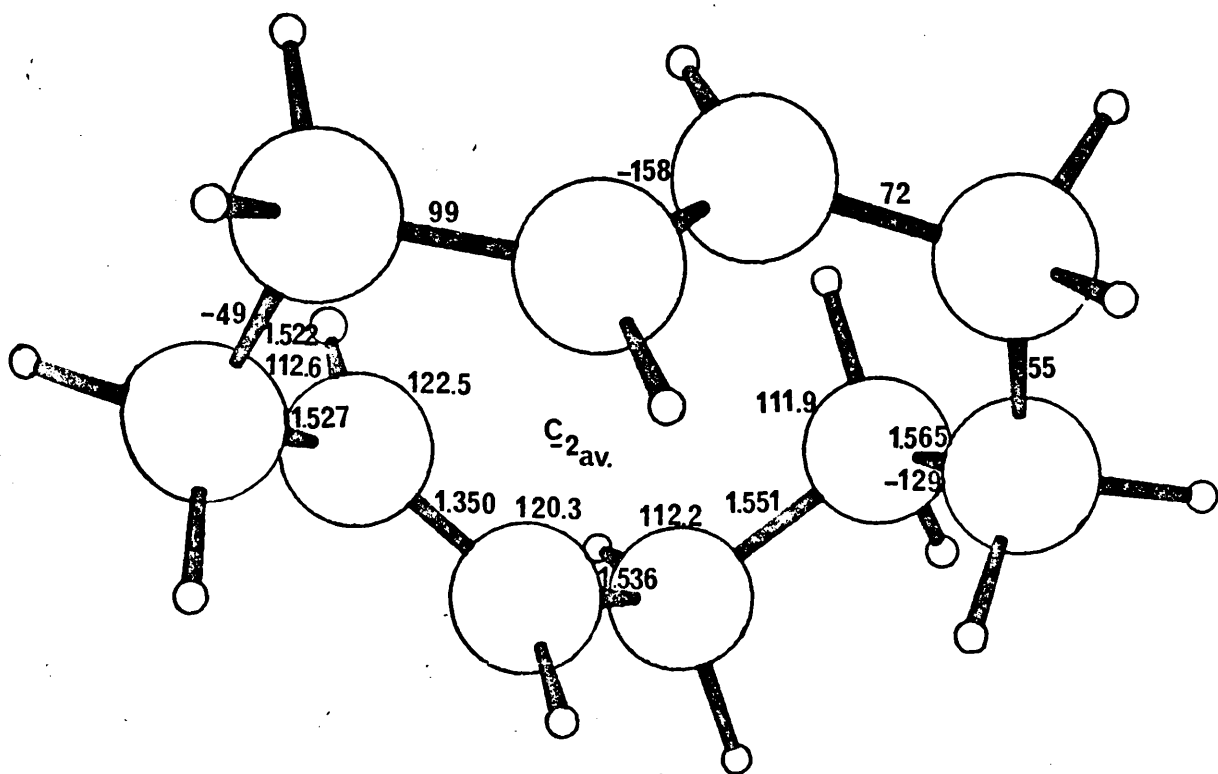


Figure 14: Calculated (a) and observed (b) geometries of the shiromodiol-type cyclodecadiene ring.



a



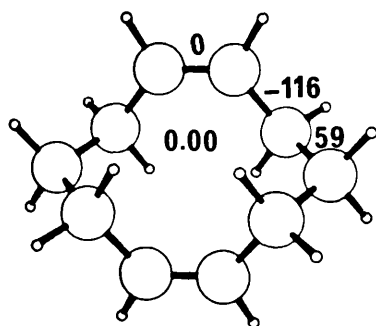
b

have been calculated with the present WBFF forcefield and results are shown in Figure 15. The global minimum is calculated to be the C_{2h} symmetric cis,cis-chair conformation, in excellent agreement with thermochemical measurements,^{11,44} and this has a molecular geometry almost exactly identical to that observed by gas phase electron diffraction⁴⁵ (see Table 4 in Chapter 2). The C_{2v} cis, cis-boat form (shown in Figure 15(b)) is, at best, barely present in the gas phase at 35°C⁴⁵ an observation which accords well with our calculated enthalpy difference of 1.2 kcal./mole between the two conformers which corresponds to 88% chair:12% boat (c.f. 0.16 kcal./mole with CFF¹⁰ and 0.30 kcal./mole with AFF⁹).

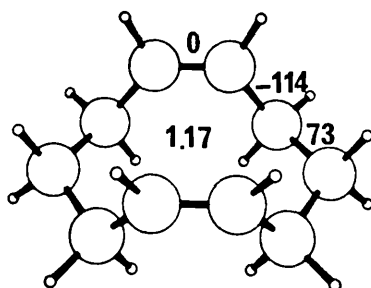
Equilibration experiments⁴⁴ indicate that although the cis,cis-isomer is certainly the predominant conformation there were detectable amounts of a cis,trans-isomer in the equilibrium mixture at 25°C and this would seem to correspond with the conformation of Figure 15(i) which has a calculated enthalpy 3.12 kcal. mole above that of the cis,cis-chair. No trans,trans-isomer was observed and therefore the calculated minimum energies for the cis,cis-chair and cis,trans-chair are probably 1-2 kcal./mole too high with respect to the trans,trans-isomer of Figure 15(d).

There is reasonable, if not conclusive evidence as to the minimum energy conformation of trans,trans-1,6-CDD. An X-ray crystal structure analysis of 2,7,-dibromo-3,8-dimethoxy derivative⁴⁶ has shown that the ten-membered ring adopts a crown conformation with C_i symmetry. Further-

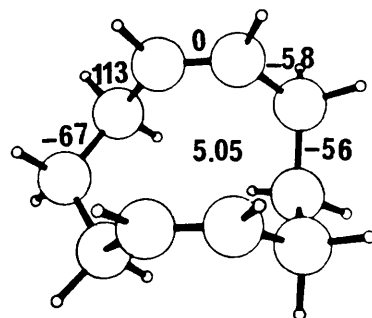
Figure 15: Calculated conformations of cyclodeca-1,6-diene
with the following symmetries (a) C_{2h} , (b) C_{2v} ,
(c) C_s , (d) C_{2h} , (e) C_s , (f) C_{2h} , (g) C_2 , (h) C_2 , (i) C_1 ,
(j) D_2 , (k) C_1 .



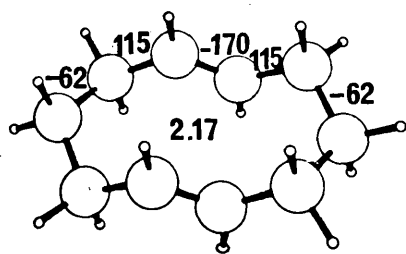
a



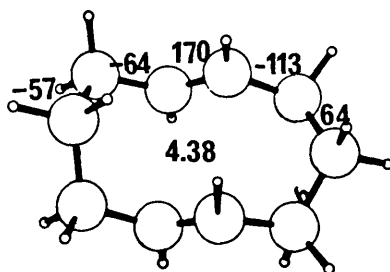
b



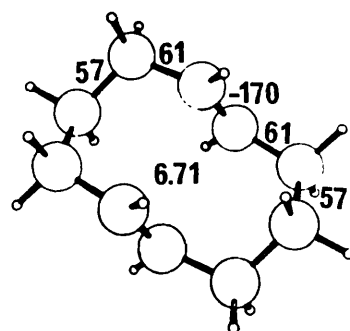
c



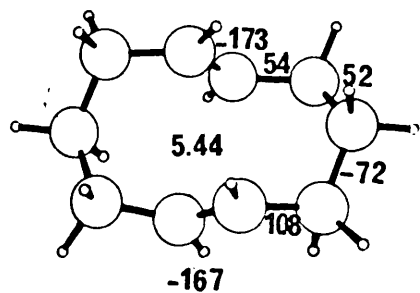
d



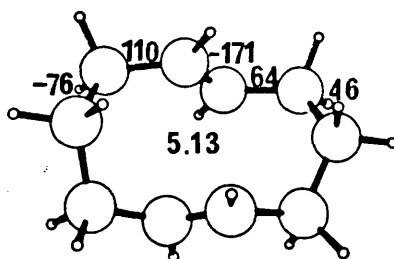
e



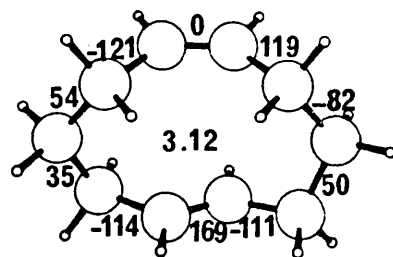
f



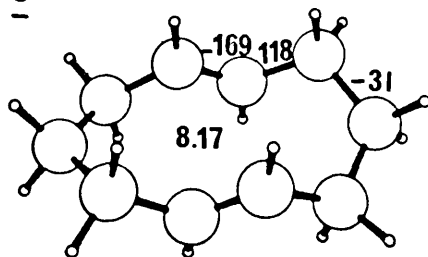
g



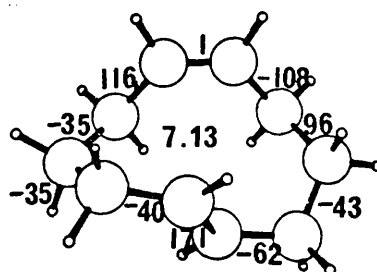
h



i

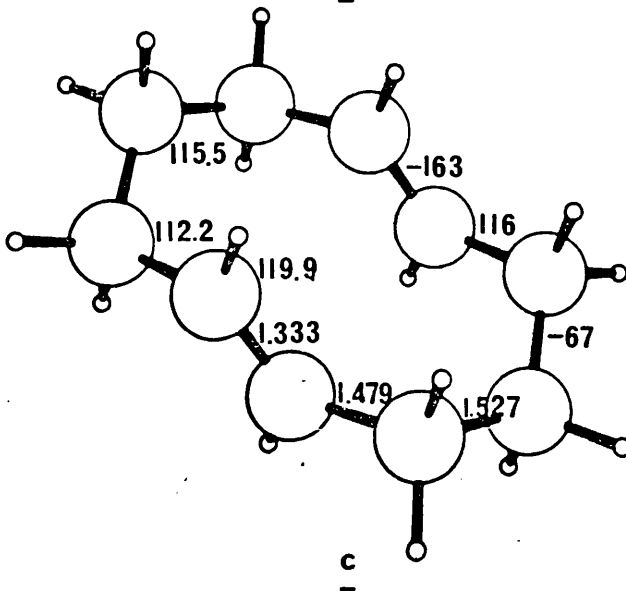
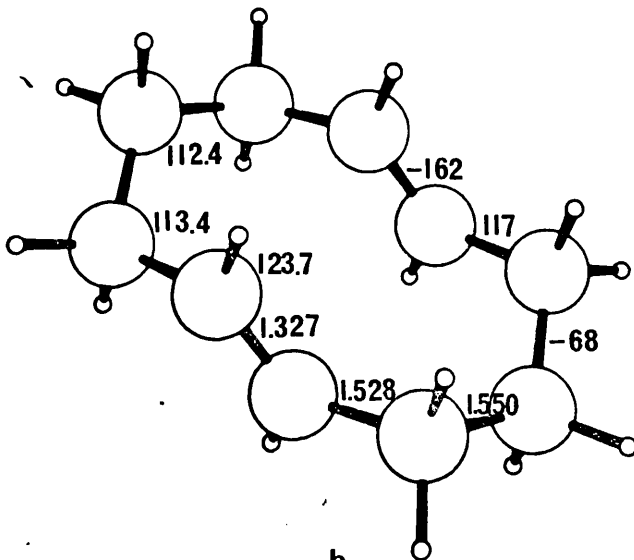
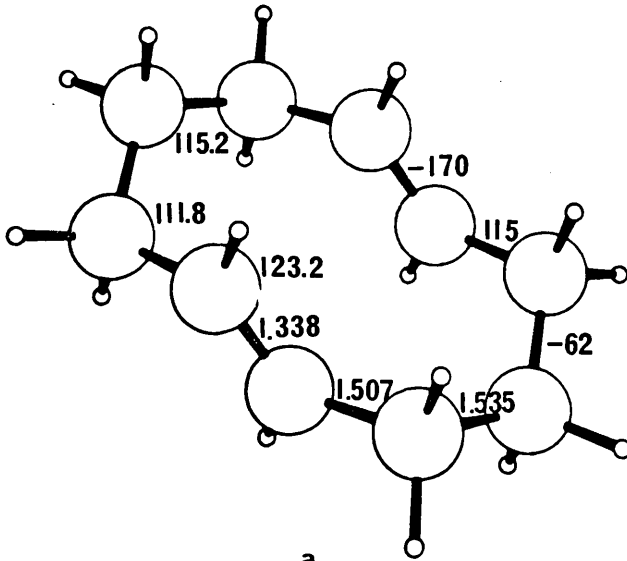


j



k

Figure 16: The calculated geometry (a) of the minimum energy trans,trans-cyclodeca-1,6-diene conformation compared with the C_{2h} averaged experimental values from X-ray crystal structure analyses of a substituted hydrocarbon (b) and 1,5-diaza-6,10-cyclodecadione (c).



more, 1,5-diaza-6,10-cyclodecadione⁴⁷ exhibits this same crown conformation with very similar ring torsion angles to the 1,6-CDD derivative. The similarities between the minimum energy conformations of medium ring alkenes and amides have been previously noted,^{10,48} and this, taken together with the fact that the same conformation occurs in two entirely different crystal structures, lends support to the calculation of the crown conformation of Figure 15(a) as the minimum energy trans,trans-variant. Our calculated conformation has C_{2h} symmetry whilst the substituents prevent the dibromo, dimethony derivative from adopting this form although the departure from a C_{2h} symmetry is not very great. The cyclic diamide has no symmetry and while the departure from C_{2h} is larger than for the dibromo, dimethony-1,6-CDD, it is still a reasonable approximation to the same. The three conformations are shown in Figure 16 with the results of the two crystal structure analyses averaged to give a C_{2h} symmetric ring.

(i) The Conformational Assignment of cis,cis,cis-1,5,9-cyclo- dodecatriene (CDDT)

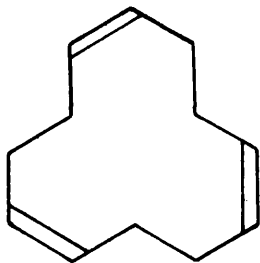
One of the most popular experimental techniques for investigating the conformations of molecules and their interconversions is nuclear magnetic resonance (NMR) analysis. The NMR spectrum of conformations which interconvert rapidly on the so-called NMR time scale will show averaged chemical shifts and coupling constants. When the interconversion is slow, each conformation will give rise to its own characteristic spectrum. In the intermediate

region, the spectrum is broadened, and suitable analysis can give the rate constants and free energies of activation (ΔG^\ddagger) for the interconversion.

When an organic chemist is interested in determining the minimum energy conformation of a particular molecule, he formulates all the conceivable contenders, and then, on the basis of the analysis of the NMR spectrum, eliminates those in which there is no correlation between the observed spectrum and the expected geometry, with the hope that the information from the spectrum will allow an unambiguous assignment of one of the postulated conformations as being the one of minimum energy. In practice, this is not usually the case as two or more of the proposed conformations are consistent with the observed spectrum.

This is therefore an area of application to which MM calculations can be applied as they calculate the steric energies and detailed geometries of all the proposed conformations and hence not only can they uniquely determine the minimum energy conformation but also verify the elimination of the other proposed conformations in a quantitative manner.

One illustrative example of the above is the attempted assignment of the minimum energy conformation of cis,cis,cis-1,5,9-cyclododecatriene (CDDT)⁴⁹ ring (XIII) by NMR analysis.



XIII

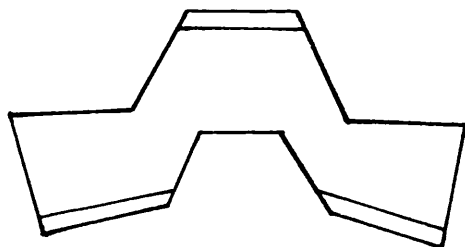
From an examination of molecular models, there seems to be four choices for the conformer of the CDDT ring - the crown (XIV(a)), the saddle (XIV(b)), the symmetrical s-trans (XIV(c)) and the unsymmetrical s-trans (XIV(d)). The crown (XIV(a)) and the saddle (XIV(b)) possess unfavourable nonbonded interactions due to the eclipsed hydrogens while the two s-trans conformations have repulsive transannular hydrogen interactions.

An NMR analysis of 1,5,9-tribromo-cis,cis,cis-1,5,9-cyclododecatriene has been performed⁴⁹ with the aim of determining its minimum energy conformation. Since molecular models indicate that the bromine atoms cause no serious steric interactions in these four conformations, we can assume that the conformation of the ring in the tribromotriene is very similar to that found in the unsubstituted compound (XIII). There is ample evidence that such an assumption is valid, e.g. the conformation of the cis,cis-cycloocta-1,5-diene ring derived from an X-ray crystal structure analysis of 3,7,-dibromo derivative⁵⁰ is very similar to that found by the electron diffraction study⁶ and MM calculations²³⁻²⁶ of the hydrocarbon itself.

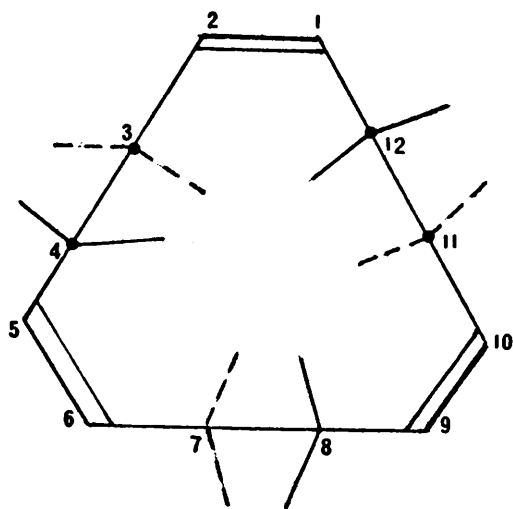
From the magnitudes of the vicinal coupling constants



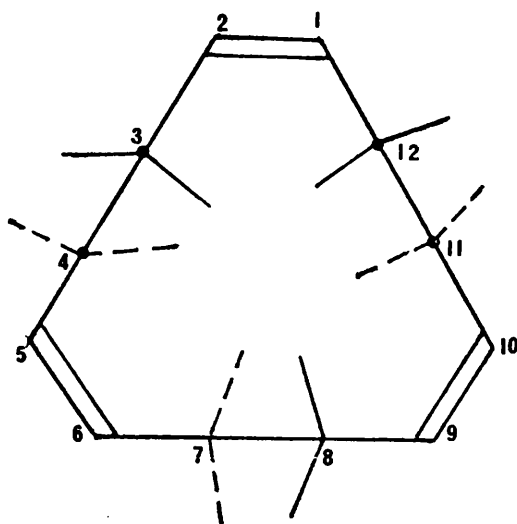
XIV (a) Crown



(b) Saddle

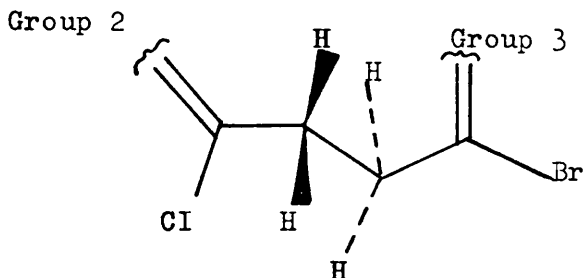


(c) unsymmetrical
s-trans



(d) symmetrical
s-trans

of the ethano hydrogens derived from the high-resolution proton spectrum of the tribromotriene,⁴⁹ it can be deduced that pairs of hydrogens are trans and pairs of hydrogens are gauche as shown below.



The only conformations of the postulated four which satisfy these conditions are the two s-trans conformations (XIV(c)) and (XIV(d)). Another factor from the NMR analysis which must be taken into account, is that the molecule is rapidly interconverting between equivalent conformations which implies that during this interconversion, the trans hydrogen pairs remain trans and the gauche pairs remain gauche - a condition that is satisfied by interconversion between equivalent s-trans conformations. In the crown conformation, however, pairs of hydrogen are cis and pairs are gauche, and the relative orientation is preserved in pairs during the rapid interconversion of equivalent crown conformations. During the interconversion among the six equivalent conformations of the saddle, the geminal hydrogens to the bromine assume all three possible orientations with respect to the ones, i.e. cis eclipsed, gauche (60°) and gauche (120°).

Therefore, on the basis of the data provided by the analysis of the nmr spectrum, the crown and saddle can be

rigorously excluded from being present to any appreciable extent, and hence one of the two s-trans conformations must be the minimum energy conformer. However, since the two s-trans conformations have identical spatial orientations of the ethano hydrogens and thus the same proton NMR spectrum, it is impossible to distinguish between them.

MM calculations, using WBFF, have been performed on the four possible conformations (XIV(a)-(d)) and the steric energies are 11.68, 11.48, 15.21 and 9.95 kcal./mole respectively which corresponds to a percentage composition of 6:7:0:87 at room temperature. These calculations thus indicate that, in fact, it is the unsymmetrical s-trans form which is the minimum energy conformation of the CDDT ring.

Molecular models indicate that repulsive interactions between transannular hydrogens at positions 4,8,12 and at positions 3,7,11 in the symmetrical conformation (XIV(c)) are more severe than the corresponding interactions at positions 3,8,12 and at positions 4,7,11 in the unsymmetrical conformation (XIV(d)). MM calculations confirm this and reveal that, in order to minimise the transannular strain, the internal bond angles in XIV(c) are increased with respect to those in XIV(d) (the average $C_{sp}^2 - C_{sp}^2 - C_{sp}^3$ angle is 1.4° and the average $C_{sp}^2 - C_{sp}^3 - C_{sp}^3$ is 1.8° greater in XIV(c) than in XIV(d)) and XIV(c) has considerably more Pitzer strain than XIV(d). Even with the angular and torsional distortions, the intra-annular H ... H distance is still only 2.07 \AA in XIV(c) compared to 2.15 \AA in XIV(d). Thus,

on account of this unfavourable nature of angular, torsional and nonbonded contributions to the steric energy, XIV(d) is found to have a lower steric energy by 5.26 kcal./mole than XIV(c).

Furthermore, the calculations indicate that the crown (XIV(a)) and the saddle (XIV(b)), not unexpectedly, suffer appreciably from the unfavourable nonbonded interactions of the eclipsed hydrogens in the ethano groups and have higher steric energies than the unsymmetrical s-trans (XIV(d)).

Moreover, from the detailed geometry and relative steric energy that MM calculations provide for each conformation, it is often possible to interpret experimental observations which is otherwise not feasible. To illustrate this, one feature of the observed vicinal coupling constants (10.57 and 5.49) of the ethano hydrogens in the tribromotriene is that they are at the lower and upper ends of the ranges for trans (10.5-12.4 cps) and gauche (2.7-5.4 cps) vicinal coupling constants for six- or larger membered rings. This can be interpreted as being a result of one of two effects:

(i) Small proportions of the crown and/or saddle conformers are present in equilibrium with the unsymmetrical s-trans conformation, and

(ii) the unsymmetrical s-trans conformer (XIV(d)) is skewed away from a pure s-trans arrangement of their ethano hydrogens in order to relieve part of the strain energy due to transannular hydrogen interactions.

Results from the force field calculations imply that the

crown and saddle conformations are only present to a very small extent (6 and 7 per cent respectively) and that the s-trans arrangement, in the unsymmetrical conformation (XIV(d)), which is calculated to be the minimum energy conformation, is found to be skewed away from the pure s-trans form by, on average, 14° . Considering the magnitudes of these two effects, MM calculation favour the latter of the two explanations.

3.5. References

1. E.L. ELIEL. "Stereochemistry of Carbon Compounds", McGraw-Hill, New York, N.Y., p 189, (1962).
2. E.L. ELIEL in M.S. Newman, ed., "Steric Effects in Organic Chemistry", John Wiley & Sons, Inc., New York, p.121 (1956).
3. V. PRELOG and M.KOBELT, Helv.Chim.Acta., 32, 1187 (1949).
4. H.C. BROWN and G. HAM. J.Amer.Chem.Soc., 78, 2735 (1956).
5. E.L. ELIEL. "Stereochemistry of Carbon Compounds", McGraw-Hill, New York, N.Y., p.192 (1962).
6. L. HEDBERG and K. HEDBERG. Abs.Papers, Nat.Meeting Amer. Cryst.Ass., 1964, Bozeman, Montana.
7. J.F. CHIANG and S.H. BAUER. J.Amer. Chem.Soc., 91, 1898 (1969).
8. G.V. SMITH and H. KRILOFF. J.Amer.Chem.Soc., 85, 2016 (1963).
9. N.L. ALLINGER and J.T. SPRAGUE. J.Amer.Chem.Soc., 94, 5734 (1972).
10. O.ERMER and S.LIFSON. J.Amer.Chem.Soc., 95, 4121 (1973)
11. R.B. TURNER, B.J. MALLON, M.TICHY, W.von E. DOERING, W.R. ROTH and G.SCHRÖDER. J.Amer.Chem.Soc., 95, 8605 (1973).
12. F.K. WINKLER, Dissertation, E.T.H. Zurich, Nr.5171 (1973).

13. E.J. COREY, F.A. CAREY and R.A.E. WINTER. J.Amer. Chem.Soc., 87, 934 (1965).
14. A.F. CAMERON, K.K. CHEUNG and J.M. ROBERTSON. J.Chem.Soc.(B), 559 (1969)
15. F.K. WINKLER and J.D. DUNITZ, J.Molec.Bio., 59, 169 (1973).
16. (a) P. GANIS, U.LEPORE, E.MARTVSCELLI, J.Phys.Chem., 74, 2439 (1970).
(b) P.C. MANOR, D.P. SHOEMAKER, A.S. PARKES, J.Amer.Chem.Soc., 92, 5260 (1970).
17. R.M. GAVIN, Jr. and Z.F. WANG. J.Amer.Chem.Soc., 95, 1425 (1973).
18. O. ERMER, Angew. Chem.Int.Ed.Engl., 13, 604 (1974).
19. M. TRAETTEBERG, Acta.Chem.Scand., Ser.B.29, 29 (1975).
20. G. FERGUSON and D. HAWLEY, Unpublished results,
21. (a) O. ERMER, H. ESER and J.D. DUNITZ, Helv.Chim.Acta, 54, 2469 (1971);
(b) P.GANIS and J.D. DUNITZ. Helv.Chim.Acta., 50, 2379 (1967).
22. F.A.L. ANET and L. KOZERSKI. J.Amer.Chem.Soc., 95, 3407 (1973).
23. F.A.L. ANET and R. ANET in Dynamic Nuclear Magnetic Resonance Spectroscopy. F.A. Cotton and L.M. Jackson, Ed., Academic Press, New York, p 571 (1975).
24. N.L. ALLINGER and J.T. SPRAGUE, Tetrahedron, 31, 21 (1975).

25. O. ERMER. J.Amer.Chem.Soc., 98, 3964 (1976).
26. M.H.P. GUY, Ph.D.Thesis, University of Glasgow, (1976).
27. K.B. WIBERG and R.H. BOYD, J.Amer.Chem.Soc., 94, 8426 (1972).
28. D.N.J. WHITE and O. ERMER. Chem.Phys.Lett., 31, 111, (1975).
29. A.C. COPE, C.F. HOWELL and A. KNOWLES, J.Amer.Chem.Soc., 84, 3190 (1962).
30. A.C. COPE, C.F. HOWELL, J. BOWERS, R.C. LORD and G.M. WHITESIDES, J.Amer.Chem.Soc., 89, 7136 (1967).
31. G.M. WHITESIDES, G.L. GOE and A.C. COPE, J.Amer.Chem.Soc., 89, 7136 (1967).
32. A.C. COPE, J.K. HECHT, H.W. JOHNSON, Jr., H. KELLER and H.J.S. WINKLER, J.Amer. Chem.Soc., 88, 761 (1966).
33. D. DEVAPRABHAKARA, C.G. CARDENUS and P.D. GARDNER, J.Amer.Chem.Soc., 85, 1553 (1963).
34. R. VAIDYANATHASWANY and D. DEVAPRABHAKARA, J.Org.Chem., 32, 4143 (1967).
35. F. ZUCCARELLO, G. BUEMI and G. FAVINI. J.Mol.Struct., 8, 459 (1971).
36. I.C. PAUL, G.A. SIM, T.A. HAMOR and J.M. ROBERTSON, J.Chem.Soc., 5502 (1963).
37. G. BUEMI, F. ZUCARELLO and G. FAVINI. J.Mol.Struct., 21, 41 (1974).
38. N.L. ALLINGER, M.T. TRIBBLE and J.T. SPRAGUE. J.Org.Chem., 37, 2423 (1972).

39. G.A. SIM in Molecular Structure by Diffraction Methods, The Chemical Society, London, Vol 2, p 131 and Vol 3 p 163 (1974).
40. A.T. McPHAIL and K.D. ONAN. J.Chem.Soc Perkin II, 578 (1976).
41. M.J. BOVILL, P.J. COX, P.D. CRADWICK, M.H.P. GUY, G.A. SIM and D.N.J. WHITE. Acta Cryst ., B32, 3203 (1976).
42. R.J. McCLURE, G.A. SIM, P. COGGON and A.T. McPHAIL. Chem.Comm., 128 (1970).
43. D.N.J. WHITE and M.J. BOVILL, Tetrahedron Letters, 2239 (1975).
44. J. DALE, Angew Chem.(Int.Ed.), 5, 1000 (1966).
45. A. ALMENNINGEN, G.G. JACOBSEN and H.M. SEIP. Acta. Chem.Scand., 23, 1495 (1969).
46. D.N.J. WHITE. Helv.Chim.Acta, 56, 1347 (1973).
47. T.SRIKRISHNAN and J.D. DUNITZ. Acta Cryst, B31, 1372 (1975).
48. D.N.J. WHITE and M.H. GUY. J.Chem.Soc.Perkin II, 43 (1975).
49. S. CASTELLANO and K.G. UNTCH. J.Amer.Chem.Soc., 88, 4238 (1966).
50. R.K. MACKENZIE, D.D. MacNICOL, H.H. MILLS, R.A. RAPHAEL, F.B. WILSON and J.A. ZABKIEWIEZ, J.Chem.Soc. Perkin II, 1632 (1972).

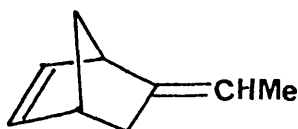
CHAPTER FOUR

Molecular mechanics calculations on the
stability of bridgehead olefins in bicyclo-
(m.n.l)alk-1-ene systems.

4.1 Introduction

On the basis of experimental data regarding anomalies associated with the bridgehead position of bridged bicyclic compounds, Bredt¹, Fawcett² and Wiseman³ proposed rules regarding the stability of bridgehead olefins.

The first aim of this study was to determine if the White-Bovill alkane/alkene force field* (referred to as WBFF) could satisfactorily reproduce the available experimental data on bridgehead olefins. On account of the fact that all the relevant experimental data was of a qualitative nature, it was impossible to include any such data in the parametrization of the WBFF. However other highly strained but isolable bicyclic olefins e.g. 5-ethylidenenorbornene (I), norbornadiene (II) and α -pinene (III) and strained trans-cycloalkenes were included in the parametrization of the WBFF, which accurately predicted the geometric and thermodynamic properties of these compounds (see Tables 3 and 4 in Chapter 2).



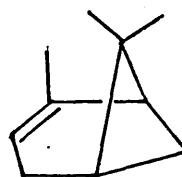
I

V_s 25.22
(kcal./mole)



II

31.32



III

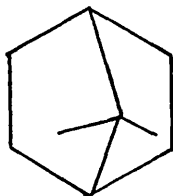
38.23

* The development and results of the WBFF are discussed fully in Chapter 2.

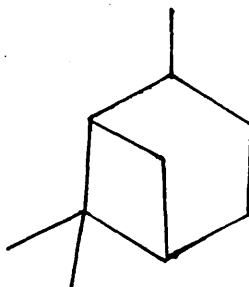
The second aim of this study is to assess the limits of application of the proposed rules and where possible, provide guidelines or rules for situations, not covered by the previous rules.

4.2 Review

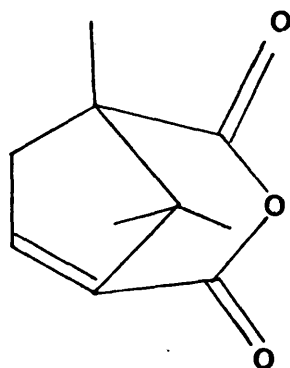
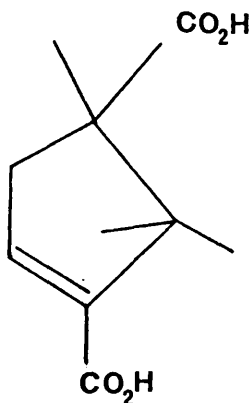
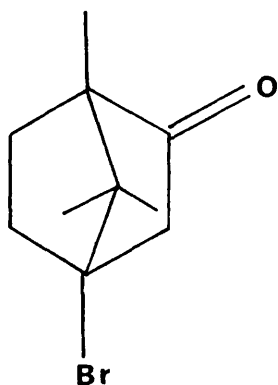
During Bredt's investigations of camphane (IV) and pinane (V) derivatives between 1900 and 1924⁴, he recognised the reluctance of bridged bicyclic systems to allow the placement of double bonds at their bridgeheads. His original formulation of the rule presently bearing his name suggests that 'double bonds at the bridgehead atoms of camphenes, pinenes and similarly constituted bicyclic compounds impose an unnatural spatial arrangement upon the involved atoms and these compounds would therefore suffer prohibitive strain' or, more precisely, when a double bond is constrained at the bridgehead position of a bicyclic compound, the four groups attached to the olefinic linkage deviate significantly from coplanarity with the trigonal centres, as a result of the torsional strain and the π -bond is therefore weakened due to poor overlap.



IV



V



Chemical evidence supporting Bredt's rule includes the failure of bromocamphor (VI) to eliminate hydrogen bromide in the presence of a base and the failure of the unsubstituted diacid (VII) to cyclise to its anhydride(VIII).

Systematic investigations of the limits of Bredt's rule were undertaken during the late 1940's by Prelog⁵. Ring closure of the diketone (A) in Figure 1 may give rise to either the fused-ring system(B) or the bridged-ring system(C). Prelog concluded from these results that

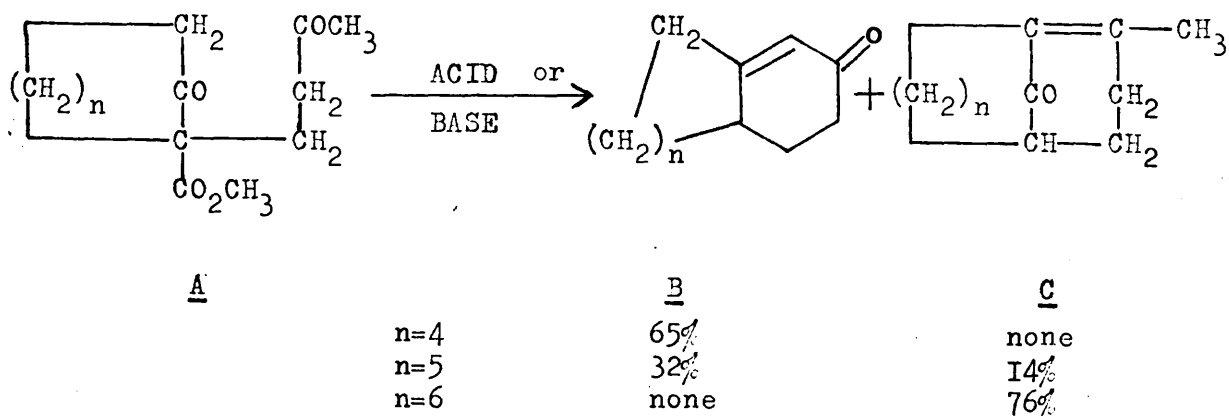
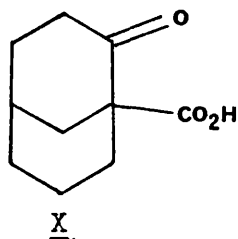
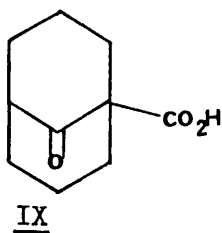


Figure 1. Limitations of Bredt's Rule

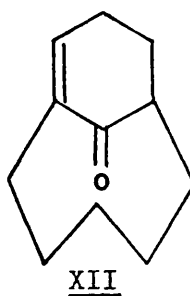
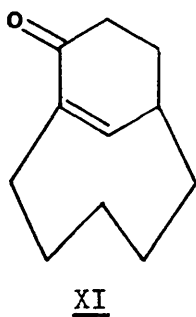
larger bicyclic ring systems can, in fact, accommodate bridgehead double bonds and that bicyclic ring systems

in the (n.3.1) series with $n = 5$ can have a bridgehead double bond, whereas the bicyclo (4.3.1) decyl and smaller systems cannot. (It has been noted^{3,6} that all these experiments were performed under equilibrating conditions and as a result, would give the thermodynamically preferred product.)

In Fawcett's review², attempts were made to define the limits of Bredt's rule more precisely and a stability (or strain) parameter S was introduced. In bicyclo (x, y, z) alk-1-enes, S is the sum of the number of atoms in the bridge, i.e. $S = x + y + z$ and the smallest observed value at the time was 9. Fawcett therefore suggested that bridged bicyclic systems with $S \geq 9$ are large enough to permit isolation of bridgehead alkene, whereas those systems, with $S = 6$ or 7, would exist solely as transient species. However, this S criterion for stability did not explain why β -keto acid (IX) resists decarboxylation⁷ while β -keto acid (X) decarboxylates readily⁸ - in (IX) and (X), $S = 7$.

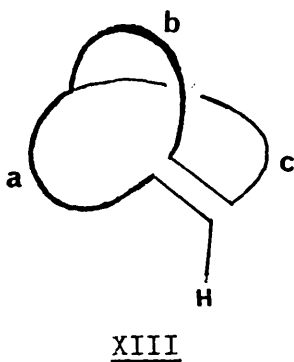


Neither does it explain the instability of the enone (XI)⁹ and the stability of enone (XII)⁹ as $S = 9$ in both enones. Despite the fact that Fawcett's proposal did not



take into account the fact that the stability of a bridgehead double bond depends on which branch of the bicyclic system contains it, it was 17 years before it was superceded.

In 1967, recognition by Wiseman³ that the determining factor was the size of the smallest ring containing a trans linkage replaced the S criterion for stability. Structure XIII represents a bicyclic alkene with a bridgehead double bond. Wiseman noted that the double



bond in XIII is exocyclic to ring ab, but endocyclic in rings ac and bc. Since the double bond is at the bridgehead of rings ac and bc, it follows that it must be cis in one ring (in this case, bc) and trans in the other (in this case, ac). He then postulated that 'the strain in bridgehead alkenes is closely related to the strain of

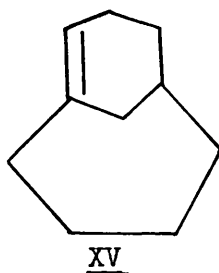
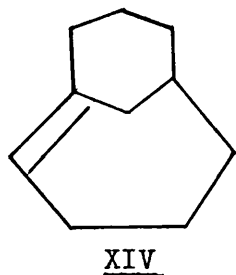
trans-cycloalkenes. Ordinarily, a bridgehead double bond will be more stable when it is trans in the larger of the two rings, in which it is exocyclic'.

The strain of trans-cycloalkenes was discussed in Chapter 3. trans-Cyclohexene has never been isolated, but has been invoked as a transient intermediate in many reactions. Bridgehead alkenes containing a trans-cyclohexene ring might be expected to be totally inaccessible. trans-Cycloheptene has been generated and trapped but not yet observed spectrophotometrically, therefore a bicyclic bridgehead olefin incorporating a trans-cycloheptene fragment may be isolable. trans-Cyclooctene and higher trans-cycloalkenes have been isolated, so that a bridgehead alkene should be isolable when the larger of the two rings containing the double bond is at eight-membered.

This hypothesis is qualitatively supported by decarboxylation studies of bicyclo β -keto acids³ and enolisation of ketones¹⁰. It explains why the decarboxylation of IX is less facile than X - IX involves a trans-cyclohexene intermediate while X involves a trans-cyclooctene intermediate. Similarly, XI contains a trans-cyclooctene ring as opposed to the more stable trans-cyclodecene ring in XII.

However, in a recent review⁶, it has been noted that this criterion is quantitatively inadequate in the respect

that it does not differentiate between bicyclo (4.3.1) dec-1(2) ene (XIV) and bicyclo (4.3.1) dec-1(9)-ene (XV), each of which contain a trans-cyclononene ring and an S value of 8.

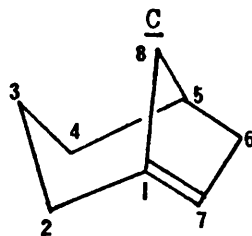
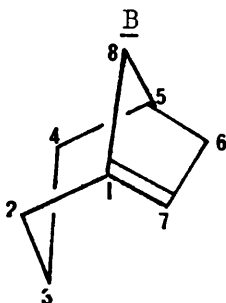
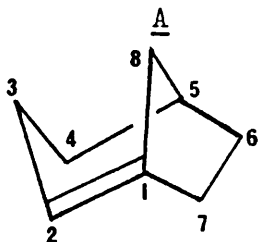


4.3 Molecular Mechanics (MM) Calculations and Results

MM calculations, using the WBFF, were performed on a carefully selected group of seventeen bridged bicyclic olefins (A-Q), sixteen of which are bridgehead olefins. All seventeen compounds are shown in Figure 2 with their corresponding steric energy, Vs (kcal/mole). All compounds were minimised until all the first derivatives of the potential energy with respect to the atomic cartesian co-ordinates were less than 10^{-7} kcal/mole⁻¹ Å⁻¹. All compounds, except G, represent energy minima. The failure of G to exhibit this feature is probably due to the instability of the calculations at such a high steric energy value (59.46 kcal/mole). The torsion angles for each bicyclic compound is given in Table 1.

Table 2 shows the bridgehead olefins listed in

(a) Bicyclo(3.2.1)octene systems.

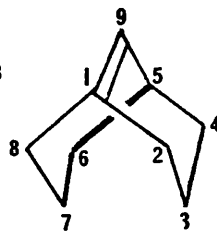
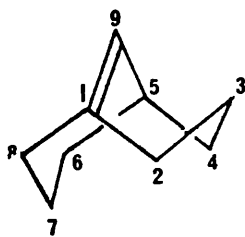
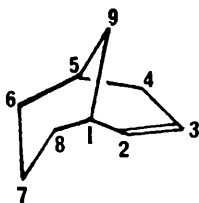
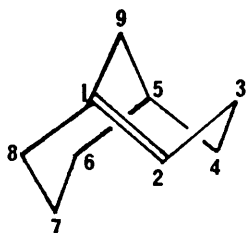
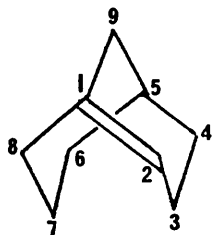


V_s 40.53
(kcal./mole)

40.15

40.99

(b) Bicyclo(3.3.1)nonene systems.



V_s 51.93
(kcal./mole)

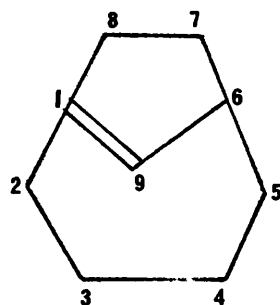
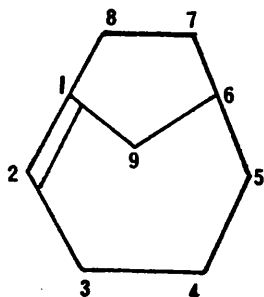
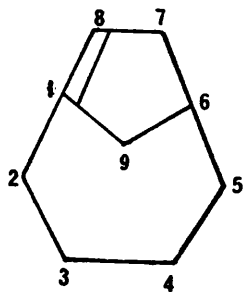
26.52

7.03

59.46

49.99

(c) Bicyclo(4.2.1)nonene systems.



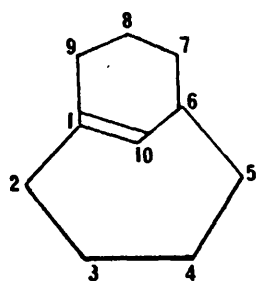
V_s 26.25
(kcal./mole)

31.14

58.51

Figure 2: The bicyclic olefins used in the study.

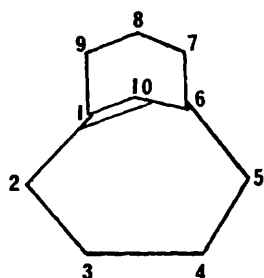
(d) Bicyclo(4.3.1)decene systems.



L

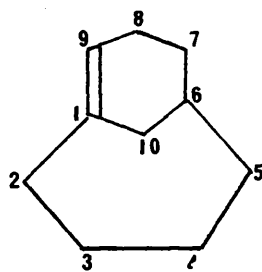
V_s 35.84

(kcal./mole)



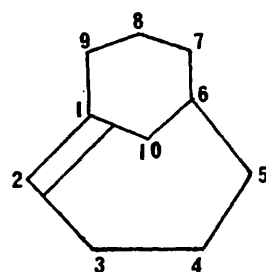
M

55.98



N

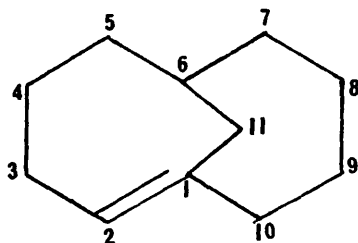
17.57



O

20.30

(e) Bicyclo(4.4.1)undecene system.

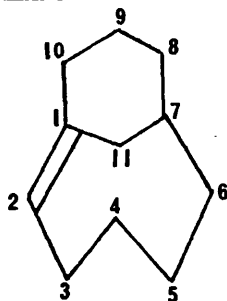


P

V_s 12.41

(kcal./mole)

(f) Bicyclo(5.3.1)undecene system.



Q

V_s 12.82

(kcal./mole)

Figure 2: (contd.)

TABLE 1: TORSION ANGLES (IN DEGREES) OF BICYCLIC BREDT COMPOUNDS.

(A) BICYCLO(3.2.1)OCTENES.

COMPOUND	A	B	C
TORSION ANGLE			
1,2,3,4	-46	-31	-14
1,7,6,5	-15	-27	-23
2,3,4,5	35	27	33
3,4,5,8	31	-50	15
3,4,5,6	-83	64	-97
4,5,8,1	-75	68	-64
4,5,6,7	93	-65	62
5,8,1,2	75	-100	103
5,8,1,7	-71	44	-45
6,5,8,1	47	-54	56
6,7,1,2	-93	128	-133
7,1,2,3	132	-66	90
7,6,5,8	-24	53	-54
8,1,2,3	-13	78	-57
8,1,7,6	56	-16	15

TABLE 1: TORSION ANGLES (IN DEGREES) OF BICYCLIC BREDT COMPOUNDS (CONTD.).

(8) BICYCLO(3.3.1)NONENES.

COMPOUND	D	E	F	G	H
TORSION ANGLE					
1,2,3,4	55	-48	7	-45	39
1,9,5,6	71	62	63	61	68
2,3,4,5	-40	42	-1	48	-44
3,4,5,6	-78	-105	-95	-116	-64
3,4,5,9	40	16	25	8	53
4,5,6,7	65	75	61	65	78
4,5,9,1	-83	-64	-57	-60	-56
5,6,7,8	39	38	51	48	34
5,9,1,2	76	66	65	65	59
6,7,8,1	-38	-43	-48	-43	-37
7,8,1,2	-87	-79	-70	-77	-82
7,8,1,9	57	77	53	49	65
8,1,2,3	63	147	84	128	91
8,1,9,5	-72	-90	-60	-61	-86
9,1,2,3	-81	-8	-39	-8	-52
9,5,6,7	-60	-49	-58	-52	-43

TABLE 1: TORSION ANGLES (IN DEGREES) OF BICYCLIC BREDT COMPOUNDS (CONTD.).

(C) BICYCLO(4.2.1)NONENES.

COMPOUND	I	J	K
TORSION ANGLE			
1,2,3,4	32	-70	46
1,9,6,7	-47	38	45
2,3,4,5	-76	69	-74
3,4,5,6	60	-44	68
4,5,6,7	62	-62	-110
4,5,6,9	-85	58	7
5,6,7,8	-74	112	87
5,6,9,1	76	-89	-77
6,7,8,1	-21	-23	10
6,9,1,2	-124	92	114
7,8,1,2	149	-101	-134
7,8,1,9	-10	56	23
8,1,2,3	-92	143	80
8,1,9,6	36	-63	-44
9,1,2,3	66	-10	-78
9,6,7,8	45	-10	-35

TABLE 1: TORSION ANGLES (IN DEGREES) OF BICYCLIC BRET COMPOUNDS (CONTD.).

(D) BICYCLO(4.3.1)DECENES.

COMPOUND	L	M	N	O
TORSION ANGLE				
1,2,3,4	52	71	-29	69
1,10,6,7	42	52	57	-53
2,3,4,5	-74	-30	82	-77
3,4,5,6	67	-36	-70	53
4,5,6,7	-127	-42	-74	76
4,5,6,10	-7	80	53	-54
5,6,7,8	59	134	115	-89
5,6,10,1	-79	-75	-71	80
6,7,8,9	51	-50	-41	-41
6,10,1,2	122	72	111	-82
7,8,9,1	-36	29	47	50
8,9,1,2	-124	-120	-164	86
8,9,1,10	27	34	4	-76
9,1,2,3	85	70	106	-153
9,1,10,6	-30	-80	-57	79
10,1,2,3	-70	-81	-62	7
10,6,7,8	-54	9	-11	41

TABLE 1: TORSION ANGLES (IN DEGREES) OF BICYCLIC BREDT COMPOUNDS (CONTD.).

(E) BICYCLO(4.4.1)UNDECANE.

COMPOUND	P
TORSION ANGLE	
1,2,3,4	-49
2,1,10,9	172
2,1,11,6	-102
2,3,4,5	69
3,4,5,6	-68
4,5,6,7	162
5,6,7,8	-65
5,6,11,1	43
6,7,8,9	-59
7,6,11,1	-85
7,8,9,10	74
8,9,10,1	-65
10,1,2,3	-94
10,1,11,6	72
11,1,2,3	79
11,1,10,9	-1

TABLE 1: TORSION ANGLES (IN DEGREES) OF BICYCLIC BREDT COMPOUNDS (CONTD.).

(F) BICYCLO(5.3.1)UNDECENE.

COMPOUND	0
TORSION ANGLE	
1,2,3,4	102
2,1,10,9	75
2,1,11,7	-61
2,3,4,5	-73
3,4,5,6	71
4,5,6,7	-81
5,6,7,8	172
6,7,8,9	-109
6,7,11,1	100
7,8,9,10	-47
8,7,11,1	-79
8,9,10,1	47
10,1,2,3	-167
10,1,11,7	63
11,1,2,3	-45
11,1,10,9	-55
11,7,8,9	63

TABLE 2: RESULTS OF THE MOLECULAR MECHANICS CALCULATIONS.

COMPOUND	V (KCAL/MOLE)	SIZE OF TRANS RING	SIZE OF CIS RING	OUT-OF-PLANE DEFORMATION ENERGY	TORSION		TORSION ANGLE ABOUT CIS DOUBLE BOND
					TRANS DOUBLE BOND	ANGLE ABOUT TRANS DOUBLE BOND	
GE(3,3,1)	59.46	6	6	5.42	65	61	61
KE(4,2,1)	58.51	7	5	5.23	78	44	44
ME(4,3,1)	55.98	6	7	6.29	80	72	72
D(3,3,1)	51.92	6	8	7.04	81	63	63
HE(3,3,1)	49.99	6	6	6.78	86	59	59
C(3,2,1)	40.99	7	5	3.22	133	15	15
A(3,2,1)	40.53	7	6	2.92	132	13	13
B*(3,2,1)	40.15	7	5	3.71	128	16	16
LE(4,3,1)	35.84	7	6	2.85	122	30	30
J(4,2,1)	31.14	8	7	1.75	143	10	10
E*(3,3,1)	26.52	8	6	1.66	147	8	8
I*(4,2,1)	26.25	8	5	1.22	149	10	10
O(4,3,1)	20.30	9	7	1.02	153	7	7
N*(4,3,1)	17.57	9	6	0.39	164	4	4
Q(5,3,1)	12.62	10	8	0.17	172	0	0
P*(4,4,1)	12.41	10	7	0.10	172	1	1

£ INDICATES THAT THE DOUBLE BOND IS ON THE BRIDGEHEAD.
 * INDICATES THE MINIMUM ENERGY CONFORMATION OF EACH SYSTEM

order of decreasing steric energy (V_s)(Column 2).

Columns 3 and 4 give information on the sizes of the trans-cycloalkene and cis-cycloalkene incorporated into the bicyclic skeleton. Column 5 shows the energy due to out-of-plane deformations calculated by the WBFF for each compound. Columns 6 and 7 give the torsion angles around the trans and cis double bonds respectively. Compound F has been excluded since it is not a bridgehead olefin.

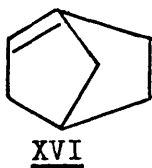
4.4 Discussion

Bicyclo (4.4.1) undec-1(2)-ene(P), which contains a trans-cyclodecene ring¹¹, and bicyclo (4.3.1) dec-1(9)-ene (N) and bicyclo(4.3.1)dec-1(2)-ene(O)¹², which contain a trans-cyclononene ring, have all been isolated - the smallest isolable members of the bicyclo (x, y, 1) alk-1-ene system are bicyclo (3.3.1) non-1(2)-ene(E)^{3b,13}, bicyclo (4.2.1)non-1(9)-ene(I)^{14,15} and bicyclo(4.2.1) non-1(2)-ene(J)^{14,15}, each of which contain a trans-cyclooctene ring. Compound E exhibits normal spectral properties but shows a high degree of reactivity in electrophilic and nucleophilic addition reactions^{36,13}. However, from a comparison of spectral properties and of the rates of electrophilic addition reactions¹⁵ of compounds E and I, it can be concluded that the double bond is slightly less strained in the latter.

The results from the MM calculations support these experimental observations. The steric energies

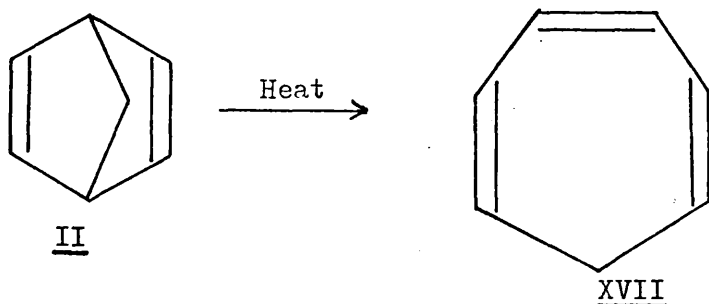
calculated for all these isolable bridgehead olefins (J, E, I, N, O and P) are not excessively high and all are indeed, less than the steric energy, V_s , of 31.32 kcal/mole which was calculated for norbornadiene (II). Therefore, on the basis of MM calculations, these bridgehead olefins (J, E, I, N, O and P) would be expected to be isolable. Furthermore, the calculated steric energy, V_s , of I is 0.3 kcal/mole less than that of E and the calculated torsion angle about the double bond is 149° in I compared with 147° in E - both these results, together with the relative magnitudes of the out-of-plane bending components of the steric energy of I and E (see column 5 in Table 2), point to the fact that the double bond is less strained in I and that E should be more reactive.

Bicyclo (3.2.1) oct-1(2)-ene(A) and bicyclo(3.2.1) oct-1(7)-ene(B), each of which contains a trans-cycloheptene ring, have been prepared but proved to be unstable and hence, after their generation, could only be trapped with diphenylisobenzofuran but not observed¹⁶. Attempts to prepare bicyclo (2.2.1) hept-1-ene (XVI), which incorporates a trans-cyclohexene fragment into it, have been unsuccessful¹⁷. These observations are in accord

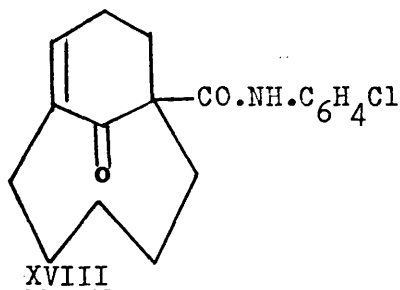


with results from MM calculations. The steric energies of the bicyclo (3.2.1) systems and similar systems

containing a trans-cyclohexene ring, are all in excess of 40 kcal/mole (see Table 2), which implies that these molecules are highly strained and hence difficult to isolate. The fact that the calculated steric energy of the compounds A and B are about 9 kcal/mole higher than that of norbornadiene (II) reinforces this opinion as norbornadiene is itself a strained bicyclic diene, as evidenced by its high heat of hydrogenation¹⁸, which averages 34 kcal/mole per double bond vs. a normal value of about 26 to 28 kcal/mole and by its rearrangement on heating, to tropyliidene (XVII), a monocyclic triene¹⁹.



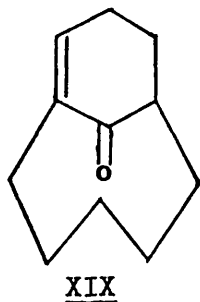
The only experimentally derived physical description of a bridgehead alkene comes from an X-ray crystal structure analysis of compound XVIII^{20,21}. This is a relatively unstrained example of an "anti-Bredt"



compound. The strain appears to manifest itself both in the warping of the double bond (by 8.6°) and bond angle

deformation, particularly around the bridgehead position. Moreover, the double bond is in a potentially conjugating position with the carbonyl position, to give an enone system. However, enones have characteristic chemical and spectroscopic properties and this example exhibits behaviour which is intermediate between the true enone and isolated double bond and carbonyl systems, i.e. the strain imposed by the bridgehead position of the double bond results in a distortion from ideal (planar) enone geometry. Empirical examination of the u.v. spectrum indicated an angle of twist of about 40° between the double bond and carbonyl plane. X-ray analysis revealed an angle of twist of 32° .

MM calculations on the corresponding unsubstituted equivalent of XVIII i.e. XIX, are in excellent agreement with the X-ray results. Figure 3 shows a comparison of the calculated geometry of XIX and the observed geometry of XVIII. The force field used in the MM calculations was an extended version of the WBFF, which is parametrised for the carbonyl function²².



From the foregoing discussion, it is clear that the results from the MM calculations, using the WBFF, are in

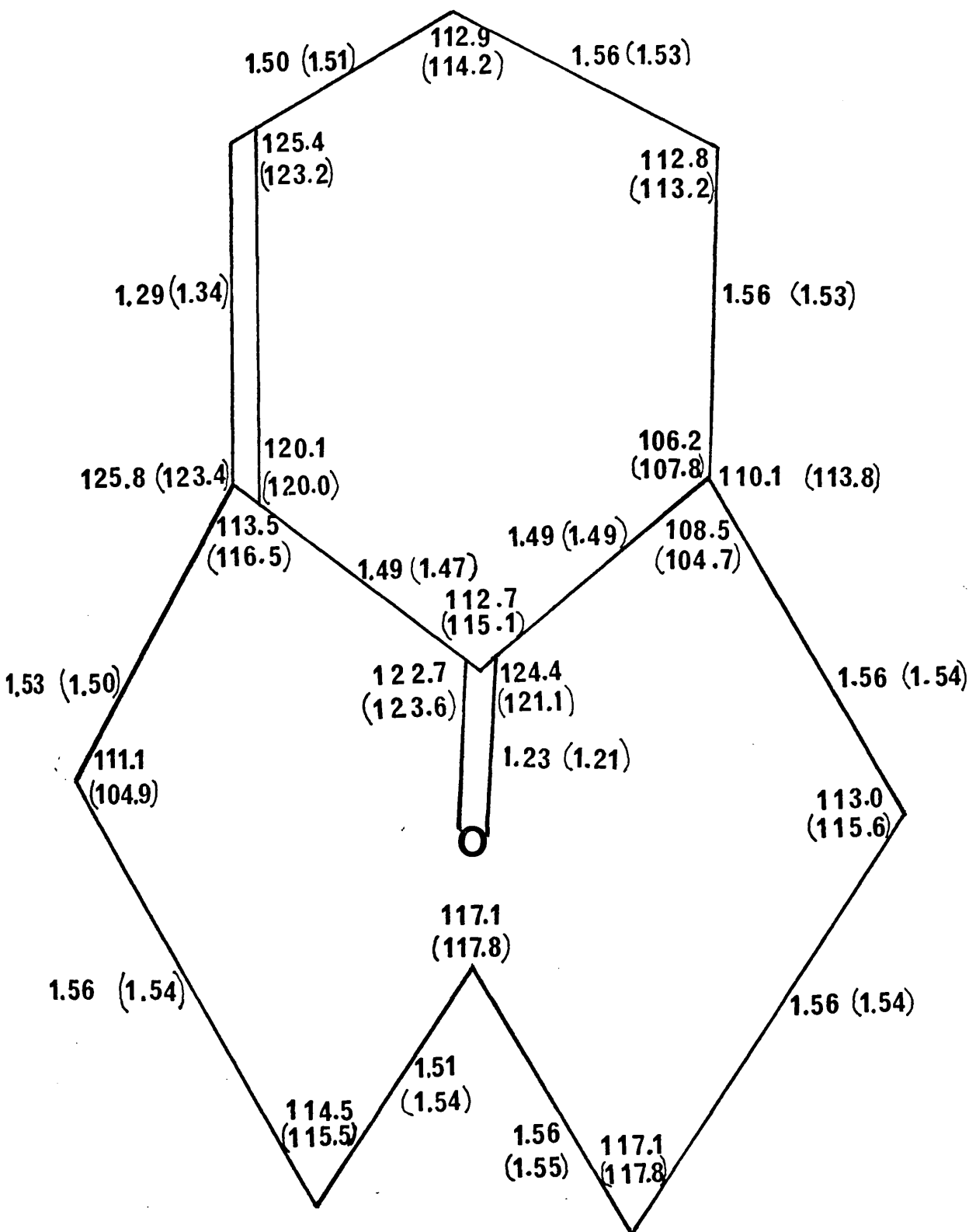


Figure 3(a): Comparison of the experimentally observed and calculated (in parentheses) bond lengths and angles for the bicyclo(5.3.1)undec-1(10)-ene-11-one system.

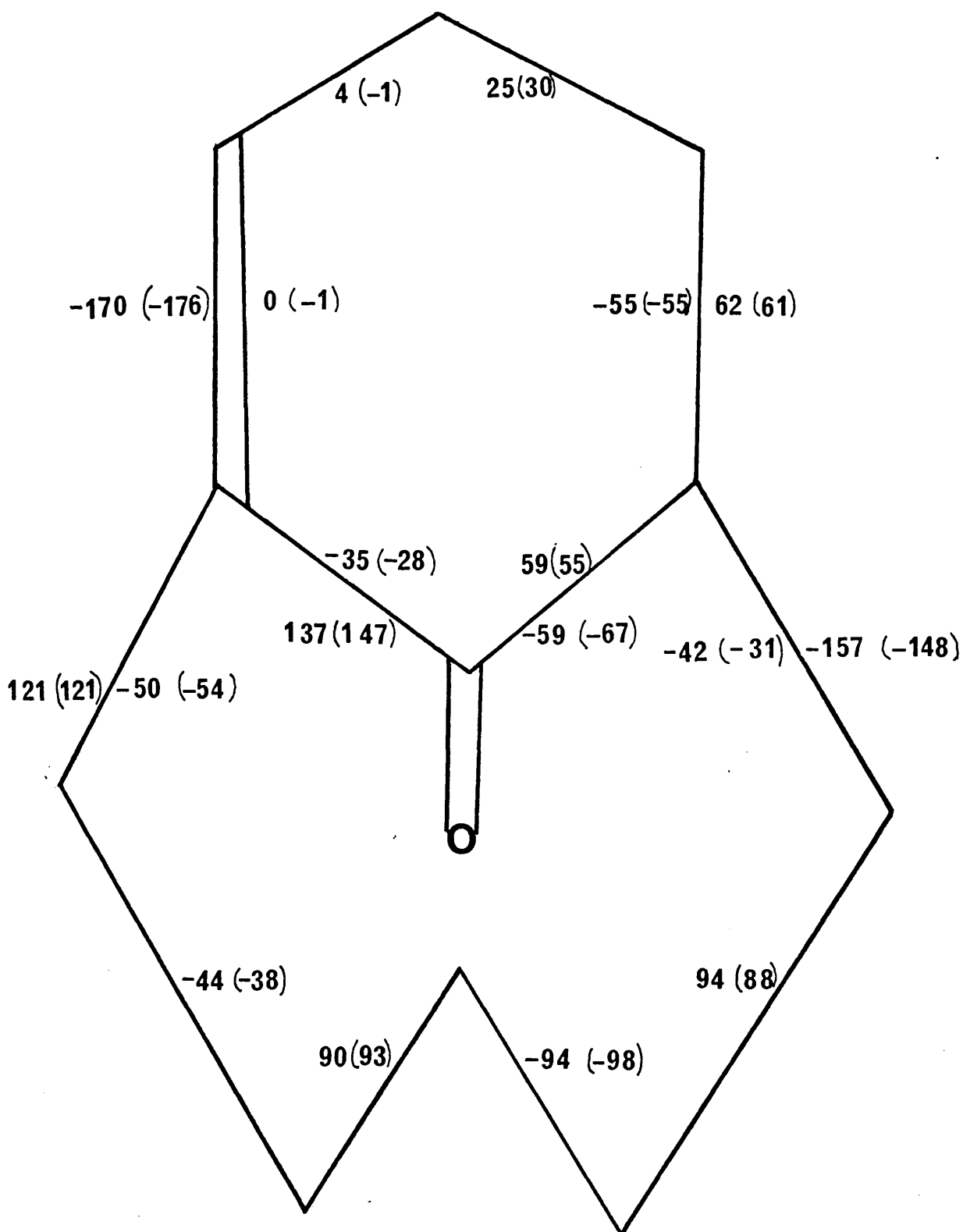
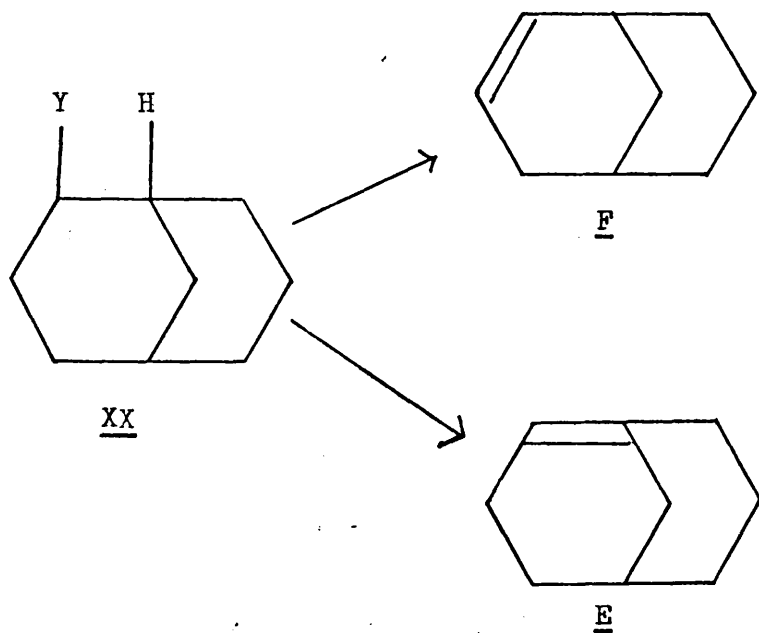


Figure 3(b): Comparison of the experimentally observed and calculated (in parentheses) torsion angles for the bicyclo(5.3.1)undec-1(10)-ene-11-one system.

sufficient agreement with the experimental observations at our disposal, to enable us to place a certain degree of confidence in the predictions and comparisons obtained from the use of the WBFF.

It can be deduced from a comparison of the steric energies of E and F, that placing a double bond in a bridgehead position as opposed to a non-bridgehead position in the bicyclo (3.3.1) nonene system results in an increase of the steric energy of about 19 kcal/mole. This increase is due to the fact that molecules possessing bridgehead double bonds are strained as a result of forcing the π -bonding system to assume an unnatural geometry and not as a result of molecular overcrowding. This is borne out by the experimental observation that elimination of HY from bicyclo (3.3.1) nonane compound (XX) leads predominantly to the 2-ene(F) rather than the 1-ene (E)¹³.



The validity of Wiseman's trans-cycloalkene analogy is vindicated by the MM calculations as systems incorporating trans-cyclodecene ring are calculated to be less strained than those with a trans-cyclononene and so on (see column 3 of Table 2). In addition, the torsion angle about the trans double bond in the bicyclo (x.y.1) alk-1-ene systems is in the same order of magnitude as in the trans-cycloalkene analogue. It is noteworthy, but not unexpected, that there is a correlation between the steric energy, V_s (column 2), the out-of-plane deformation energy (column 5) and the torsion angle about the trans double bond (column 6). The dominant factor controlling the inherent degree of strain of a bicyclo (x,y,1)alk-1-ene compound is therefore the size of the trans-cycloalkene fragment.

Bridgehead olefins have been divided into two classes by Fawcett² - those which are isolable and those which are transient intermediates. The steric energies of the former are all calculated to be less than or equal to 31.14 kcal/mole, while those of the latter class are greater than or equal to 35.84 kcal/mole. It would appear that if the steric energy, V_s , of a bicyclic bridgehead olefin is less than about 33 kcal/mole with respect to the WBFF, it should be isolable. Whereas if the calculated steric energy exceeds this value, the bridgehead olefin would

be expected to be highly strained and exist as a transient intermediate. Furthermore, the large distortion from coplanarity of the four groups attached to the olefinic linkage in bicyclic systems containing trans-cyclohexene rings (see column 6 in table 2) suggest that such compounds must have substantial diradical character.

As previously mentioned, Wiseman's hypothesis tells us nothing about the relative stabilities within a given ring system i.e. for bicyclo(x.y.1) alk-1-ene systems where $x \neq y$, with a double bond at, but not on, the bridgehead, it is not possible to predict whether it is energetically more expensive to place the double bond in the smaller ring or in the larger ring.

On the basis of Wiseman's postulate, no distinction can be made between isomers A and B, I and J and N and O. MM calculations using the WBFF, indicate that it is more favourable to place the double bond in the second largest bridge so that B is less strained than A, I is less strained than J and N is less strained than O (see Figure 2). A similar conclusion has been drawn from MM calculations performed by Burkert²³ using Allinger's force field.

Examination of bicyclo (3.2.1) oct-1-ene systems, A and B reveals that incorporation of the double bond into largest bridge of this trans-cycloheptene analogue, as in A results in the formation of a high energy boat conformation of cis-cyclohexene which is characterised by

unfavourable torsional and nonbonded interactions. If, on the other hand, the double bond is placed in the second largest bridge (as in B), this enables the six-membered ring to assume an energetically preferred chair conformation. Similarly, compound B is more stable than compound C, since the former possess a chair cyclohexane ring and the latter a boat cyclohexane ring.

Molecular models of bicyclo (4.2.1) non-1(8)-ene (I) and bicyclo(4.2.1) non-1(2) -ene (J) and of bicyclo(4.3.1) dec-1(9)-ene (N) and bicyclo(4.3.1) dec-1(2)-ene(O) indicate that the double bond is distorted more when it is placed in the largest bridge (as in J and O) as compared to when it is placed in the second largest bridge (as in I and N) within a given skeleton. This is due to the fact that when a double bond is introduced into a ring system, the system becomes less flexible. Thus, when a cis double bond is placed in the second largest bridge so as to form a rigid cis - cyclopentene, as in I, or a cis-cyclohexene, as in N, the other saturated seven membered ring in I and N has more degrees of freedom, by which it can act to minimise the distortion of the double bond and its substituents from the preferred planar geometry and the strain suffered by the compound, than when

the double bond is placed in the largest bridge to form a cis-cycloheptene ring (as in J and O) and the unfavourable strain components minimised by only five - and six-membered rings, as in J and O respectively. Thus, from models, one would expect I to be less strained than O.

MM calculations confirm these proposals - the steric energy of I is calculated to be 4.89 kcal/mole less than J and the steric energy of N is 2.73 kcal/mole less than O. The substituents on the double bond deviate from planarity, on average by 17° in I and by 21° in J. The torsion angle about the trans double bond is 149° in I as opposed to 143° in J. The bridge bond angle is 91.4° in I compared to 88.5° in J. Similarly, the deviation of the substituents from planarity in N is 10° as opposed to 16° in O. The torsion angle about the trans double bond is 164° in N and 153° in O, the bridge bond angle is 101.9° in N and 101.6° in O.

It is also interesting to note that the calculated steric energy for compound I is less than that of compound E, which, in turn, is less than that of compound J (see Table 2). Compounds I, E and J all incorporate a trans-cyclooctene ring into their skeleton. Compound I

has a cis-cyclopentene and cycloheptane ring, compound E has a cis-cyclohexene and cyclohexane ring, while J has a cis-cycloheptene and cyclopentane ring. The deviation of double bond substituents from planarity is 17° in I, 20° in E and 21° in J. The torsion angle about the trans double bond is 149° in I, 147° in E and 143° in J.

These results, together with the results for the bicyclo(4.2.1)-nonenes I and J and bicyclo(4.3.1.) decenes N and O, support the theory that, within a given skeleton, which has a double bond at, but not on, the bridge, the double bond is more favourable when it is placed in the second largest bridge or alternatively, the system with a cis-cyclopentene ring is more stable than one with a cis-cyclohexene ring which in turn is more stable than one with a cis-cycloheptene ring. Similar deduction can be drawn from the results of P and Q.

Unfortunately, the only experimental confirmation of this theory is the aforementioned data that the double bond is more strained in E than it is in I¹⁵. To obtain conclusive experimental proof, it would be necessary to determine the heats of hydrogenation and/or heats of formation of the appropriate bridgehead olefins. Many

reactions which yield these olefins occur under equilibrium conditions and thus yield thermodynamically preferred products, or alternatively, the relative percentage of products from a reaction may not reflect their relative stabilities, but rather the stabilities of the transition states, whose conformations do not resemble those of the products.

When the double bond is placed in the smallest bridge (usually referred to 'the bridgehead'), the trans double bond as a consequence is located in a relatively small trans-cycloalkene ring. MM calculations indicate that on account of the fact of the large distortions of the trans torsion angle from 180° and of the cis torsion angle from 0° , e.g. the corresponding values in H are 86° and 59° , these compounds are usually highly strained and in some cases, it becomes difficult to differentiate between situations in which the double bond is trans and those in which it is cis.

In general, within a given skeleton, systems with a double bond placed in the second largest bridge will be less strained than those with a double bond located in the

largest bridge, which in turn is less strained than those with a double bond situated on the smallest bridge.

4.5 References

1. J. Brecht, H. Thouet and J. Schmitz, Annalen, 437,
1 (1924).
2. F.S. Fawcett, Chem. Rev., 47, 219(1950).
- 3(a). J.R. Wiseman, J. Amer. Chem. Soc., 89, 5966(1967)
(b). J.R. Wiseman and W.A. Fletcher, J. Amer. Chem. Soc.,
92, 956 (1970).
4. J. Brecht, J. Houben and P. Levy, Ber., 35, 1286(1902)
5. V. Prelog, J. Chem. Soc., 420 (1950) and references
cited.
6. G.L. Buchanan, Chem. Soc. Rev., 3, 41 (1974)
7. A.C. Cope and M.E. Synerholm, J. Amer. Chem. Soc.,
72, 5228 (1950)
8. H. Meerwein, F. Kiel, G. Klosgen and E. Schoch,
J. Prakt. Chem., 104, 163, 166(1922)
9. G.L. Buchanan and G. Jamieson, Tetrahedron, 28,
1129 (1972)
10. K.W. Turnbull, S.J. Gould and D. Arigoni, J.C.S.
Chem. Comm., 597 (1972).
11. T. Westman, Ph.D. Dissertation, University of
California, 1962.
12. F.T. Bond, Ph.D. Dissertation, University of
California, 1962.
13. J.A. Marshall and H. Faubl, J. Amer. Chem. Soc.,
89, 5965 (1967).
14. J.R. Wiseman, H. Chan and C.J. Ahola, J. Amer. Chem.
Soc., 91, 2812 (1969).
15. K.B. Becker, Tetrahedron Lett., 2207 (1975)

16. J.A. Chong and J.R. Wiseman, J. Amer. Chem. Soc., 94, 8627 (1972).
17. W.G. Dauben and J.D. Robbins, Tetrahedron Lett., 151 (1975).
18. R.B. Turner, W.R. Meador and R.E. Winkler, J. Amer. Chem. Soc., 79, 4116 (1957)
19. Shell Chemical Corporation, New York, private communication (circular), June 1956.
20. A.F. Cameron and G. Jamieson, J. Chem. Soc.(B), 1581(1971).
21. G.L. Buchanan and G. Jamieson, Tetrahedron, 28, 1123 (1972).
22. D.N.J. White and H.P. Flitman, private communication.
23. U. Burkert, Chem. Ber., 110, 773 (1977).

CHAPTER FIVE

Prediction of the stereoselectivity of hindered substrates

5.1 Introduction

Steric and electronic effects strongly influence the rates and equilibria of many reactions in organic and inorganic chemistry. It is therefore necessary to examine closely the steric and electronic properties of the reacting species, both in their ground and excited states, if the nature of the products and rate of a particular reaction are to be predicted.

Stereoselectivity is of great importance in the design of organic reactions, particularly in the syntheses of natural products. A 'stereoselective' reaction is one in which of two (or more) possible stereoisomeric products, one is produced in (great) predominance over the other(s). Although it has long been recognised that steric hindrance is an important factor in stereo-selective transformations¹, few attempts have been made to deal with this concept in a quantitative manner.

Most organic chemists try to estimate the degree of steric congestion at sites of chemical attack from a visual inspection of a molecular model of the compound of interest. However, molecular models can be misleading and this approach becomes increasingly complex particularly when there is very little steric hindrance from the immediate neighbours and the medium-and long - range steric effects become dominant factors in controlling the stereoselectivity of a reaction² and when more than one

conformation of the molecule may react.

Wipke and Gund³ have devised an algorithm for calculating semi-quantitative estimates of the relative steric congestion at possible reaction sites. This technique is extremely useful for predicting which of the possible products will dominate in reactions, which are controlled by steric influence of neighbouring atoms in the molecule. A certain degree of success has been achieved when this type of method has been applied to the prediction of ratio of products which result from stereoselective nucleophilic additions to sterically hindered ketones^{3,4} (see Figure 1).

In Wipke and Gund's method³, the term 'steric

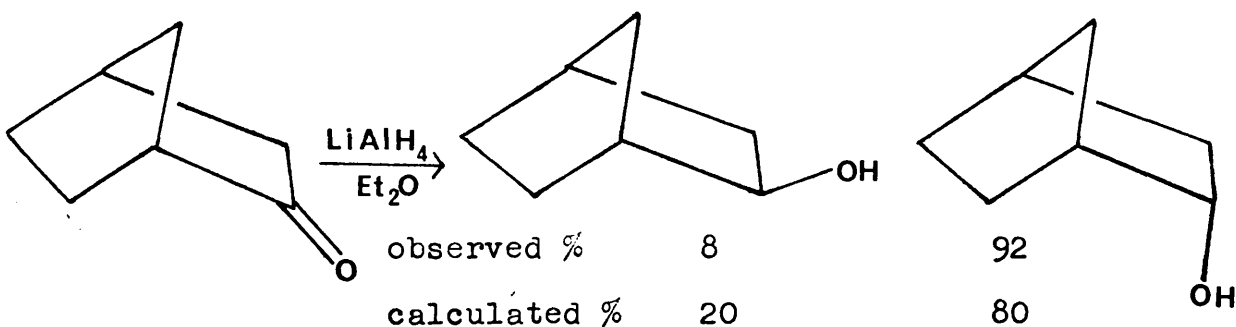


Figure 1. Comparison of the observed and calculated stereoselectivity for the reduction of 2-norbornanone, a congested ketone.

congestion' at a reaction centre refers to the steric environment of the isolated substrate in its ground state, and is independent of reaction partners or transition-state structure. The term 'steric hindrance' refers to steric environment with respect to the approach

of a specific reacting partner. The Wipke and Gund method generates a cone of preferred approach for each sterically hindering atom and works in the following way:

Consider attack on a carbonyl group by a reagent R whose size is considered negligible (Figure 2). If the reagent attacks C_x along a line perpendicular to the plane containing the carbonyl group, it will be hindered by the various atoms i above the plane. A measure of each atom's ability to hinder the incoming reagent is its van der Waals radius r_i . For each hindering atom i , a cone of preferred approach, centred on the perpendicular and tangent to the sphere of van der Waals radius r_i surrounding atom i , is defined. This cone intersects a sphere of unit radius centred on the carbon C_x , to generate a solid angle A_{xa} . The magnitude of this angle is equated with the accessibility $A_{xa(i)}$ of the carbon atom with respect to atom i . It can be seen that large solid angles are found in situations of high accessibility and conversely, a small solid angle is indicative of low accessibility. From solid geometry:

$$A_{xa(i)} = 2\pi(1 - \cos \theta).$$

The congestion at C_x caused by atom i is defined as the inverse of the accessibility:

$$C_{xa(i)} = 1/A_{xa(i)}$$

The total congestion at C_x is generated by summing the individual congestion terms for all the atoms above the

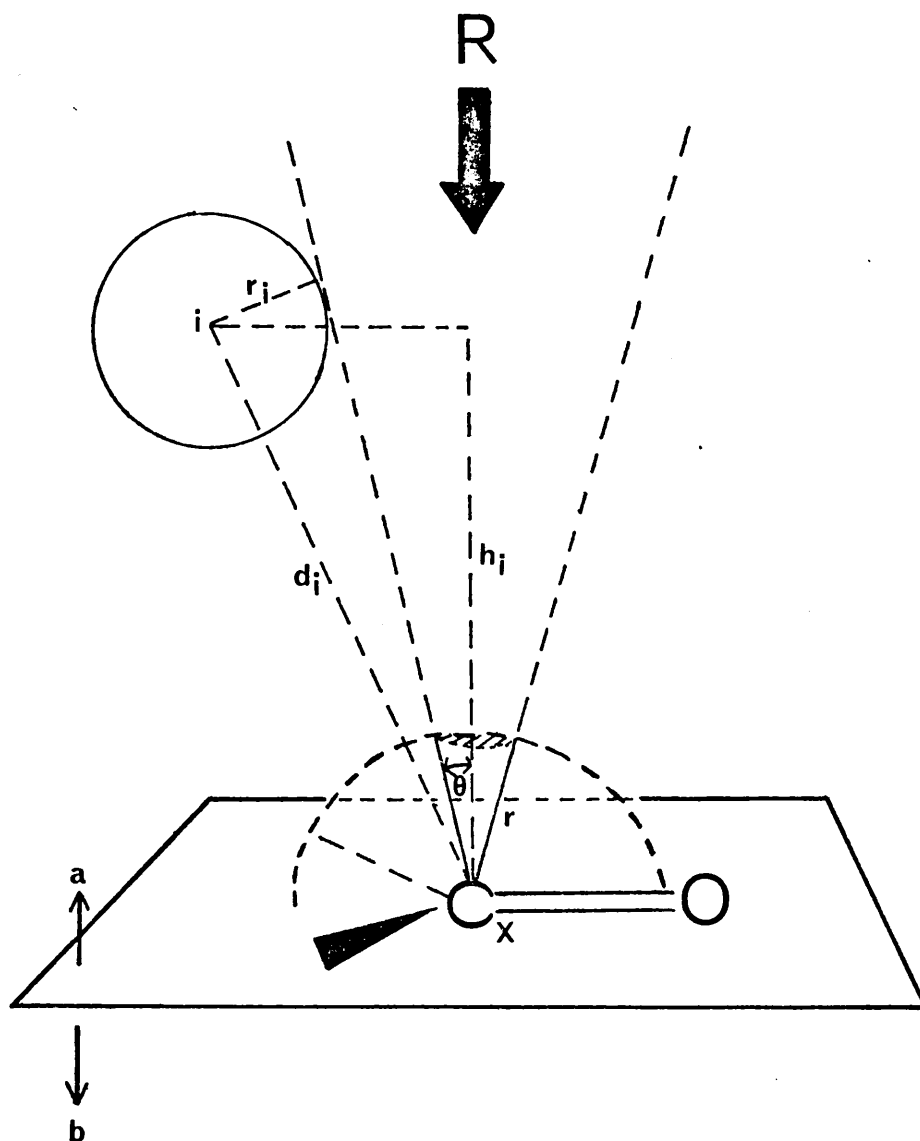


Figure 2: Cone of preferred approach of reagent R to carbon x defined by hindering atom i . The accessibility of x on side a with respect to i is defined by this solid angle and is numerically equal to the area on a unit sphere cut by this cone (shaded area).

carbonyl plane:

$$C_{xa} = \sum_i C_{xa(i)}$$

The calculation is then repeated for attack below the plane of the carbonyl group to give C_{xb} . The preferred direction of attack of the incoming reagent is that which gives the minimum value of C . The percentage of product resulting from attack below the plane of the j^{th} conformation, p_{Bj} is given by:

$$p_{Bj} = \frac{C_{xa}}{C_{xa} + C_{xb}}$$

Similarly, the percentage of product resulting from attack above the plane of the j^{th} conformation, p_{Aj} is given by:

$$p_{Aj} = \frac{C_{xb}}{C_{xa} + C_{xb}}$$

Angle θ is easily derived:

$$\theta = 90 - \theta_1 - \theta_2$$

where $\theta_1 = \sin^{-1} (r_1/d_1)$, d_1 is the distance of atom 1 from the centre of attack, and $\theta_2 = \sin^{-1} (h_1/d_1)$, h_1 is the distance of atom 1 above (or below) the plane of the carbonyl group.

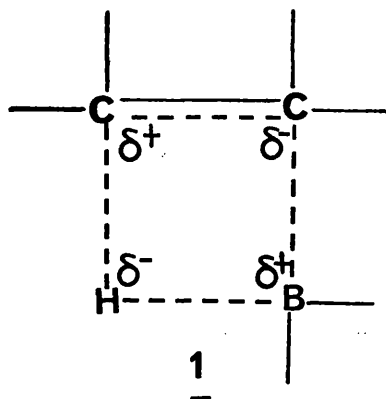
Wipke and Gund have found that the calculated congestions do reflect observed stereoselectivities in a semi-quantitative manner and that steric control appears to dominate when the difference in congestion of the two sides is large and the larger of the two values is greater than ca.30.

It is noteworthy that results from this method may be inaccurate in cases where the size of reagents, inductive effects, transition-state conformational effects or

equilibration of products are dominant factors in determining the stereoselectivity of a given reaction.

5.2 Prediction of the Stereoselectivity in the Hydroboration of Hindered Cyclohexenes using Molecular Mechanics Calculations and Steric Congestion Calculations.

Wipke and Gund³ suggested that these types of congestion calculations may be extended to include electrophilic additions to double bonds by calculating the degree of steric crowding or congestion on each side of the mid-point of the double bond. However, in the case of hydroboration of an alkene, which involves a cis anti-Markovnikov addition of the B-H bond to the double bond of the olefin, the reaction does not therefore take place via reagent attachment to the mid-point of the double bond but through the four-centre transition state 1⁵.



It therefore appeared more realistic to adopt a two-fold attack on two atomic centres (see Figure 3) rather than a bond centred approach as the latter approach would imply that the double bond can be considered as infinitesimally small compared with the rest of the reagent-substrate complex. This appears to be too gross an

approximation for general use and therefore it would be preferable to treat this type of addition in terms of the sum of two atom centred congestions.

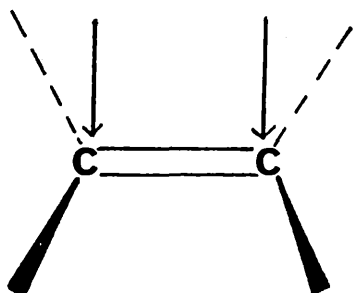


Figure 3. Simultaneous Attack on Two Atomic Centres.

The congestion function developed by Wipke and Gund was utilised in the SAUCE computer program, which was written at the University of Glasgow by M.J. Bovill and C.J. Gilmore and which has proved useful in the study of electrophilic attack on nitrogen lone-pairs² and hydroboration of hindered cyclohexenes⁶, which will be discussed fully in this chapter.

The recent publication of results of a series of hydroboration/oxidation experiments on hindered 1,3,5-tri- and tetra- substituted alkylcyclohexenes⁷ provides reference data for testing the applicability of summed atom centred congestion ratio's (SACR'S) in the prediction of the outcome of stereoselective additions to hindered double bonds since hydroboration is known to be sensitive to the balance of steric hindrance to the two faces of the double bond⁸ (see Figure 4).

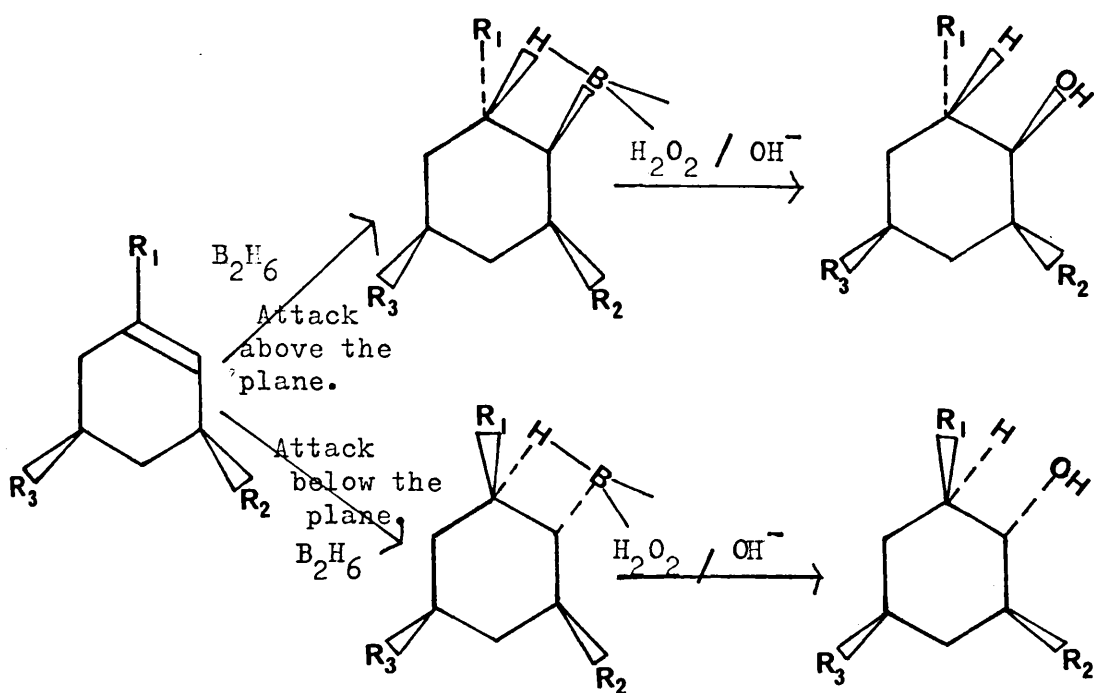
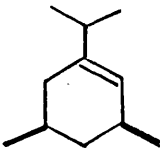
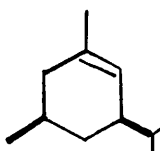
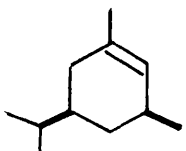
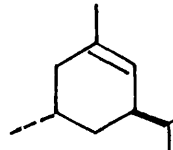
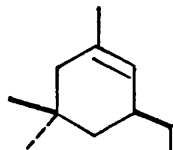
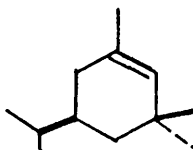
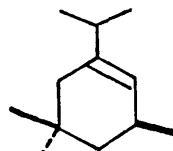
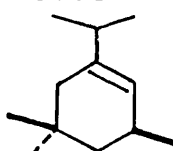


Figure 4.

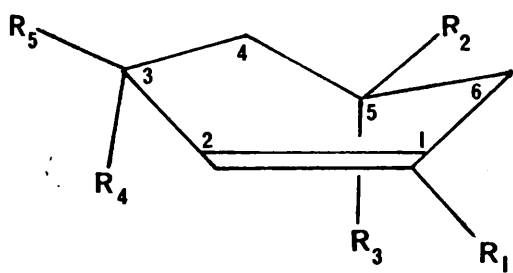
Gordon and Robinson⁷ propose that the olefins 2-4 and 6-9 (Table 1) strongly prefer the half-chair conformation 10 while, for olefin 5, conformations 10 and 11 are of comparative stability. These proposals are borne out by molecular mechanics calculations using the White-Bovill alkane/alkene force field, the development of which is described in Chapter 2. The results of these calculations on olefins 2-9 are given in Table 1. Olefins 2-4 and 6-9 which adopt half-chair conformer 10 are found to be between 1.29 and 2.48 kcal/mole more stable than when the same olefins adopt the other half-chair conformation 11. (N.B. A difference in strain energy of 1.29 kcal/mole corresponds to 90% of the more

Table 1. Results of Molecular Mechanics Calculations and Congestion Calculations

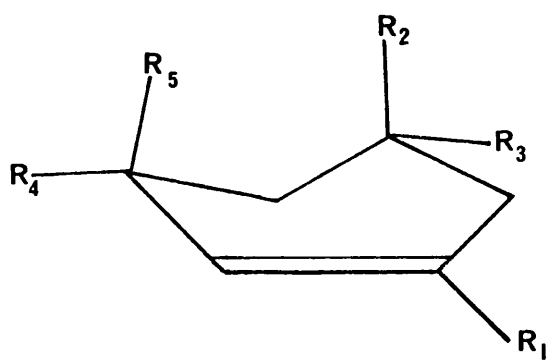
		Rotamers which adopt half-chair conformation					
		10			11		
<u>2</u>		E_{sj}^a	x_j^b	p_{bj}^c	E_{sj}	x_j	p_{bj}
		<u>4.09</u>	45	46	<u>6.00</u>		
		4.36	29	66			
		4.42	26	49			
<u>3</u>		<u>4.30</u>	57	95	<u>6.78</u>		
		4.74	28	93			
		5.15	15	61			
<u>4</u>		<u>5.36</u>	37	55	<u>7.19</u>		
		5.37	36	58			
		5.54	27	60			
<u>5</u>		<u>4.95</u>	31	91	<u>5.19</u>	21	3
		5.40	15	91	5.36	16	94
		5.73	9	32	5.78	8	75
<u>6</u>		<u>5.35</u>	56	93	<u>7.26</u>		
		5.79	28	83			
		6.12	16	30			
<u>7</u>		<u>6.02</u>	38	58	<u>7.70</u>		
		6.12	32	41			
		6.19	30	38			
<u>8</u>		<u>4.81</u>	43	57	<u>6.49</u>		
		5.05	29	40			
		5.06	28	52			
<u>9</u>		<u>5.17</u>	42	28	<u>6.46</u>		
		5.30	34	32			
		5.51	24	45			

- a E_{sj} denotes the steric energy (in kcal/mole) of the j^{th} conformation.
- b x_j denotes the percentage of conformation j amongst the various possibilities.
- c p_{bj} represents the percentage of product resulting from attack below the plane of the j^{th} conformation.

The underlining is used to indicate the most stable rotamer of each type of half-chair conformation that the olefin can adopt.



10

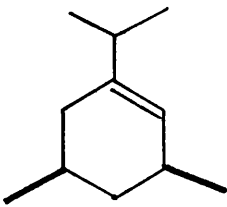
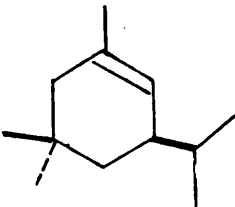
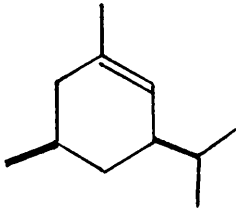
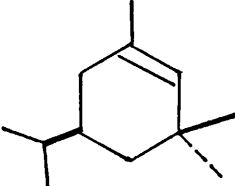
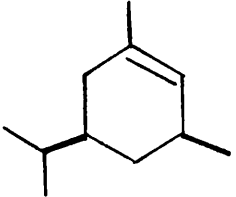
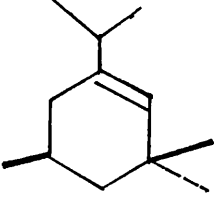
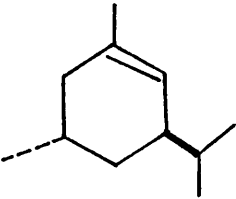
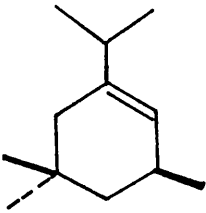


11

stable conformer being present in an equilibrium mixture at room temperature.) In the case of olefin 5, the half-chair conformation 10 is calculated to be only 0.24 kcal/mole lower in potential energy than the half-chair conformation 11. Since olefins 2-4 and 6-9 with half-chair conformation 11 are barely present, they are not included in further computations.

On account of the presence of the isopropyl group in each of the olefins 2-9, it is necessary to consider each of the three rotameric states that the isopropyl group can assume in each olefin. Molecular mechanics calculations indicate that each rotameric form of each olefin is present to an appreciable extent (see Table 1) and since the congestion ratio will depend strongly upon the exact molecular conformation, it was considered vital, for the validity of the results, that the SACR's of each rotameric state of each olefin should be taken into account when determining the overall SACR of each olefin. The results of the SACR calculations are compared with the experimental results in Table 2 where P_B is calculated from $P_B = 0.01 \sum_{j=1}^n p_{Bj} x_j$ with p_{Bj} representing the percentage of product resulting from attack below the plane of the j^{th} conformation (i.e. alternative half-chairs and/or rotamers) and x_j the percentage of conformation j amongst the various possibilities. The individual p_{Bj} and x_j values for each conformation are given in Table 1.

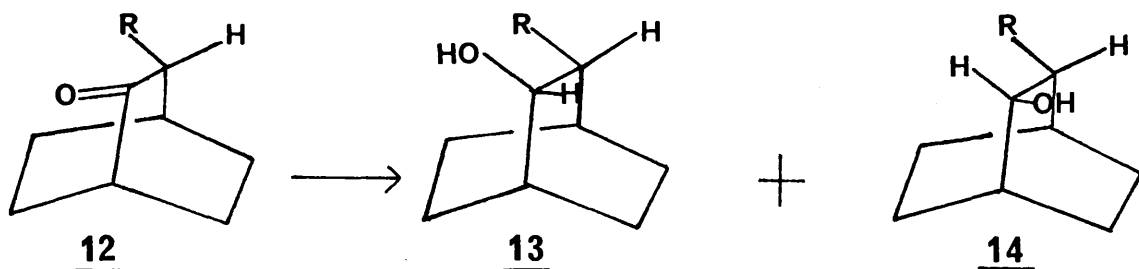
Table 2.

		<u>P_B</u>				<u>P_B</u>	
		<u>Obs.</u>	<u>Calc.</u>			<u>Obs.</u>	<u>Calc.</u>
<u>2</u>		100	53	<u>6</u>		65	80
<u>3</u>		100	89	<u>7</u>		35	46
<u>4</u>		100	58	<u>8</u>		35	50
<u>5</u>		90	75	<u>9</u>		30	33

5.3 Discussion

From Table 2, it can be seen that the calculated value of P_B correlates well with the experimentally observed stereoselectivities in the hydroboration of these hindered cyclohexenes in most cases - for olefins 3 and 5 - 9, the calculated value of P_B is within $\pm 15\%$ of the observed value. This comparison is favourable when it is taken into account that experimental results, from one laboratory have associated errors and differ from the results from different laboratories. In olefins 2 and 4, the difference in absolute congestion values of the two sides is not large (7 and 5 respectively) and the larger of the two values is less than 30 in both cases, which would be interpreted by Wipke and Gund as being due to steric control not dominating. Torsional effects in the substrate-reagent complex can be important³, but, in the case of 2 and 4, would favour the reverse stereoselectivity to that observed. Furthermore, since the major products of the hydroboration of olefins 7 - 9 are the less stable possible products and olefins 5 and 6 also produce significant amounts of the less stable products, this would imply that the transition state in these reactions clearly resembles the starting materials (olefins) rather than the products and that this reaction is governed by 'steric approach control'⁹ rather than product development control (i.e. where the more thermodynamically stable product is preferentially formed). It is therefore difficult to envisage reactions of olefins 2 - 4 being

controlled differently as all the reactions are mechanistically very similar. This then points to the fact that the reason for the poor results in the case of 2 and 4 lie with the ground state congestion algorithm or with some other factor which has been so far neglected. One such factor may be the inductive effect of the alkyl group. In the hydride reduction of 3-alkyl bicyclo (2.2.2) octan-2-ones, (12), ($R=Me, Et, Pr^i$) there is an unexpectedly large



proportion of trans alcohol (14) formed in the reaction, especially when $R=Pr^i$ ¹⁰, in conflict with chemical intuition and theoretical calculations. This has been attributed to an anisotropic inductive effect of the alkyl groups, which leads to an anomalously high rate of attack from the more hindered side (i.e. the alkyl side) of the carbonyl group. In the case of the hydroboration (electrophilic reaction) of olefins, it is conceivable that there is a similar factor operating. The inductive effect of the electron-releasing groups (methyl and iso-propyl) is also anisotropic and that this effect is activating on the side of the double bond remote from the substituents R_2 and R_5 in olefins 2 - 4. This would account for the high stereoselectivity of olefins 2 - 4.

This anisotropic inductive effect, (if present) would appear to exert a relatively weak influence, since in olefins 2 - 9, which contain an axial R_3 or an axial R_4 group and are therefore congested on the side of the double bond remote from R_2 and R_5 groups, 'steric approach control' once again dominates.

Whatever the reason for this failure in the predictions, the SACR's calculations lend support to Gordon and Robinson's hypothesis that the high stereoselectivity shown by 2 - 4 is due to the effect of the R_5 hindering attack from the upper face of the double bond, only when R_5 is an isopropyl group (as in 3) and not when R_5 is a methyl group (as in 2 and 4).

In conclusion, the congestion function is reliable in predicting the stereoselectivity of hindered cyclohexenes when the difference in the congestion of the two sides is greater than about 10 and the larger of the two values is greater than about 30. Furthermore, this method requires only small amounts of computer time as each SACR calculation for one olefin takes only 0.25 second. In cases where steric control does not dominate, a more complex approach is obviously required. One such approach involves the construction of models of chair-like and twist-like transition complexes (since it is impossible to deduce the conformation of the transition state from the products) of alkylcyclohexene/ BH_3 followed by full relaxation energy minimisation of the complex keeping a B-H vector locked parallel to and, say 1.5A

above, the double bond⁴ in one case, and the same distance below in the other. The ratio of products would then be estimated from the calculated energy difference between the model complexes. This approach allows the substrate to relieve and spread the strain induced by reagent approach and would include torsional, dipolar, solvent, entropic and reagent size effects as well as illuminating the nature of the transition complex.

5.4 References

1. Reviews: (a) J.D. Morrison and H.S. Mosher, "Asymmetric Organic Reaction", Prentice-Hall, Englewood Cliffs, N.J., 1971;
(b) L. Velluz, J. Valls, and G. Nomine, Angew. Chem., Int. Ed. Engl., 4, 181 (1965);
(c) L. Velluz, J. Valls and J. Mathiez, ibid., 6, 778 (1967);
(d) J.W. Scott and D. Valentine Jr., Science, 184, 943 (1974).
2. C.J. Gilmore, R.F. Bryan and S.M. Kupchan, J. Amer. Chem. Soc., 98, 1947 (1976).
3. W. Todd Wipke and P. Gund, J. Amer. Chem. Soc., 98, 8107 (1976).
4. P. Muller and J-C. Perlberger, Helv. Chim. Acta, 59, 1880 (1976).
5. H.C. Brown, R. Liotta and C.G. Scouten, J. Amer. Chem. Soc., 98, 5297 (1976).
6. D.N.J. White and M.J. Bovill, Tetrahedron Lett., submitted (1977).
7. M.H. Gordon and M.J.T. Robinson, Tetrahedron Lett., 3867 (1975).
8. M.H. Gordon and Kwang-Ting Liu, J. Amer. Chem. Soc., 93, 7335 (1971).
- 9(a). W.G. Dauben, G.J. Fonkin and D.S. Noyce, J. Amer. Chem. Soc., 78, 2579 (1956);
(b). W.G. Dauben, E.J. Blanz, J. Jiu and R.A. Micheli, ibid., 78, 3752 (1956).
10. M. Cherest, H. Felkin and P. Tacheau, J. Chem. Soc. Commun., 372 (1977).

CHAPTER SIX

The correlation of Raman optical activity
in methyl torsion modes with molecular
mechanics calculations of chiral hindering
potentials.

6.1 Introduction

A molecule is said to be optically active if it rotates the plane of polarization of a linearly polarized light beam. This is attributed to the fact that an optically active medium has different refractive indices for left and right circularly polarized light, that is right and left circularly polarized light travel through the medium at different speeds. The necessary and sufficient condition for a molecule to show optical activity is that such a molecule should not be superimposable with its mirror image i.e. when a molecule has no elements of symmetry or has only a simple axis of symmetry. Conversely, a molecule that has a plane of symmetry, a centre of symmetry or an alternating axis of symmetry, is superimposable with its mirror image and optically inactive.

Since about 1955, chiroptical effects (effects upon light passing through an optically active medium) i.e. optical rotatory dispersion (ORD) and circular dichroism (CD) have been of great value as a probe of chirality in stereochemical studies of molecules containing a chromophore which absorbs in a readily accessible region of the ultra-violet and which has a low extinction coefficient.

Recently, complete vibrational optical activity spectra of chiral molecules have been obtained from a

small difference in the intensity of Raman scattered light in right and left circularly polarized incident light¹⁻⁵. This technique is potentially more powerful than ORD and CD, since every part of a molecule contributes to a vibrational spectrum, which is therefore considerably richer in structural information than the visible or near ultraviolet part of an electronic spectrum. The relevant experimental quantity in measurements of Rayleigh and Raman optical activity is the dimensionless circular intensity differential (CID).

$$\Delta = (I^R - I^L) / (I^R + I^L) \quad (1).$$

where I^R and I^L are the scattered intensities in right and left circularly polarized light.

The largest Raman CID's are usually found in molecules with rigid, twisted skeletons e.g. α -pinene. Since mirror-image isomers give identical optical activity spectra but with reversed signs, as illustrated in Figure 1, it is usually best to run the two isomers to have confidence in the marginal effects; but for the larger effects, a single isomer suffices.

Although the interpretation of depolarized Raman CID spectra is still in its infancy, it has been established that chiral organic molecules containing methyl groups often show large optical activity in broad, weak depolarized Raman bands between 200 and 300 cm^{-1} that originate in methyl torsion modes of vibration⁶. It has

Figure 1(a): Part of the Raman CID spectra of the two enantiomers of tartaric acid .

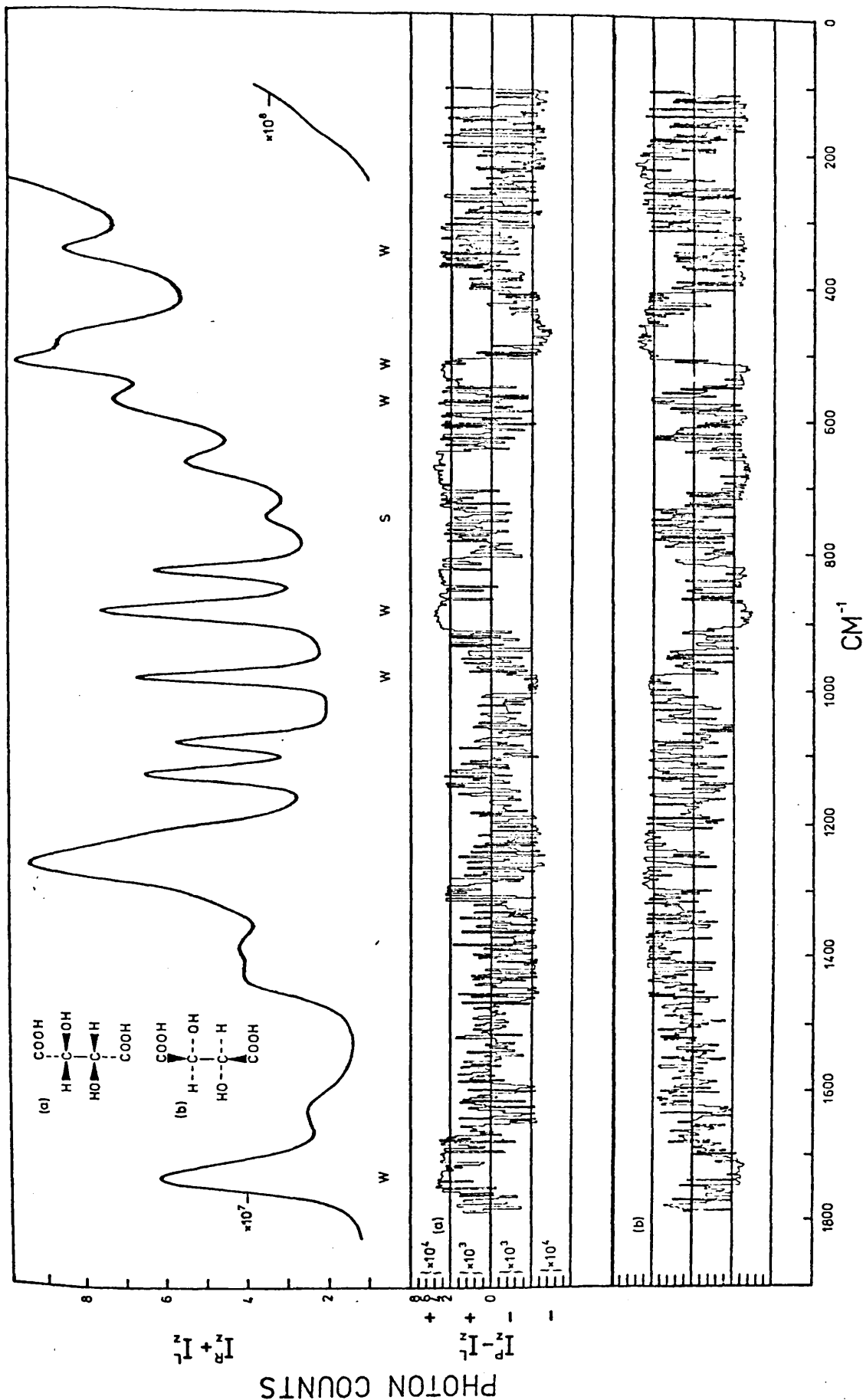


Figure 1(b): Part of the Raman CID spectrum of (-)- α -phenylethylamine.

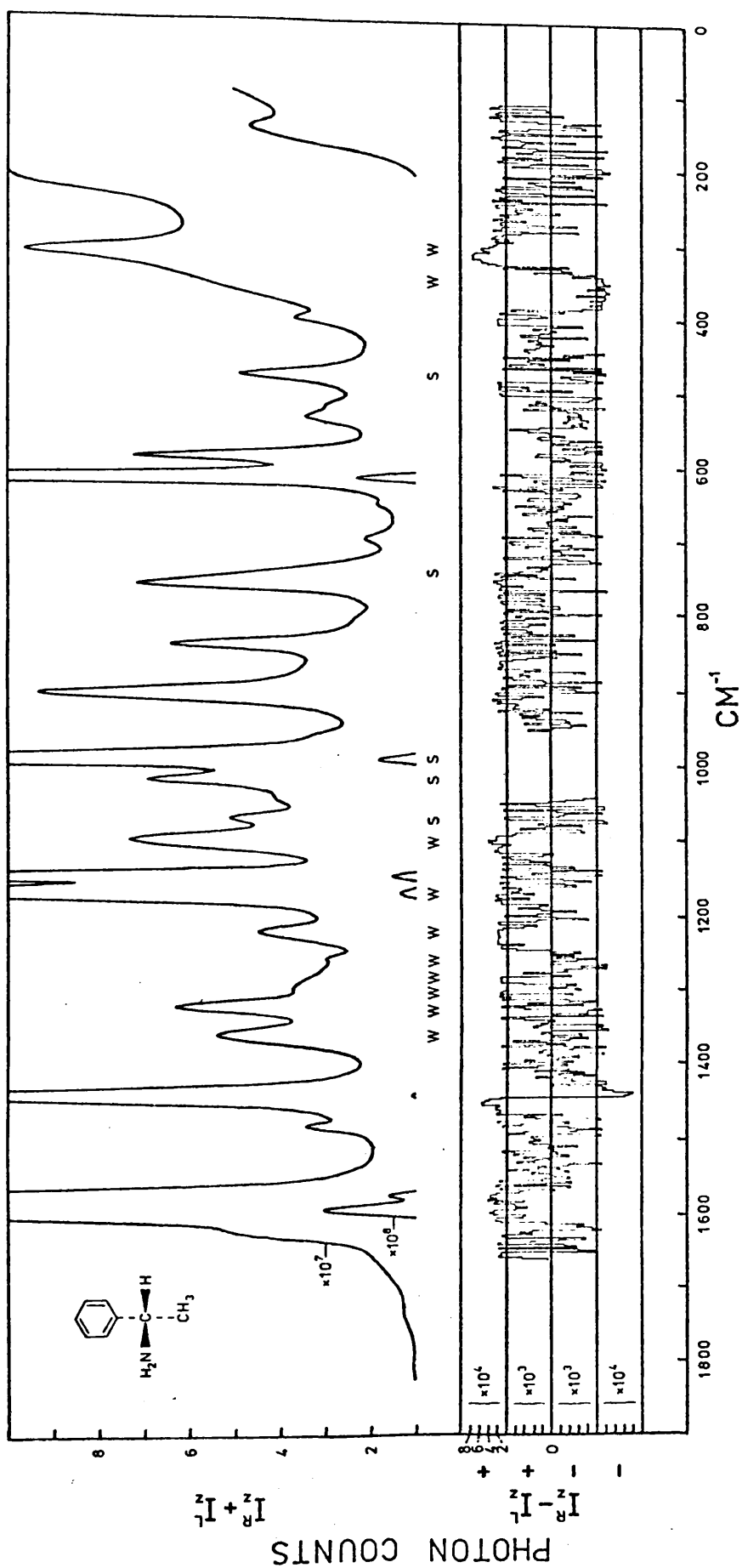
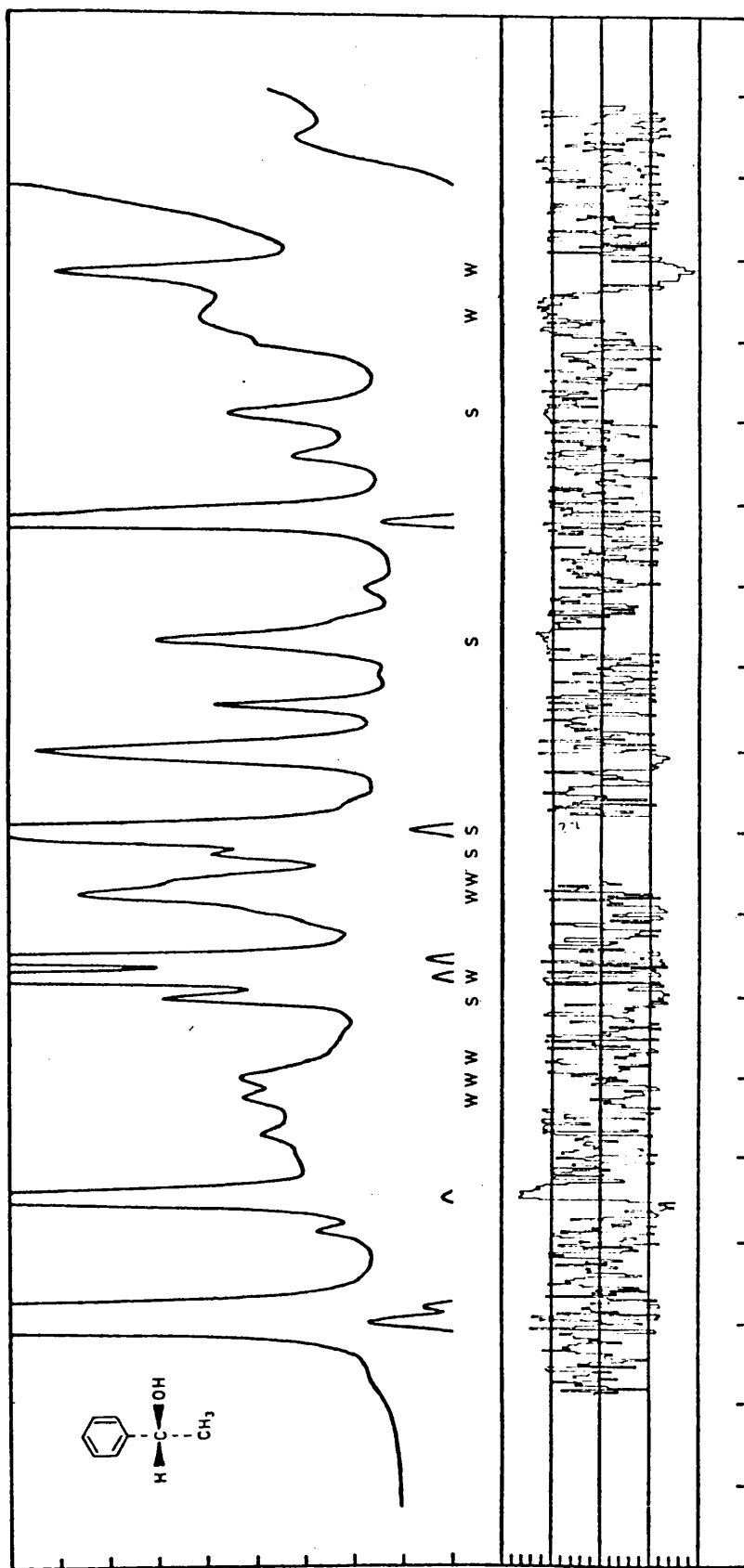


Figure 1(b): Part of the Raman CID spectrum of (+) α -phenylethanol.



been suggested⁷ that this Raman optical activity can be correlated with the chiral part of the electronic potential barrier hindering the rotation of the methyl group and as such it could provide a novel approach to conformational analysis and to the assignment of absolute configuration of chiral molecules.

The dominant part of the three-fold potential barrier that hinders the rotation of the methyl group has the form⁸

$$V(\theta) = \frac{1}{2} V_3 (1 - \cos 3\theta) \quad (2)$$

where V_3 is the barrier and θ is the torsion angle with three equivalent equilibrium values 0° , 120° and 240° .

In the perturbed harmonic oscillator approximation approach, it is suggested that the barrier in a chiral molecule can be written³

$$V(\theta) = \frac{1}{2} V_3 (1 - \cos 3\theta) \pm V_3^1 \sin 3\theta \quad (3)$$

The second term, $V_3^1 \sin 3\theta$, has the effect of displacing the positions of the maxima and minima to one side or the other of the symmetrical position (Figure 2), so that, in an equilibrium position, the methyl group and the hindering groups now constitute a chiral structure with absolute configuration depending on the sense of displacement.

In addition, using the elementary theory of the one-dimensional harmonic oscillator, the barrier height ought

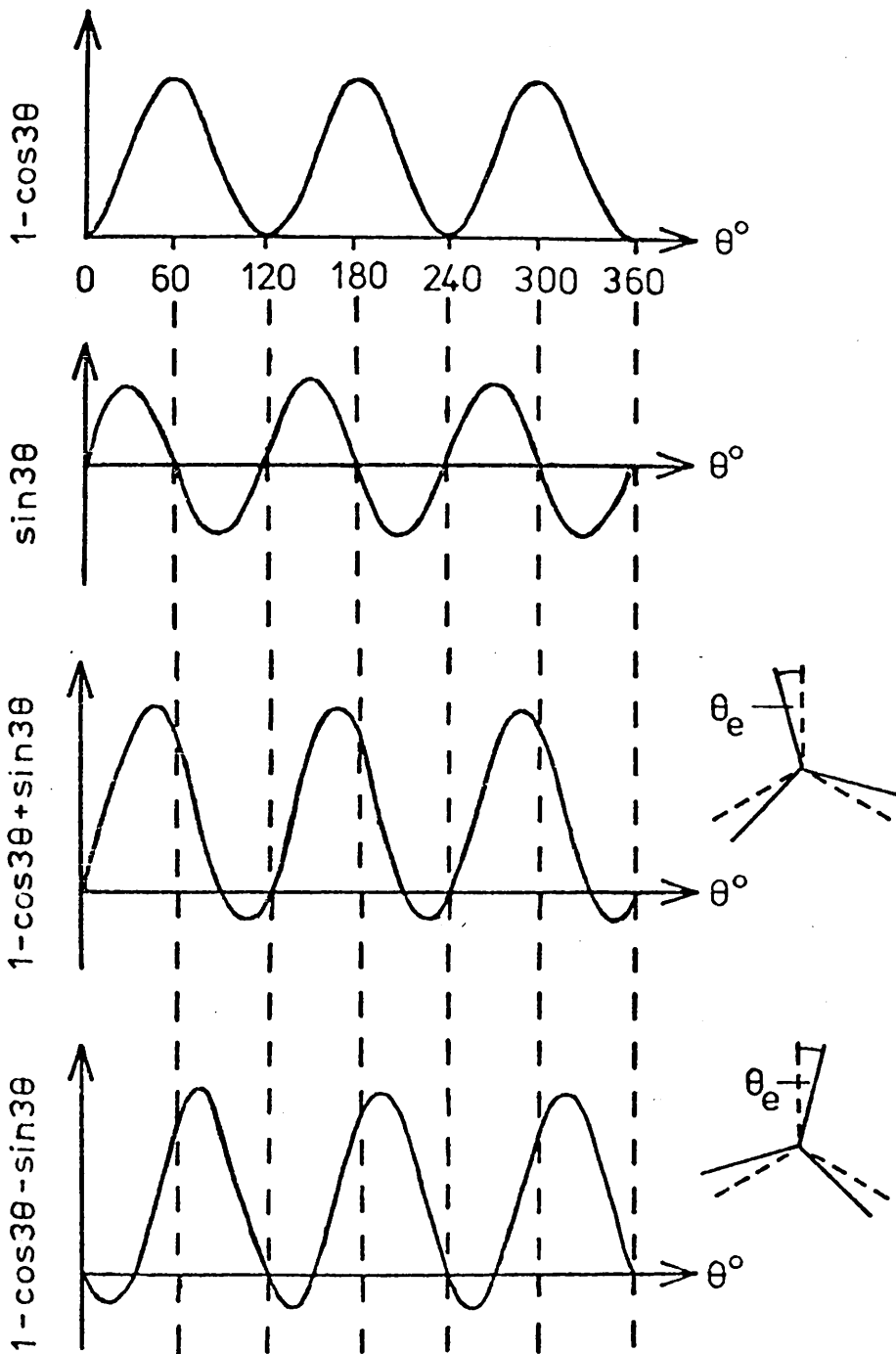


Figure 2: The generation of chiral threefold potential barriers.

to be⁸

$$V_3 \text{ (erg)} = \frac{8}{9} \pi^2 c^2 \bar{V}_t^2 I_r \quad (4)$$

where \bar{V}_t is the torsion frequency in cm^{-1} and I_r is the reduced moment of inertia for the internal rotation. This frequency correlation is not expected to be reliable because it has been assumed that the methyl torsion does not couple with other modes, which is probably not a good approximation in low-symmetry molecules.

The first two terms in the series expansion of the chiral barrier (3) are

$$V(\theta) = \frac{9}{4} V_3 \theta^2 \pm 3 V_3^1 \theta \quad (5)$$

The presence of the term linear in θ means that

$(\partial V / \partial \theta)_{\theta=0} \neq 0$ so $\theta = 0$ is no longer the equilibrium position: in fact if $\theta = \theta_e$ is now the equilibrium position, then

$$V_3^1 = \mp \frac{3}{2} V_3 \theta_e \quad (6)$$

where V_3 is the amplitude of the symmetric part of the electronic potential barrier, V_3^1 is the amplitude of the chiral part of the electronic potential barrier and θ_e is the displacement of the equilibrium position of the methyl group from the symmetric position. $V_3 \theta_e$ thus gives a measure of the chiral part of the barrier and is thus proportional to the methyl torsion Raman optical activity.

At this stage, molecular mechanics (MM) calculations were employed to obtain the chiral parts of the

electronic potential barriers hindering the methyl torsion in several molecules, with the hope that it would prove possible to obtain a correlation between the observed methyl torsion Raman optical activity and the sign and magnitude of $V_3^{\Theta e}$ supplied by the MM calculations.

6.2 Molecular Mechanics Calculations

The White-Bovill alkane/alkene force field (WBFF)⁹ and the minimisation procedure¹⁰, which were discussed in Chapter 2, were used in the MM calculations. Since (+)-3-methylcyclopentanone and (+)-3-methylcyclohexanone contain a carbonyl group, it was necessary to represent the $>C=O$ as a $>C=CH_2$ in the WBFF, which is considered to provide a suitable model¹¹. In the case of (+)-carvone, which was included in the later stages of the calculations, a carbonyl force field¹² which was based on the WBFF, was used.

For each of the molecules of interest, all possible conformations were built and minimised until the first derivatives of the potential energy with respect to the cartesian co-ordinates were less than 10^{-9} kcal/mole to ensure a credible and reproducible minimum energy geometry. In every molecule except (+)-3-methylcyclopentanone, it was found that there was only one major conformation present. For (+)-3-methylcyclopentanone, MM calculations indicated that two conformations were significantly populated at room temperature - 70% of the

half-chair conformation with the methyl in an equatorial position and 30% of the half-chair with the methyl in an axial position. The results for (+) -3-methyl-cyclopentanone in Table 1 correspond to the Boltzmann-weighted mean over the two conformers.

Energy mapping of the methyl rotations through 120° in 10° steps, in all compounds, was accomplished by means of the Wiberg-Boyd algorithm¹³. The resulting potential energy profile $V(\theta)$ for (+)-3-methylcyclohexanone is plotted in Figure 3. In addition, the $V(\theta)$ is subtracted from the symmetric potential barrier $\frac{1}{2}V_3(1-\cos 3\theta)$ and the resultant is plotted as a function of θ in Figure 3. It can be seen that the chiral part of the potential barrier does indeed have the form $\sin 3\theta$, as suggested by equation 3.

Table 1 lists the calculated displacement θ_e of the equilibrium position of the methyl groups from the symmetric position in the series of molecules being studied, together with the calculated height of the completed barrier which we take, for simplicity, to be V_3 . A positive θ_e corresponds to a clockwise displacement when viewed along the threefold axis of the methyl group towards the hindering structure and to negative Raman optical activity and vice versa. In the case of (+)-3-methylcyclopentanone, it is the less stable isomer that shows the largest chiral part of the hindering potential and thus dominates the methyl torsion Raman optical activity.

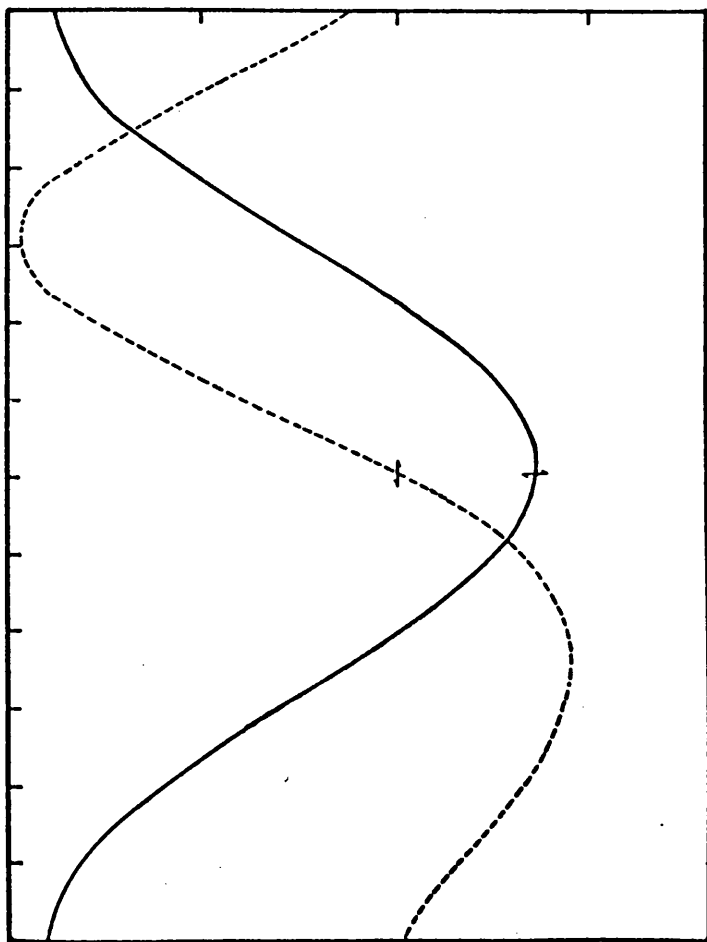


Figure 3: The calculated potential energy profile $V(\theta)$ (solid line) for rotation of the methyl group in (+)-3-methylcyclohexanone. The minimum is at 58.64° and the barrier height $V_3(\text{calc.})$ is 2.51 kcal./mole. The broken line shows the residual $\frac{1}{2}V_3(\text{calc.})(1+\cos 3\theta)-V(\theta)$.

TABLE 1. MOLECULAR MECHANICS DATA FOR THE METHYL GROUP IN A SERIES OF CHIRAL MOLECULES.

MOLECULE	θ_e DEGREES	V_3 KCAL/MOLE	$V_3\theta_e$ SIGN OF OBSERVED RAMAN OPTICAL ACTIVITY
(+)-3-METHYLCYCLOHEXANONE	1.4	2.51	3.51
(+)-3-METHYLCYCLOPENTANONE	0.2	2.55	0.51
(-)-MENTHOL (RING METHYL)	-1.3	2.37	-3.00
(-)-LIMONENE (ISOPROPENYL METHYL)	1.34	0.89	1.19
(-)-LIMONENE (RING METHYL)	-2.3	0.69	-1.59
(+)-CARVONE (ISOPROPENYL METHYL)	-0.27		(-)

Figure 4: The depolarized Raman circular intensity sum ($I_z^R + I_z^L$) and difference ($I_z^R - I_z^L$) spectra of neat (+)-3-methylcyclohexanone

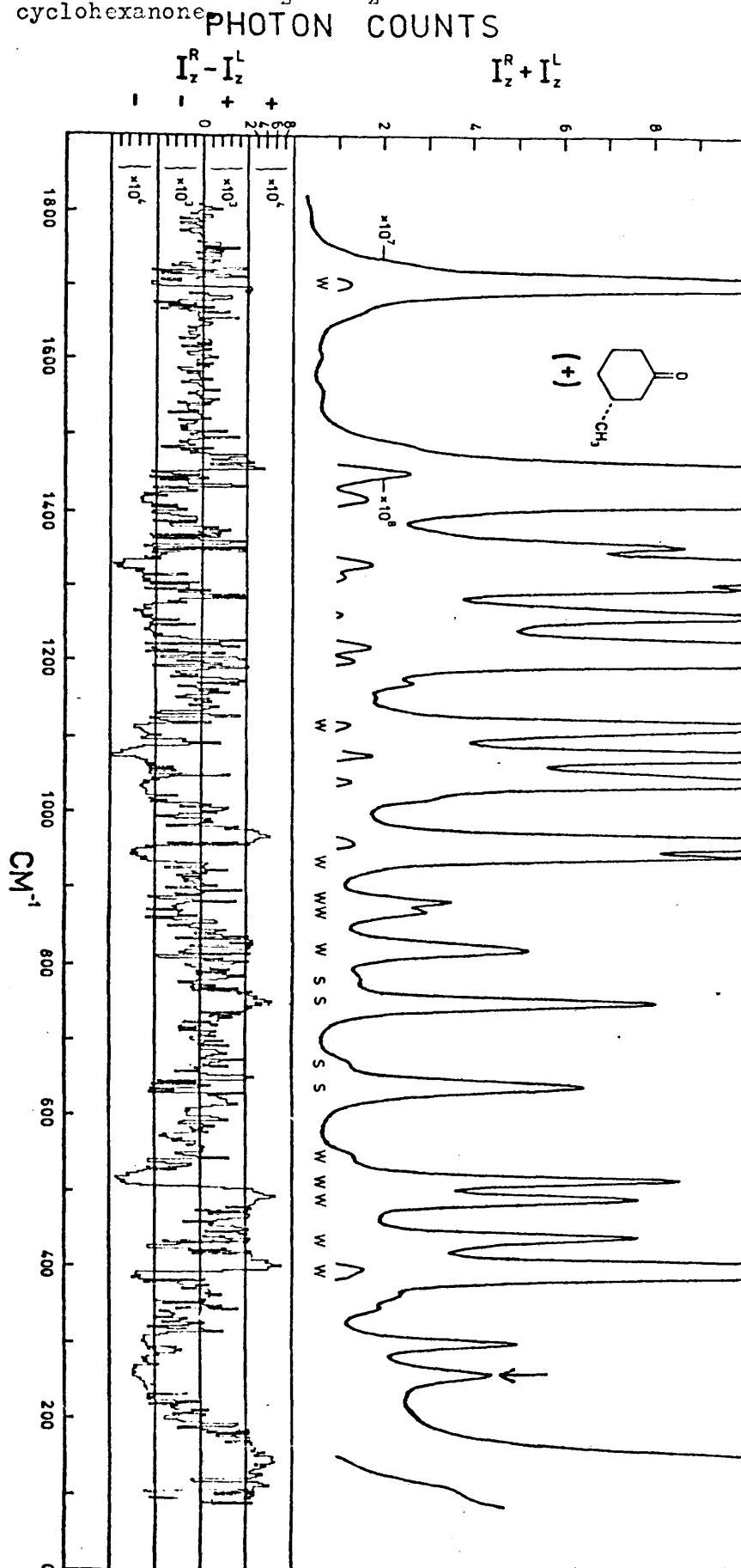


Figure 5: The depolarized Raman circular intensity sum and difference spectra of neat (+)-3-methylcyclopentanone.

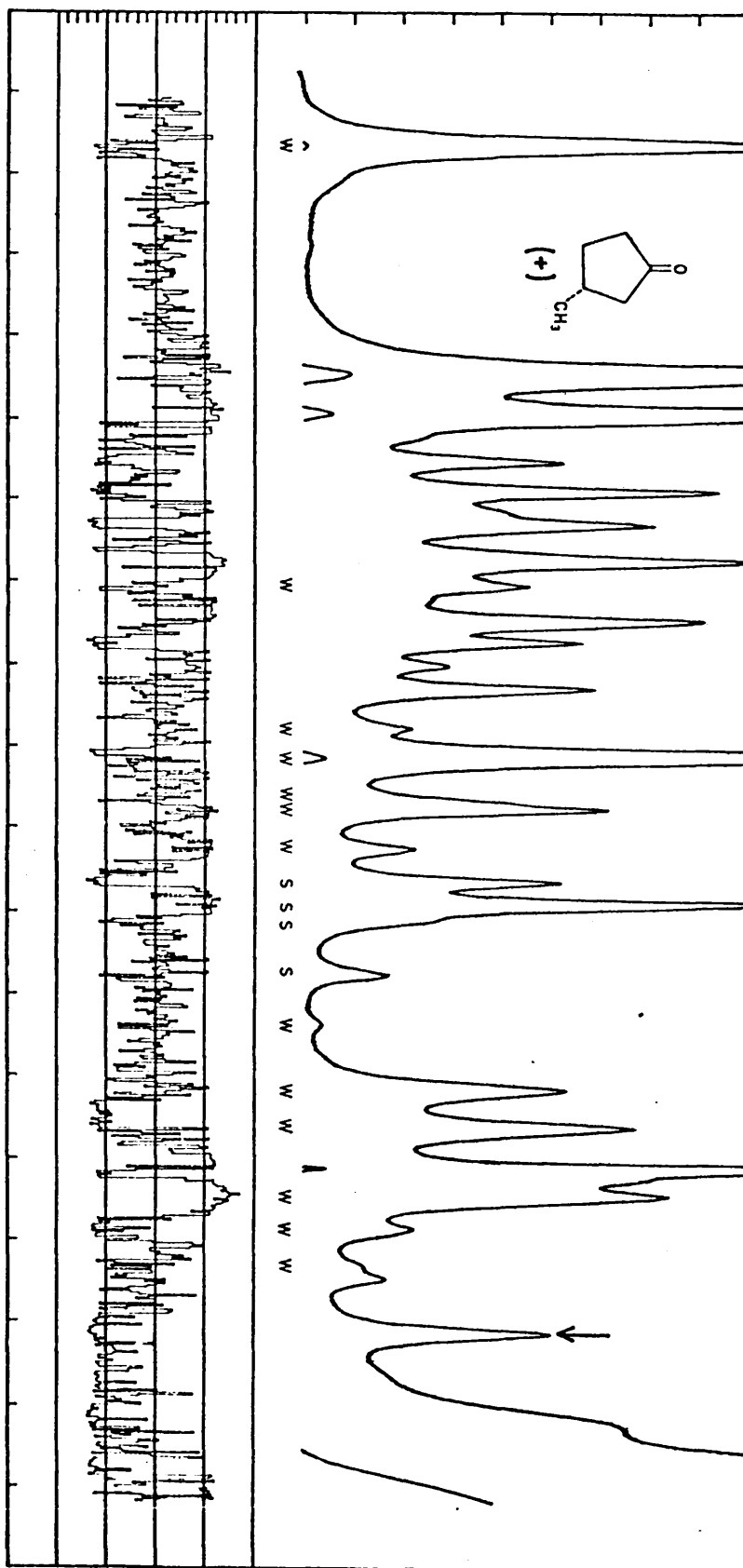


Figure 6: The depolarized Raman circular intensity sum and difference spectra of (-)-menthone diluted with about 30% methanol.

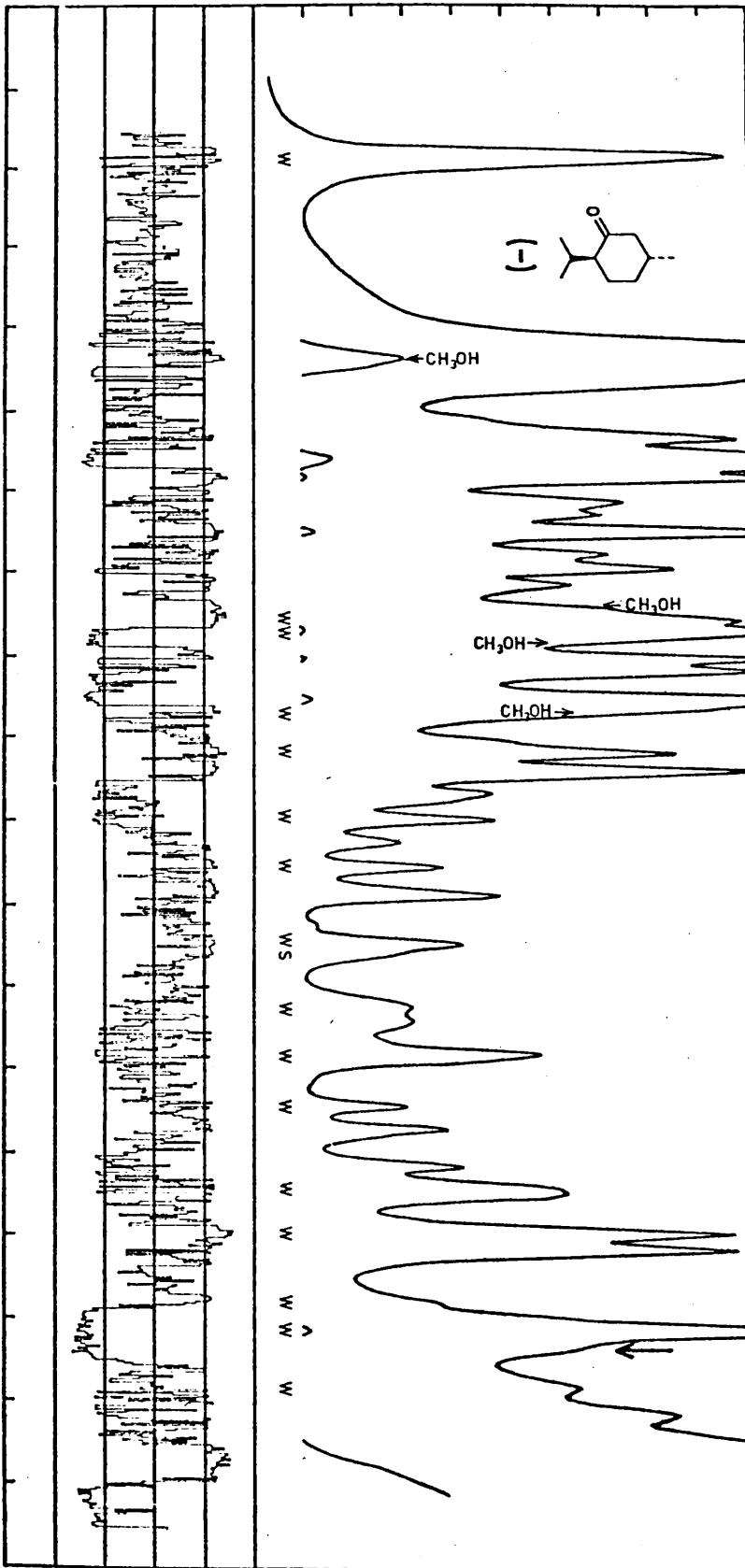


Figure 7: The depolarized Raman circular intensity sum and difference spectra of (-)-menthol.

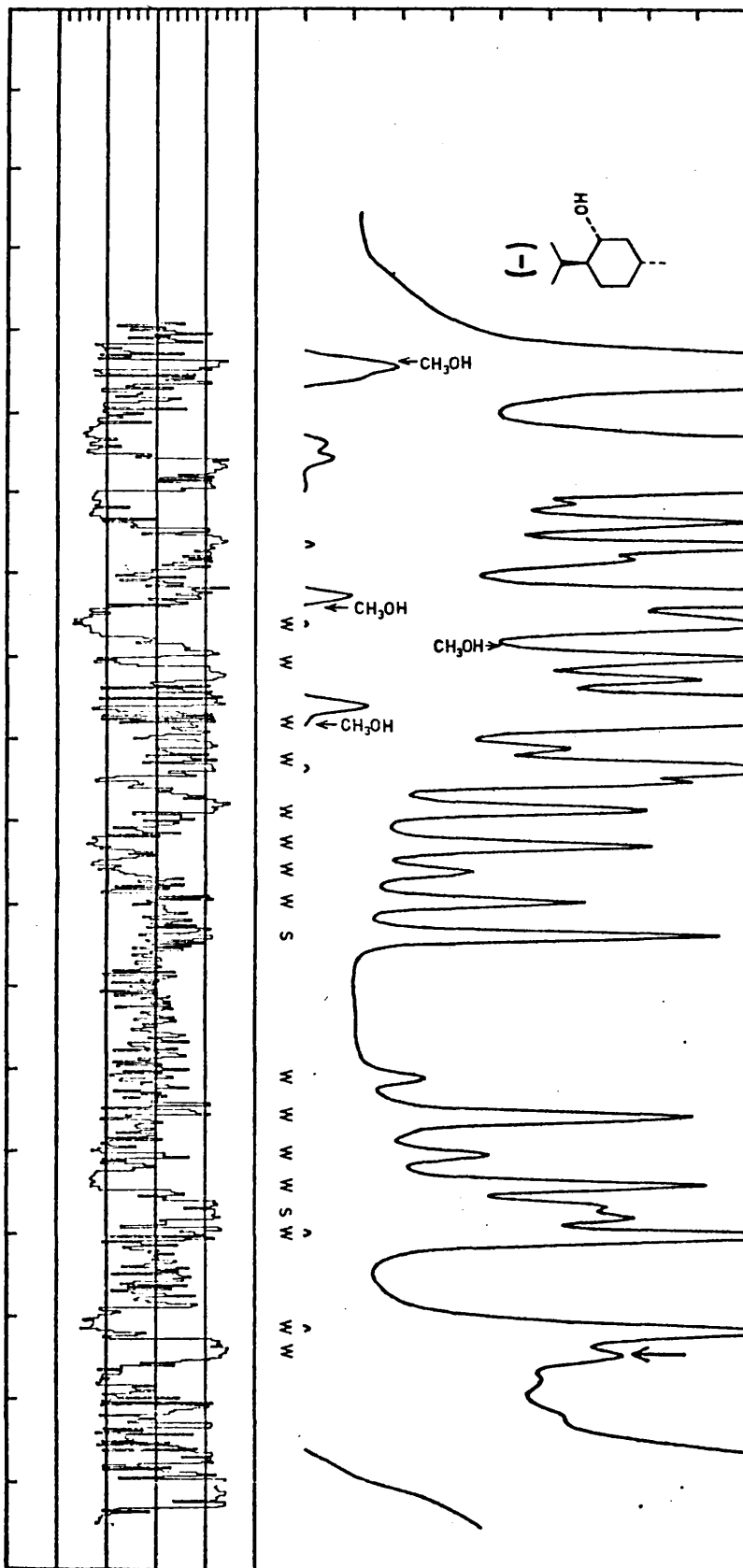


Figure 8: The depolarized Raman circular intensity sum and difference spectra of neat (-)-menthyl chloride.

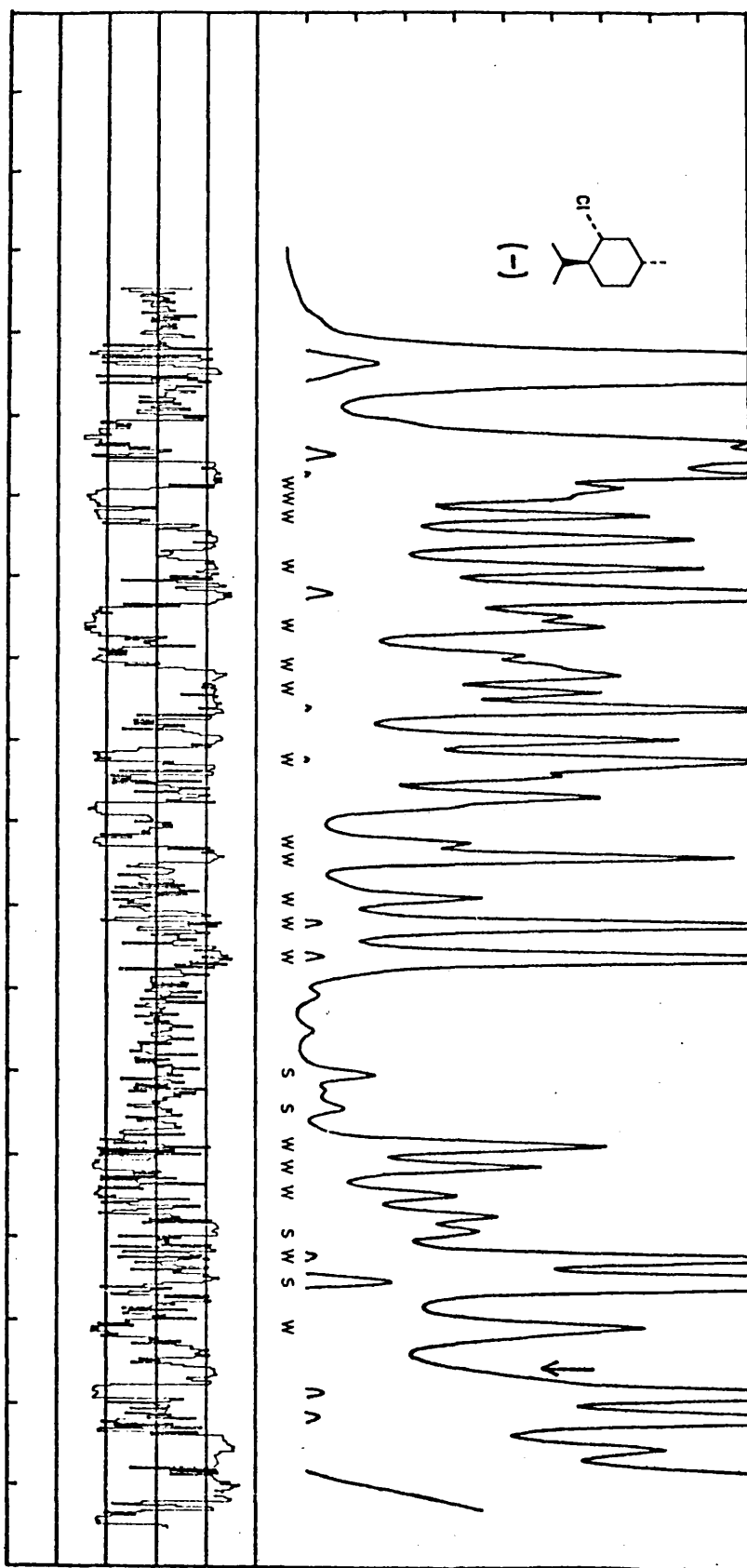


Figure 9: The depolarized Raman circular intensity sum and difference spectra of neat (-)-isopulegol.

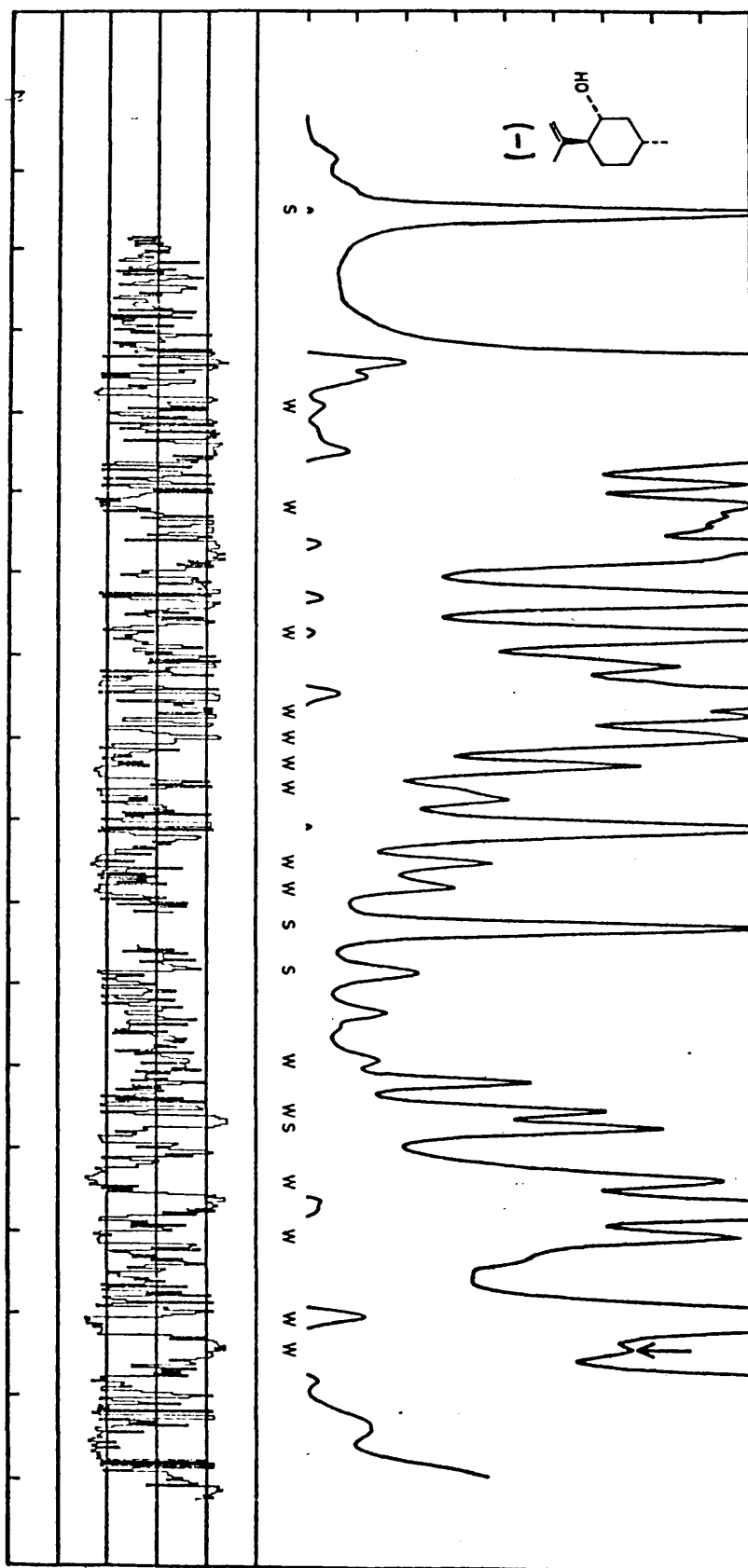


Figure 10: The depolarized Raman circular intensity sum and difference spectra of neat (-)-limonene.

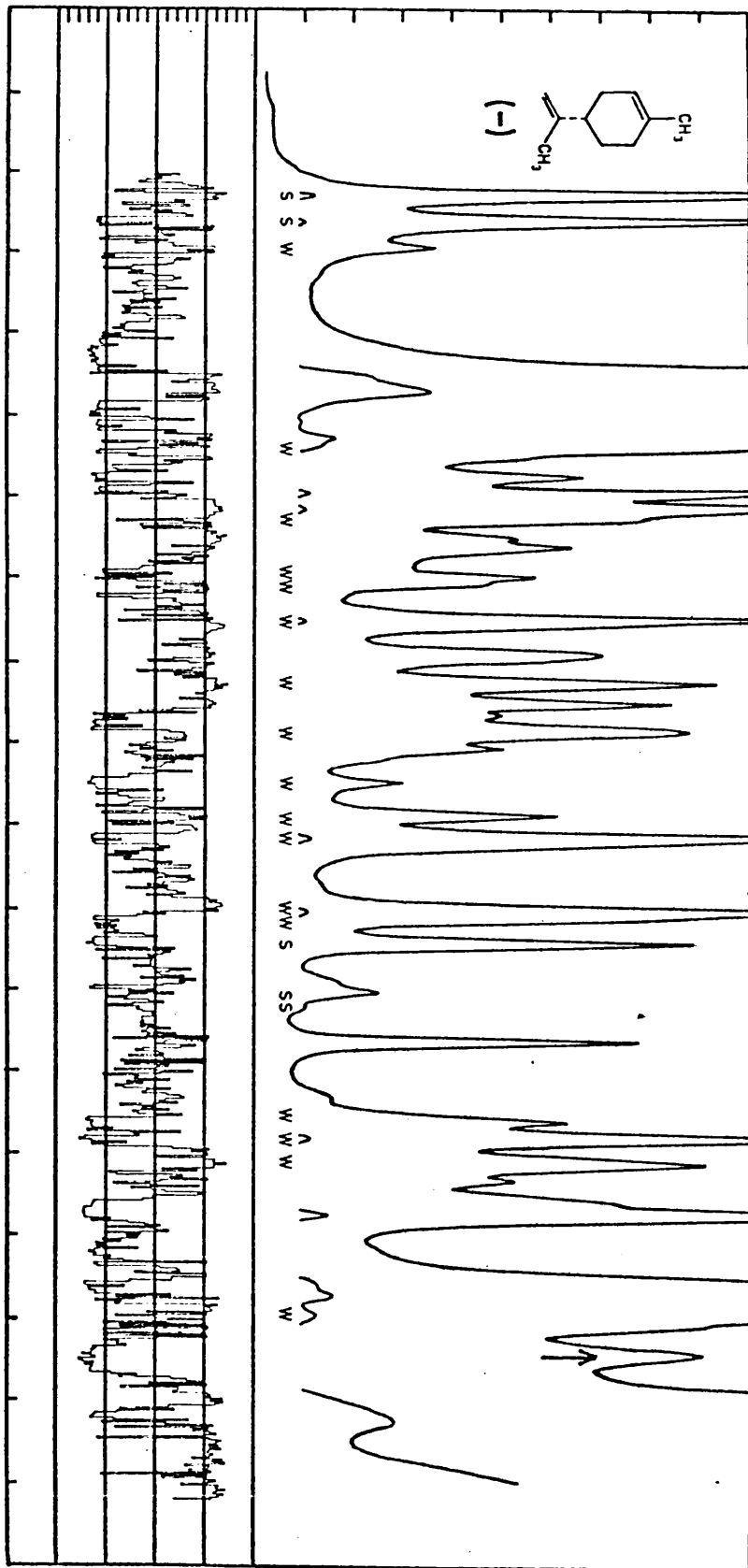
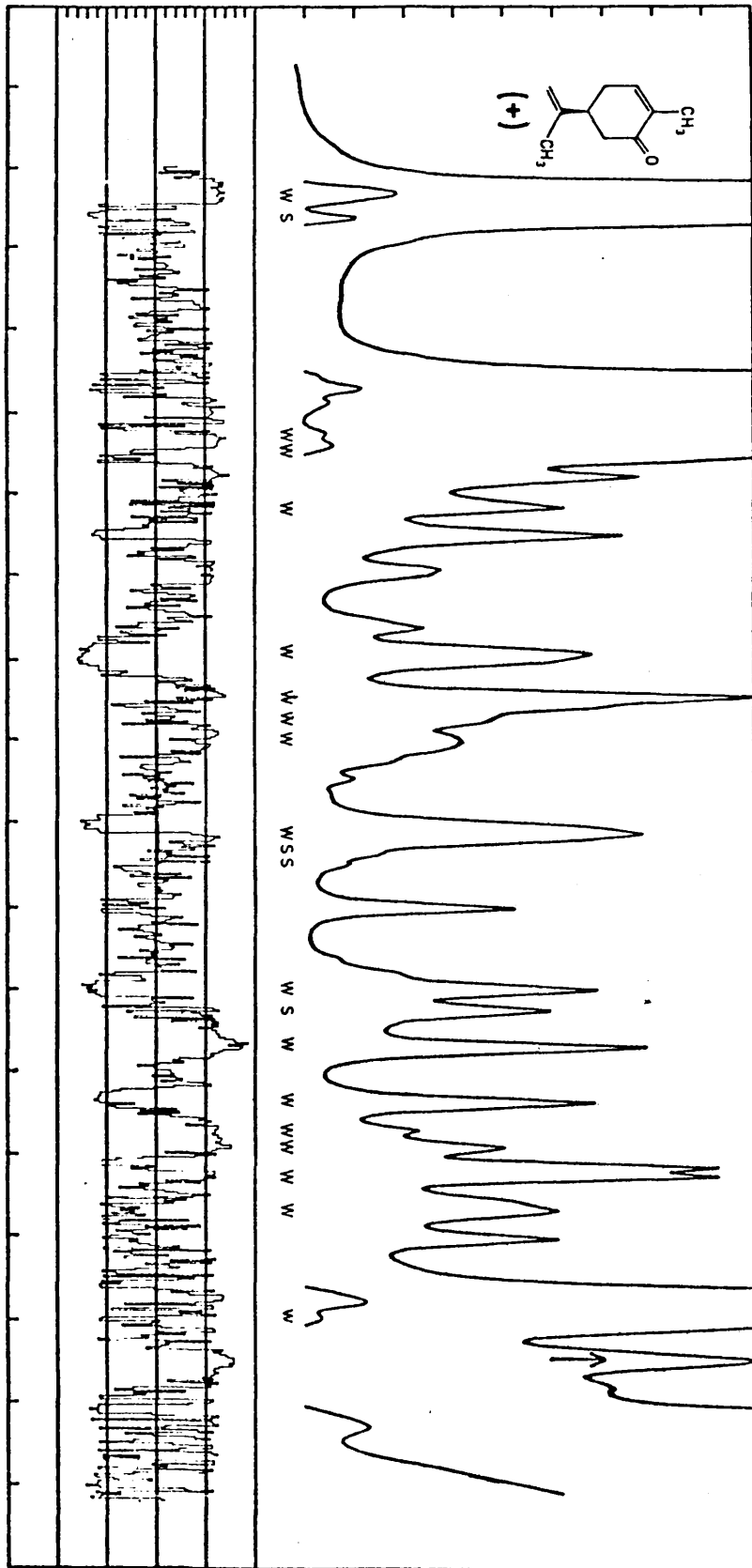


Figure 11: The depolarized Raman circular intensity sum and difference spectra of neat (+)-carvone.



In practice, however, it has been found that the only method which gives a reliable measure of θ_e (and thus the absolute configuration of chiral molecules) is MM calculations as they take account of all the steric interactions in a molecule and minimise the energy with respect to the geometry. Moreover, MM calculations can assess the relative proportion of isomers that compose an equilibrium mixture of a chiral molecule. Molecular models are ineffective in the derivation of these two features of chiral molecules.

6.3 Discussion

It can be seen from Table 1 and from Figures 4,5, 7,10 and 11, that in all molecules studied, there is a strong correlation between the sign of $V_3\theta_e$, which is obtained from MM calculations and the sign of the corresponding methyl torsion CIDs. There is only an approximate correlation between the magnitudes of $V_3\theta_e$ and the corresponding magnitudes of the CIDs but this is due, in part, to the fact that Raman intensities are not standardized. As anticipated, the correlation between frequency of the methyl torsion band and the barrier height, V_3 , as implied by equation 4, is not reproduced by the MM calculations.

Although the assignment of most Raman bands is still tentative, the torsion modes of methyl groups attached to saturated ring systems can be assigned with a certain degree of confidence as they are usually broad

and weak, and occur between 200 and 300 cm^{-1} . In the Raman spectrum of (+)-3-methylcyclohexanone (Figure 4) the broad, weak band at about 260 cm^{-1} probably originates in the methyl torsion. In a similar way, the band at 290 cm^{-1} in (+)-3-methyl-cyclopentanone (Figure 5) is assigned to the methyl torsion mode. The former band is large and negative, whereas the latter is small and negative. These relative signs and magnitudes are consistent with the MM calculations (Table 1) which give V_3^{Me} of the same sign (positive) but much larger for the cyclohexanone than for the cyclopentanone. The assignment of a higher methyl torsion frequency in the cyclopentanone than in the cyclohexanone is supported by the calculated barrier heights, V_3 .

This type of correlation has been extended, without calculation, to some additional related molecules. For example, the methyl group attached directly to the ring in (-)-menthone has a very similar stereochemical environment and the same absolute configuration to that in (+)-3-methyl-cyclohexanone. It is therefore possible to assign the large negative Raman optical activity associated with the weak Raman band at about 260 cm^{-1} in (-)-menthone (Figure 5) to the methyl torsion mode.

MM calculations on (-)-menthol indicate that the methyl group attached to the ring will give rise to a torsion mode which will have large and positive Raman optical activity. These calculations are in accord with

the experimental observation of a weak, broad Raman band at about 260 cm^{-1} in (-)-menthol (Figure 7) which shows large positive optical activity. Similarly, the Raman optical activity spectrum of (-)-menthyl chloride (Figure 8) shows band shoulders at about 260 and 230 cm^{-1} which show small positive optical activity and the Raman optical activity spectrum of (-)-isopulegol (Figure 9) has a band at about 260 cm^{-1} which shows a positive optical activity. Since these three molecules have the same absolute configuration in the region of the methyl group, it seems that these bands can be assigned to torsion of the methyl group attached to the ring in each molecule.

The Raman optical activity spectrum of (-)-limonene (Figure 10) shows a large negative effect associated with a broad, weak Raman band at 250 cm^{-1} . In a similar way, (+)-carvone (Figure 11) shows a large positive effect associated with a Raman band of similar shape at the same frequency. These effects might originate in torsions of the isopropenyl methyl groups since the corresponding potential barriers would be very similar in the two molecules but with opposite chiral parts. This is supported by MM calculation on (-)-limonene (Table 1) which give a positive $V_3\theta_e$ value (and implies negative Raman optical activity) for the isopropenyl methyl group and a negative and smaller $V_3\theta_e$ value (and therefore positive Raman optical activity) for the methyl group attached directly to the ring. The torsion of the latter methyl group may therefore give rise to the Raman bands of positive optical

activity at about 200 cm^{-1} or between about 100 and 180 cm^{-1} . MM calculations on (+)-carvone give a negative $V_{3\theta e}$ value for the isopropenyl methyl group and thus imply positive Raman optical activity which agrees with the assigned Raman band at about 250 cm^{-1} .

An illustration, which demonstrates the reliability of correlations of absolute configurations obtained from Raman optical activity data, is available. The similarity of a number of Raman optical activity features of menthol and menthyl chloride, in Figures 7 and 8, implied that the two chiral molecules should have the same absolute configuration. The menthol enantiomer was known, with certainty, to be the (-)-isomer. Reference 14, however, wrongly assigned the menthyl chloride molecule used as the (+)-isomer. This incorrect assignment was subsequently found to be due to a typographical error and the isomer of menthyl chloride used in the Raman studies was in fact the (-)-isomer as the Raman optical activity spectrum suggested.

6.4 References

1. L.D. Barron, M.P. Bogaard and A.D. Buckingham, J. Amer. Chem. Soc., 95, 603(1973)
2. L.D. Barron and A.D. Buckingham, Ann. Rev. Phys. Chem., 26, 381 (1975).
3. L.D. Barron, Advances in Infra red and Raman Spectroscopy, (Edited by R.J.H. Clark and R.E. Hester), Volume 3, Heyden, London, in the press.
4. W. Hug, S. Kint, G.F. Bailey, and J.R. Scherer, J. Amer. Chem. Soc., 97, 5589 (1975)
5. M. Diem, M.J. Diem, B.A. Hudgens, J.L. Fry and D.F. Burow, J.C.S. Chem. Comm., 1028 (1976).
6. L.D. Barron, Nature, 255, 458 (1975)
7. L.D. Barron, M.J. Bovill and D.N.J. White, J.C.S. Perkin II, in preparation (1977)
8. C.H. Townes and A.L. Schawlow, Microwave Spectroscopy, McGraw-Hill, New York, 1955
9. D.N.J. White and M.J. Bovill, J.C.S. Perkin II, in the press (1977)
10. D.N.J. White, Computers and Chemistry, in the press (1977)
11. D.F. DeTar, J. Amer. Chem. Soc., 96, 1254 (1974)
12. D.N.J. White and H.P. Flitman, to be published.
13. K.B. Wiberg and R.H. Boyd, J. Amer. Chem. Soc., 94, 8426 (1972)
14. W. Klyne and J. Buckingham, Atlas of Stereochemistry, Chapman and Hall, London, 1974.

CHAPTER SEVEN

Some aspects of crystallography.

7.1. Historical

In 1912, Max von Laue predicted that the array of atoms in the lattice structure of a crystal could act as a three-dimensional diffraction grating for X-rays, which are electromagnetic waves having wavelengths in the range of 0.5 - 2.5 Å. In the experiments of Friedrich and Knipping, a crystal of zinc blende was exposed to X-rays and a pattern consisting of a central image surrounded by spots was formed on a photographic plate. These diffraction photographs lent definite support to the view that X-rays consisted of waves as well as supporting the hypothesis of the lattice structure of crystals. W.H. Bragg and his son, W.L. Bragg assumed that the X-rays were 'reflected' from families of regularly spaced planes throughout the crystals and the famous Bragg Law was derived:

$$n\lambda = 2d \sin \theta;$$

where n is the order of the spectrum, λ is the wavelength of the incident X-rays, θ is the angle of incidence between the rays and the plane and d is the distance between adjacent layers of atoms in the crystal. A powerful and precise tool had now been put in the hands of scientists interested in the structure of matter.

X-rays are so penetrating that they cannot be focused by any material. To circumvent this problem, various calculations, which will be discussed in subsequent sections, are substituted for the lenses. From the intensities of the three-dimensional array of reflections collected

from a given single crystal either photographically or from an automatic diffractometer, which has only been in use for about fifteen years, it is possible to obtain an electron density distribution in the crystal which, in turn, provides direct images of the atoms in the unit cell. X-ray analyses of hundreds of crystal structures have led to detailed knowledge of the geometrical properties of different groups of atoms. The resulting stereochemical principles in conjunction with the complex mathematical techniques of modern crystallography and the advent of the data-processing computers have been of great help in the determination of the molecular architecture of complicated biological molecules, which are composed of small basic units, e.g. proteins.

7.2. Corrections to the measured intensities

Before proceeding to the actual structure analysis, it is vital that certain corrections, which allow for various geometrical and physical factors, be applied to the intensity data from the crystal.

(a) Lorentz-Polarisation

Lorentz

Diffraction corresponding to a particular reciprocal lattice point hkl occurs whenever that point intersects the Ewald sphere, but in view of the fact that each reciprocal lattice point is smeared out, the intersection of any given point with the Ewald sphere is not a precise event occurring at the single instant when the Bragg condition is exactly satisfied. The time required for a reciprocal lattice point to pass through the sphere of reflection depends on

both the Bragg angle, θ and on the technique used to measure the intensities. For the equi-inclination Weissenberg technique, the Lorentz factor, L is given by

$$L = \frac{\sin \theta}{\sin 2\theta (\sin^2 \theta - \sin^2 \mu)^{\frac{1}{2}}}, \quad (1)$$

where μ is the equi-inclination setting angle. For data collected on a four circle diffractometer, L is given by

$$L = \frac{1}{\sin 2\theta}. \quad (2)$$

Polarisation

Most methods of data collection use an incident X-ray beam which is unpolarised. The emergent radiation is, however, partially polarised because electric vectors which are parallel to the surface of the reflecting plane are reflected more efficiently than electric vectors perpendicular to the aforementioned plane. The intensity of the reflected beam can be corrected by the polarisation factor, p , which is independent of the mode of data collection employed and which is given by

$$p = \frac{1}{2}(1 + \cos^2 2\theta). \quad (3)$$

The combined Lorentz-Polarisation factor, L_p , for a four circle diffractometer may then be written as follows:

$$L_p = \frac{1 + \cos^2 2\theta}{2 \sin 2\theta} \quad (4)$$

(b) Counting Loss

In recent years, proportional counters and scintillation counters have been used in the measurement of X-ray

intensities. It has been pointed out that, because of the dead time of the counter tubes, which is about 0.25μ sec, the linearity of counting rate with intensity is limited to regions below a certain counting rate. For intense reflections, i.e. greater than about 10,000 to 20,000 counts/sec, the counting rate is beyond the linearity limit, and so, if full use is to be made of the inherent accuracy of the diffractometer, this counter saturation effect must be taken into consideration and this is usually accomplished by reducing the intensity of the direct beam by interposing a suitable number of calibrated foils or, more commonly, by lowering the voltage. A number of low order reflections are then remeasured and, from an analysis of the counts of the weaker low order reflections at the reduced and normal beam intensities, it is possible to derive a conversion factor which may then be applied to the more intense reflections.

The relationship between the intensity of one reflection at normal beam intensity, I , and the intensity of the same reflection at reduced beam intensity, J , is given by

$$J = P_1 I + P_2 I^2, \quad (5)$$

where P_1, P_2 are constants to be determined. Each observation J has an assigned weight, W , which is proportional to the inverse of the square of the standard deviation of J , i.e.

$$W = 1/(\sigma J)^2$$

The residual Δ is the difference between the intensities for a given reflection under the two sets of conditions such

that

$$\Delta = J - (P_1 I + P_2 I^2). \quad (6)$$

By the method of least squares, M is set equal to $\sum W \Delta^2$ and the conditions for M to be a minimum are given by

$$\frac{\partial M}{\partial P_1} = \frac{\partial M}{\partial P_2} = 0. \quad (7)$$

Solution of the resulting simultaneous equations provides the values of \underline{P}_1 and \underline{P}_2 which can be resubstituted into the appropriate equation, together with the count of a strong reflection at reduced beam intensity, \underline{J} , thus making it possible to obtain corrected \underline{I} values for strong reflections.

7.3 Structure Factors

The proper measure of the scattering power per unit cell is given by a complex quantity known as the structure factor, represented by F . The intensity $I(hkl)$ of each diffracted beam is proportional to the square of its amplitude, i.e. $I(hkl) \propto |F(hkl)|_{\text{obs}}^2$ where $|F(hkl)|_{\text{obs}}$ is the so-called "observed" structure factor amplitude and where $F(hkl)$ represents the radiation scattered in the order (hkl) by the crystal. Each of the diffracted beams also has a phase $\alpha(hkl)$ associated with it which expresses the extent to which the diffracted beam is in phase with other diffracted beams. If the positions of the atoms in the unit cell are known, both the "calculated" amplitude $|F(hkl)|_{\text{calc}}$ and "calculated" phase $\alpha(hkl)$ for each reflection can be obtained from the structure factor equation,

$$F(hkl) = \sum_{j=1}^n f_j \exp 2 \pi i (hx_j + ky_j + lz_j) \quad (8)$$

$$= A(hkl) + i B(hkl),$$

$$\text{where } A(hkl) = \sum_{j=1}^n f_j \cos 2 \pi (hx_j + ky_j + lz_j);$$

$$B(hkl) = \sum_{j=1}^n f_j \sin 2 \pi (hx_j + ky_j + lz_j);$$

and i is the imaginary number $\sqrt{-1}$. The summation is over all n atoms in the unit cell, with x_j, y_j, z_j representing the fractional coordinates of the j^{th} atom. From the structure factor equation, it follows that

$$|F(hkl)| = \sqrt{A(hkl)^2 + B(hkl)^2}$$

$$\text{and } \tan \alpha (hkl) = B(hkl) / A(hkl). \quad (9)$$

The term f_j in equation (8) represents the scattering power of the j^{th} atom and is known for an atom at rest. At zero angle scattering, for which all electrons scatter in phase, f_j is equal to the total number of electrons in the atom (viz. the atomic number). With increasing diffraction angle θ , f_j decreases rapidly, in the order of $\sin \theta / \lambda$ due to a greater phase difference between the waves scattered by the electron cloud of the atom.

Atoms in crystals are vibrating and this results in the electron cloud being spread over a wider region of space.

Allowance must be made for this effect in work of even moderate accuracy and this can be accomplished by effectively diminishing f_o , the scattering power of the stationary atom. Thus for isotropic vibration, the scattering factor f_j is given by

$$f_j = f_o \exp \left[-B (\sin^2 \theta) / \lambda^2 \right] , \quad (10)$$

where $B = 8\pi^2 \bar{U}^2$, the Debye-Waller factor or the isotropic thermal parameter. It usually lies in the range $2-4 \text{ \AA}^2$ for carbon and oxygen atoms in a typical organic crystal and is temperature dependent.

\bar{U}^2 = the mean square amplitude of vibration perpendicular to the reflecting plane and lies in the range $0.1 - 0.01 \text{ \AA}^2$.

In general, however, atoms vibrate with different amplitudes in different directions and are best represented by an ellipsoid of electron density, rather than a sphere. To describe such an ellipsoid, six parameters are required - three give the radii along its principal axes and three more to describe the orientation of the ellipsoid in space. Thus, for anisotropic vibration,

$$f_j = f_o \exp \left[- (B_{11} h^2 a^{*2} + B_{22} k^2 b^{*2} + B_{33} l^2 c^{*2} + 2B_{13} h l a^* c^* + 2B_{23} k l b^* c^* + 2B_{12} h k a^* b^*) / 4 \right] , \quad (11)$$

where B_{ij} = the anisotropic thermal parameter; a^*, b^*, c^* = the lengths of reciprocal cell edges.

Alternatively, equation (11) may be rewritten in the more

commonly used form:

$$f_j = f_o \exp \left[-2\pi^2 (U_{11}h^2a^{*2} + U_{22}k^2b^{*2} + U_{33}l^2c^{*2} + 2U_{13}hla^{*}c^{*} + 2U_{23}klb^{*}c^{*} + 2U_{12}hka^{*}b^{*}) \right] \quad (12)$$

where $U_{ij} = U_{ij}^2 = B_{ij}/8\pi^2$, the thermal parameters expressed in terms of mean-square amplitudes of vibrations.

7.4 Structure factors and the electron density distribution

Since the electron density in a crystal varies continuously and periodically in three-dimensional space, the electron density can be expressed as the following three-dimensional Fourier series:

$$\rho(xyz) = V^{-1} \sum_h \sum_k \sum_l F(hkl) \exp \left[-2\pi i(hx + ky + lz) \right] \quad (13)$$

where $\rho(xyz)$ is the electron density at the point with fractional coordinates x, y, z in the unit cell of Volume V . The triple summation is taken over all diffracted beams. It can be shown that

$$F(hkl) = |F(hkl)| \exp 2\pi i \propto (hkl). \quad (14)$$

Using equation (14), it is now possible to substitute for $F(hkl)$ in equation (13) and thus obtain a more useful form of the Fourier expression,

$$\rho(xyz) = V^{-1} \sum_h \sum_k \sum_l |F(hkl)| \exp \left[-2\pi i(hx + ky + lz - \propto(hkl)) \right] \quad (15)$$

If both the amplitude $|F(hkl)|$ and the phase $\alpha(hkl)$ of each diffracted beam are known, the electron density within the unit cell of the crystal can be calculated directly from equation (15) at fractional intervals along each of the cell edges to give a three-dimensional grid of electron density points and the positions of the atoms in the unit cell may be deduced. Equation (15) separates the $|F(hkl)|$'s which can be obtained experimentally from the intensity data from the phase $\alpha(hkl)$ which, unfortunately, cannot be derived from the experimental data and which must therefore be derived by some other strategy, e.g. by trial-and-error, the heavy-atom method, isomorphous replacement, Patterson methods or Direct methods. This search for a self-consistent set of phases is termed the 'phase problem' of crystallography.

7.5 Direct Methods of Phase Determination

Direct methods seek to determine phase information objectively by examination of structure factor magnitudes derived from the study of a single crystal, without reference to chemical knowledge or isomorphous derivatives. Starting from the fundamental physical fact that the electron density within the unit cell can never be negative, a number of inequalities, equalities and probabilities may be derived which, in favourable cases, allow phases to be determined.

Direct methods involve the comparison of the structure factor magnitudes, and in order to generalise the mathematics, it is necessary to define the Unitary Structure Factor $U(\underline{h})$, in direct method vector notation, as

$$U(\underline{h}) = \frac{F(\underline{h})}{\sum_{j=1}^N f_j} \quad (16)$$

where the summation is carried out over the N atoms in the cell and f_j is the scattering factor for atom j compensating for both theta fall-off and thermal effects.

Since

$$F(\underline{h}) = \sum_{j=1}^N f_j \exp 2 \pi i \underline{h} \cdot \underline{r}_j \quad (17)$$

then $|F(\underline{h})| \leq \sum_{j=1}^N f_j$

and so $|U(\underline{h})| \leq 1.$

The maximum value of 1 for $U(\underline{h})$ occurs when all atoms scatter in phase and $|U(\underline{h})|$'s of 1 are rarely if ever found. By defining the Unitary Atomic Scattering Factor n_j , in the following manner:

$$n_j = \frac{f_j}{\sum_{j=1}^N f_j}, \quad (18)$$

it is possible to write

$$U(\underline{h}) = \sum_{j=1}^N n_j \exp 2 \pi i \underline{h} \cdot \underline{r}_j. \quad (19)$$

If all the atoms in the unit cell are alike, n_i then becomes equal to the reciprocal of the number of atoms in the unit cell, N , i.e.

$$n_i = \frac{1}{N},$$

and it can be easily deduced that, in a reasonably sized

organic molecule, there may be so few large $|U(h)|$'s among the data that there will not be enough constraints to determine the structure. As a result of this, Karle and Hauptman formulated a normalised structure factor, $E(\underline{h})$, which is given by

$$E(\underline{h})^2 = \frac{|F(\underline{h})|^2}{\epsilon \sum_{i=1}^N f_i^2} \quad (20)$$

where ϵ is an integer, which is normally unity and which corrects for space group extinctions. The advantage of $E(\underline{h})$ is that the average value of $|E(\underline{h})|^2$ is unity, and it has been shown that the use of $E(\underline{h})$ is tantamount to regarding the atoms within a structure as points which do not suffer thermal motion.

Inequalities

The first direct methods to be introduced were the Harker-Kasper inequalities, from which it is possible to obtain certain phase information. In a crystal which has a centre of symmetry, equation (19) may be rewritten in the form

$$U(\underline{h}) = 2 \sum_{j=1}^{N/2} n_j \cos 2\pi i \underline{h} \cdot \underline{r}_j \quad (21)$$

Using Cauchy's inequality, which states that

$$\left| \sum_j a_j b_j \right|^2 \leq \left(\sum_j |a_j|^2 \right) \left(\sum_j |b_j|^2 \right),$$

equation (21) then becomes

$$U^2(\underline{h}) \leq \frac{1}{2} [1 + U(2\underline{h})] \quad (22)$$

Relation (22) relates information concerning the reciprocal lattice site \underline{h} to that for the site $2\underline{h}$ and since, both the magnitude and sign (+) of $U^2(\underline{h})$ are known, the sign of $U(2\underline{h})$ may be unambiguously deduced if the intensity at \underline{h} is strong enough.

In general, they give unambiguous information only if there are a large number of intensity maxima associated with unitary structure factors of value of about one half or greater. As molecular size increases, the probability of any general $U(\underline{h})$ being greater than one half decreases, and so this reduces the applicability of inequalities to larger structures. Although different inequalities may be generated for all the 230 space groups, the general use of inequalities is restricted to centrosymmetric crystals. The resolution of the positive/negative ambiguity is a far simpler problem than the identification of a phase angle anywhere between 0 and 2π , and no general inequalities for the noncentrosymmetric case have been found to be useful.

Equalities

In 1952, certain equalities, which give more specific information than do the inequalities, were introduced. Sayre derived the following relationship between the structure factors of three reflections represented as \underline{h} , \underline{k} , $\underline{h-k}$:

$$F(\underline{h}) = \phi(\underline{h}) \sum_{\underline{k}} F(\underline{k}) \cdot F(\underline{h} - \underline{k}), \quad (23)$$

where $\phi(\underline{h})$ is a calculable scaling factor.

By considering a structure of identical resolved atoms, Sayre derived the following 'Sigma two' relationships,

between the signs of three reflections:

$$S(\underline{h}) = S(\underline{k}) \cdot S(\underline{h} - \underline{k}) \quad (24)$$

where S indicates 'the sign of'.

Thus knowledge of the signs of two reflections permit the sign of the third reflection to be determined. These particular relationships are true only for the hypothetical case of a structure composed of identical atoms. For organic crystals, the predominant components carbon, oxygen and nitrogen have about the same atomic weight, and so equation (24) has been shown to hold if the associated structure factors are large.

'S' may be used to denote 'the phase of', thus allowing the Sayre equation to be used for non-centrosymmetric cases.

Probabilities

When the magnitudes of the structure factors are not large enough for equation (24) to be strictly true, it has been shown that they are probably correct, although in some cases, the sign equalities may break down and the 'equals' sign in equation (24) should be replaced by ' \approx ' which means 'probably equals'.

Various analyses have been carried out by Cochran and Woolfson to determine the statistical interpretation of relation (24) and the probability of its being correct may be quantified in terms of E values in the following way:

$$P(E) = \frac{1}{2} + \frac{1}{2} \tanh (|E(\underline{h}) \cdot E(\underline{k}) \cdot E(\underline{h}-\underline{k})| \cdot N^{-\frac{1}{2}}). \quad (25)$$

By regarding each phase indication as a vector of length $|E(\underline{k}) \cdot E(\underline{h} - \underline{k})|$ and direction $[\phi(\underline{k}) + \phi(\underline{h} - \underline{k})]$, they may be summed vectorially. This operation leads to the Tangent formula:

$$\tan \phi(\underline{h}) = \frac{\sum_{\underline{k}} |E(\underline{k}) \cdot E(\underline{h}-\underline{k})| \sin [\phi(\underline{k}) + \phi(\underline{h} - \underline{k})]}{\sum_{\underline{k}} |E(\underline{k}) \cdot E(\underline{h}-\underline{k})| \cos [\phi(\underline{k}) + \phi(\underline{h} - \underline{k})]} \quad (26)$$

For non-centrosymmetric space groups, it is often found only partial structure information is obtained. However, if the calculated structure factors, based on the partial structure, agree reasonably well with the observed amplitudes, then the phases associated with other large E values may be included in further tangent formula calculations. This recycling process may be repeated until all the atoms are located.

Phase Determination in Practice

Numerous computer programmes have been prepared to determine phases by utilising the symbolic addition procedure of the Karles and equations (24-26). The MULTAN system is one such package of crystallographic computer programmes which will perform all the necessary direct methods calculations. The main subprogrammes which comprise the complete system are:

(a) The NORMAL programme computes the normalised structure amplitudes, $|E|$'s from the intensity data.

(b) The MULTAN programme consists of three sections:

(i) SIGMA 2 generates the Sigma two interactions (Equation(24)).

(ii) CONVERGE finds the starting reflections for the Tangent formula (Equation (26)) by application of the Sigma one formula (which is a special case of the Sigma two relationship in which two of the reflections are the same) and by assigning phase values to reflections which define the origin and enantiomorph. A small number of reflections, which appear to provide a good starting point for phase determination, are chosen and are given all possible combinations of $\pm \pi/4$ or $\pm 3\pi/4$ for non-centrosymmetric space groups and 0 or π for centrosymmetric space groups, thus producing a multiple starting point for the tangent formula.

(iii) FASTAN generates each starting set of phases and, by using a weighted version of the Tangent formula and the phase relationships output by SIGMA 2, it determines the phases of other high value $|E|$'s and a figure of merit based on the degree of internal consistency for each complete phase set.

(c) The FOURIER programme computes an E-map from a set of normalised structure factors which has the highest combined figure of merit. From the E-map, it is possible, in most cases, to deduce the location of atoms.

MULTAN is most successful when dealing with centrosymmetric crystals of small organic molecules, and complete structures solutions are often possible. The problem is more complicated for the non-centrosymmetric case, but it is not impossible. Very often, figures of merit can be unreliable and it is necessary to examine a large number of E-maps before the correct solution is found.

7.6. Fourier synthesis

Once the initial estimates for the phases $\alpha(hkl)$ have been obtained by some strategy, they can be used, in conjunction with the observed structure factor amplitudes, to compute a three-dimensional electron density map, by using equation (15). If the initial phases are close enough to the true values, this synthesis will allow some of the structural information "locked" in the observed structure factor amplitude values to be released either by revealing peaks with reduced density of additional atoms, which were not used in the derivation of the initial sets of phases, or by indicating any minor errors in the coordinates of the atoms previously located. A new set of phases are then recalculated from the corrected coordinates of the previous set of atoms and the coordinates of the newly located atoms, using equation (8) and this new set of phases represent an improvement over the initial set of phases because there is more, or more precise, information used in their derivation. The reiterative process of recalculation of the phases together with the subsequent computation of another Fourier electron density map (based

on the observed amplitudes and calculated phases) is known as "successive Fourier synthesis" and is continued until a model which reproduces itself is obtained.

Having obtained a more reliable set of phases, we then calculate a Fourier synthesis using the quantities $|F_o| - |F_c|$. This gives a difference Fourier map which has certain features which enable the correct model to be further refined and which may be expressed in the form:

$$\Delta\rho = v^{-1} \sum_h \sum_k \sum_l \Delta F_{\text{exp}} - 2 \pi i(hx + ky + lz), \quad (27)$$

$$\text{where } \Delta F = |F_o| - |F_c|$$

$|F_o|$ = observed structure factor amplitude,
obtained from intensity data.

and $|F_c|$ = calculated structure factor amplitude,
obtained from structure factor equation (8).

Specifically, a difference Fourier map is particularly useful for the more precise location of atomic positions, for the identification of missing atoms and for refinement of thermal parameters.

7.7 Least squares refinement

This is a statistical treatment of the data so that a model, which represents the best fit with the observed data, is obtained.

The electron density maxima obtained from the Fourier synthesis, discussed in the previous section, does not

necessarily correspond to the best atomic co-ordinates which can be attained. This is mainly due to the fact that, in these Fourier synthesis, the summation is only taken over all the diffracted beam instead these Fourier series should be infinite. Thus termination of series errors will always be present. To overcome this obstacle, the structure can be further refined by the method of least squares. Since there is a large excess of observational data (F_o) over the numbers of parameters, e.g. atomic coordinates, temperature factors, this situation is suited to least squares analysis, which is well adapted to automatic computing. The computation is set up so as to yield small shifts in the parameters which will minimise the quantity D which is given by

$$D = \sum_{hkl} W (|F_o| - |F_c|)^2 = \sum_{hkl} W \Delta^2, \quad (28)$$

where W = a weighting factor for each observation and the summation is over all the observed reflections.

Since $|F_c|$ is a function of parameters P_1, P_2, \dots, P_n , which may be scale, positional or thermal parameters, the conditions for D to be a minimum are the equations

$$\frac{\partial D}{\partial P_j} = 0 = \sum_{hkl} W \Delta \frac{\partial |F_c|}{\partial P_j} \quad \text{for } j = 1, 2, \dots, n. \quad (29)$$

There are \underline{n} such equations corresponding to the \underline{n} possible values of j. Since for each atom which is refined anisotropically, there are nine parameters and for each atom which is refined isotropically, there are four parameters, it can be seen that \underline{n} will usually be a large number in most

crystal structure analyses. The Fourier syntheses provide satisfactory estimates, a_j , for the values of parameters, P_j , and thus provide a good starting point for the least squares analysis, which, in turn, supplies the values for the small changes, ΔP_j , in the values of the parameters, P_j , such that a better approximation, a'_j , for the value of the parameters, P_j , can be obtained,

$$\text{i.e. } a'_j = a_j + \Delta P_j, \quad j = 1, 2, \dots, n \quad (30)$$

The function $|F_c|$ can now be expressed as a Taylor series, which is truncated after the linear term to make the subsequent calculations more manageable:

$$\begin{aligned} |F_c(P_1, P_2, \dots, P_n)| &= |F_c(a_1, a_2, \dots, a_n)| \\ &+ \sum_{i=1}^n \frac{\partial |F_c|}{\partial P_i} \cdot \Delta P_i. \end{aligned} \quad (31)$$

Substituting equation (31) in equation (29) gives, on rearrangement:

$$\sum_{i=1}^n \left(\sum_{hkl} w \frac{\partial |F_c|}{\partial P_i} \cdot \frac{\partial |F_c|}{\partial P_j} \right) \Delta P_i = \sum_{hkl} w \Delta \frac{\partial |F_c|}{\partial P_j}. \quad (32)$$

The system of n equation in (32) corresponds to the n normal equations for the "best" values of ΔP_i and may be rewritten as:

$$\sum_i a_{ij} \Delta P_i = C_j \quad (33)$$

or, in matrix notation, as:

$$A \cdot \Delta P = C \quad (34)$$

Having obtained the least squares solution from one cycle, i.e. the values of shifts ΔP_i , it is usually necessary to perform several cycles of least-squares before there is convergence. This is because the Taylor series, which relates $|F_c|$ to the parameters, P_j , has been truncated (equation (31)) and so the 'best values' of the parameters are not given after one cycle.

The crystallographic least squares refinement can utilise either block diagonal or full matrix methods. The latter is the preferred approach as the full matrix technique has better convergence properties and also supplies useful information on the interdependence or correlation of parameters used in the least squares analysis, but it is important to note that it places greater demands on computer resources.

Once the optimum values of the parameters, P_j , have been obtained, it is important to obtain a measure of the error in such values and this is accomplished by calculating the standard deviation, σ , for each parameter in the following way:

$$\sigma(P_j) = \left((a^{-1})_{jj} \frac{\sum w \Delta^2}{m - n} \right)^{\frac{1}{2}} \quad (35)$$

where $\sigma(P_j)$ = estimated standard deviation of parameter P_j

$(a^{-1})_{jj}$ = the j^{th} diagonal element in the inverse matrix of A (see equation (34)).

m = number of observations

n = number of parameters.

From statistical considerations, the proper weight, W , should be proportional to the inverse of the square of the standard deviation of the amplitude $|F_o(hkl)|$, i.e.

$$W(hkl) = \frac{1}{\sigma^2 [F_o(hkl)]}, \quad (36)$$

where the standard deviations can be estimated by making repeated measurements of each reflection, which is clearly not feasible. It is therefore customary to use empirical weighting schemes which are designed so as to minimise the deviation from constant $W\Delta^2$ over a range of magnitudes of $|F_o|$ and $\sin \theta$.

The least squares refinement process is followed by computing the weighted residual R at each stage:

$$R = \frac{\sum W (|F_o| - |F_c|)^2}{\sum W |F_o|^2} \quad (37)$$

If the refinement process is giving a progressively more accurate electron density map, then R should decrease steadily.

CHAPTER EIGHT

An X-ray analysis of 1,8-dimethyl-2-naphthyl acetate.

8.1 Introduction

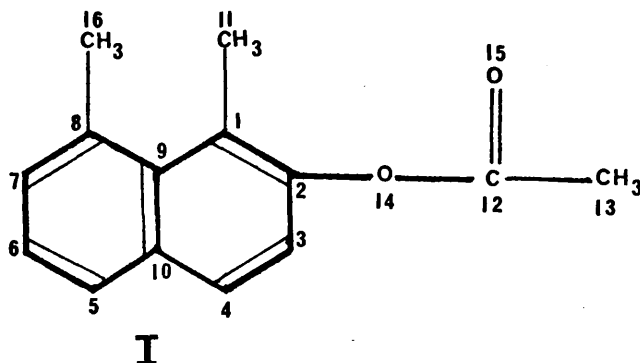
In the naphthalene molecule, the 1-and 8-positions are said to be peri to each other and substituents located at these positions are in much closer proximity than similar substituents located ortho to each other. This closer proximity has been responsible for the appearance of several unique properties of peri-substituted naphthalenes, e.g. the relative ease of acid-catalysed isomerisation of 1,8-dimethylnaphthalene to the 1,7-isomer compared to other dimethylnaphthalenes has been attributed to the relief of strain in the leading to the carbon-1 protonated derivative.¹

Peri-strain can be relieved by four modes of molecular deformation² - (a) stretching of bonds C1-C9 and C8-C9, (b) in-plane deflection of the substituents such that the C9-C8-C16 and C9-C1-C11 valency angles are increased from their equilibrium values of 120° , (c) out-of-plane bending of the substituents on the naphthalene nucleus, δ_i , and (d) a distortion or buckling of the nucleus itself. In many peri-substituted naphthalenes, considerable in-plane and out-of-plane deviations of the exocyclic bonds occur; reported cases of nuclear distortions are relatively limited. In such molecules, two competing influences are in operation, namely the loss on resonance energy due to nuclear distortions and deviation of substituents from the mean molecular plane on one hand and the decrease in steric strain energy on the other.

In naphthalene, the distance between the peri-carbon

atoms is only about 2.4-2.5 Å. In aromatic molecules, the normal nonbonded C ... C distance is about 3.0 Å. It is therefore logical to expect that with substituents other than hydrogen at the peri positions in naphthalene, there will be considerable steric interaction.

The crystallographic study of 1,8-dimethyl-2-naphthyl acetate³ (I) was undertaken so that some light may be thrown on the nature of the peri interaction and the mechanism by which the steric strain is minimised. This, in turn, may



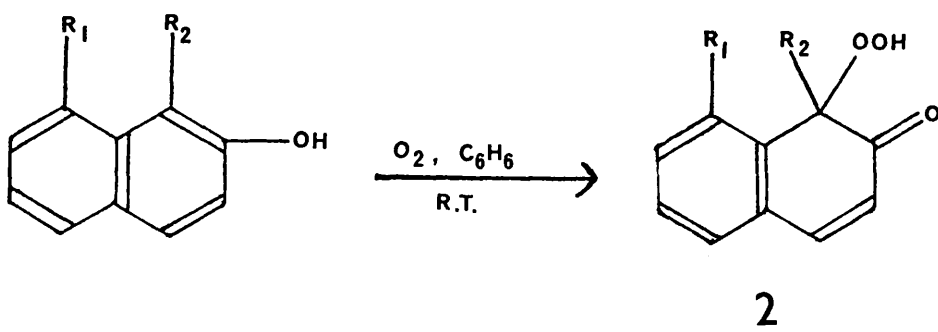
help to explain the effect of the peri-strain on the rate of the autoxidation of substituted 2-naphthols. The order of reactivity of the 2-naphthols known to autoxidise was found to be,⁴

1-Me(inert) « 1-Ethyl « 1-c-hexyl < 1-isopropyl

< 1,8-dimethyl < 1-t-butyl.

Brady and Carnduff⁴ proposed that the major factor controlling the overall rate of the autoxidation of substituted 2-naphthols, which show the characteristics of a radical chain process, is the degree of steric strain within the molecule, and especially the magnitude of the peri-interaction between substituents at C1 and C8 and/or C4 and C5. This

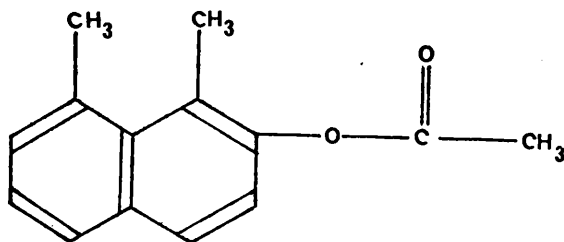
peri-interaction is absent in the 1-hydroperoxy-2(1H)-naphthalenones (2) produced in the autoxidation reactions. The resulting strain relief is thought to be the factor controlling the rates.



On account of the fact that 1,8-dimethyl-2-naphthol will autoxidise readily, the X-ray crystal structure analysis was performed on the acetate of the naphthol, since the first step in the reaction is the homolytic fission of the O-H bond.

8.2. Experimental

Crystal Data



1,8-Dimethyl-2-naphthyl acetate: $C_{14}O_2H_{14}$

Unit Cell Dimensions:

\underline{a}	=	9.54 Å	$\alpha = 90.0^\circ$
\underline{b}	=	6.63 Å	$\beta = 110.2^\circ$
\underline{c}	=	19.87 Å	$\gamma = 90.0^\circ$

Space Group	P2 ₁ /C (C _{2h} ⁵)
M	214 a.m.u.
V	1180 Å ³
D _m	1.18 g cm ⁻³
D _c	1.21 g cm ⁻³
λ	0.7107 Å
μ (Mo K α)	0.86 cm ⁻¹
F (000)	456
Z	4

The space group was uniquely determined by the systematic absences:

h0l when $l = 2n + 1$ and Ok0 when $k = 2n + 1$. The crystal used in this analysis was a needle of dimensions 1.5 x 1.0 x 0.5 mm³.

Data Collection

Precession photographs were used to measure the cell dimensions and to determine the space group. The crystal was then mounted and aligned on the goniometer head of a Hilger and Watts Y290 computer-controlled four-circle diffractometer. The cell dimensions quoted in the crystal data are those obtained from a least-squares analysis of the angular settings of 12 reflections. The intensities were obtained by the ω -2 θ step scan procedure which consisted of forty steps of 0.02° at 2 sec./step with background counts for 20 seconds at each end of the scan range and periodic monitoring of two standard reflections. The integrated intensity, \underline{I} of a reflection can be calculated from the peak, \underline{P} , and background $\underline{B1}$, $\underline{B2}$, counts using equation (1):

$$I = P - (B1 + B2) \cdot \frac{t_p}{2t_b} \quad (1)$$

where t_p = counting time at peak

and t_b = counting time for one of the background counts (both the same),

and the standard deviation of \underline{I} (σI), can be obtained from equation (2):

$$\sigma I = \left(P + (B1 + B2) \cdot \frac{t_p}{2t_b} \right)^{\frac{1}{2}} \quad (2)$$

The integrated intensities (I) of 1877 independent reflections ($2\theta \leq 52^\circ$) with $I \geq 2 \sigma(I)$ were obtained. Reduced beam intensity was employed to remeasure the reflections for which $2\theta \leq 16^\circ$ in order to correct for counter saturation errors. No correction for absorption was applied.

TABLE 1 SUMMARY OF STRUCTURE DETERMINATION

A. INITIAL SET OF PHASES

REFLECTION	PHASE *	MOD. E
6 3 -14 +	360	3.14
1 5 -8 +	360	2.70
4 1 11 +	360	2.56
6 2 6	360 OR 180	3.06
5 3 -13	360 OR 180	3.04
7 4 -18	360 OR 180	2.93
7 2 38	360 OR 180	2.57

B. STATISTICS

THEORETICAL FOR CENTRIC	E1	E2	E3	E4	E5	E6
THEORETICAL FOR ACENTRIC	0.798	1.000	0.968	31.7	4.6	0.3
FOUND	0.886	1.000	0.736	36.8	1.8	0.0
	0.828	1.000	0.929	28.8	5.00	0.4

* IN DEGREES
 + ORIGIN DEFINING
 MOD. E MODULUS OF E FOR REFLECTION CONCERNED
 E1 MEAN VALUE FOR MODULUS OF E
 E2 MEAN VALUE FOR MODULUS OF E**2
 E3 MEAN VALUE FOR MODULUS OF ((E**2)-1)
 E4 % OF REFLECTIONS WITH MODULUS OF E > 1.0
 E5 % OF REFLECTIONS WITH MODULUS OF E > 2.0
 E6 % OF REFLECTIONS WITH MODULUS OF E > 3.0

Structure Analysis

The atomic coordinates of all the non-hydrogen atoms were obtained by the multiresolution direct phase determining programme MULTAN. $|E|$ values were derived from the intensities, on the basis of an overall isotropic temperature factor $B \ 3.80 \text{ \AA}^2$, and triplet relationships were generated for the 200 reflections with $|E| > 1.5$. The starting set of 7 reflections, which consisted of three to define the origin and four reflections to which the values of 0 and π were given, were selected by the programme (Table 1). This procedure gave sixteen possible phase sets which were then calculated for the 200 reflections with the largest values of $|E|$ and an E-map computed from the set showing the highest combined figure of merit revealed all the non-hydrogen atoms.

The initial structure-factor calculation gave an R of 29.8% and three cycles of full-matrix least-squares refinement, using the 1824 independent structure amplitudes for which $|F_o| > 4 \sigma(|F_o|)$ with isotropic thermal parameters, lowered R to 16.7%. Subsequent calculations with anisotropic thermal parameters reduced R further to 10.4%. After making allowance for errors caused by counter saturation, R was 9.7%. A difference electron-density distribution revealed the sites of the hydrogen atoms, which were then included in the least-squares calculations with isotropic thermal parameters and convergence was reached at 6.6%. The weighting scheme employed was $\omega = 1/(A + B |F_o| + C |F_o|^2)$ with $A = 0.1508$, $B = -0.0051$

and $C = 0.0038$. The values of constants A, B and C were chosen so that the deviation from $\omega \Delta^2$ over the range of $|F_o|$ and $\sin \theta$ was minimised. The refinement then converged at $R = 6.1\%$. The ratio of observations to parameters was 9 to 1.

8.3 Results

The atomic coordinates, thermal parameters, bond lengths, valency angles, torsion angles, deviations of the atoms from the various planes in the molecules and a listing of the observed and calculated structure factors are given in Tables 2-8. The molecular and crystal structures are shown in Figures 1 and 2.

Table 2 : Fractional atomic coordinates ($\times 10^4$) with estimated
standard deviations in parentheses.

The hydrogen atoms are numbered according to the
atoms to which they are attached.

The table shows:

Atom	x	y	z
------	---	---	---

C(1)	4869(2)	4257(3)	5901(1)
C(2)	3468(2)	4879(3)	5488(1)
C(3)	2780(2)	6633(4)	5598(1)
C(4)	3526(2)	7806(3)	6164(1)
C(5)	5694(3)	8567(4)	7212(1)
C(6)	7061(3)	8124(4)	7677(1)
C(7)	7803(3)	6433(4)	7553(1)
C(8)	7188(2)	5132(3)	6985(1)
C(9)	5702(2)	5517(3)	6496(1)
C(10)	4980(2)	7293(3)	6621(1)
C(11)	5436(4)	2276(4)	5714(2)
C(12)	1539(2)	2591(4)	4875(1)
C(13)	0837(4)	1561(6)	4171(2)
O(14)	2690(2)	3763(3)	4864(1)
O(15)	1156(2)	2453(3)	5380(1)
C(16)	8176(3)	3424(6)	6914(2)

H(3)	1778(29)	7058(38)	5248(12)
H(4)	3102(25)	9003(40)	6303(12)
H(5)	5133(27)	9772(40)	7276(12)
H(6)	7520(30)	9084(43)	8121(14)
H(7)	8824(30)	6083(41)	7868(13)
H(111)	6375(40)	2350(51)	5573(18)
H(112)	5791(32)	1401(51)	6109(16)
H(113)	4708(41)	1904(52)	5289(18)
H(131)	0084(54)	2646(68)	3881(23)
H(132)	0055(37)	0517(51)	4169(16)
H(133)	1493(42)	1438(56)	3950(19)
H(161)	7716(55)	2000(77)	6947(25)
H(162)	9223(47)	3535(62)	7268(20)
H(163)	8288(37)	3483(53)	6427(19)

Table 3: Thermal parameters ($\times 10^4$) with e.s.d.'s in parentheses.

Carbon and oxygen values are anisotropic.

Hydrogen values are isotropic.

The anisotropic temperature factor expression used was of the form described by equation (12) in chapter seven, the coefficients being in terms of the mean square amplitudes of vibration U_{ij} .

The table shows:

Atom	U_{11} or U	U_{22}	U_{33}	U_{12}	U_{13}	U_{23}
------	-----------------	----------	----------	----------	----------	----------

C(1)	631(11)	482(9)	600(10)	-62(8)	309(8)	12(8)
C(2)	613(11)	655(11)	538(10)	-113(9)	251(8)	-45(9)
C(3)	578(10)	819(14)	659(12)	39(10)	227(9)	56(11)
C(4)	681(12)	606(12)	736(12)	71(10)	329(10)	9(10)
C(5)	915(16)	627(13)	652(12)	-138(11)	350(11)	-96(10)
C(6)	942(17)	832(17)	652(13)	-265(14)	223(12)	-83(12)
C(7)	633(12)	927(17)	697(13)	-193(12)	104(10)	148(12)
C(8)	576(10)	662(12)	710(12)	-18(9)	222(9)	153(10)
C(9)	554(9)	505(10)	549(9)	-39(8)	267(8)	58(8)
C(10)	641(10)	513(10)	567(10)	-42(8)	287(8)	7(8)
C(11)	995(18)	524(12)	877(17)	18(12)	413(15)	-60(12)
C(12)	637(12)	772(14)	661(12)	-129(10)	162(10)	-26(10)
C(13)	927(19)	1140(25)	827(17)	-334(19)	195(15)	-277(17)
O(14)	796(10)	978(12)	617(8)	-323(8)	262(7)	-158(8)
O(15)	941(12)	1169(15)	763(10)	-422(11)	345(9)	-89(9)
C(16)	705(15)	1004(23)	1311(27)	245(15)	204(17)	98(20)

H(3)	489(63)
H(4)	444(60)
H(5)	512(68)
H(6)	620(74)
H(7)	532(66)
H(111)	871(101)
H(112)	713(90)
H(113)	872(109)
H(131)	1236(158)
H(132)	788(92)
H(133)	893(118)
H(161)	1438(175)
H(162)	1114(125)
H(163)	827(106)

Table 4: Intramolecular bonded distances (angstroms) with standard deviations (angstroms) in parentheses.

ATOM1	ATOM2	DIST.	ATOM1	ATOM2	DIST.
C1	C2	1.369(2)	C12	O14	1.350(2)
C1	C9	1.442(2)	C12	O15	1.185(2)
C1	C11	1.514(3)	C3	H3	1.009(26)
C2	C3	1.389(3)	C4	H4	0.973(25)
C2	O14	1.413(2)	C5	H5	0.993(26)
C3	C4	1.351(3)	C6	H6	1.053(27)
C4	C10	1.412(2)	C7	H7	0.987(28)
C5	C6	1.344(3)	C11	H111	1.027(40)
C5	C10	1.417(2)	C11	H112	0.940(31)
C6	C7	1.393(3)	C11	H113	0.924(35)
C7	C8	1.380(3)	C13	H131	1.039(46)
C8	C9	1.438(2)	C13	H132	1.017(35)
C8	C16	1.510(4)	C13	H133	0.882(40)
C9	C10	1.429(2)	C16	H161	1.053(51)
C12	C13	1.492(3)	C16	H162	1.007(43)

Table 5: Valency angles (degrees) with the standard deviations (degrees) in parentheses.

ATOM1	ATOM2	ATOM3	ANGLE	ATOM1	ATOM2	ATOM3	ANGLE
C9	C1	C2	117.7(1)	C11	C1	C2	118.1(1)
C11	C1	C9	124.1(1)	O14	C2	C1	118.5(1)
C3	C2	C1	125.0(1)	O14	C2	C3	116.3(1)
C4	C3	C2	118.2(2)	C10	C4	C3	121.0(2)
C10	C5	C6	120.9(2)	C7	C6	C5	119.0(2)
C8	C7	C6	123.4(2)	C9	C8	C7	118.9(1)
C16	C8	C7	116.2(2)	C16	C8	C9	124.8(2)
C10	C9	C1	117.3(1)	C8	C9	C1	125.9(1)
C10	C9	C8	116.8(1)	C9	C10	C5	120.9(1)
C5	C10	C4	118.3(1)	C9	C10	C4	120.8(1)
O14	C12	C13	110.7(2)	O15	C12	C13	126.1(2)
O15	C12	O14	123.1(2)	C12	O14	C2	118.2(1)
H3	C3	C2	120.8(14)	H3	C3	C4	120.9(14)
H4	C4	C3	123.7(13)	H4	C4	C10	115.2(13)
H5	C5	C6	121.7(14)	H5	C5	C10	117.3(14)
H6	C6	C5	117.9(16)	H6	C6	C7	123.0(16)
H7	C7	C6	121.8(15)	H7	C7	C8	114.9(15)
H112	C11	C1	112.8(19)	H113	C11	C1	103.7(22)
H111	C11	C1	116.4(18)	H112	C11	H111	99.3(27)
H113	C11	H111	102.3(30)	H113	C11	H112	122.6(29)
H131	C13	C12	101.8(24)	H132	C13	C12	114.0(17)
H133	C13	C12	110.0(24)	H131	C13	H131	96.0(33)
H133	C13	H131	105.2(36)	H132	C13	H132	125.4(31)
H161	C16	C8	112.3(29)	H162	C16	C8	112.3(24)
H163	C16	C8	109.6(20)	H161	C16	H161	110.8(36)
H163	C16	H161	106.2(33)	H162	C16	H162	105.1(32)

Table 6: Torsion angles (degrees) with the standard deviations
(degrees) in parentheses.

ATOM1	ATOM2	ATOM3	ATOM4	ANGLE	ANGLE
C9	C1	C2	C3	-0.2(3)	174.2(1)
C11	C1	C2	C3	178.7(2)	-6.8(2)
C2	C1	C9	C8	-179.4(1)	1.9(2)
C11	C1	C9	C8	1.8(3)	-177.0(1)
C1	C2	C3	C4	-1.6(3)	-176.2(1)
C1	C2	C14	C12	106.7(2)	-78.4(2)
C2	C3	C4	C10	1.6(3)	-179.0(2)
C3	C4	C10	C9	0.0(3)	2.9(3)
C6	C5	C10	C4	178.1(2)	-1.0(3)
C5	C6	C7	C8	-2.2(3)	-0.5(3)
C6	C7	C8	C16	177.5(2)	-176.4(1)
C7	C8	C9	C10	2.3(2)	5.7(3)
C16	C8	C9	C10	-175.5(2)	-1.9(2)
C1	C9	C10	C5	177.2(1)	179.3(1)
C8	C9	C10	C5	-1.6(2)	179.0(2)
O15	C12	C14	C2	-0.1(3)	118.3(22)
C2	C1	C11	H112	-128.0(21)	6.8(23)
C9	C1	C11	H111	-62.9(22)	50.9(21)
C9	C1	C11	H113	-174.3(23)	175.0(17)
O14	C2	C3	H3	0.4(17)	-175.1(17)
H3	C3	C4	C10	-174.9(17)	8.4(24)
H4	C4	C10	C5	-2.1(16)	177.1(15)
C10	C5	C6	H6	-177.2(17)	-178.9(17)
H5	C5	C6	H6	1.0(24)	-0.1(16)
H5	C5	C10	C9	-179.3(16)	177.4(18)
H6	C6	C7	C8	177.9(18)	-2.5(26)
H7	C7	C8	C9	179.9(17)	-2.1(17)
C7	C8	C16	H161	119.6(30)	-6.2(26)
C7	C8	C16	H163	-122.6(21)	-62.5(30)
C9	C8	C16	H162	171.7(26)	55.3(22)
O14	C12	C13	H131	-85.7(26)	172.3(20)
O14	C12	C13	H133	25.5(26)	93.4(26)
O15	C12	C13	H132	-8.6(21)	-155.5(26)

THE ANGLE 1-2-3-4 IS DEFINED AS POSITIVE IF, WHEN VIEWED ALONG THE 2-3 BOND, ATOM 1 HAS TO BE ROTATED CLOCKWISE TO ECLIPSE ATOM 4

TABLE 7 MEAN PLANE CALCULATION

ATOMS IN THE PLANE	ATOMS OUT OF THE PLANE	DEVIATION (ANGSTROMS)
C(1)		0.030(3)
C(2)		0.023(3)
C(3)		-0.007(4)
C(4)		-0.018(4)
C(5)		0.003(4)
C(6)		0.040(4)
C(7)		0.001(4)
C(8)		-0.036(3)
C(9)		-0.017(3)
C(10)		-0.019(3)
	H(3)	-0.098(34)
	H(4)	0.055(36)
	H(5)	-0.016(36)
	H(7)	-0.002(36)
	C(11)	0.094(5)
	C(12)	1.049(4)
	C(13)	0.769(6)
	O(14)	-0.066(2)
	O(15)	2.084(3)
	C(16)	-0.137(6)

THE EQUATION OF THE PLANE IS:

$$-0.6256X - 0.5249Y + 0.5772Z = 4.4718$$

Table 8: Final structure factors

The table shows:

L^*	$ F_o $	$ F_c $	(Phase)
-------	---------	---------	---------

* Reflections sorted into groups with common
H,K indices (shown in each group heading)

0,-6,L	7	49	45	4	168	-169	0,0,L	-10	14	-15
1	39	-38	-89	5	60	-54	2	314	319	90
2	76	-76	-62	6	35	38	4	455	501	-189
4	70	70	-62	8	129	-114	6	205	-199	139
5	43	43	-64	10	40	40	8	71	-61	25
6	34	-37	-64	11	67	63	10	64	-63	46
7	52	-53	21	12	69	-65	12	69	61	38
8	26	-26	-30	13	36	-35	14	38	38	26
9	25	23	-21	14	31	31	16	33	-32	33
10	10	-10		15	11	9	18	15	14	28
				16	11	-9				38
0,-5,L				17	56	-55				76
1	28	-27	103	18	55	-52				11
3	53	-50	-153				1,-6,L			-74
4	205	209	-95	2	240	-251	-10	14	16	-149
5	110	118	-171	3	47	-33	-7	58	-61	-19
6	106	101	-242	4	31	24	-5	19	17	15
7	28	-30	-156	5	322	321	-4	30	-32	-20
8	72	-73	-84	6	345	344	-3	33	-38	-18
9	50	-52	9	7	81	71	-1	18	-19	66
10	31	-31	-60	8	132	-121	0	40	39	-48
11	50	-53	97	9	148	-140	1	73	74	
12	12	-13	-41	10	58	-49	2	9	6	
			15	11	37	31	3	72	-70	
0,-4,L			-37	12	63	-63	4	141	-145	-52
0	130	117	-45	13	19	-19	5	37	-35	25
1	101	-97		14	73	-76	6	37	-35	44
2	135	137		15	33	30	7	12	-14	-19
3	174	170	-694	16	67	-70	8	50	-48	-43
4	110	-106	225	17	36	-33	9	20	18	134
5	119	114	-277	18	25	-26				-202
6	108	104	-58	19	34	33	1,-5,L			125
							-13	17	17	-49
							-12	27	-30	38

[illegible]

[illegible]

3,-6,L			3,-4,L			3,-3,L			3,-2,L			3,-1,L		
-3	48	-47	7	89	-87	-18	15	15	-20	28	30	-20	21	-21
-2	45	47	8	131	132	-17	20	-17	-19	12	13	-19	33	35
-1	25	22	9	22	23	-16	20	21	-18	68	66	-18	9	8
0	111	111	10	34	-37	-15	77	-76	-17	23	22	-17	107	108
1	109	107	3,-4,L			-14	190	207	-16	12	13	-16	78	-80
2	56	53	-17	41	-42	-13	164	-173	-15	65	65	-15	48	48
3	35	36	-16	27	-25	-12	84	82	-13	52	-50	-14	131	-139
4	48	48	-15	13	-13	-11	45	46	-12	44	-42	-13	33	31
6	11	9	-14	86	-90	-10	100	-99	-11	16	21	-12	55	-57
3,-5,L			-13	115	118	-9	133	-133	-10	187	-192	-11	10	-14
-14	45	-44	-12	103	-105	-8	46	-42	-9	426	-417	-10	75	-79
-13	16	-14	-11	12	-14	-7	105	106	-8	442	-481	-9	148	-142
-12	30	35	-10	52	53	-6	120	-114	-7	113	111	-8	374	-398
-11	30	-29	-8	86	-81	-5	51	44	-6	423	428	-7	145	-153
-10	37	-36	-7	50	-46	-4	324	-313	-5	258	-243	-6	55	50
-9	81	-86	-6	32	-29	-3	120	-116	-3	11	3	-5	543	503
-8	20	-22	-5	30	25	-2	110	-115	-2	228	212	-4	188	216
-7	64	-66	-4	79	-69	-1	44	-47	-1	77	-68	-3	130	127
-6	50	52	-3	18	-16	0	21	18	0	288	280	-2	475	444
-5	27	-31	-2	47	-46	1	84	80	1	51	-46	-1	213	235
-4	70	72	-1	80	74	2	137	-135	2	109	111	0	152	135
-3	38	38	1	89	-91	3	127	-113	3	162	-155	1	81	-83
-2	27	28	2	168	-164	4	96	-88	4	133	125	2	86	-75
-1	48	48	3	101	-97	5	32	32	5	146	-134	3	193	200
0	14	13	4	20	-24	6	95	-93	6	71	62	4	265	-287
1	43	39	5	41	-42	7	45	-40	7	28	-31	5	51	-43
2	18	22	6	158	-155	8	46	-44	8	25	31	6	22	-18
3	41	39	7	82	80	10	12	-11	9	20	-21	7	86	-81
4	39	-34	8	11	15	12	17	-17	10	27	-23	8	85	-90
5	21	17	9	13	17	13	20	-21	11	75	-77	9	23	26
6	84	84	10	19	19	14	19	-20	13	22	-27	10	13	-14
			11	14	-16				14	14	-14			
			12	27	-31				15	19	-20			

4,-1,L	-8	192	190	-2	88	86	5,-4,L	-12	43	49	-9	14	3
-7	20	17	0	183	188	-16	55	-11	104	-104	-8	124	-126
-6	198	201	6	78	77	-15	30	-10	94	-94	-7	65	-68
-5	62	57	8	109	-112	-14	136	-9	72	68	-6	60	-62
-4	38	37	10	54	-57	-13	45	-8	34	-34	-5	117	109
-3	87	81	12	33	-35	-12	63	-7	25	-26	-4	91	86
-2	76	69	14	185	195	-11	27	-6	27	-28	-3	32	33
-1	246	268	14	37	37	-10	27	-5	16	-17	-2	108	100
0	62	60	5,-6,L			-9	27	-4	15	16	-1	116	109
1	98	88	-6	24	-27	-8	44	-3	53	-57	0	96	92
2	27	18	-4	19	-19	-7	58	-2	148	136	1	31	27
3	93	-78	-3	18	-22	-6	37	-1	82	-83	2	77	68
4	8	-16				-5	82	0	170	169	3	16	12
6	115	-118	5,-5,L			-4	92	1	159	155	4	58	-58
7	55	-52	-13	26	28	-3	27	2	26	26	5	26	27
8	232	-246	-11	35	38	-2	30	3	124	126	6	105	108
10	55	55	-10	22	-22	-1	97	4	128	124	7	174	176
11	153	156	-9	40	42	0	63	5	58	61	8	79	82
12	21	26	-8	25	24	2	160	6	134	131	9	16	-14
13	21	21	-7	16	-21	3	97	7	85	85	10	55	-56
14	20	17	-6	8	10	4	17	8	10	10	11	74	75
			-5	39	-44	5	19	10	50	52			
			-4	13	-12	7	10	11	41	-44	5,-1,L		
4,0,L	-20	41	35	69	72	8	18	5,-2,L			-20	67	-68
-18	20	-21	-2	24	23	9	30	-19	73	-72	-19	37	35
-16	59	-58	0	36	-34			-18	62	60	-18	21	-23
-14	58	51	1	14	-13	5,-3,L		-17	52	-52	-17	25	-24
-12	84	72	2	60	-62	-18	71	-16	64	-68	-16	53	-55
-10	208	205	3	15	-13	-17	89	-15	17	14	-15	22	20
-8	30	31	4	121	-123	-16	35	-14	12	-11	-14	17	-20
-6	114	114	5	34	-36	-15	19	-13	83	82	-12	26	-23
-4	28	31	6	17	-11	-14	140	-12	77	76	-11	34	-32
						-13	188	-10	214	-229			

[illegible]

[illegible]

[illegible]

[illegible]

[illegible]

8,-4,L	8,0,L	-12	14	-13	9,0,L	-16	16	13
6 22 17	-22 29 -26	-11 29 -33	29 15 -10	-33 38 -10	-20 19 -15	-14 24 -24		
8,-3,L	-18 40 43	-4 15 38	38 66 65	38 65 75	-18 56 -58	-13 21 -20		
-18 19 20	8 26 24	-3 38 66	66 74 75	65 75 14	-16 30 -30	-11 10 -9		
-17 38 36	10 37 35	-2 1 17	74 17 14	75 14 19	6 22 -26	-10 60 59		
-16 22 -24	9,-5,L	-1 1 17	17 14 19	14 19 -7	8 29 26	-9 38 -38		
-15 45 45	-10 10 15	2 22 22	22 10 -7	-19 -7 -14		-8 12 9		
3 13 13	-7 19 17	3 10 10	10 14 -11	-14 -11 -11	10,-4,L	-5 17 -17		
4 20 -21	-6 49 -45	4 14 14	14 14 -11	-11 -11 -11	-11 23 -24	-4 23 -24		
5 30 31	-5 10 -14	5 14 14	14 14 -11	-11 -11 -11	-8 21 -16	-3 31 -30		
7 14 -13	-4 37 36	9,-2,L	9,-2,L	-11 -11 -11	-7 44 39	0 10 -7		
8 10 -9	-3 18 19	-19 50 -49	50 21 2	-49 21 2	-6 48 48	1 11 4		
8,-2,L	-2 12 16	-18 22 2	22 10 37	2 37 23	-5 32 33	2 10 11		
-19 27 27	9,-4,L	-15 10 11	10 38 23	37 23 9	-4 13 9	10,-1,L		
-18 14 15	-14 19 -20	-14 38 37	38 22 23	23 23 9	-3 30 -30	-15 25 -23		
8 23 -22	-12 26 -26	3 22 11	22 11 11	11 11 9		-12 58 -56		
9 19 19	-11 17 -14	4 11 11	11 11 11	11 11 9		-11 82 82		
8,-1,L	-6 18 -20	9,-1,L	9,-1,L	-9 9 9		-10 107 -103		
-21 14 -15	-5 16 -17	-21 17 17	17 17 17	17 17 17		-6 17 -14		
-20 19 19	-4 14 -11	-20 13 13	13 13 13	13 13 13		-3 54 -52		
-19 33 34	-3 70 67	-19 25 25	25 25 25	25 25 25		-2 27 -27		
-18 67 67	-2 60 64	-18 34 34	34 34 34	34 34 34		-1 11 -14		
6 45 47	2 37 36	-15 17 17	17 17 17	17 17 17		0 26 28		
7 18 21	9,-3,L	2 33 33	33 33 33	33 33 33		2 12 -12		
8 24 24	-18 20 -21	4 46 46	46 46 46	46 46 46		10,0,L		
10 35 33	-16 18 16	5 12 12	12 12 12	12 12 12		-16 24 -23		
	-14 32 32	6 47 47	47 47 47	47 47 47		-14 35 -35		
	-13 28 26	7 18 18	18 18 18	18 18 18		-12 104 102		
		8 25 20	25 20 20	20 20 20		-10 14 16		
						-4 24 -22		

10,0,L	13	11	11,-1,L	-6	20	-22	-14	77	74
-2	12	-12	-15	-4	22	23	-12	61	-60
53	19	-16	51	-3	19	18	-10	29	30
2	22	-20	40	-1	14	11	-8	23	-23
-29	22	-20	23				-2	35	36
11,-2,L	16	14	-10		11,0,L		0	24	22
-12			-8						
12			15	-16	67	65			
2			25	-7					
			-23						

Figure 1: A view of 1,8-dimethyl-2-naphthyl acetate.

Apical values	Bond angles ($^{\circ}$)
Others	Bond lengths (\AA)

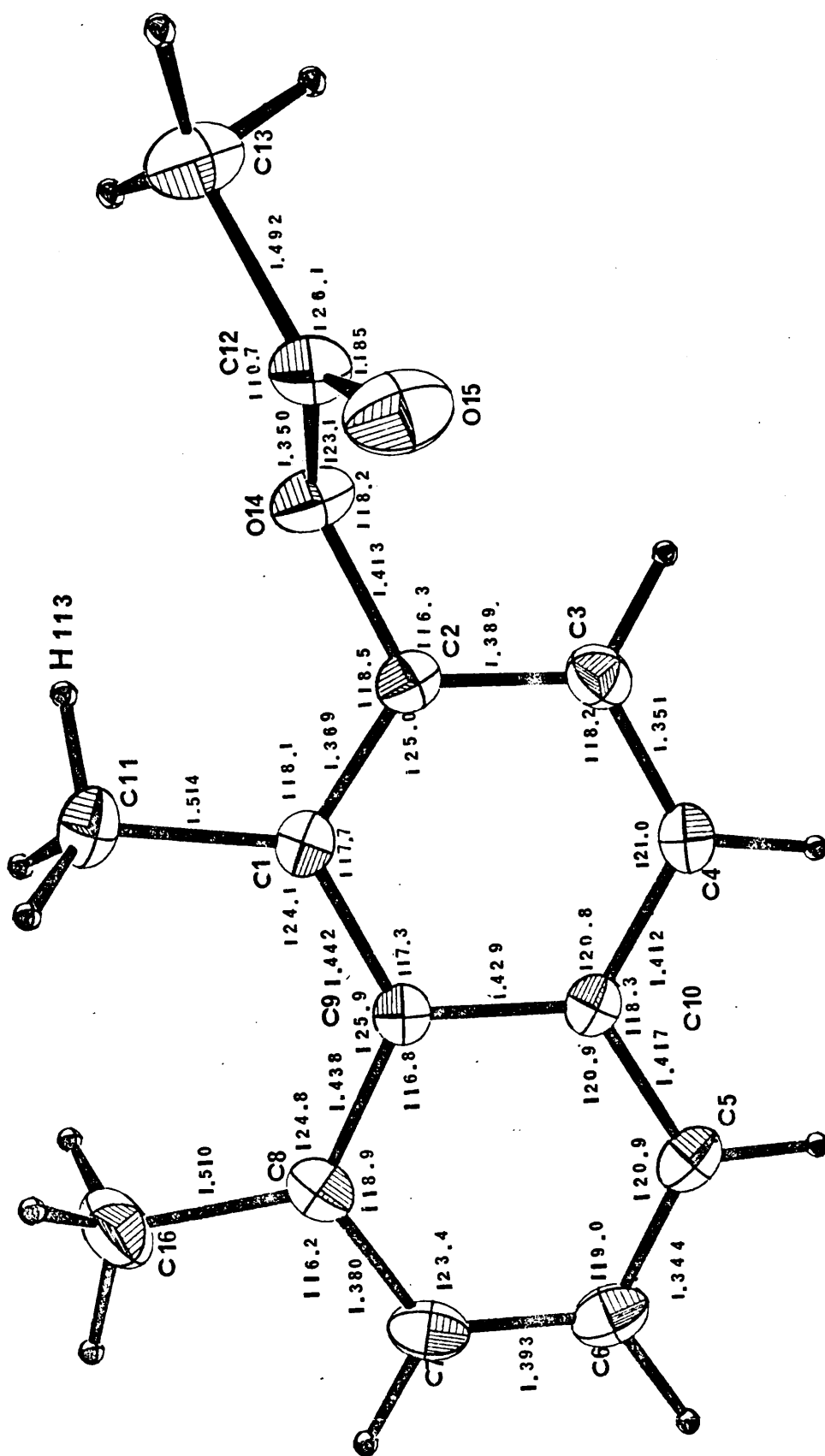
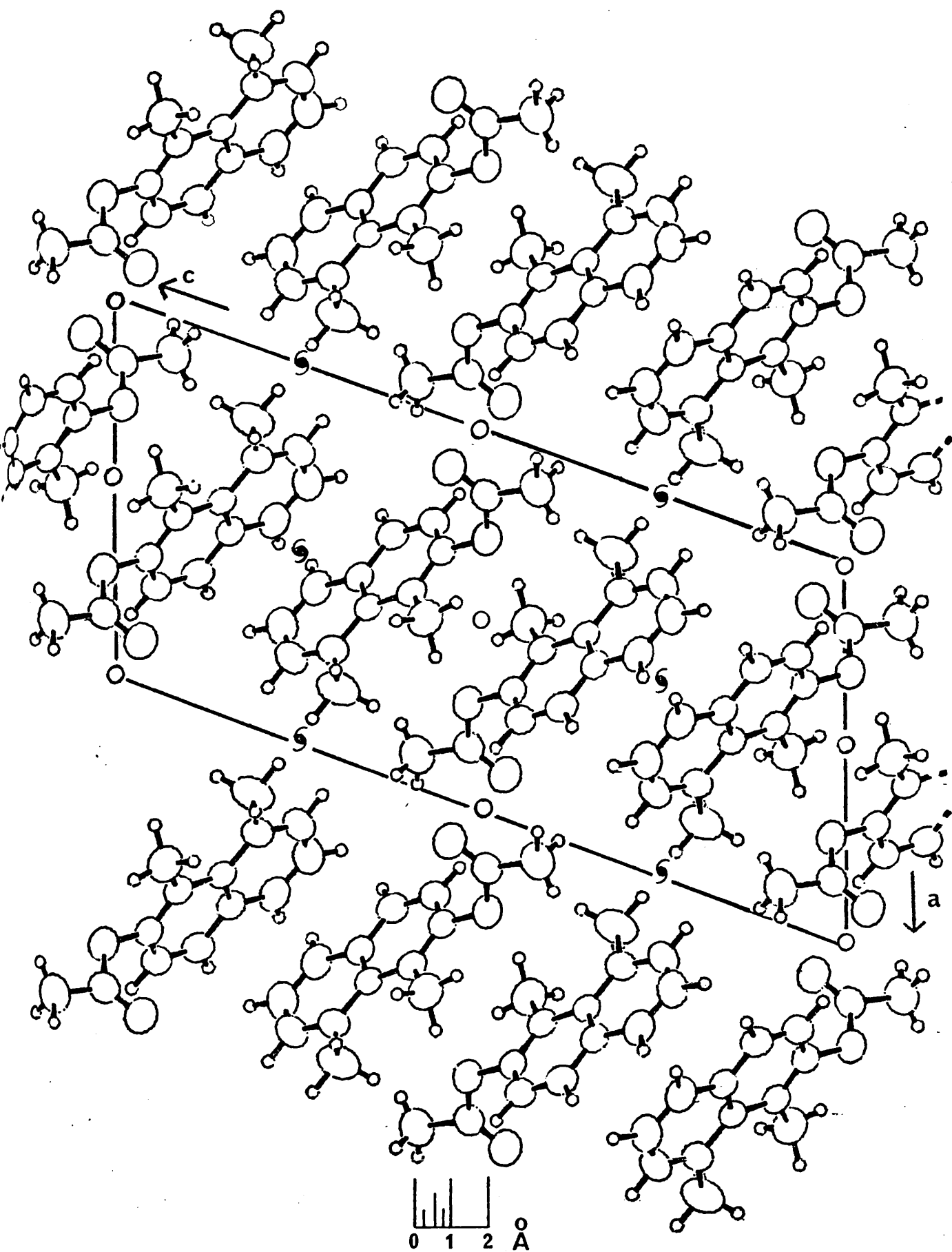


Figure 2: Crystal packing

A view down the b axis



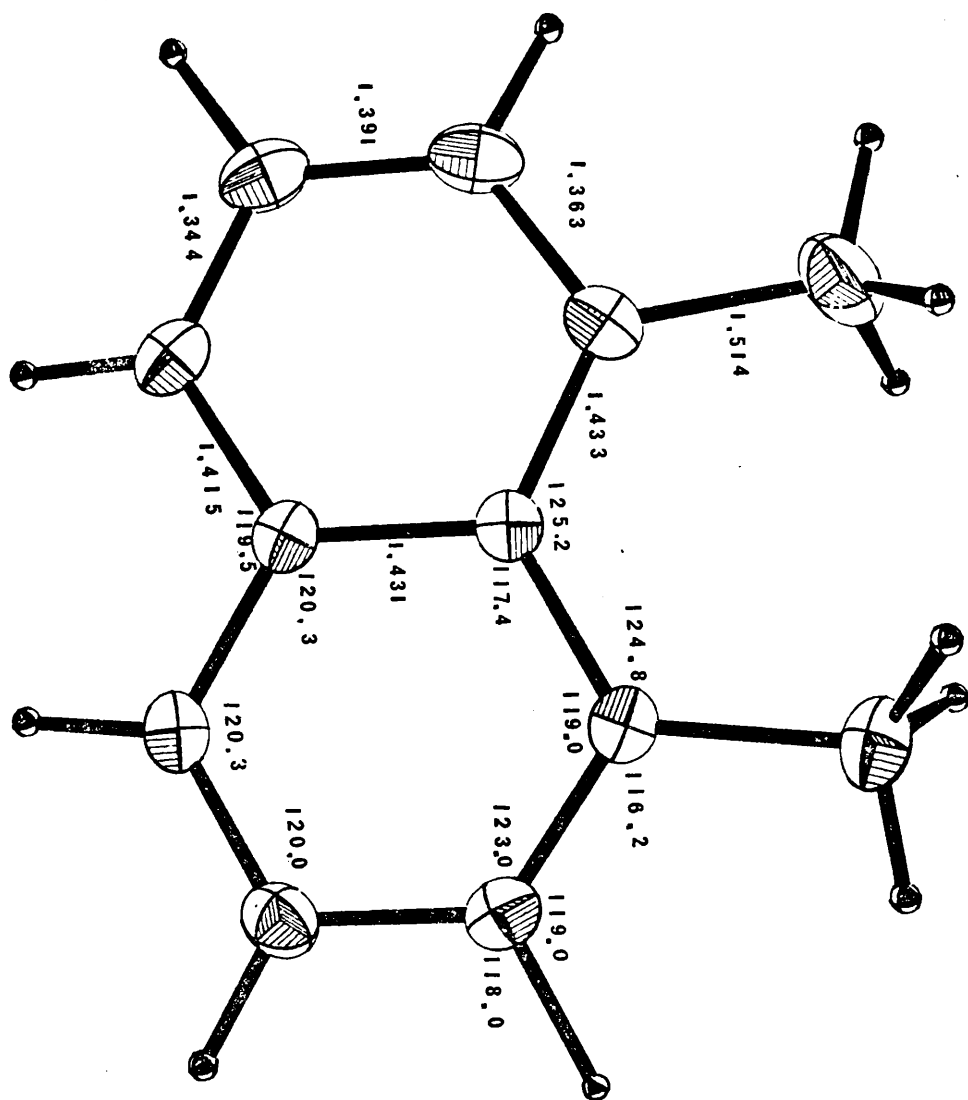
8.4 Discussion of Results

The overall geometry of 1,8-dimethyl-2-naphthyl acetate (1,8-DMNA) differs significantly from that of naphthalene⁵ but is very similar to that observed in 1,8-dimethyl-naphthalene (1,8-DMN)⁶ (Figures 1 and 3). This would imply that the addition of substituents on the naphthalene nucleus in positions 1 and 8 has introduced additional strain into the system as a result of the strong nonbonded interactions between the methyl substituents.

The most marked distortions occur at the junction of the two benzene rings in the naphthalene nucleus. The C1-C9-C8 valence angle in 1,8-DMNA is 125.9° compared to 125.2° in 1,8-DMN. The C1-C9 and C8-C9 bond lengths are observed to be significantly longer than the corresponding bond distances in naphthalene, while the C4-C10 and C5-C10 bond lengths are found to be correspondingly shortened. In 1,8-DMNA, the inner valence angles C9-C1-C11 and C9-C8-C16 are increased from the ideal 120° to 124.1° and 124.8° respectively, while the outer angles C2-C1-C11 and C7-C8-C12 are decreased to 118.1° and 116.2° respectively. The C9-C1-C11 valence angle is smaller than the C9-C8-C16 valence angle, in 1,8-DMNA, because further opening of the former angle would lead to more repulsive interactions between the outer hydrogen on C11(H113) and the substituent on C2. In 1,8-DMN, the inner angle is increased to 124.8° and the outer angle is decreased to 116.2° . The aforementioned deformations result in the C1 ... C8 and C11 ... C16 nonbonded distances being 2.565° \AA and 2.965° \AA respectively

Figure 3: 1,8-dimethyl-naphthalene

Apical values	Bond angles ($^{\circ}$)
Others	Bond lengths ($^{\circ}$)



in 1,8-DMNA, and 2.543 \AA , and 2.932 \AA , respectively in 1,8-DMN, as compared to 2.44 \AA , which is the corresponding value for these distances in naphthalene.

The naphthalene nucleus in 1,8-DMNA is essentially planar (Table 6) as the maximum ring torsion angle (ω) is 3° , with the sum of the absolute values of the torsion angles, $\sum|\omega|$, being 18° and the sum of the signed values of the torsion angles, $\sum\omega$, being 0° . The largest displacements from the mean plane of the ring is 0.04 \AA at C6 and -0.03 \AA at C8 (Table 7). The largest deviation from the best least-squares plane in 1,8-DMN is ca. 0.02 \AA . Thus the steric strain, resulting from peri-interactions, will not be relieved by a buckling of the naphthalene nucleus, in these molecules. The substituents on C1, C2 and C8 in 1,8-DMNA deviate from the mean plane of the naphthalene nucleus. The C16 atom deviates from the mean plane by -0.134 \AA , the C11 atom deviates to $+0.099 \text{ \AA}$, and O14 atom by -0.058 \AA , i.e. the C16 and O14 atoms deviate from the mean plane in an opposite direction from C11 as this would help to decrease the repulsive interactions between the substituents. In addition, the carbon atoms bearing the methyl groups are also forced out of the plane of the molecule in the direction of the substituent (Table 7), resulting in slight nuclear distortions. This out-of-plane deflection effect is observed in 1,8-dinitronaphthalene⁷ and 3-bromo-1,8-dimethylnaphthalene⁸ but not in 1,8-DMN. This must be due to the extra nonbonded interactions of the substituent in position 2 which are present in 1,8-DMNA but

are absent in 1,8-DMN. In 1,8-DMNA, the angle between the planes defined by C11,C1,C8 and C16,C8,C1 is 6° , which provides further evidence of the out-of-plane bending of the substituents on C1 and C8 on opposite sides of the mean plane of the naphthalene ring.

The conformation of the methyl hydrogen atoms on C11 and C16 in 1,8-DMNA and 1,8-DMN is unexpected. The two hydrogens on the outside of the C ... C interaction practically lie in the plane of the aromatic rings while the other four hydrogens face each other in pairs such that the H ... H distances are ca. $2.0 \overset{\text{O}}{\text{\AA}}$ (Figure 4). Strain energy minimization calculations⁶ have shown that this is indeed the most stable configuration for the methyl groups. This conclusion was arrived at by starting with different starting orientations of the methyl groups. The resulting minimized geometries all had the same orientation of the methyl groups as found in the two crystal structures. This configuration then must minimize the H ... H interactions. The calculations also indicate that the fixed orientation of the methyl groups in the crystal structures results from intra- rather than inter-molecular forces.

Table 9 shows the values of certain geometric parameters which are considered to be indicative of peri-strain, for a series of increasingly crowded C1 and/or C8 substituted naphthalenes. The out-of-plane bending, $|\delta_1| + |\delta_8|$, appears to be almost random and although the general trend of the lengthening of bonds C1 - C9 and C8 - C9 is upwards, it is irregular, as is the accompanying reduction in the

Figure 4: A view of 1,8-dimethyl-2-naphthyl acetate through
the naphthalene ring.

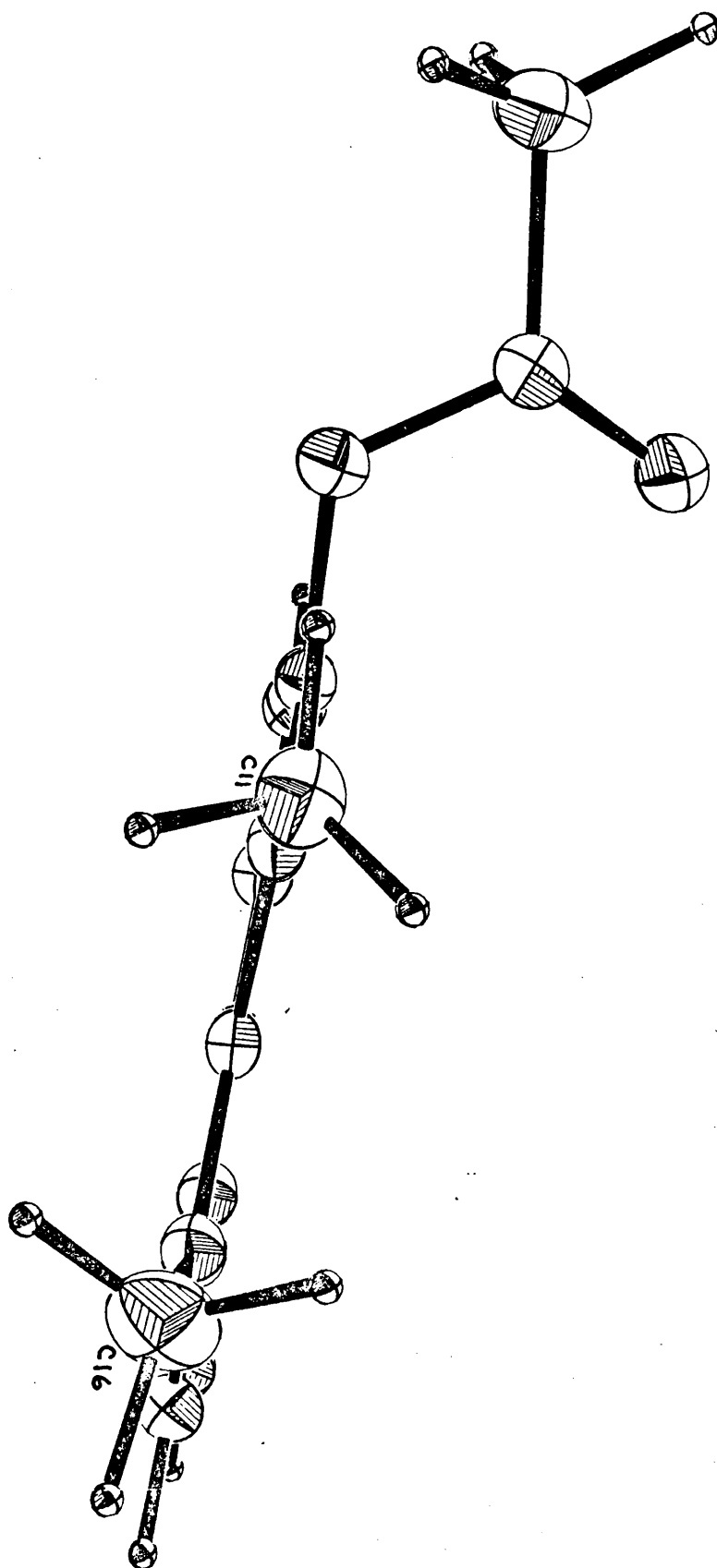


TABLE 9. SOME GEOMETRICAL PARAMETERS THOUGHT TO BE INDICATIVE OF PERI-STRAIN IN 1,8-DISUBSTITUTED NAPHTHALENES.

COMPOUND	C1...C8	θ_{1-9-8} (DEG)	$l_{1-9} + l_{8-9}$ (Å)	$l_{4-10} + l_{5-10}$ (Å)	$l_{6_1} + l_{6_2}$ (Å)
(1) H/H	2.44	120.2	2.846	2.846	0.00
(2) H/ME	2.49	122.0	2.845	2.838	0.07
(3) H/I-Pr	2.52	123.2	2.859	2.832	0.05
(4) Me ₂ H/I-Pr	2.56	125.8	2.878	2.828	0.01
(5) Me ₂ H/Me	2.57	125.9	2.880	2.829	0.23
(6) NO ₂ /NO ₂	2.57	127.0	2.870	2.840	0.42
(7) t-Bu/t-Bu	2.62	127.5	2.922	2.836	0.79
(8)	2.62	129.9	2.897	2.832	0.56
(1) H/H	REFERENCE 5				
(2) H/ME	REFERENCE 9				
(3) H/I-Pr	REFERENCE 10				
(4) Me ₂ H/I-Pr	REFERENCE 11				
(5) Me/Me	THIS WORK				
(6) CH ₂ Pr/CH ₂ Pr	REFERENCE 2				
(7) NO ₂ /NO ₂	REFERENCE 7				
(8) t-Bu/t-Bu	REFERENCE 13				

C4-C10, C5-C10 bond lengths. In contrast, θ_{1-9-8} and C1 ... C8 increase smoothly with increasing crowding of the substituents and are the only consistent indicator of steric crowding for peri-substituted naphthalenes.

The crystal structures of 1-methyl⁹, 1-isopropyl¹⁰ and 1,8-dimethyl-2-naphthyl acetates³ support the hypothesis that the rate of autoxidation of the corresponding naphthols is dependent on the steric strain present.⁴ It is however possible that although the reaction is driven by relief of strain when the intermediate is formed, steric factors, in particular the accessibility of the reaction site, may be of some importance. The difference in congestion at the reaction site would increase with the size of the alkyl group and would show a corresponding decrease in rate, in contrast to the observed increase in rate. The Wipke and Gund steric congestion algorithm,¹² which was discussed in Chapter 5, was used to check the latter point and no significant increase in congestion in progressing from the 1-methyl to the 1,8-dimethyl-2-naphthyl acetate was found. In order to gain some idea of the relative energies of the 1-methyl and 1,8-dimethyl compounds were computed by M.H.P. Guy at the University of Glasgow³ using an ad hoc force-field and the 1-methyl compound was found to be of lowest strain-energy and 4.5 kcal./mole more stable than the 1,8-dimethyl compound.

Finally, there is no evidence to support the proposal of Bright et al⁶ that peri-strain between C1 and C8 substituents is transmitted to H4 and H5 by a buttressing

mechanism involving H2, H3, H6 and H7. Were this the case then one would expect to find systematic distortions of the bond angles involving these latter four atoms. Although the hydrogen atoms are relatively poorly defined by X-ray analyses, the fact that no such distortions are found in the three alkyl-2-naphthylacetates^{3,9,10}, 1,8-DMN⁶ and 1,8-di (bromomethyl) naphthalene² makes this argument reasonably conclusive. In any case, it is extremely unlikely that this hypothetical strain transmission system would concentrate its effect at H4 and H5 but would distribute it, insofar as was possible, amongst all the naphthalenic hydrogens. The key to the non-parallel C4-H4 and C5-H5 vectors is contained in the lengthening of the C1-C9 and C8-C9 bonds with a corresponding shortening of C4-C10 and C5-C10 - this pushes C11 and C16 apart and H4 and H5 together without affecting H2, H3, H6 or H7, such that, for instance H5, C5, C8 and C16 still lie on a straight line and such would not be the case if a buttressing mechanism was operative.

8.5. References

1. V. BALASUBRAMANIAN, Chem.Rev., 66, 567 (1966).
2. J.B. ROBERT, J.S. SHERFINSKI, R.E. MARSH and J.D. ROBERTS, J.Org.Chem., 39, 1152 (1974).
3. D.N.J. WHITE, J. CARNDUFF, M.H.P. GUY and M.J. BOVILL, Acta Cryst., B33, in press (1977).
4. P.A. BRADY and J. CARNDUFF, Chem.Comm., 816 (1974).
5. G.S. PAWLEY and E.A. YEATS, Acta Cryst., B25, 2009 (1969).
6. D. BRIGHT, I.E. MAXWELL and J. de BOER, J.C.S. Perkin II., 2101 (1973).
7. Z.A. AKOPYAN, A.I. KITAIGORODSKII and Yu.T. STRUCHKOV, Zh.Struct.Khim., 6, 729 (1965).
8. M.D. JAMESON and B.R. PENFOLD, J.Chem.Soc., 528 (1965).
9. D.N.J. WHITE, J. CARNDUFF, M.H.P. GUY and M.J. BOVILL, Acta Cryst., B33, in press (1977).
10. D.N.J. WHITE, J. CARNDUFF, P.R. MALLINSON, M.H.P. GUY and M.J. BOVILL, Acta Cryst., B33, in press (1977)
11. H. EINSPAHR, J.B. ROBERT, R.E. MARSH and J.D. ROBERTS, Acta Cryst., B29, 1611 (1973).
12. W.T. WIPKE and P. GUND, J.Amer.Chem.Soc., 98, 8107 (1976).
13. J. HANDAL, J.G. WHITE, R.W.FRANCK, Y.H. YUH and N.L. ALLINGER, J.Amer.Chem.Soc., 99, 3345 (1977).

CHAPTER NINE

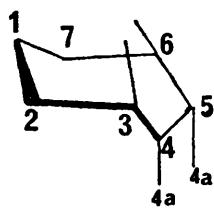
The crystal structure of bicyclo(4.4.1)undecane-1,6-diol.

9.1 Introduction

X-ray crystal structure analysis has played an important role in the development of conformational analysis of common- and medium-sized cycloalkanes.¹ This technique gives very detailed information about the geometry of suitable crystalline derivatives and thus establishes the most stable conformation that a particular cycloalkane can adopt in the solid state. On account of the fact that intramolecular forces are usually much stronger than intermolecular forces, the conformation adopted in the solid state is qualitatively similar to that in solution or in the gas phase.² This structural information is not only of chemical interest but it also provides accurate data that are extremely useful in the parametrisation of force-fields, which are used in molecular mechanics (MM) calculations. The resulting force-fields can then be used to predict, with a certain degree of confidence, geometric and thermodynamic properties of the rapidly increasing number of naturally occurring compounds that incorporate cycloalkanes into their molecular framework. This latter technique of calculating the probable preferred conformation is much quicker and less expensive than determination of it by X-ray diffraction. Moreover, the preferred conformation of a cycloalkane ring cannot be determined by X-ray crystal structure analysis with certainty in some cases, as many of the possible conformations are approximately isoenergetic and the observed conformation depends on the nature and position of the substituents on the cycloalkane ring.^{3,4}

It is now widely accepted that conformations of cycloheptane exist in families of chairs and boats (Figure 1). The two families are separated by a potential energy barrier of ca. 8 kcal./mole and they contain a number of flexible forms which are readily interconvertible.⁵ The \underline{C}_s form of the chair has an extremely serious H H repulsion across the axial C3 and C6 positions which it may relieve by pseudorotation to the \underline{C}_2 twist-chair. There seems to be agreement^{5,6} that the most stable conformation of cycloheptane is actually the \underline{C}_2 twist-chair form, which has less torsional strain and less nonbonded repulsions than the \underline{C}_s chair. For similar reasons, the \underline{C}_2 twist-boat form is more stable than the \underline{C}_s boat. The boat family is less stable than the chair family by about 3-4 kcal./mole. Within each family, the \underline{C}_s boat or \underline{C}_s chair conformations are energy maxima 1-2 kcal./mole above the twist-minima. On this basis, Hendrickson predicted that cycloheptane pseudorotates in the gas phase at room temperature and the fact that the crystal structures of calcium cycloheptane-carboxylate pentahydrate⁷ and 1-aminocycloheptane-1-carboxylic acid hydrobromide monohydrate⁸ are disordered and appear to contain a mixture of conformations of the 7-ring suggest that this process may also occur in the solid state when the hydrocarbon is lightly or non-substituted.

Several X-ray analyses of naturally occurring guianolides, which contain cycloheptane rings fused to cyclopentane and γ -lactone rings, have been performed⁹⁻¹³ and the results indicate that the cycloheptane ring does not always adopt

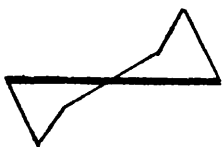


Chair

$\underline{C_s}$



Boat



Twist-chair

$\underline{C_2}$



Twist-boat

Figure I: Major conformations of cycloheptane.

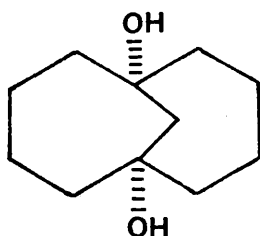
the C_2 twist-chair form and, regardless of the actual conformation assumed, appreciable deviations from the symmetrical forms have been noted⁹ - these two features of the cycloheptane ring in crystal structures result from the steric requirements of the gross structures being accommodated.

It would therefore seem that the minimum energy conformation (MEC) of cycloheptane is only likely to be observed in the crystal structure of a suitable derivative in which the 7-ring is locked into the C_2 twist-chair MEC. Inspection of Dreiding models reveals that two MEC cycloheptane rings can be 1,3-fused, in a cis manner, to form bicyclo(4.4.1)undecane with minimal changes in the individual 7-ring conformations. The cycloheptane rings will be locked into the C_2 -symmetric twist-chair form and, barring the introduction of any serious steric compression by 1,3-fusion, this hybrid conformation should also be the MEC of bicyclo(4,4,1)-undecane.

An X-ray crystal structure analysis of bicyclo(4,4,1)-undecane-1,6-diol¹⁴ therefore not only provides details of the MEC of the parent hydrocarbon but also provides structural details of the MEC of cycloheptane. One might expect also that the conformation of the 10-ring would correspond to one of the previously studied possibilities for cyclodecane.⁹

9.2 Experimental

Crystal Data



Bicyclo(4,4,1)undecane-1,6-diol: $C_{11}H_{20}O_2$

Unit Cell Dimensions

$$\begin{aligned} \underline{a} &= 11.73 \text{ \AA} \\ \underline{b} &= 11.73 \text{ \AA} \\ \underline{c} &= 15.47 \text{ \AA} \end{aligned} \quad \alpha = \beta = \gamma = 90.0^\circ$$

Space Group $P4_3 2_1 2 (D_4^8)$ or $P4_1 2_1 2 (D_4^4)$

M 184.3 a.m.u.

V 2129 Å³

D_m 1.17 g cm⁻³

D_c 1.15 g cm⁻³

λ 0.71069 Å

$\mu(M_o K\alpha)$ 0.83 cm⁻¹

F(000) 816

Z 8

The possible groups were determined by the systematic absences:

h00 when $h = 2n + 1$, 0k0 when $k = 2n + 1$ and 00l when $l \neq 4n$.

The crystal used in this analysis was of dimensions

ca. 0.8 x 0.5 x 0.3 mm³.

Data Collection

Initial values for the cell dimensions, obtained from precession photographs, were subsequently adjusted by a least-squares analysis of the angular settings for a number of reflections measured on a Hilger and Watts Y290 four-circle computer-controlled diffractometer. The intensities of 1087 independent reflections ($\theta < 30^\circ$) with $I > 3 \sigma(I)$ were measured by means of $\omega - 2\theta$ scans which consisted of 40 steps of 0.02° at 2 sec./step, with background counts for 20 seconds on each side of peak maximum and two standard reflections being measured after every 40 intensity measurements.

The data in the range $2\theta < 16^\circ$ were also collected with reduced beam intensity so that allowance could be made for counter errors. No corrections were made for absorption.

Structure Analysis

The coordinates of all the carbon and oxygen atoms were obtained from an E-map calculated with the set of phases having the highest combined figure of merit produced by the MULTAN direct phasing program for the space group $P4_32_12$. Normalised structure factors were derived from the intensities, on the basis of an overall isotropic temperature $B2.0013 \text{ \AA}^2$ and the triplet relationships for the 240 reflections with $|E| > 1.2$. The starting set of 4 reflections (Table 1) was selected by the program on the basis that phases with a probability in excess of 0.95 were acceptable and gave

TABLE 1 SUMMARY OF STRUCTURE DETERMINATION

A. INITIAL SET OF PHASES

REFLECTION	PHASE *	MOD. E
2 2 3 +	90	3.14
5 0 3 +	135	2.64
1 1 2	0 OR 180	2.59
7 6 3	45, 135, 225 OR 315	2.48
9 2 0	0 OR 180	2.02
2 1 12	45, 135, 225 OR 315	2.00

B. STATISTICS

	E1	E2	E3	E4	E5	E6
THEORETICAL FOR CENTRIC	0.798	1.000	0.968	31.7	4.6	0.3
THEORETICAL FOR ACENTRIC	0.886	1.000	0.736	36.8	1.8	0.0
FOUND	0.912	1.000	0.655	37.6	1.7	0.1

* IN DEGREES
+ ORIGIN DEFINING
MOD. E MODULUS OF E FOR REFLECTION CONCERNED
E1 MEAN VALUE FOR MODULUS OF E
E2 MEAN VALUE FOR MODULUS OF E**2
E3 MEAN VALUE FOR MODULUS OF ((E**2)-1)
E4 % OF REFLECTIONS WITH MODULUS OF E > 1.0
E5 % OF REFLECTIONS WITH MODULUS OF E > 2.0
E6 % OF REFLECTIONS WITH MODULUS OF E > 3.0

rise to 64 phase sets.

The initial structure-factor calculation using the 1060 independent structure amplitudes for which $|F_o| \geq 4\sigma |F_o|$ gave an R of 22.2% and full-matrix least-squares adjustment of the positional and isotropic thermal parameters of the non-hydrogen atoms converged at R 12.4%. R was lowered to 9.6% when anisotropic thermal parameters for these atoms were used. The positions of the hydrogen atoms were located in a difference map and least-squares refinement continued with the positional and isotropic thermal parameters of the hydrogen atoms included in the model. A weighting scheme of the form $\sqrt{W} = 1 / \sigma(|F_o|)$ was employed and the refinement converged at R = 3.8%. The ratio of observations to parameters was 5.3 to 1.

9.3. Results

The crystal and molecular structures are shown in Figures 2 and 3 and the atomic coordinates, thermal parameters, bond lengths, valency angles, torsion angles a listing of the observed and calculated structure factors are given in Tables 2-7.

Figure 2: The crystal packing viewed down b.

Inter-molecular hydrogen bonds are indicated
by broken lines.

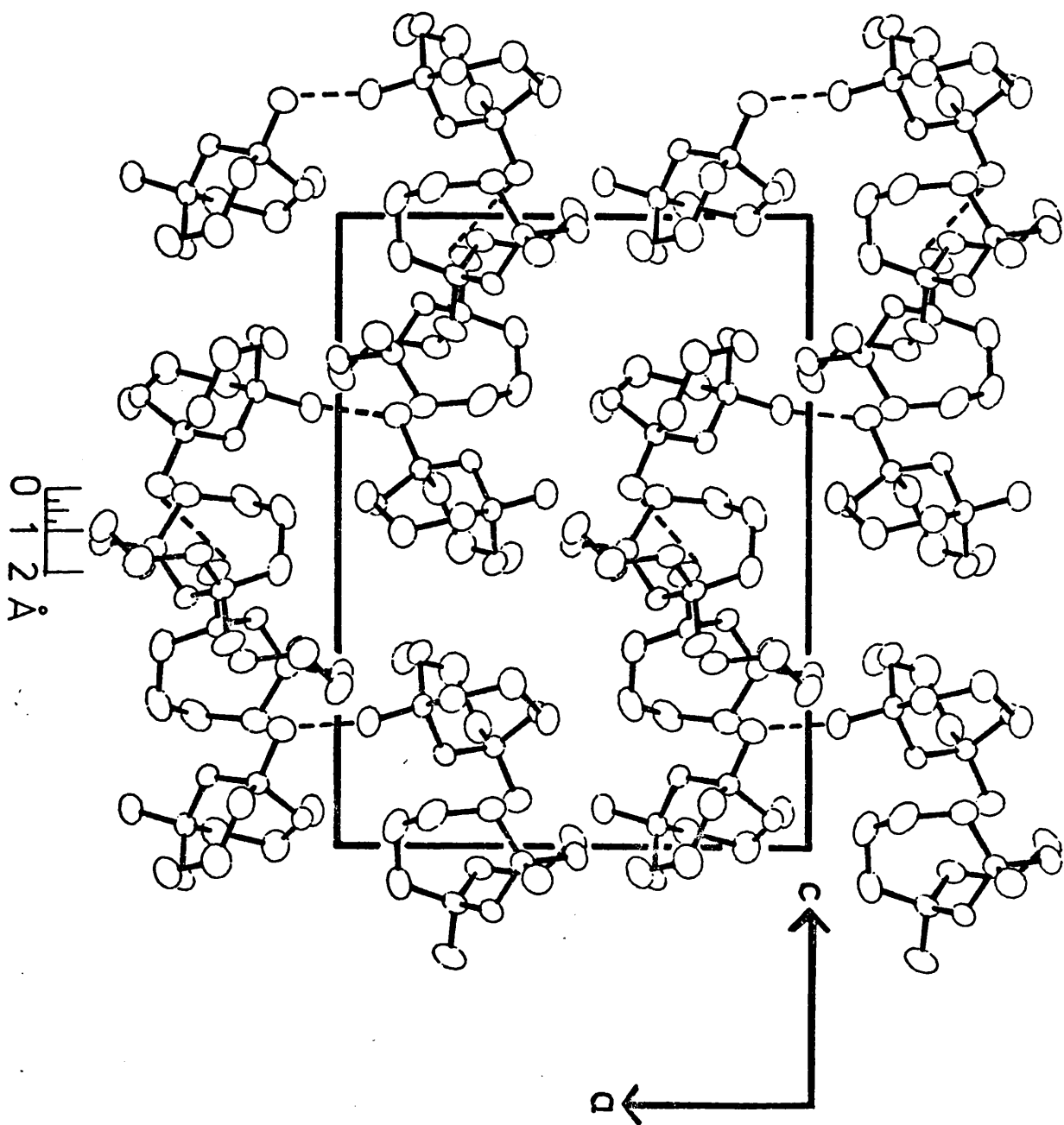


Figure 3 (a) and (b): Two views of the molecule in approximately perpendicular directions.

Figure 3(a)

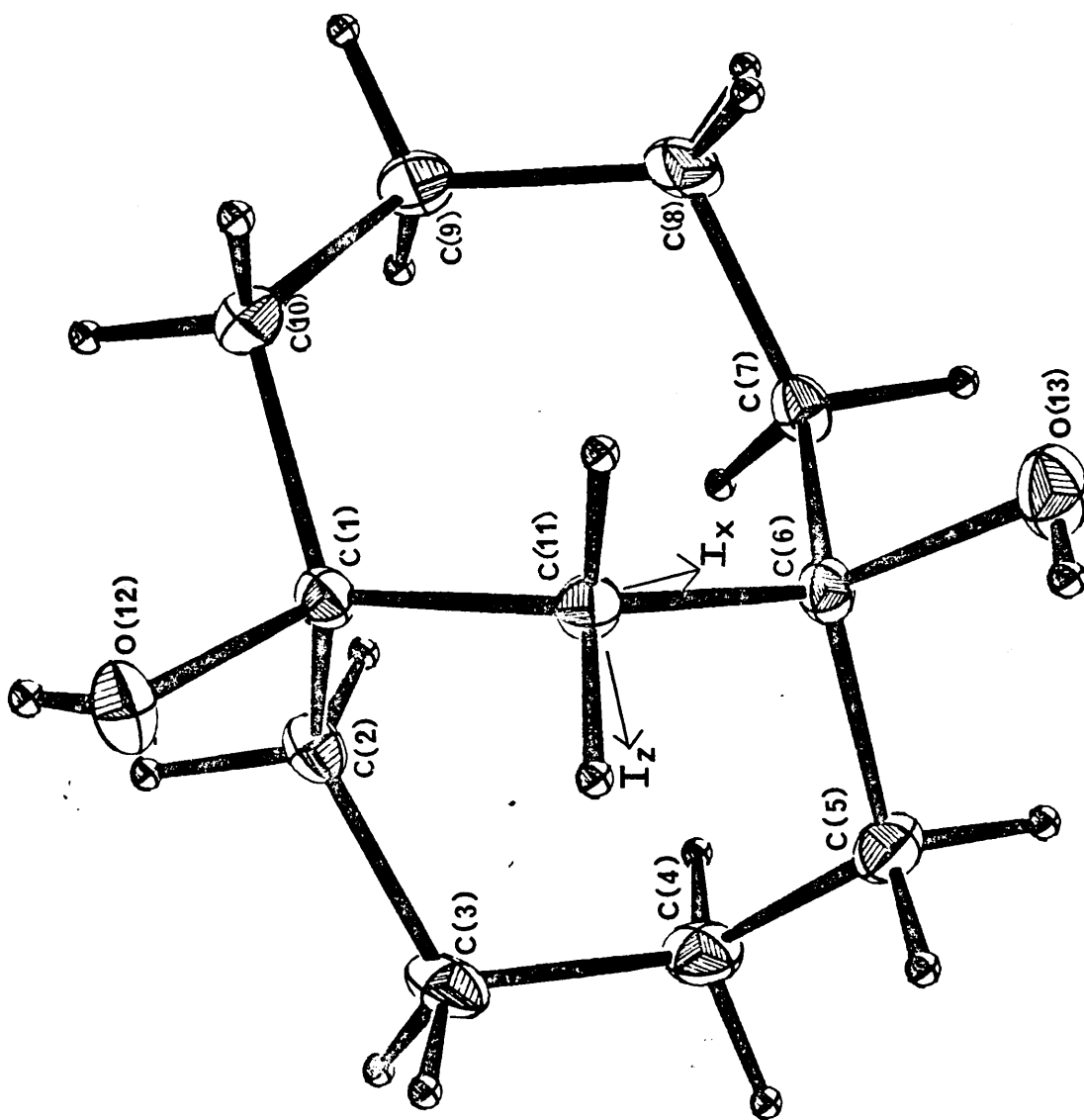


Figure 3(b)

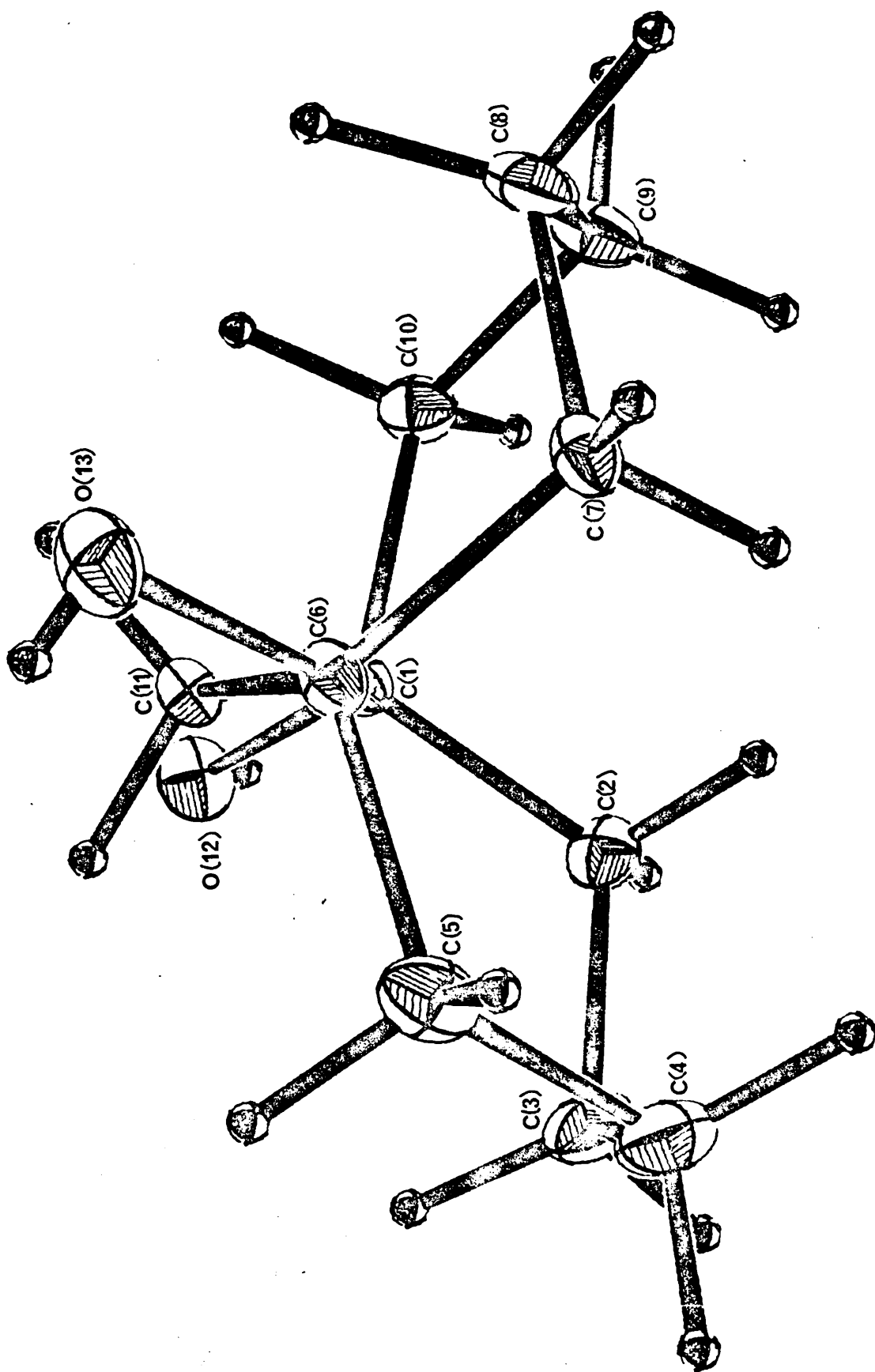


Table 2: Fractional atomic coordinates ($\times 10^4$) with estimated standard deviations in parentheses.

The hydrogen atoms are numbered according to the atoms to which they are attached.

The table shows:

Atom	x	y	z
------	---	---	---

C(1)	8238(2)	8897(2)	2191(2)
C(2)	8303(3)	8231(3)	3038(2)
C(3)	8606(3)	6967(3)	2948(2)
C(4)	7584(3)	6193(3)	2770(2)
C(5)	7070(3)	6269(3)	1854(2)
C(6)	6720(2)	7460(2)	1540(2)
C(7)	5782(2)	7968(3)	2101(2)
C(8)	5575(3)	9237(3)	1981(2)
C(9)	6339(3)	9980(3)	2540(2)
C(10)	7606(3)	10036(2)	2302(2)
C(11)	7771(2)	8232(2)	1417(2)
O(12)	9387(2)	9210(2)	1933(2)
O(13)	6225(3)	7343(3)	0687(2)

H(21)	7617 (28)	8312 (26)	3379 (18)
H(22)	8852 (29)	8635 (27)	3426 (20)
H(31)	9224 (36)	6863 (34)	2502 (26)
H(32)	8922 (26)	6742 (26)	3438 (19)
H(41)	7784 (30)	5379 (33)	2847 (22)
H(42)	6996 (30)	6384 (31)	3212 (22)
H(51)	6384 (29)	5800 (27)	1803 (19)
H(52)	7599 (30)	5982 (28)	1434 (20)
H(71)	5917 (25)	7814 (24)	2724 (18)
H(72)	5088 (29)	7527 (30)	1959 (20)
H(81)	4802 (30)	9367 (27)	2145 (20)
H(82)	5654 (30)	9401 (29)	1298 (23)
H(91)	6277 (28)	9653 (27)	3148 (22)

H(92)	6084 (28)	10764 (28)	2593 (21)
H(101)	7980 (27)	10445 (26)	2829 (18)
H(102)	7722 (30)	10443 (28)	1699 (21)
H(111)	7606 (25)	8786 (26)	0947 (18)
H(112)	8371 (27)	7761 (27)	1215 (19)
H(12)	9577 (34)	9480 (33)	2182 (24)
H(13)	6548 (33)	7100 (36)	0558 (27)

Table 3: Thermal parameters ($\times 10^4$) with e.s.d.'s in parentheses.

Carbon and oxygen values are anisotropic.

Hydrogen values are isotropic.

The anisotropic temperature factor expression used was of the form described by equation (12) in chapter seven, the coefficients being in terms of the mean square amplitudes of vibration U_{ij} .

The table shows:

Atom	U_{11} or U	U_{22}	U_{33}	U_{12}	U_{13}	U_{23}
------	-----------------	----------	----------	----------	----------	----------

C(1)	272(12)	362(14)	356(12)	5(11)	-12(10)	-30(11)
C(2)	378(16)	529(18)	374(13)	-10(14)	-101(13)	31(14)
C(3)	438(18)	608(21)	635(21)	112(16)	-118(18)	221(18)
C(4)	560(21)	409(17)	748(22)	55(16)	-28(19)	177(17)
C(5)	477(18)	351(15)	666(20)	-19(14)	31(16)	-74(15)
C(6)	307(13)	386(14)	303(11)	-7(11)	-12(10)	-79(12)
C(7)	277(13)	521(17)	331(13)	-9(12)	20(11)	-56(12)
C(8)	331(16)	591(20)	621(20)	212(15)	-30(15)	-95(18)
C(9)	481(18)	460(18)	649(21)	165(15)	16(17)	-182(17)
C(10)	485(17)	335(14)	497(15)	26(13)	-39(14)	-64(13)
C(11)	300(13)	347(14)	328(11)	13(11)	44(10)	-57(11)
O(12)	342(12)	613(16)	566(15)	-132(11)	-22(11)	-41(14)
O(13)	525(16)	681(18)	399(12)	-21(15)	-35(12)	-195(12)

H(21)	114(74)
H(22)	188(81)
H(31)	412(109)
H(32)	77(74)
H(41)	290(98)
H(42)	275(98)
H(51)	172(80)
H(52)	195(86)
H(71)	75(72)
H(72)	212(82)
H(81)	177(85)
H(82)	286(97)
H(91)	174(81)

$\pi(92)$	127 (83)
$\pi(101)$	128 (76)
$\pi(102)$	242 (89)
$\pi(111)$	99 (70)
$\pi(112)$	141 (79)
$\pi(12)$	100 (121)
$\pi(13)$	97 (136)

Table 4: Intramolecular bonded distances (angstroms) with standard deviations (angstroms) in parentheses.

ATOM1	ATOM2	DIST.	ATOM1	ATOM2	DIST.
C1	C2	1.527(4)	C3	H32	0.883(29)
C1	C10	1.537(3)	C4	H41	0.992(38)
C1	C11	1.530(3)	C4	H42	0.996(34)
C1	O12	1.452(3)	C5	H51	0.977(33)
C2	C3	1.530(4)	C5	H52	0.960(33)
C3	C4	1.528(5)	C7	H71	0.994(28)
C4	C5	1.541(5)	C7	H72	0.988(34)
C5	C6	1.535(4)	C8	H81	0.953(34)
C6	C7	1.521(3)	C8	H82	1.078(35)
C6	C11	1.540(3)	C9	H91	1.018(33)
C6	O13	1.447(3)	C9	H92	0.970(33)
C7	C8	1.520(4)	C10	H101	1.042(29)
C8	C9	1.519(4)	C10	H102	1.057(32)
C9	C10	1.531(4)	C11	H111	0.994(29)
C2	H21	0.965(31)	C11	H112	0.948(31)
C2	H22	1.000(32)	O12	H12	0.547(38)
C3	H31	1.008(40)	O13	H13	0.514(40)

Table 5: Valency angles (degrees) with the standard deviations
(degrees) in parentheses.

ATOM1	ATOM2	ATOM3	ANGLE	ATOM1	ATOM2	ATOM3	ANGLE
C10	C1	C2	111.9(2)	C11	C1	C2	115.4(2)
O12	C1	C2	108.6(2)	C11	C1	C10	111.0(2)
O12	C1	C10	105.0(2)	O12	C1	C11	104.2(2)
C3	C2	C1	115.4(2)	C4	C3	C2	114.2(2)
C5	C4	C3	116.0(2)	C6	C5	C4	116.6(2)
C7	C6	C5	111.6(2)	C11	C6	C5	111.2(2)
O13	C6	C5	108.0(2)	C11	C6	C7	114.7(2)
O13	C6	C7	105.5(2)	O13	C6	C11	105.3(2)
C8	C7	C6	115.4(2)	C9	C8	C7	113.5(2)
C10	C9	C8	117.3(2)	C9	C10	C1	117.2(2)
C6	C11	C1	119.2(2)	H21	C2	C1	112.1(17)
H22	C2	C1	107.7(18)	H21	C2	C3	109.8(18)
H22	C2	C3	111.4(18)	H22	C2	H21	99.2(25)
H32	C3	C2	108.0(19)	H31	C3	C4	111.6(23)
H32	C3	C4	107.8(20)	H31	C3	C2	110.2(22)
H32	C3	H31	104.4(30)	H41	C4	C5	105.1(20)
H42	C4	C5	110.3(20)	H41	C4	C3	111.4(20)
H42	C4	C3	106.5(20)	H42	C4	H41	107.3(29)
H52	C5	C6	105.2(19)	H51	C5	C4	111.3(17)
H52	C5	C4	110.4(20)	H51	C5	C6	105.5(18)
H52	C5	H51	106.2(27)	H71	C7	C6	111.6(16)
H72	C7	C6	105.3(19)	H71	C7	C8	108.7(16)
H72	C7	C8	110.8(20)	H72	C7	H71	104.5(24)
H82	C8	C7	106.2(18)	H81	C8	C9	108.5(19)
H82	C8	C9	113.9(18)	H81	C8	C7	106.0(19)
H82	C8	H81	108.3(26)	H91	C9	C10	107.9(18)
H92	C9	C10	106.1(19)	H91	C9	C8	105.5(18)
H92	C9	C8	114.3(19)	H92	C9	H91	104.9(26)
H102	C10	C9	110.9(19)	H101	C10	C1	106.6(17)
H102	C10	C1	103.4(18)	H101	C10	C9	103.8(17)

VALENCY ANGLES (CONTINUED)

ATOM1	ATOM2	ATOM3	ANGLE
H102	C10	H101	115.3(24)
H112	C11	C1	106.8(18)
H112	C11	C6	106.9(19)
H12	O12	C1	109.2(41)
ATOM1	ATOM2	ATOM3	ANGLE
H111	C11	C1	108.0(17)
H111	C11	C6	108.6(17)
H112	C11	H111	106.6(24)
H13	O13	C6	96.5(46)

Table 6. Bond angles (degrees) with the standard deviations (degrees) in parentheses.

Table 6: Torsion angles (degrees) with the standard deviations
(degrees) in parentheses.

ATOM1	ATOM2	ATOM3	ATOM4	ANGLE	ANGLE	ATOM1	ATOM2	ATOM3	ATOM4	ANGLE
C10	C1	C2	C3	163.5(2)	35.4(3)	C11	C1	C2	C3	
O12	C1	C2	C3	-81.1(3)	-64.9(3)	C2	C1	C10	C9	
C11	C1	C10	C9	65.5(3)	177.5(2)	O12	C1	C10	C9	
C2	C1	C11	C6	43.0(3)	-85.6(2)	C10	C1	C11	C6	
O12	C1	C11	C6	162.0(2)	-85.4(3)	C1	C2	C3	C4	
C2	C3	C4	C5	72.8(3)	-54.2(4)	C3	C4	C5	C6	
C4	C5	C6	C7	-62.5(3)	67.0(3)	C4	C5	C6	C11	
C4	C5	C6	O13	-178.0(2)	166.0(2)	C5	C6	C7	C8	
C11	C6	C7	C8	38.4(3)	-77.0(3)	O13	C6	C7	C8	
C5	C6	C11	C1	-86.1(2)	41.8(3)	C7	C6	C11	C1	
O13	C6	C11	C1	157.3(2)	-86.7(3)	C6	C7	C8	C9	
C7	C8	C9	C10	70.9(3)	-51.9(3)	C8	C9	C10	C1	
C10	C1	C2	H21	36.8(19)	-71.4(19)	C10	C1	C2	H22	
C11	C1	C2	H21	-91.3(19)	160.5(19)	C11	C1	C2	H22	
O12	C1	C2	H21	152.2(19)	44.0(19)	O12	C1	C2	H22	
C2	C1	C10	H101	50.8(17)	172.8(18)	C2	C1	C10	H102	
C11	C1	C10	H101	-178.8(17)	-56.8(18)	C11	C1	C10	H102	
O12	C1	C10	H101	-66.8(17)	55.2(18)	O12	C1	C10	H102	
C2	C1	C11	H111	167.5(17)	-78.2(19)	C2	C1	C11	H112	
C10	C1	C11	H111	38.9(18)	153.2(19)	C10	C1	C11	H112	
O12	C1	C11	H111	-73.5(18)	40.8(19)	O12	C1	C11	H112	
C2	C1	O12	H12	-60.9(43)	58.9(43)	C10	C1	O12	H12	
C11	C1	O12	H12	175.6(42)	41.2(24)	C1	C2	C3	H31	
C1	C2	C3	H32	154.6(20)	42.5(19)	H21	C2	C3	C4	
H21	C2	C3	H31	169.1(31)	-77.5(28)	H21	C2	C3	H32	
H22	C2	C3	C4	151.4(20)	-82.0(31)	H22	C2	C3	H31	
H22	C2	C3	H32	31.4(28)	-167.1(22)	C2	C3	C4	H41	
C2	C3	C4	H42	-50.5(21)	-53.1(25)	H31	C3	C4	C5	
H31	C3	C4	H41	67.0(33)	-176.3(32)	H31	C3	C4	H42	
H32	C3	C4	C5	-167.2(20)	-47.1(30)	H32	C3	C4	H41	
H32	C3	C4	H42	69.6(29)	-175.3(20)	H32	C3	C4	H51	
C3	C4	C5	H52	67.1(21)	-177.6(21)	C3	C4	C5	C6	
H41	C4	C5	H51	61.2(29)	-56.4(30)	H41	C4	C5	H52	

TORSION_ANGLES (CONTINUED)

ATOM1	ATOM2	ATOM3	ATOM4	ANGLE	ATOM1	ATOM2	ATOM3	ATOM4	ANGLE
H42	C4	C5	C6	67.1(21)	H42	C4	C5	H51	-54.1(29)
H42	C4	C5	H52	-171.7(30)	H51	C5	C6	C7	61.6(19)
H51	C5	C6	C11	-168.9(19)	H51	C5	C6	O13	-53.9(19)
H52	C5	C6	C7	174.0(20)	H52	C5	C6	C11	-56.5(20)
H52	C5	C6	O13	58.5(20)	C5	C6	C7	H71	41.2(18)
C5	C6	C7	H72	-71.5(20)	C11	C6	C7	H71	-86.4(18)
C11	C6	C7	H72	160.8(20)	O13	C6	C7	H71	158.2(17)
O13	C6	C7	H72	45.5(20)	C5	C6	C11	H111	149.7(18)
C5	C6	C11	H112	35.0(19)	C7	C6	C11	H111	-82.5(18)
C7	C6	C11	H112	162.9(19)	O13	C6	C11	H111	33.0(18)
O13	C6	C11	H112	-81.6(19)	C5	C6	O13	H13	-49.7(46)
C7	C6	O13	H13	-169.2(46)	C11	C6	O13	H13	69.1(46)
C6	C7	C8	H81	154.3(20)	C6	C7	C8	H82	39.3(19)
H71	C7	C8	C9	39.5(17)	H71	C7	C8	H81	-79.4(27)
H71	C7	C8	H82	165.5(26)	H72	C7	C8	C9	153.8(20)
H72	C7	C8	H81	34.8(29)	H72	C7	C8	H82	-80.2(28)
C7	C8	C9	H91	-49.3(19)	C7	C8	C9	H92	-164.0(21)
H81	C8	C9	C10	-171.5(20)	H81	C8	C9	H91	68.3(28)
H81	C8	C9	H92	-46.4(29)	H82	C8	C9	C10	-50.9(20)
H82	C8	C9	H91	-171.1(28)	H82	C8	C9	H92	74.2(29)
C8	C9	C10	H101	-169.0(17)	C8	C9	C10	H102	66.5(19)
H91	C9	C10	C1	67.0(19)	H91	C9	C10	H101	-50.1(26)
H91	C9	C10	H102	-174.6(27)	H92	C9	C10	C1	179.1(20)
H92	C9	C10	H101	61.9(26)	H92	C9	C10	H102	-62.6(28)

THE ANGLE 1-2-3-4 IS DEFINED AS POSITIVE IF, WHEN VIEWED ALONG THE 2-3 BOND, ATOM 1 HAS TO BE ROTATED CLOCKWISE TO ECLIPSE ATOM 4

Table 7: Final structure factors

The table shows:

L*	F _o	F _c	Phase (°)
----	----------------	----------------	-----------

* reflections sorted into groups with common
H,K indices (shown in each group heading)

-12	0,0,L	260	267	180	-4	646	636	270	-16	72	77	0	-13	163	161	90
-8		835	826	180	-3	826	874	45	-14	57	66	90	-11	354	341	270
-4		1007	1024	0	-2	938	947	180	-13	66	63	225	-10	48	47	180
					-1	537	580	315	-11	218	230	135	-9	79	77	90
									-10	143	126	90	-8	190	186	180
	0,2,L					1,1,L			-9	325	325	225	-7	341	342	90
-7		39	5	46	-15	141	137	90	-8	54	55	0	-6	152	150	180
					-14	283	282	180	-6	173	169	270	-5	501	489	270
					-11	73	70	90	-5	130	127	225	-4	649	643	180
	0,8,L				-10	52	45	180	-4	521	532	0	-3	1201	1266	90
-10		32	33	270	-9	287	288	270	-3	40	38	315	-2	251	244	0
					-8	278	276	180	-2	139	133	270	0	196	213	0
					-7	125	131	270	-1	502	513	45				
	0,9,L				-6	321	301	180	0	1062	1086	180		2,7,L		
					-5	326	316	270		2,1,L			-13	39	29	326
-4		25	9	90	-4	269	265	180								
					-3	138	140	270	-14	57	58	21				
	0,12,L				-2	1484	1505	0	-13	210	206	23		2,12,L		
					-1	346	350	270	-12	274	279	308	0	32	30	180
-3		46	39	225					-11	80	85	286				
						1,9,L			-10	161	167	331		3,0,L		
									-9	95	94	276				
-16		102	95	90	-1	40	43	18	-8	233	226	230	-15	105	102	225
-15		55	52	225					-7	498	475	128	-14	136	143	180
-13		123	121	315		1,11,L			-6	464	459	289	-13	131	137	135
-12		109	111	270	-2	49	50	212	-5	466	464	257	-12	28	37	90
-11		141	147	45					-4	46	37	129	-11	69	64	225
-10		176	181	0		1,12,L			-3	445	434	112	-10	266	268	180
-9		293	281	135					-2	703	726	269	-9	219	210	315
-8		362	349	270	-1	43	47	18	-1	491	497	21	-7	331	325	45
-7		166	158	45					0	59	51	0	-6	274	281	180
-6		126	119	0		2,0,L							-5	322	326	315
-5		203	207	135						2,2,L			-4	211	207	90

-3	3,0,L	-6	146	151	343	0	35	38	0	4,2,L	-15	60	57	291
-2	52	-5	241	239	310						-14	97	99	291
-1	24	-4	265	257	177		4,0,L				-13	38	40	33
	73	-3	341	339	35						-12	77	79	165
		-2	251	253	251		51	48	315		-11	125	121	77
		-1	317	317	18		86	83	90		-10	29	32	185
	3,1,L	0	652	883	160		91	87	0		-9	61	54	45
-15	144						326	333	315		-8	268	276	149
-13	148		3,3,L				120	118	270		-7	63	57	278
-12	146	-15	45	52	90		261	255	0		-6	175	172	289
-11	46	-14	116	122	0		170	162	135		-5	169	174	194
-10	282	-13	119	112	90		51	46	180		-4	362	338	79
-9	269	-1	114	114	90		366	377	135		-3	143	150	199
-8	121	0	827	855	0		39	55	90		-2	164	164	270
-7	256						187	177	45		-1	344	339	115
-6	216		3,6,L				140	140	180		0	550	540	0
-5	429	-10	41	36	118		4,1,L							
-4	329													
-3	355		3,7,L				35	23	6	4,3,L	-14	68	74	344
-2	418						127	128	154		-13	75	78	313
-1	659	0	35	37	180		203	206	141		-12	131	129	285
0	376						182	177	134		-11	68	58	315
			3,8,L				69	78	320		-10	51	45	165
	3,2,L						80	76	163		-9	213	211	42
-15	145	-10	38	37	254		146	158	48		-8	238	235	26
-14	287						71	73	2		-7	37	35	212
-13	294		3,10,L				190	189	320		-6	154	155	137
-12	124						214	216	14		-5	204	200	51
-11	150	-4	34	36	284		102	91	46		-4	249	249	79
-10	190						248	232	234		-3	285	272	22
-9	199		3,11,L				303	295	23		-2	286	277	231
-8	292						230	233	332		-1			
-7	170	-6	31	33	209		304	286	0		0			

-1 0	4,3,L		5,1,L		5,3,L		5,10,L	
	300	293	212	157	50	49	65	56
	548	543	180	160	124	128	62	64
				61	57	59	38	34
				85	133	139	236	247
-12 -10 -9 -8 -7 -6 -5 -4 -3 -2 -1 0	4,4,L		5,2,L		5,4,L		6,0,L	
	61	62	180	150	193	193	41	45
	76	69	180	150	124	128	39	36
	188	189	270	150	29	42	39	38
	152	157	0	75	193	193	125	128
-14 -13 -12 -11 -10 -9 -8 -7 -6 -5 -4 -3 -2 -1 0	5,0,L		5,5,L		5,6,L		5,7,L	
	73	75	0	148	152	180	190	192
	88	91	135	0	156	180	136	138
	96	98	90	251	235	102	85	88
	187	201	225	148	152	180	255	247
-12 -11 -10 -9 -8 -7 -6 -5 -4 -3 -2 -1 0	5,8,L		5,9,L		5,10,L		5,11,L	
	124	129	180	200	198	198	274	279
	214	206	90	200	198	198	274	279
	251	257	45	200	198	198	274	279
	303	294	180	200	198	198	274	279
-14 -13 -12 -11 -10 -9 -8 -7 -6 -5 -4 -3 -2 -1 0	5,12,L		5,13,L		5,14,L		5,15,L	
	187	201	225	200	198	198	274	279
	124	129	180	200	198	198	274	279
	214	206	90	200	198	198	274	279
	251	257	45	200	198	198	274	279

6,1,L			6,3,L			6,6,L			6,8,L			7,1,L			7,2,L			
-13	108	113	245	-13	73	74	86	-12	91	100	277	-11	31	32	45			
-12	54	54	264	-12	93	98	37	-11	141	135	101	-10	28	28	0			
-11	72	80	180	-11	71	72	73	-10	59	60	277	-9	126	137	315			
-10	61	60	159	-9	35	34	233	-9	53	55	114	-8	56	57	90			
-9	42	37	88	-8	158	157	246	-8	151	160	4	-7	264	270	225			
-7	58	60	280	-7	185	190	49	-7	141	135	243	-6	114	114	180			
-6	113	110	122	-6	199	202	247	-6	168	170	21	-5	53	52	315			
-5	233	225	53	-5	70	72	145	-5	148	148	102	-4	298	298	90			
-4	94	90	324	-4	109	115	208	-4	184	183	239	-3	35	42	45			
-3	310	303	41	-3	219	204	286	-3	46	53	227	-2	78	80	0			
-2	178	185	54	-2	154	159	308	-2	43	44	290	-1	231	240	135			
-1	354	337	99	-1	123	115	15	0	185	186	175	7,1,L						
0	194	188	180	0	100	103	0	0	339	336	180	7,2,L						
6,2,L			6,4,L			6,6,L			6,8,L			7,0,L			7,5,L			
-14	76	74	76	-13	52	55	254	-11	58	69	90	-12	70	67	320			
-13	67	72	282	-12	47	55	19	-10	38	43	0	-12	90	100	193			
-12	30	33	26	-11	73	77	337	-9	97	104	270	-11	138	141	192			
-11	45	48	109	-10	141	145	110	-8	197	198	180	-10	93	93	143			
-10	81	84	312	-9	88	83	35	-7	176	173	270	-9	231	242	349			
-9	178	178	183	-8	68	67	267	-6	33	39	180	-8	30	33	244			
-8	120	121	353	-7	73	66	84	-5	80	76	90	-7	77	76	238			
-7	44	40	103	-6	233	228	75	-4	114	118	0	-6	218	220	175			
-6	137	137	239	-5	103	94	312	-3	225	223	270	-5	49	56	19			
-5	359	354	150	-4	227	229	175	-2	34	36	0	-4	308	309	267			
-4	242	234	264	-3	55	50	264	-1	163	163	270	-3	122	122	337			
-3	172	170	318	-2	150	147	106	0	0	0	0	-2	97	94	10			
-2	110	114	196	-1	143	151	160	-5	44	46	215	-1	122	123	167			
-1	89	80	277	0	143	131	0	0	0	0	0	0	188	192	180			
0	530	528	180	6,5,L			7,0,L			7,5,L			7,10,L			7,15,L		

7,2,L		-5	165	167	38	7,7,L		-6	196	203	116
-8	149	158	28			-7	34	41	270		
-7	111	107	8			-6	111	111	0		
-6	164	160	68			-5	157	152	90		
-5	153	155	255			-4	72	77	180		
-4	108	110	114			-3	43	41	270		
-3	124	128	236			-2	142	145	180		
-2	415	424	355			-1	155	169	90		
-1	214	213	357			0	213	220	180		
0	399	407	180								
7,3,L		7,5,L		7,10,L		8,2,L		8,3,L		8,4,L	
-12	80	78	290	-11	51	55	2	-12	50	41	0
-11	70	70	298	-10	142	152	1	-11	122	127	34
-10	138	137	190	-9	140	142	356	-10	78	88	225
-9	132	142	169	-8	155	161	147	-8	179	183	338
-8	158	161	279	-7	159	163	289	-6	86	85	276
-7	207	203	162	-6	130	130	226	-5	135	142	10
-6	141	141	46	-5	72	70	88	-4	82	83	158
-5	157	163	115	-4	41	36	210	-3	181	184	195
-4	148	151	198	-3	92	90	122	-2	106	101	332
-3	242	237	167	-2	52	51	182	0	262	268	180
-2	188	192	3	-1	283	283	87				
-1	61	63	77	0	59	53	0				
7,4,L		7,6,L		8,1,L		8,2,L		8,3,L		8,4,L	
-12	39	42	304	-10	139	141	334	-11	96	89	139
-10	44	39	352	-9	81	80	123	-9	46	51	121
-9	68	69	146	-7	170	177	155	-8	156	160	92
-8	98	99	222	-6	86	88	20	-7	214	211	305
-7	135	145	260	-5	194	199	156	-6	89	85	120
-6	65	59	4	-4	161	164	329	-5	240	244	9
				-3	340	345	209	-4	49	51	342
				-2	87	85	199	-3	269	272	313
				-1	70	77	213	-2	290	290	152
				0	72	70	0	-1	126	123	327
								0	34	37	0

-10	8,4,L	45	46	331	0	228	231	0	-1	84	85	135	-3	191	200	252
-9		58	61	114		8,7,L				9,1,L			-2	122	125	177
-8		140	143	139		72	72	76	-11	82	96	17	-1	81	78	289
-7		34	30	256		52	45	271	-10	81	83	342				
-6		165	165	279		57	67	359	-9	96	98	233	-9	85	77	56
-5		245	254	136		124	125	209	-7	74	69	191	-8	86	85	319
-4		213	211	9		129	134	192	-6	78	71	42	-7	91	92	348
-3		110	111	203		81	77	178	-5	254	259	306	-6	48	57	350
-2		156	157	279		69	74	211	-4	190	190	121	-5	82	77	67
-1		141	139	348		68	75	0	-2	128	128	176	-4	177	175	89
0		230	229	0					0	36	32	180	-3	173	182	299
						8,8,L				9,2,L			-2	98	96	246
						168	164	0	-10	89	84	304	-1	93	97	81
-10		50	50	190		204	206	90	-9	68	72	270	0	161	168	180
-8		168	175	188		83	88	90	-8	173	181	114				
-7		32	24	233		215	206	0	-7	34	45	162				
-6		169	180	165					-6	65	69	259	-9	58	61	218
-5		126	130	55		8,9,L			-5	38	34	91	-8	45	49	301
-4		224	228	83		47	50	65	-4	94	98	304	-6	67	60	32
-3		124	127	323					-3	135	132	87	-5	53	65	9
-2		127	125	165		9,0,L			-2	65	63	44	-4	134	137	310
-1		85	88	19					-1	167	169	151	-3	116	118	338
0		153	146	0					0	280	282	0	-2	95	100	225
													-1	81	82	161
													0	115	116	0
						8,6,L				9,3,L						
-9		66	62	103		139	145	180	-10	120	127	355				
-8		43	43	327		95	100	135	-7	119	121	297	-7	73	75	66
-4		71	78	263		218	217	270	-6	127	128	292	-6	64	62	218
-3		100	102	230		43	42	225	-5	205	205	154	-5	54	53	264
-2		65	62	93		58	64	180	-4	134	135	305				
-1		44	52	29		269	272	135								
						70	76	225								
						24	30	180								

-4	9,6,L	52	51	179	-6	91	102	277	-5	64	67	143	-6	88	84	2
-3		198	203	73	-5	75	79	343	-3	107	106	266	-5	91	89	59
-1		37	33	347	-4	92	95	284	-2	87	80	136	-4	52	57	36
0		87	98	0	-3	157	155	131	-1	130	136	205	-3	71	66	264
					-2	159	163	49					-1	215	215	344
					-1	154	161	16		10,5,L						
					0	160	157	0						11,2,L		
	9,7,L					10,2,L			-6	85	82	9				
-6		46	54	202	-5			300	-5	117	122	300	-6	83	85	286
-5		133	137	242	-3			37	-3	85	79	159	-5	74	70	189
-4		66	70	145	-2	129	132	90	-2	91	100	159	-4	62	66	64
-3		42	47	49	-8	57	65	135	0	111	108	0	-3	88	93	330
-1		158	156	244	-6	63	68	77		10,6,L			-2	87	86	262
0		32	19	0	-5	144	141	129					-1	49	52	143
					-4	107	113	191					0	80	85	0
	9,8,L				-3	53	51	254	-5	90	91	263				
-2		57	53	200	-2	124	131	146	-3	126	111	120		11,3,L		
0		49	49	180	-1	141	143	16	-2	111	114	296				
					0	114	119	180		10,7,L						
	10,0,L					10,3,L							-5	76	83	316
-9		51	47	225	-8	59	61	187	-2	58	55	71	-3	101	102	25
-8		64	65	0	-7	100	103	265	-1	70	64	273	-2	53	50	223
-6		47	48	90	-6	55	53	82					-1	94	89	159
-5		118	126	45	-5	117	114	119		11,0,L				11,4,L		
-4		93	94	0	-3	69	68	212	-6	69	70	180	-5	99	97	172
-1		97	99	225	-2	101	105	341	-4	103	102	270	-4	123	124	276
					-1	118	122	86	-3	247	253	225	-3	96	90	156
	10,1,L				0	43	54	0	-2	95	96	180	-1	64	65	232
						10,4,L			-1	101	105	315	0	89	91	0
-9		89	88	220										11,5,L		
-8		147	148	187	-7	72	78	141		11,1,L			-3	103	95	141
-7		111	109	120	-6	42	47	104	-7	139	136	352				

	4,12,L			5,9,L	6,5,L	7,3,L
-14	67	66	153	-13 58 57 227	-14 83 82 196	-13 93 96 10
	5,0,L			-12 36 37 134	-13 112 111 222	
				-10 32 22 152		7,4,L
-17	33	41	135	5,11,L	6,6,L	
-16	39	37	270			
-15	90	91	225	-8 44 45 84	-15 76 74 90	-14 29 25 309
	5,1,L			6,0,L	6,7,L	7,5,L
-17	35	26	173	-15 47 44 315	-12 38 44 193	-14 57 54 149
-16	52	44	80			-13 60 58 285
-15	77	80	208	6,1,L	6,8,L	-12 104 108 77
	5,2,L			44 46 171	-11 35 35 176	7,6,L
-17	49	51	340	107 104 133	6,9,L	-11 48 41 188
-16	55	53	151	6,2,L		7,7,L
	5,4,L			-17 53 49 317	-9 39 45 301	-10 56 54 180
				-16 46 45 183	6,12,L	
-17	46	50	275	-15 60 61 67	-5 34 29 23	7,12,L
-15	51	53	51		-1 61 59 177	-5 34 31 275
-14	79	82	302	6,3,L		8,2,L
	5,5,L			-16 68 69 320	7,1,L	
				-15 47 45 106		
-15	104	105	90	-14 52 50 140	-16 62 57 212	-14 45 47 271
-14	89	77	0		-15 56 59 53	-13 72 75 147
	5,8,L			6,4,L	7,2,L	
				-15 108 102 262		
-13	29	29	331	-14 53 62 56	-16 46 34 250	
					-15 45 35 191	

8,3,L		8,12,L		-4	72	75	260	-12	48	45	107
-13	67	63	210					-11	86	80	139
-12	96	73	169	-1	68	71	20	-9	84	74	183
8,4,L		9,0,L		-8	83	81	180	10,5,L			
				-7	58	54	270				
-14	47	55	157	-6	37	41	0	-10	46	55	24
-13	86	71	351	-5	49	41	270	-9	28	34	316
-12	58	55	199	0	48	47	180	-7	128	122	27
8,5,L		9,10,L						10,6,L			
				-4	41	39	0				
-11	102	104	253	-3	57	56	338	-9	61	63	298
8,6,L		10,0,L						-8	83	86	217
								-7	65	65	158
-12	31	36	104	-13	42	46	45	-6	56	57	291
8,8,L		9,4,L		-11	39	37	135	10,7,L			
				-10	48	55	90				
-8	82	62	180					-10	66	66	11
-7	89	85	90	-13	50	57	273	-9	79	71	235
8,9,L		9,6,L		-11	61	61	60	-7	73	71	212
				-10	54	61	347	-6	95	94	58
-6	50	44	24	-13	50	57	273	-4	41	41	113
8,10,L		9,7,L		-11	61	61	60	10,8,L			
				-10	62	62	339				
-8	29	20	178					-7	69	67	340
0	52	51	0	-11	42	40	331	-6	79	81	262
8,11,L		9,8,L		-10	62	54	287	-3	62	56	83
				-9	72	73	271	-1	83	76	30
								10,9,L			
				-7	118	118	38	0	29	23	0

-12	11,0,L	51	53	270	-8	55	49	204	-10	54	60	226	-1	74	70	160
-11		63	62	45	-6	37	34	15	-8	65	64	184				
-9		68	70	135	-5	156	153	355	-7	49	52	30		13,0,L		
-8		65	69	90	-3	87	81	29	-5	85	80	45				
	11,1,L				-1	64	66	57	-4	47	49	68	-7	35	32	225
					0	61	61	0					-5	74	77	135
-12		53	45	229									-4	51	55	270
-9		50	48	309									-2	100	92	180
	11,2,L									12,3,L						
		58	60	124	-8	75	61	110	-9	87	81	127		13,1,L		
-9		29	32	292	-5	61	55	214	-2	54	47	40				
-8		109	106	218	-3	54	60	161	-1	58	52	6				
-7		81	83	246						12,4,L			-7	59	63	214
													-3	97	92	223
	11,3,L															
		54	56	49	-6	87	85	169	-2	75	67	219		13,2,L		
					0	123	121	180	-1	69	62	320				
										12,5,L			-7	68	71	8
-8													-4	59	48	142
	11,4,L				-3	65	65	300	-3	83	85	149	-3	76	76	230
					0	45	36	0	-2	37	41	156				
									0	29	40	0		13,3,L		
-10		38	36	125						12,6,L			-7	30	25	309
-9		51	36	203	-5	68	71	225	-6	81	74	268	-6	87	87	343
	11,5,L								-1	60	59	3	-4	102	104	45
													-3	74	72	76
													0	59	56	0
-10		86	80	60						12,7,L				13,4,L		
-7		61	64	112	-10	71	70	16								
-6		99	93	30	-6	79	71	71	-4	89	83	107	-6	41	41	202
-4		87	91	85	-5	39	33	159	-2	66	64	358	-5	86	88	275

	13,4,L	1,0,L	4,2,L	6,6,L	
-4	55	40	-19	47	50
-3	62	44	90	117	116
0	97	1,5,L		6,9,L	0
	13,5,L	41	37	61	55
			350	-14	51
					341
-5	33	1,13,L		6,14,L	
-2	62				
-1	77	56	53	50	54
			350	-3	41
				-1	42
					348
	13,6,L	1,15,L		7,1,L	
-2	76	44	48	66	70
			142	-10	315
			168		
	14,1,L	44	46	4,13,L	
		72	73		
			180		
0	54	2,2,L	-7	76	70
					7
	14,2,L	64	69	5,2,L	
			0		
-1	32	2,5,L	-18	65	55
					350
	14,3,L	61	55	5,3,L	
			10		
-2	67	3,1,L	-18	51	53
					331
	0,0,L	62	57	6,0,L	
			78		
		57	56		
			335		
-20	71	3,15,L	-18	33	32
					90
	0,15,L			6,1,L	
		-1	62		
		0	55		
-2	37		-18	30	29
					44

-13	7,9,L	34	42	101	-16	9,2,L	48	57	102	-12	10,7,L	73	66	324	-11	46	49	135
					-15		61	55	329							12,1,L		
	7,12,L										10,9,L				-12	41	35	88
-9	48	48	120		-15	9,4,L				-9	60	63	55		-11	127	127	128
	7,13,L					56	49	65								12,3,L		
-4	40	40	240			9,5,L				-13	55	55	135		-11	55	55	291
-3	30	41	127		-15	60	53	54							-10	85	87	160
	8,1,L					9,11,L				-13	45	40	230			12,5,L		
-17	80	76	228		-4	65	60	101							-9	72	65	236
-16	60	61	141			10,0,L					11,3,L					12,6,L		
	8,3,L				-15	58	54	135		-13	60	63	12		-8	62	64	194
-17	80	80	81			10,2,L				-12	58	57	13			13,0,L		
	8,5,L										11,4,L							
-15	32	40	164		-14	42	39	237		-13	62	66	36		-11	52	50	45
	8,12,L					10,3,L					11,8,L					13,1,L		
-7	49	45	284		-14	72	63	199		-7	38	43	211		-10	70	65	335
-6	74	68	281			10,6,L					11,9,L					13,4,L		
	9,0,L				-12	70	67	255		-8	100	101	312		-8	80	71	182
-1										-5	63	55	32			13,5,L		
-16	69	63	270								12,0,L				-8	81	82	35

[illegible]

	12,10,L		13,0,L		14,0,L		15,0,L		16,0,L		17,0,L					
-6	82	75	235	-7	40	35	307	-2	41	38	76	-16	33	25	142	
-3	86	69	63													
	13,0,L		13,0,L		13,0,L		13,0,L		13,0,L		13,0,L		13,0,L		13,0,L	
-13	43	48	315	-1	57	55	249	-2	87	76	30	-4	44	39	131	
-12	85	66	50					0	37	29	180					
	13,5,L		14,0,L		14,0,L		14,0,L		14,0,L		14,0,L		14,0,L		14,0,L	
-10	65	60	357	-6	29	24	205	-19	37	33	135	-19	42	44	13	
	13,6,L		14,0,L		14,0,L		14,0,L		14,0,L		14,0,L		14,0,L		14,0,L	
-9	54	47	331	-5	73	73	320	-20	52	55	0	-16	45	31	252	
	13,6,L		14,0,L		14,0,L		14,0,L		14,0,L		14,0,L		14,0,L		14,0,L	
				-1	91	87	229	-20	45	43	84	-16	83	77	0	

9.4 Discussion of Results

This X-ray crystal structure analysis of bicyclo(4,4,1)undecane-1,6-diol reveals that the ring system consists of two cycloheptane rings, both in a twist-chair conformation, fused back-to-back to one another across positions 1 and 3, as defined in Figure 1. The molecule possesses an approximate C_2 symmetry axis passing through C(11) normal to the plane of least inertia (Figure 3).

Molecular mechanics calculations, using the White-Bovill alkane/alkene force-field¹⁵ and a two-stage Newton-Raphson minimisation procedure were performed on a number of plausible conformations of bicyclo(4,4,1)undecane. The gas phase MEC appears to be an exactly C_2 symmetric structure corresponding very closely to that in the solid state and the calculated and observed geometries are compared in Figure 4. The shortest observed transannular H ... H contacts are 2.15 and 2.14 Å between H(21) ... H(91) and H(42) ... H(71) (C-H bond vectors corrected to a length of 1.08 Å from the foreshortened length of 0.990 Å, which is observed in the X-ray analysis) and the corresponding calculated values are 2.21 Å. There is no evidence of anomalous methylene scissoring modes^{17,18} in the IR spectrum of solid bicyclo(4,4,1)undecane and so by analogy with 9-thiabicyclo(3,3,1)nonan-2,6-dione where the effect is also absent and the distance is known to be 2.07 Å from a recent neutron diffraction study,¹⁹ it seems reasonable to conclude that the actual distances in bicyclo(4,4,1)undecane are, at least, greater than 2.07 Å.

Figure 4(a): The calculated torsion angles (degrees) for the bicyclo(4.4.1)undecane system are shown to the left-hand side of each set of numbers. The observed torsion angles for bicyclo(4.4.1)undecane-1,6-diol are given to the right of each set of numbers, along with the corresponding e.s.d.'s (in parentheses). Multiple torsion angles are distinguished by appending the label of the fourth atom to the value.

Figure 4(b): The bond lengths (\AA) with e.s.d.'s $\times 10^3$ and bond angles (degrees) with e.s.d.'s $\times 10$.

Figure 4(a)

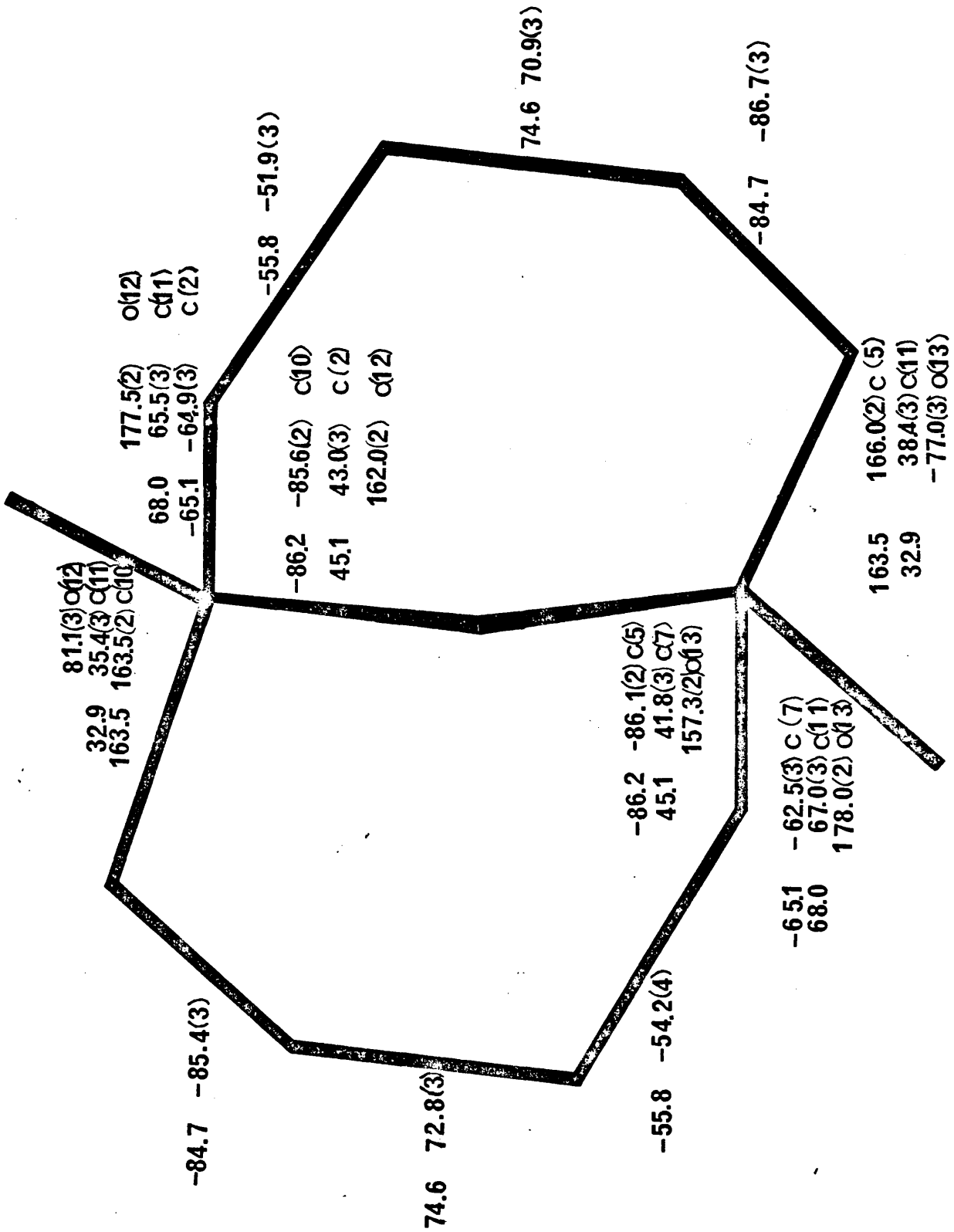
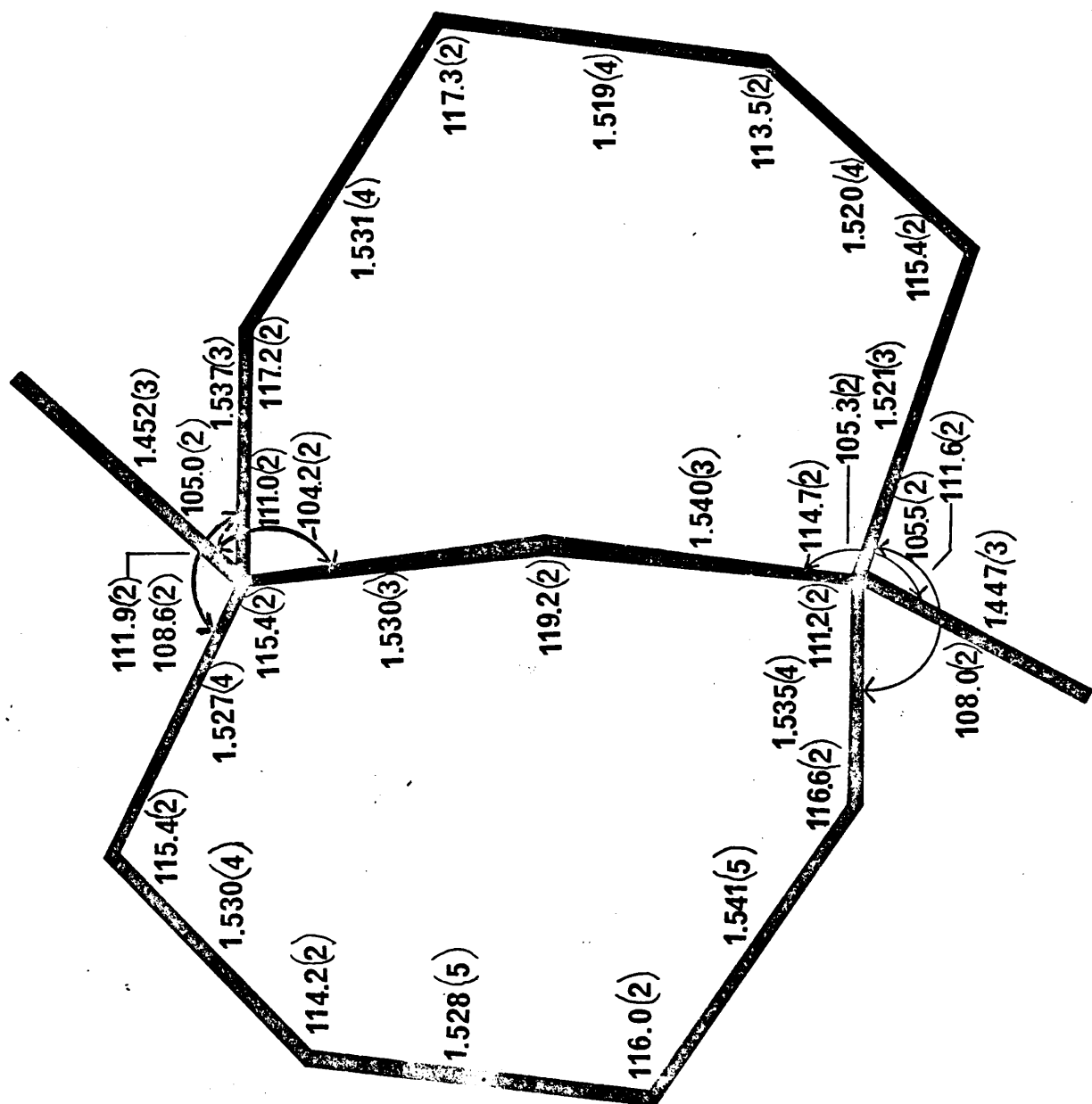


Figure 4(b)



Torsion angles and relative energies for the other calculated conformations are given in Table 8. Conformation I corresponds to a twist-chair cycloheptane ring fused to a chair cycloheptane ring and is 4.88 kcal./mole higher than the MEC, on account of the unfavourable torsional interactions, mainly associated with the chair, and the repulsive nonbonded interactions of atoms across the ring. These strain components are minimized, to a large extent, by bond angle deformation. Conformation II relates to a twist-chair being 1,3-fused to a boat and is 4.34 kcal./mole higher in steric energy than the MEC. This difference can be attributed, in large part, to the nonbonded interactions and torsional strain that characterise the boat cycloheptane ring, which is calculated to be 3.79 kcal./mole less stable than the twist-chair 7-ring. Conformation III represents a twist-chair, which is 3,5-bridged by a twist-boat saturated 7-ring and is 6.43 kcal./mole less stable than the MEC. Two cycloheptane boats fused back-to-back, as in Conformation IV raises the steric energy with respect to the MEC by 8.26 kcal./mole, which is approximately twice the calculated energy difference between the twist-chair and boat conformations of cycloheptane. Two cycloheptane chair conformations fused together result in two extremely serious H ... H interactions (ca. $1.0 \overset{\text{O}}{\text{\AA}}$), which involve the four 4-a hydrogens (see Figure 1) of the two cycloheptane rings, and as such, would appear to be energetically unstable.

The conformation of the ten-membered ring in bicyclo (4,4,1)undecane-1,6-diol is interesting because it appears to be representative of a class which has so far escaped

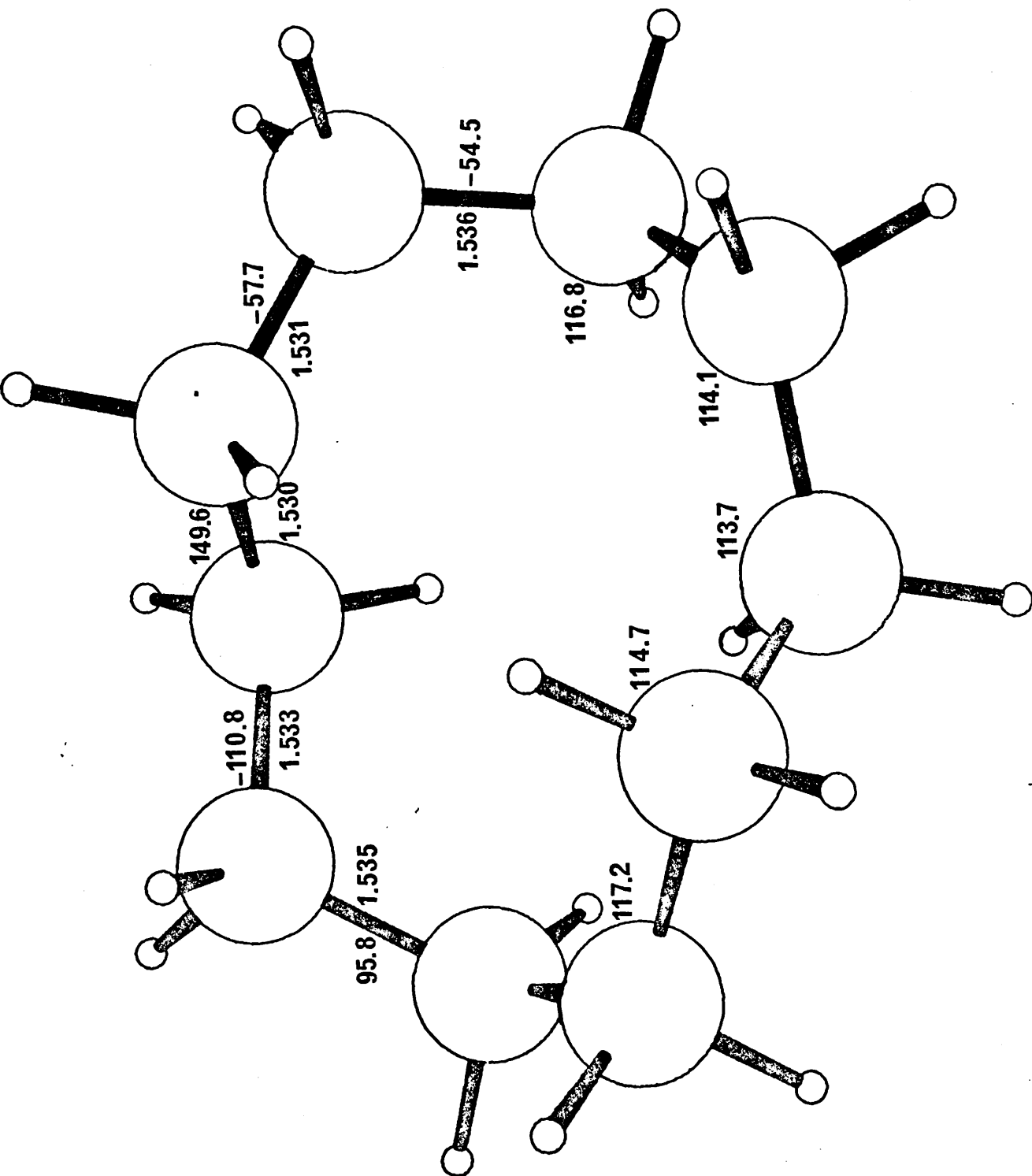
TABLE 8: Torsion angles (deg) and steric energies relative to the MEC (k.cal.mol⁻¹) for some low-energy conformations of bicyclo(4,4,1)undecane.

	I	II	III	IV
$\omega_{10,1,2,3}$	-56	-162	-151	-156
$\omega_{1,2,3,4}$	-59	73	72	68
$\omega_{2,3,4,5}$	-8	-6	-13	0
$\omega_{3,4,5,6}$	70	-69	-64	-68
$\omega_{4,5,6,7}$	57	170	168	155
$\omega_{5,6,7,8}$	-120	-108	-53	-156
$\omega_{5,6,11,1}$	60	50	51	64
$\omega_{6,7,8,9}$	58	49	-34	68
$\omega_{7,8,9,10}$	-87	-88	-33	0
$\omega_{8,9,10,1}$	63	70	76	-68
$\omega_{9,10,1,2}$	85	78	60	155
$\omega_{10,1,11,6}$	75	76	68	64
E_s	4.88	4.34	6.43	8.26

attention. The low-energy conformations of cyclodecane studied by Hendrickson and others^{5,20} are either asymmetric or have mirror planes/two-fold axes bisecting bonds and/or passing through atoms. In the present instance, the sole symmetry element is a two-fold axis passing through the centre of the ring and the conformation resembles a trans, trans-cyclodeca-1,6-diene variant which was discussed in Chapter 3²¹ and which is only 2.40 kcal./mole less stable than the MEC conformation of cyclodecane, the BCB. The geometry (derived from MM calculations) of the observed 10-ring conformation is shown in Figure 5.

An algorithm, derived by Cremer and Pople,²² provided a means whereby it was possible to compare the various observed and calculated cycloheptane structures with the calculated C_2 symmetric twist-chair MEC which is characterised by amplitudes $q_2 = 0.499$, $q_3 = 0.673 \text{ \AA}$ and phase angles $\phi_2 = 270^\circ$, $\phi_3 = 270^\circ$. The geometry is not significantly different to that calculated by other workers,⁷ and therefore forms a valid reference point for the following discussion. The amplitudes and phase angles for the two observed 7-rings of bicyclo(4,4,1) undecane system are 0.512, 0.644 \AA , 273, 271 $^\circ$ and 0.535, 0.630 \AA , 271, 270 $^\circ$ and the corresponding calculated values are 0.512, 0.656 \AA , 276, 272 $^\circ$. Although the values of q_2 and q_3 vary slightly from 7-ring to 7-ring, the value of $Q = \left(\sum_m q_m^2 \right)^{\frac{1}{2}}$ for each ring is nearly constant at $0.83 \pm 0.01 \text{ \AA}$, so that 1,3 fusion appears to have little effect on the total puckering amplitude. The differences between the calculated q and ϕ

Figure 5: The calculated cyclodecane conformation derived from the 10-ring of bicyclo(4.4.1)undecane.



for cycloheptane and bicyclo(4,4,1)undecane system indicate a small amount of distortion consequent upon fusion of the two twist-chair 7-rings to form the bicyclic molecule, so that the observed conformations probably do not correspond exactly to the MEC of cycloheptane although the deviation is small.

Differences between the two observed 7-rings amount to $\langle \Delta l \rangle = 0.008 \text{ \AA}$, $\langle \Delta \theta \rangle = 0.5^\circ$ and $\langle \Delta \omega \rangle = 1.5^\circ$ compared with $3 \langle \sigma(l) \rangle = 0.012 \text{ \AA}$, $3 \langle \sigma(\theta) \rangle = 0.6^\circ$ and $3 \langle \sigma(\omega) \rangle = 1.5^\circ$, where l, θ and ω denote bond length, bond angle and torsion angle. It can therefore be deduced that, with one exception, the departure of bicyclo(4,4,1)undecane-1,6-diol from C_2 molecular symmetry are probably not significant in the solid state. The exception concerns the orientation of the O-H bond vectors (see Figure 3) which might be expected to vary independently in order that the intermolecular hydrogen bonding is optimised.

An analysis of the thermal motion parameters²³ of the non-hydrogen atoms of bicyclo(4,4,1)undecane-1,6-diol was carried out and the components of the translation (T), libration (L) and screw (S) tensors are given in Table 9. The reasonable agreement between the r.m.s. $\sigma(U_{ij}^{obs})$ of 0.0015 \AA^2 and the calculated value $\langle (U_{ij}^{obs} - U_{ij}^{calc})^2 \rangle^{\frac{1}{2}} = 0.0024 \text{ \AA}^2$ implies that the bicyclic system behaves as a rigid body and is not disordered. The eigenvector corresponding to the largest eigenvalue of the L tensor is almost exactly parallel to the vector between the two oxygen atoms, so that the intermolecular hydrogen bonds are

TABLE 9: Components of the translation (T), libration (L) and screw (S) tensors describing the rigid body motion of bicyclo(4,4,1)undecane. All values $\times 10^4$

	Components			Eigenvalues	Eigenvectors		
T_{ij}	307	33	28	348	7166	4668	5183
		255	39	265	-6846	3286	6506
			275	223	1334	-8211	5550
L_{ij}	71	-9	6	76	9022	-2701	3363
		41	-5	54	-3643	-597	9294
			56	38	-2309	-9610	-1523
S_{ij}	-15	0	2				
		-1	4				
			10				
				$\langle (U_{ij}^{obs} - U_{ij}^{calc})^2 \rangle^{\frac{1}{2}} = 24 \text{ \AA}^2$ $\langle (\sigma(U_{ij}^{obs}))^2 \rangle^{\frac{1}{2}} = 15 \text{ \AA}^2$			

The tensor components are in units of $\text{\AA}^2(\underline{T})$, $\text{rad}^2(\underline{L})$ and $\text{rad } \text{\AA}(\underline{S})$ and the eigenvalues in $\text{\AA}^2(\underline{T})$ and $\text{rad}^2(\underline{L})$. The normalised eigenvectors are referred to the molecular inertial axes shown in Figure 2.

minimally perturbed by this librational mode in a similar way to those in cyclodecane-1,6-diol.²⁴

9.5. References

1. J.D. DUNITZ, Perspectives in Structural Chemistry, 2, 1-70 (1968). (J.D. Dunitz and J.A. Ibers, editors) New York: John Wiley.
2. E. HULER and A. WARSHEL. Acta Cryst., B30, 1822 (1974).
3. M. BIXON, H. DECKER, J.D. DUNITZ, H. ESER, S. LIFSON, C.MOSSELMAN, J. SICHER and M.SVOBODA, Chem.Comm., 360 (1967).
4. J.D. DUNITZ and H.M.M. SHEARER, Helv.Chim.Acta, 43, 18 (1960).
5. J.B. HENDRICKSON, J.Amer.Chem.Soc., 89, 7047 (1967).
6. R. PAUNCZ and D. GINSBURG, Tetrahedron, 9, 40 (1960).
7. W.M.J. FLAPPER and C. ROMERS, Tetrahedron, 31, 1705 (1975)
8. K.K. CHACKO, R. SRINIVASAN and R.ZAND, J.Cryst. Molec.Struct. 1, 213 (1971).
9. A.T. McPHAIL and G.A. SIM, Tetrahedron, 29, 1751 (1973).
10. J.D.M. ASHER and G.A. SIM, J. Chem.Soc., 1584 (1965).
11. MAZHOR-UL-HAQUE and C.N. CAUGHLAN, J.Chem.Soc., B., 956 (1969).
12. MAZHOR-UL-HAQUE and C.N. CAUGHLAN, J. Chem.Soc., B., 355 (1967).
13. A.T. McPHAIL and K.D. ONAN, J.Chem.Soc., Perkin II, in press, (1977).
14. D.N.J. WHITE and M.J. BOVILL, Acta Cryst., B33, in press (1977).

15. D.N.J. WHITE and M.J. BOVILL, J.Chem.Soc., Perkin II,
in press (1977).
16. D.N.J. WHITE and O. ERMER, Chem.Phys.Letters, 31, 111
(1975).
17. J. MARTIN, Ph.D. Thesis, University of Glasgow, 1974
18. R.K. MACKENZIE., D.D. MACNICOL, H.H. MILLS, R.A.RAPHAEL,
F.B. WILSON and J.A. ZABKIEWICZ, J.Chem.Soc., Perkin II,
1632 (1972).
19. M.J. BOVILL, P.J. COX, H.P. FLITMAN, M.H.P. GUY, A.D.U.
HARDY, P.McCABE, G.A. SIM and D.N.J. WHITE, Acta Cryst., B,
in preparation (1977).
20. O. ERMER, Structure and Bonding, 27, 161 (1976).
Berlin: Springer-Verlag.
21. D.N.J. WHITE and M.J. BOVILL, Tetrahedron Letters, 2239,
(1975).
22. D. CREMER and J.A. POPLE, J.Amer.Chem.Soc., 97, 1354
(1975).
23. V. SCHOMAKER and K.N. TRUEBLOOD, Acta Cryst., B24, 63
(1968).
24. O. ERMER, J.D. DUNITZ and I. BERNAL. Acta Cryst.,
B29, 2278 (1973).